Stability and Error Analysis of Numerical Schemes for 1D and 2D Fractional Differential Equations

Aniruddha Seal

Department of Mathematics
Indian Institute of Technology Guwahati
Guwahati - 781039, India.

May, 2024

Stability and Error Analysis of Numerical Schemes for 1D and 2D Fractional Differential Equations

A Thesis Submitted

in the Fulfillment of the Requirements

for the Degree of

DOCTOR OF PHILOSOPHY

by

Aniruddha Seal

(Roll Number: 196123002)

Department of Mathematics

Indian Institute of Technology Guwahati

Guwahati - 781039, India.

May, 2024

DECLARATION

I do hereby declare that the work contained in this thesis entitled **"Stability and Error Analysis of Numerical Schemes for 1D and 2D Fractional Differential Equations"** was completed by me, under the supervision of **Dr. Natesan Srinivasan, Professor, Department of Mathematics, Indian Institute of Technology Guwahati** for the award of the degree of Doctor of Philosophy and this work has not been submitted elsewhere for a degree.

IIT Guwahati
May, 2024

Aniruddha Seal
(Roll No. 196123002)
Department of Mathematics
Indian Institute of Technology Guwahati.

CERTIFICATE

This is to certify that the work contained in this thesis entitled **"Stability and Error Analysis of Numerical Schemes for 1D and 2D Fractional Differential Equations"** by **Aniruddha Seal**, a student of **Department of Mathematics, Indian Institute of Technology Guwahati**, for the award of the degree of Doctor of Philosophy has been carried out under my supervision and this work has not been submitted elsewhere for a degree.

IIT Guwahati
May, 2024

Prof. Natesan Srinivasan
Professor
Department of Mathematics
Indian Institute of Technology Guwahati

Dedicated to

"Maa"

Mrs. Namita Seal,

and

"Baba"

Mr. Amitava Seal.

ACKNOWLEDGMENT

"Celebrate the blessing of God and praise him for his kindness towards you. Thank him, for his precious gift."

I begin with a gratitude to "The God Almighty" for giving me the blessings and opportunity to achieve my goal and to be successful in this part. It is with immense pleasure and honor that I express my heartfelt gratitude to everyone who has supported me along my journey. First and foremost, I would like to express my gratefulness to Professor Natesan Srinivasan for his exceptional supervision of my thesis. His guidance, mentorship, and patience have been a constant source of hope and encouragement throughout my research. No matter the circumstances, he stood by me, providing unwavering support. His dedication, tolerance, and enthusiasm have deeply motivated me. This dissertation would not have been possible without his leadership and continuous support. His knowledge and advice have been indispensable to me, and I am truly thankful for his efforts to ensure my success.

Besides my supervisor, I would like to extend my gratitude to my doctoral committee members, Prof. D. C. Dalal, Prof. R. K. Sinha, Prof. S. N. Bora, and Prof. B. Deka for their cooperation and insightful feedback as my research work progressed.

I am profoundly grateful to the Indian Institute of Technology Guwahati for providing the essential resources for my research. I am equally grateful for the financial assistance provided by the Ministry of Human Resource Development, Government of India, which played a crucial role in enabling me to complete my thesis.

I also acknowledge the support provided by the department's office staff, including Mr. Sridhar Samal, Mrs. Trishna Choudhury, Mr. Phatik Kumar, and Mr. Jayanta Kumar Kalita, as well as our technical superintendent, Mr. Pranpratim Borgohain, Mr. Santanu Majumdar, and Mr. Pranab Jyoti Boro.

I am thankful to my family for their continuous support and encouragement. Their presence throughout this journey has been invaluable, and I am deeply appreciative of their role in my achievements. I want to express special gratitude to my parents, Mrs. Namita Seal and Mr. Amitava Seal, for their constant support and belief in me. Their sacrifices have paved the way for my success, and I am forever grateful for their unwavering faith in my abilities.

I am deeply thankful to Ankita for consistently providing me with strong emotional support and keeping me motivated. Despite the challenges, you have been a constant source of strength during both the highs and lows, lifting me up whenever I felt down. Your words of encouragement have been invaluable, helping me stay focused and on track. I am truly appreciative of your patience and understanding.

I am indebted to my teachers, Mr. Debajit Chatterjee and Dr. Gurudas Bajani, who shared their knowledge of Mathematics with utmost care during my school days. I extend my gratitude to Prof. Basudeb Mukhopadhyay (Dept. of Math, IIEST Shibpur) and Prof. Ujjal Debnath (Dept. of Math, IIEST Shibpur) for inspiring me and offering invaluable guidance during my postgraduate time and for motivating me to pursue further studies in mathematics. Additionally, I am thankful to Prof. Kalyan Chakraborty (Dept. of Math, HRI Allahabad) for providing valuable suggestions regarding the advancement of my research during my project periods at Harish-Chandra Research Institute, Allahabad.

I am eternally grateful to my friends for their unwavering friendship and understanding throughout this journey. They have consistently lent a listening ear and provided invaluable mental support during my toughest moments. I am thankful to my friends Dr. Avijit Das, Dr. Mrityunjoy Barman, Dr. Dipesh Barman, Abhijit, Mijanur, Sagar, Sandip, Sunil, Imran, Rik, Gopinath, Soumalya, Dipankar, Pratyasha for sharing many cheerful memories and supportive presence during my journey. I would like to take the opportunity to convey my gratitude to my senior Dr. Gautam Singh for his valuable suggestions at various times. Additionally, I would like to express my gratefulness towards Dr. Şuayip Toprakseven (Artvin Çoruh University) for his valuable discussion and collaboration.

Furthermore, I wish to extend my heartfelt appreciation to my juniors, including Rupchand, Deb Narayan, Saurabh, Arindam, Sachin, Aayushman, Achyuta, Bivakar, Ramesh, Sumit, Amit, Nayan, Pankaj, Anindita, Arijit, and many others, for enriching the journey with their contributions and creating unforgettable memories. I am also thankful to my school friends Subham, Anirudha, Subrata, Rupam, Pranay, and Rajsekhar for sharing cherished memories from our school days until now. Although, words may not suffice to fully convey my gratitude to all of my remarkable friend, nonetheless, I will forever cherish the wonderful memories we have created together over the past few years.

The beauty of the IIT Guwahati campus has truly defined my experience over the years. Its scenic charm exudes a refreshing vibe, contributing to an uplifting atmosphere that has left a lasting impression on me. Moreover, the campus's sports and cultural facilities played a crucial role in maintaining my mental well-being during my research days. These amenities provided opportunities to meet many new people that have become an integral part of my life.

I extend my heartfelt thanks to Prof. Swarup Bag, Prof. Amaresh Dalal, Prof. Kalyanasis Sahu, Dr. Subhamay Saha, Dr. Sukanta Bhattacharjee, Dr. Araghni Bhattacharya, Anjishnu Biswas, Sanket Das, Debabrata Paul, Rajnandan Choudhury Das, Deepak Mishra, Sanu Gangwar, Shashi Bhushan Singh, Alik Pramanik, Mijanur Islam, Angan Sarkar, Nilmadhab Das, and many others for sharing unforgettable moments with me during my PhD journey. Besides all these, I would like to extend my sincere appreciation to my beloved "Disang Hostel" and the staff members of my hostel, including the security personnel and mess staff, for their constant support and for creating a nurturing environment that has played a significant role in my journey towards achieving my goals.

I want to acknowledge the efforts of all those who have directly or indirectly helped me along the way. This thesis would not have been possible without their support.

Thank you.

IIT Guwahati, May, 2024 **Aniruddha Seal**

"Arise, awake, and stop not till the goal is reached."

— **Swami Vivekananda**

"All of us do not have equal talent. But, all of us have an equal opportunity to develop our talents."

— **Dr. A.P.J Abdul Kalam**

"The truth always turns out to be simpler than you thought."

—**Richard P. Feynman**

ABSTRACT

The aim of this thesis is to construct and analyze some simple, yet very efficient numerical methods to approximate solutions to fractional differential equations (FDEs) which find wide-ranging applications across numerous fields. From understanding fluid dynamics in engineering to modeling chemical reactions in chemistry, and from analyzing electrical networks in physics to optimizing control systems in robotics, these mathematical models underpin crucial aspects of modern technology and scientific inquiry. In FDEs, weakly singular kernels play a significant role. These kernels have singularities that are milder compared to classical calculus. Since most FDEs lack analytical solutions, we look towards different numerical methods as the optional way. However, when dealing with FDEs with weakly singular kernels, standard numerical techniques may not suffice, and thus specialized techniques are needed to ensure accurate and efficient computations. The non-uniform mesh generation strategies help us to get rid of this issue of singularities by distributing a sufficient number of mesh points near the singular point.

In this work, the investigation begins with the analysis of a one-dimensional (1D) steady-state fractional boundary-value problems (FBVPs) featuring a fractional convection term and variable coefficients. Through rigorous analysis, the existence and uniqueness of solutions are established, followed by numerical exploration using the well-known $L1$-method. Henceforth, the discrete comparison principle is discussed and the error analysis is performed using the properly chosen discrete barrier function. Attention then turns to a second-order scheme utilizing spline techniques for FBVPs with integral boundary conditions. The existence and uniqueness theorem for the considered FBVP is exposed. Then the error analysis is conducted with subsequent discussions on discretization methods. Theoretical findings are substantiated through numerical experiments.

Then we discuss the numerical solution of 1D nonlinear time-tempered **k**-Caputo fractional diffusion equations. Initially, Newton's quasilinearization technique is employed to simplify the model problem and then we apply ${}_{\mathbf{k}}L2\text{-}1_{\sigma}$ scheme for the discretization. conduct stability analysis for the proposed scheme. Exploring further, 1D nonlinear time-fractional diffusion equations (TFDEs) with generalized memory kernels are addressed in the next chapter. The same linearization technique is used for simplification of the model and then we use non-uniform discretization methods to overcome the singularity. A generalized discrete fractional Grönwall inequality is developed with the help of complementary discrete generalized memory kernel. Further stability analysis, and error estimation are also established in L^2-norm. Few numerical experiments are addressed to justify the theoretical error estimates.

Furthermore, two-dimensional (2D) FDEs are also focused in this thesis. A dimensional-splitting weak Galerkin (WG) approach is introduced for numerically solving 2D TFDEs, aiming to reduce computational complexity and storage requirements. Initially, the 2D model problem is splitted into a set of individuals 1D problems in x- and y-directions, and

then the stability analysis is provided in each direction. Also, an overall error estimate of the proposed method is established in L^2-norm. Lastly, we deal with a locally one-dimensional (LOD) method for tackling the complexities of 2D nonlinear space-fractional diffusion equations (SFDEs). The model problem is first linearized and then decomposed into two 1D subproblems to minimize computational cost and storage necessities. Thereafter the discrete maximum principle in each direction and the overall convergence analysis is described in the maximum norm with the help of appropriately selected discrete barrier function. In each problem few numerical examples are incorporated for empirical validation of the theory. The thesis concludes with a summary of research findings and suggestions for future exploration within this dynamic field, underlining the practical significance of the developed numerical methods in diverse real-world applications critical for advancing technology and scientific knowledge.

Contents

ABBREVIATION

ADI	Alternating direction implicit
BVP	Boundary-value problem
DGMK	Discrete generalized memory kernel
FBVP	Fractional boundary-value problem
FDE	Fractional differential equation
FDM	Finite difference method
FEM	Finite element method
FIBVP	Fractional initial boundary-value problem
IBVP	Initial boundary-value problem
LOD	Locally one-dimensional
ODE	Ordinary differential equation
PDE	Partial differential equation
RL	Riemann-Liouville
RLC	Riemann-Liouville-Caputo
SFWG	Stabilizer-Free Weak Galerkin
TFDE	Time-Fractional Differential Equation
SFDE	Space-Fractional Differential Equation
STFDE	Space-Time-Fractional Differential Equation
WGFEM	Weak-Galerkin Finite Element Method

NOMENCLATURE

$\mathbb{N}$	Set of all natural numbers
$\mathbb{R}$	Set of all real numbers
$\mathbb{C}$	Set of all complex numbers
$\mathfrak{Re}(z)$	Real part of a complex number z
$\mathcal{C}(\overline{G})$	Space of continuous functions defined on some domain $\overline{G}$
$\mathcal{C}^k(\overline{G})$	Space of k times continuously differentiable functions defined on some domain $\overline{G}$
$L^1(G)$	Space of integral functions on the domain G
α	Fractional order $0 < \alpha < 1$
γ	Fractional order $1 < \gamma < 2$
β	Any arbitrary fractional order with $\mathbf{n} - 1 < \beta \leq \mathbf{n}$, $\mathbf{n} \in \mathbb{N}$
T	Final time
Ω_x	The domain $\{x : x \in (x_l, x_r)\}$ in the x-direction
Ω_y	The domain $\{y : y \in (y_l, y_r)\}$ in the y-direction
Ω_t	The domain $\{t : t \in (0, T]\}$ in the temporal direction
$\mathcal{D}$	Continuous space $\Omega_x \times \Omega_t$
$\mathcal{V}$	Continuous spatial domain $\Omega_x \times \Omega_y$ in 2D
h, h_x, h_y	Mesh-size in the spatial direction
τ, τ_n	Mesh-size in the temporal direction
C	Generic constant which takes different positive values according to its presence in required place
$\|\|\cdot\|\|_\infty$	Standard supremum-norm
$\|\|\cdot\|\|_2$	Discretre L^2-norm
$\|\cdot\|_W^{(+)}$, $\|\cdot\|_W$	WG Energy-norm
M_x, M_y	Number of mesh intervals in the x- and y-direction respectively
N	Number of mesh intervals in the time direction
$\overline{\Omega}^{M_x}$	Uniform mesh for the domain Ω
$\overline{\Omega}_x^{M_x}$, $\overline{\Omega}_y^{M_y}$	Uniform mesh along the x-direction and y-direction
$\overline{\Omega}_t^N$	Discretized temporal mesh

$\overline{\mathcal{D}}_{M_x}^N := \overline{\Omega}_x^{M_x} \times \overline{\Omega}_t^N$	The computational mesh for the domain $\mathcal{D}$
$\overline{\Omega}_{M_x,M_y}^N := \overline{\Omega}_x^{M_x} \times \overline{\Omega}_y^{M_y} \times \overline{\Omega}_t^N$	The computational mesh for the domain $\mathcal{V} \times \Omega_t$
E_{M_x}, $E_{M_x}^N$, E_M^N	Errors
$\widetilde{D}_{M_x}$	Maximum double-mesh differences
CO_{M_x}, CO_N, CO_M, CO_M^N, $\widehat{CO}_{M_x}$	Order of convergences

List of Figures

List of Tables

CHAPTER 1

Introduction and Mathematical Preliminaries

The objective of this thesis is to design and analyze efficient numerical methods for different types of fractional differential equations (FDEs). Numerical solutions of FDEs draw significant attention in various fields of applied sciences, engineering and medicines like acoustics, fluid mechanics, astrophysics, earthquake science, viscoelasticity etc. This chapter is introductory and includes a description of the problems, some notations, and preliminary material. It also includes a brief survey of the relevant literature and motivation behind the current study. The chapter-wise description of the thesis is reported in the last section of this chapter.

1.1 Background

1.1.1 Genesis of classical calculus

The birth of classical calculus in the late seventeenth century created a monumental shift in mathematical thinking, catalyzed by the pioneering contributions of luminaries such as Sir Isaac Newton and Gottfried Wilhelm Leibniz. In 1687, Newton's magnum opus [64], the Philosophiae Naturalis Principia Mathematica, revolutionized scientific inquiry by formulating the laws of motion and universal gravitation through the language of calculus. Concurrently, Leibniz's development of the symbolic notation for differentiation and integration provided a powerful toolkit for solving various kinds of scientific and engineering problems.

Classical calculus developed around the idea of integer-order derivatives and integrals, quickly emerged as a fundamental tool in the study of mathematical applications. It played a pivotal role in advancing various fields including physics, astronomy, engineering, and economics. From calculating planetary orbits and optimizing mechanical systems to modeling population dynamics and analyzing financial markets, classical calculus has deeply influenced virtually every aspect of scientific and technological progress. Its widespread application has significantly reshaped the landscape of human knowledge and innovation.

As demands increased, scientific inquiry expanded to include more complex phenomena. However, classical calculus shows its limitations in accurately describing certain complex behaviors like memory effects, non-local interactions, and fractal geometries. These limitations prompted the search for a more generalized mathematical framework capable of addressing these difficulties and ultimately encourages the scientists to search different but better tool to replace the classical calculus, and this ultimately leading to the emergence of the fractional calculus, a study or non-integer order derivatives and integration.

1.1.2 Birth of fractional calculus

The origin of fractional calculus dates back to the late 17th century through the works by Gottfried Wilhelm Leibniz during this period. One of the earliest remarks on the meaning of non-integer derivatives can be found in a letter [80] from Leibniz to L'Hospital dated 30.09.1695, where Leibniz gives a first answer to a question posed by L'Hospital about the meaning of non-integer derivatives, especially the case $1/2$. Leibniz acknowledges the question raised by L'Hospital and produced a conclusion by writing that "one day very useful

consequences will be drawn from this paradox, since there are little paradoxes without usefulness." The topic of non-integer order derivatives also comes up in the correspondence between Johann Bernoulli and Leibniz. In a letter [48] written to Leibniz in December 1695 Bernoulli reiterates the problem of "fractional or irrational" derivatives. Further advancements in fractional calculus occurred in the late 18th century, notably with Leonhard Euler's introduction of the Gamma function [21] in 1783, which indirectly touched upon fractional derivatives. Since then, lots of mathematicians have worked on fractional calculus, making it clearer and more useful in math.

In the realm of fractional calculus, differential equations play a crucial role as they serve as the mathematical framework for describing the behavior of systems with fractional-order dynamics. These equations involve fractional derivatives, which capture memory and non-local effects, making them suitable for modeling phenomena exhibiting complex behaviors such as anomalous diffusion, viscoelasticity, and some complex geometries.

The modern formulation of fractional calculus is the outcome of tireless efforts of some famous mathematicians and physicists. Some figures such as Joseph Liouville, Bernhard Riemann, Marcel Riesz, Hadamard, Michele Caputo, Mauro Fabrizio, Abdon Atangana, Dumitru Baleanu, etc. have played pivotal roles in refining the theory, providing rigorous definitions and properties of fractional derivatives and integrals, and establishing the theoretical results necessary for the study of fractional differential equations (FDEs). Their contributions have illuminated the advancement of modern mathematical analysis within the framework of fractional differential equations.

1.1.3 Applications of fractional calculus

Fractional calculus, though as old as classical calculus, has not been given so much important compared to classical calculus due to its complexity and lack of clear practical applications. At the earlier stage, it was mainly studied as a theoretical concept without much consideration for real-world applications. However, in recent years, there has been a surge in interest among researchers exploring its applications in various fields like viscoelasticity [9], electromagnetism [19], control systems [59], biomedicine and biology [35], option pricing [4], earthquake modelling [56], hydrology [11], etc. One key advantage is that fractional calculus helps us to understand systems with memory [76], which classical calculus doesn't fully address.

Classical calculus focuses on instant changes, but fractional calculus allows us to account for past influences. This makes it incredibly valuable for predicting long-term behavior, such

as how materials age or how complex biological processes unfold.

With each new discovery, it is becoming evident that fractional calculus is not just a niche topic—it is a powerful tool with the potential to solve real-world problems and drive innovation across various scientific and engineering disciplines. Its applications, from understanding the behavior of materials over time to unraveling the mysteries of living organisms, highlight its versatility and importance in advancing our understanding of the world around us.

1.2 Some important definitions and preliminaries

This section delves into some fundamental definitions and well-established results that play a pivotal role in the theoretical framework of this thesis.

In mathematics, some simple concepts are used to develop more intricate ideas. For example, some concepts, true for natural numbers, can be extended in case of $\mathbb{R}^+$, space of all positive real numbers. Like, the product of all positive integers less than or equal to some positive integer $\mathbf{n}$, gives the factorial of $\mathbf{n}$, denoted by $\mathbf{n}!$. But now the following steps show how this concept will be extended to some number $\mathbf{r} \in \mathbb{R}^+$.

1.2.1 Gamma function

Definition 1.2.1 ([21]). *If z is a complex number with $\mathfrak{Re}(z) > 0$, then the Euler gamma function is defined by,*

$$\Gamma(z) = \int_0^\infty \zeta^{z-1} e^{-\zeta}\, d\zeta. \tag{1.2.1}$$

It is noticeable that when $\mathbf{r} \in \mathbb{R}^+$, then the gamma function $\Gamma(\mathbf{r}+1)$ can be represented as $\Gamma(\mathbf{r}+1) = \mathbf{r}\Gamma(\mathbf{r})$ and for $\mathbf{n} \in \mathbb{Z}^+$, $\Gamma(\mathbf{n}+1) = \mathbf{n}!$.

Now, we use this concept of gamma function to extend the concept of classical order derivative to non-integer order derivative.

Let us consider a function $g(x) = x^k$, $x \geq 0$. Then the $\mathbf{n}$-th order derivative of $g(x)$ can be written as

$$\frac{d^{\mathbf{n}}}{dx^{\mathbf{n}}} g(x) = \frac{k!}{(k-\mathbf{n})!} x^{k-\mathbf{n}} = \frac{\Gamma(1+k)}{\Gamma(1+k-\mathbf{n})} x^{k-\mathbf{n}}, \tag{1.2.2}$$

where k and $\mathbf{n}$ are non-negative integer numbers.

Then we can generalize the above equation (1.2.2) by extending the integer $\mathbf{n}$ to a real

value $\mathbf{r}$ such as:

$$\frac{d^{\mathbf{r}}}{dx^{\mathbf{r}}}g(x) = \frac{\Gamma(1+k)}{\Gamma(1+k-\mathbf{r})}x^{k-\mathbf{r}}. \tag{1.2.3}$$

Considering the above concept of non-integer order derivative, there are so many interesting properties *e.g.* the above derivative (1.2.3) of a constant number is not zero *i.e.,*

$$\frac{d^{\mathbf{r}}}{dx^{\mathbf{r}}}(x^0) = \frac{\Gamma(1)}{\Gamma(1-\mathbf{r})}x^{-\mathbf{r}} = \frac{x^{-\mathbf{r}}}{\Gamma(1-\mathbf{r})}.$$

All these definitions approach to classical-order derivative in integer order limit- this method is called fractionalization algorithm *i.e.,*

$$\lim_{\mathbf{r}\to\mathbf{n}} \mathbf{D}^{\mathbf{r}} f(x) = \mathbf{D}^{\mathbf{n}} f(x),\ \mathbf{n} \in \mathbb{N}\cup\{0\},$$

where $\mathbf{D}$ is a differential operator.

Now, we define an extension of the Euler gamma function, namely $\mathbf{k}$-gamma function [14]. We first define the Pochhammer $\mathbf{k}$-symbol that will be utilized in further extension of the gamma function.

Definition 1.2.2 ([14])**.** *Let $z \in \mathbb{C}, \mathbf{k} \in \mathbb{R}$, and $\mathbf{n} \in \mathbb{N}$. Then the Pochhammer $\mathbf{k}$-symbol is defined as*

$$(z)_{\mathbf{n},\mathbf{k}} = z(z+\mathbf{k})(z+2\mathbf{k})\dots(z+(\mathbf{n}-1)\mathbf{k}). \tag{1.2.4}$$

Definition 1.2.3 ($\mathbf{k}$-gamma function)**.** *For any real number $\mathbf{k} > 0$, the $\mathbf{k}$-gamma function $\Gamma_{\mathbf{k}}$ is defined by*

$$\Gamma_{\mathbf{k}}(z) = \lim_{\mathbf{n}\to\infty} \frac{\mathbf{n}!\mathbf{k}^{\mathbf{n}}(\mathbf{nk})^{\frac{z}{\mathbf{k}}-1}}{(z)_{\mathbf{n},\mathbf{k}}}, \quad z \in \mathbb{C}\setminus\mathbf{k}\mathbb{Z}^-, \tag{1.2.5}$$

and the integral representation of the $\mathbf{k}$-gamma function is as follows:

$$\Gamma_{\mathbf{k}}(z) = \int_0^\infty \zeta^{z-1} e^{\left(-\zeta^{\mathbf{k}}/\mathbf{k}\right)} d\zeta.$$

Properties: Some properties of the $\mathbf{k}$-gamma function are:

1. $\Gamma_{\mathbf{k}}(z+\mathbf{k}) = z\Gamma_{\mathbf{k}}(z)$.
2. $\Gamma_{\mathbf{k}}(z) = \mathbf{k}^{\frac{\alpha}{\mathbf{k}}-1}\,\Gamma\left(\frac{z}{\mathbf{k}}\right)$.
3. For $\mathbf{k} \to 1$, we can get back the Euler gamma function *i.e.,* $\Gamma_{\mathbf{k}}(\cdot) \to \Gamma(\cdot)$.
4. For $\mathbf{k} \to 2$, it reduces to an integral of Gaussian functions *i.e.,*

$$\Gamma_2(z) = \int_0^\infty \zeta^{z-1} e^{\left(-\zeta^2/2\right)} d\zeta.$$

1.2.2 Mittag-Leffler function

The Mittag-Leffler function arises naturally in the solution of fractional-order differential equations. This function was first introduced by a Swedish Mathematician Gosta Mittag-Leffler [60] in the year 1903 as a generalization of the exponential function $exp(z), z \in \mathbb{C}$. It is found particularly in the investigations of the fractional generalization of the kinetic equation, random walks, Lévy flights, super-diffusive transport and in the study of complex systems.

Definition 1.2.4. *The one-parameter Mittag-Leffler function is defined as a power series expansion*

$$E_{\zeta_1}(z) = \sum_{j=0}^{\infty} \frac{z^j}{\Gamma(1 + j\,\zeta_1)}, \quad \text{for } \zeta_1,\, z \in \mathbb{C} \quad \text{with } \mathfrak{Re}(\zeta_1) > 0.$$

The two-parameter Mittag-Leffler function is a generalization of the one-parameter Mittag-Leffler function $E_{\zeta_1}(z)$ and it was introduced by Wiman [88] in the year 1905. The two-parameter Mittag-Leffler function or Wiman's function is defined by

$$E_{\zeta_1,\zeta_2}(z) = \sum_{j=0}^{\infty} \frac{z^j}{\Gamma(\zeta_2 + j\,\zeta_1)}, \quad \text{for } \zeta_1,\, \zeta_2,\, z \in \mathbb{C} \quad \text{with } \mathfrak{Re}(\zeta_1),\ \mathfrak{Re}(\zeta_2) > 0.$$

After a gap, in the year 1971, Prabhakar [66] discovered another generalized form of the Mittag-Leffler function which is known as the three-parameter Mittag-Leffler function and is defined as a power series expansion

$$E^{\zeta_3}_{\zeta_1,\zeta_2}(z) = \sum_{j=0}^{\infty} \frac{(\zeta_3)_j}{\Gamma(\zeta_2 + j\,\zeta_1)} \frac{z^j}{j!}, \quad \text{for } \zeta_1,\, \zeta_2,\, \zeta_3,\, z \in \mathbb{C} \quad \text{with } \mathfrak{Re}(\zeta_1),\ \mathfrak{Re}(\zeta_2),\ \mathfrak{Re}(\zeta_3) > 0.$$

where $(\zeta_3)_j$ is the Pochhammer symbol with $\mathbf{k} = 1$ in (1.2.4).

1.2.3 Definitions of fractional integrals and derivatives

In this subsection, we explore some key definitions of fractional order integrals and derivatives, building upon the concepts from integer-order calculus.

Let us define the following space:

$$\mathcal{AC}^{\mathbf{n}}([a,b]) = \left\{ v \in \mathcal{C}^{\mathbf{n}-1}([a,b]) : v^{(\mathbf{n}-1)} \text{ is absolutely continuous on } [a,b]\, i.e., v^{(\mathbf{n})} \in L^1([a,b]) \right\}, \tag{1.2.6}$$

where $v^{(\mathbf{n})}(x) = \dfrac{d^{\mathbf{n}} v}{dx^{\mathbf{n}}}$.

The classical Cauchy formula for the $\mathbf{n}$-fold integration of any function $v(x)$ with $\mathbf{n} \in \mathbb{N}$ is given by,

$$I_{a,x}^{\mathbf{n}} v(x) = \frac{1}{(\mathbf{n}-1)!} \int_a^x (x-\zeta)^{\mathbf{n}-1} v(\zeta)\, d\zeta.$$

Then using the fractionalization algorithm to expand the integer-order to arbitrary real order $\beta \geq 0$ with $\mathbf{n} \to \beta$ gives

$$I_{a,x}^{\beta} v(x) = D_{a,x}^{-\beta} v(x) = \frac{1}{\Gamma(\beta)} \int_a^x (x-\zeta)^{\beta-1} v(\zeta)\, d\zeta, \tag{1.2.7}$$

and it is known as the Riemann-Liouville (RL) fractional integral of order β.

Definition 1.2.5. *The Riemann-Liouville fractional derivative of order β for any function $v(x) \in \mathcal{AC}^{\mathbf{n}}([a,b])$, proposed by Riemann in 1847, is defined by*

$${}^{RL}D_{a,x}^{\beta} v(x) = \frac{d^{\mathbf{n}}}{dx^{\mathbf{n}}} \left(D_{a,x}^{-(\mathbf{n}-\beta)} v(x) \right) = \frac{1}{\Gamma(\mathbf{n}-\beta)} \frac{d^{\mathbf{n}}}{dx^{\mathbf{n}}} \int_a^x (x-\zeta)^{\mathbf{n}-\beta-1} v(\zeta)\, d\zeta, \tag{1.2.8}$$

where $\mathbf{n} = \lfloor \beta \rfloor + 1$, $x > a$.

The Riemann–Liouville fractional derivative stands as the well-established and in many regards the most natural definition. However, its application in modeling physical phenomena comes with certain disadvantages because a model including Riemann–Liouville fractional derivative demands for fractional initial value conditions. To overcome these difficulties, Caputo fractional derivative [12] was introduced by Michele Caputo in 1967 as a preferable choice for physical scenarios, as it includes only classical initial conditions, makes it more suitable for real-world circumstances.

Definition 1.2.6. *The Caputo fractional derivative of order β for any function $v(x) \in \mathcal{AC}^{\mathbf{n}}([a,b])$, where $\mathbf{n} = \lfloor \beta \rfloor + 1$ is defined as*

$${}^{C}D_{a,x}^{\beta} v(x) = D_{a,x}^{-(\mathbf{n}-\beta)} (v^{(\mathbf{n})}) = \frac{1}{\Gamma(\mathbf{n}-\beta)} \int_a^x \frac{v^{(\mathbf{n})}(\zeta)}{(x-\zeta)^{\beta-\mathbf{n}+1}}\, d\zeta, \quad x > a. \tag{1.2.9}$$

1.2.4 Relation between the Riemann-Liouville and Caputo fractional derivatives

The Riemann-Liouville and Caputo fractional derivative of a function $v(x)$ are connected by following relationship

$${}^{RL}D_{a,x}^{\beta} v(x) = \sum_{k=0}^{\mathbf{n}-1} \frac{v^{(k)}(a) x^{k-\beta}}{\Gamma(k+1-\beta)} + {}^{C}D_{a,x}^{\beta} v(x), \quad \mathbf{n} = \lfloor \beta \rfloor + 1,$$

and if $\beta \in (0,1)$ then we have ${}^{RL}D^{\beta}_{a,x}[v(x)-v(a)] = {}^{C}D^{\beta}_{a,x}v(x)$.

Thus, whenever $\beta \to \mathbf{n}$, Riemann-Liouville derivative, Caputo fractional derivative all tend to the classical derivative of order $\mathbf{n}$, but for non-integer order derivative, we have different behaviour of same function under different fractional derivative, for example, Riemann-Liouville derivative of a constant is non-zero but Caputo fractional derivative of that is zero as the later one includes $v'(x)$ inside integral sign.

1.2.5 Generalization of the fractional integral and fractional derivatives

In the recent days, various types of extended versions of the fractional integral and fractional derivatives have been introduced to capture the more realistic behaviour of the real-world problems. Few of them are defined below.

Definition 1.2.7 ([73]). *The tempered Riemann-Liouville fractional integral of order $\beta > 0$ and with tempering factor $\lambda \geq 0$ is defined as*

$$I^{\beta,\lambda}_{a,x}\, v(x) = \frac{1}{\Gamma(\beta)} \int_a^x (x-\zeta)^{\beta-1} e^{-\lambda(x-\zeta)} v(\zeta)\, d\zeta = e^{-\lambda x} I^{\beta}_{a,x} \left(e^{\lambda x} v(x)\right), \quad x > a. \tag{1.2.10}$$

Definition 1.2.8 ([73]). *The tempered Caputo fractional derivative of order $\beta > 0$ is defined as*

$${}^{C}D^{\beta,\lambda}_{a,x} v(x) = \frac{e^{-\lambda x}}{\Gamma(\mathbf{n}-\beta)} \int_a^x \frac{1}{(x-\zeta)^{\beta-\mathbf{n}+1}} \frac{d^{\mathbf{n}}}{d\zeta^{\mathbf{n}}} \left(e^{\lambda\zeta} v(\zeta)\right) d\zeta = e^{-\lambda x}\, {}^{C}D^{\beta,\lambda}_{a,x}(e^{\lambda x} v(x)), \quad x > a. \tag{1.2.11}$$

where $\mathbf{n} = \lfloor \beta \rfloor + 1$.

It is worth to mention that if $\lambda = 0$, then the tempered Riemann-Liouville fractional integral (1.2.10) and the tempered Caputo fractional derivative (1.2.11) reduce to the Riemann-Liouville fractional integral (1.2.7) and the Caputo fractional derivative (1.2.9) respectively.

In 2012, Mubeen and Habibullah [62] introduced a variant of the fractional integrals, namely $\mathbf{k}$-fractional integral with $\mathbf{k} \geq 1$ based on the $\mathbf{k}$-gamma function, defined in (1.2.5).

Definition 1.2.9. *The $\mathbf{k}$-fractional integral of order $\beta > 0$ for any function $v(x) \in \mathcal{AC}^{\mathbf{n}}([a,b])$, where $\mathbf{n} = \lfloor \beta \rfloor + 1$ is defined as*

$${}_{\mathbf{k}}I^{\beta}_{a,x}\, v(x) = \frac{1}{\mathbf{k}\Gamma_{\mathbf{k}}(\beta)} \int_a^x (x-\zeta)^{\beta/\mathbf{k}-1} v(\zeta)\, d\zeta, \quad x > a. \tag{1.2.12}$$

An additional generalization of the Caputo fractional derivative was introduced in [22], known as the $\mathbf{k}$-Caputo fractional derivative utilizing the $\mathbf{k}$-gamma function.

Definition 1.2.10. *For any function* $v(x) \in \mathcal{AC}^{\mathbf{n}}([a,b])$*, where* $\mathbf{n} = \lfloor \beta \rfloor + 1$*, the* $\mathbf{k}$*-Caputo fractional derivative of order* $\beta > 0$ *is defined as*

$$ {}^{C}_{\mathbf{k}}D^{\beta}_{a,x}\, v(x) = \frac{1}{\mathbf{k}\Gamma_{\mathbf{k}}\left(\mathbf{n} - \beta/\mathbf{k}\right)} \int_a^x \frac{v^{(\mathbf{n})}(\zeta)}{(x-\zeta)^{\beta/\mathbf{k}-\mathbf{n}+1}}\, d\zeta, \quad x > a. \tag{1.2.13} $$

In particular, when $\mathbf{k} \to 1$, then the equations (1.2.12) and (1.2.13) transform into the familiar Riemann-Liouville fractional integral (1.2.7) and the Caputo fractional derivative (1.2.9) respectively.

1.2.6 Some important integral transforms and their properties

Integral transforms are very much useful in solving differential and integral equations. It allows one to turn a complicated differential equation into an equation, often an algebraic equation one can solve easily. Laplace transform is one of the mostly used integral transforms in the study of differential equations. A novel integral transform was proposed by G. K. Watugala [85] in 1993, and its application over the ordinary differential equations and control engineering problems have been studied by the author. After that in 1994, S. Weerakoon [87] applied the Sumudu transform over different partial differential equations and derived the complex inversion for the Sumudu transform.

Definition 1.2.11. *Let us consider the following space*

$$ \mathbb{D}_{\mathbf{s}} = \left\{ z(t) : \exists\, \mathcal{M}, \mu_1, \mu_2 > 0,\ |z| < \mathcal{M} e^{\frac{|t|}{\mu_j}},\ \text{if } t \in (-1)^j \times [0,\infty) \right\}. \tag{1.2.14} $$

Definition 1.2.12. *The Sumudu transform of a function* $z \in \mathbb{D}_{\mathbf{s}}$ *is defined as*

$$ \mathbb{S}\left[z(t); \vartheta\right] = \mathbf{W}\left(\vartheta\right) = \int_0^{\infty} z\left(\vartheta t\right) e^{-t}\, dt, \quad t \geq 0,\ -\mu_1 < \vartheta < \mu_2. \tag{1.2.15} $$

Some basic properties of the Sumudu transforms are discussed in [10] by Belgacem and Karaballi.

Lemma 1.2.13. *Let* $\mathbf{W}\left(\vartheta\right)$ *and* $\mathbf{Z}\left(\vartheta\right)$ *be the Sumudu transforms of two functions* $w(t)$ *and* $z(t)$ *respectively. Then the Sumudu transform of the convolution*

$$ \left(w * z\right)(t) = \int_0^t w\left(\zeta\right) z\left(t - \zeta\right)\, d\zeta, \tag{1.2.16} $$

is given by $\mathbb{S}\left[\left(w * z\right)(t); \vartheta\right] = \vartheta\, \mathbf{W}\left(\vartheta\right) \mathbf{Z}\left(\vartheta\right)$.

Lemma 1.2.14. *If* $\mathbf{W}(\vartheta)$ *is the Sumudu transforms of the function* $w(t)$*, then the Sumudu transform of the* $\mathbf{n}$*-th order derivative,* $w^{(\mathbf{n})}(t)$*, denoted by* $\mathbf{W}_{\mathbf{n}}(\vartheta)$ *is given by*

$$\mathbf{W}_{\mathbf{n}}(\vartheta) = \vartheta^{-\mathbf{n}} \left[\mathbf{W}(\vartheta) - \sum_{k=0}^{\mathbf{n}-1} w^{(k)}(0)\vartheta^k \right], \quad \mathbf{n} \geq 1. \tag{1.2.17}$$

Then the Sumudu transform has been extended to fractional integrals and derivatives by Katatbeh and Belgacem in [41], and also authors used it to solve fractional differential equations. The Sumudu transform of the Caputo fractional derivative is discussed in the next lemma.

Lemma 1.2.15. *If for a positive integer* $\mathbf{n}$*,* $\mathbf{n}-1 < \beta \leq \mathbf{n}$*, and* $\mathbf{W}(\vartheta)$ *is the Sumudu transform of a function* $w(t)$*, then the Sumudu transform* $\mathbf{W}_C^{\beta}(\vartheta)$ *of the Caputo fractional derivative of* $w(t)$ *of order* β*,* ${}^{C}D_{0,t}^{\beta}w(t)$*, is given by*

$$\mathbf{W}_C^{\beta}(\vartheta) = \mathbb{S}\left[{}^{C}D_{0,t}^{\beta}w(t)\right] = \vartheta^{-\beta}\left[\mathbf{W}(\vartheta) - \sum_{k=1}^{n}\vartheta^{k-1}\left[\frac{d^{k-1}w(t)}{dt^{k-1}}\right]_{t=0}\right]. \tag{1.2.18}$$

Another novel integral transform, namely Elzaki transform was developed by T. Elzaki [16] in 2011, and was applied on different ordinary differential equations to show its efficiency. Thereafter, Elzaki and Elzaki [15] have shown the application of Elzaki transform on five different partial differential equations that basically occur in many branches of physics, in applied mathematics as well as in engineering.

Definition 1.2.16. *The Elzaki transform of a function* $z \in \mathbb{D}_{\mathbf{s}}$ *is defined as*

$$\mathbb{E}[z(t);\nu] = \mathbf{T}(\nu) = \nu\int_0^{\infty} z(t)\, e^{-t/\nu}\, dt, \quad t \geq 0,\ -\mu_1 < \nu < \mu_2. \tag{1.2.19}$$

Later, Elzaki et. al. [18] have studied the properties of the Elzaki transform and Laplace-Elzaki duality result has been used to invoke a complex inverse Elzaki transform. In the next lemma, we state the Laplace-Elzaki duality result.

Lemma 1.2.17. *Let,* $\mathbf{F}(s)$ *be the Laplace transform of the function* $z(t)$*, defined by*

$$\mathbf{F}(s) = \mathbb{L}[z(t);s] = \int_0^{\infty} e^{-s\,t} z(t)\, dt, \quad \mathfrak{Re}(s) > 0,$$

and $\mathbf{T}(\nu)$ *be the Elzaki transform of the function* $z(t)$*. Then the Laplace-Elzaki duality relation is expressed as*

$$\mathbf{T}(\nu) = \nu\mathbf{F}\left(\frac{1}{\nu}\right), \quad \mathbf{F}(s) = s\mathbf{T}\left(\frac{1}{s}\right). \tag{1.2.20}$$

Next lemma provides the Elzaki transform of the convolution operator $*$ between two functions $w(t)$ and $z(t)$.

Lemma 1.2.18 ([17]). *Let* $\mathbf{V}(\nu)$ *and* $\mathbf{T}(\nu)$ *be the Elzaki transforms of two functions* $w(t)$ *and* $z(t)$ *respectively. Then the Elzaki transform of the convolution*

$$(w * z)(t) = \int_0^t w(\zeta)\, z(t-\zeta)\, d\zeta, \tag{1.2.21}$$

is given by $\mathbb{E}[(w * z)(t); \nu] = \frac{1}{\nu}\mathbf{V}(\nu)\mathbf{T}(\nu)$.

Then, Khalid et. al. have extended the use of Elzaki transform to the fractional derivatives in [43] and established the application of the Elzaki transform technique to some non-homogeneous fractional differential equations.

1.2.7 Discretization of the domain

To study the numerical solution of a differential equation, we first need to consider the discretized form of the given domain. We consider the spatial domains $\Omega_x = (x_l, x_r)$ and $\Omega_y = (y_l, y_r)$ in the x- and y- directions respectively. The spatial domains are discretized in following manner under the uniform mesh

$$\overline{\Omega}_x^{M_x} = \{x_i : x_i = x_l + ih_x,\ i = 0, 1, 2, \ldots, M_x,\ h_x = (x_r - x_l)/M_x\},$$
$$\overline{\Omega}_y^{M_y} = \{y_j : y_j = y_l + jh_y,\ j = 0, 1, 2, \ldots, M_y,\ h_y = (y_r - y_l)/M_y\},$$

where h_x and h_y are the step-size in the x- and y- directions respectively.

The time domain $\Omega_t = (0, T]$ is discretized as

$$\overline{\Omega}_t^N = \{t_n : 0 = t_0 < t_1 < t_2 \ldots < t_{N-1} < t_N = T,\ 0 \le n \le N\},$$

with the time-step size $\tau_n = t_n - t_{n-1}$, $1 \le n \le N$. If the temporal mesh is uniform then the mesh size can be written as $\tau = T/N$.

1.2.8 Numerical approximation of the space and time fractional derivatives

In the study of FDEs, numerical approximation of fractional derivative plays a crucial role due to the unavailability of closed-form analytical solution of FDEs in many cases. One

of the commonly used numerical methods to approximate the fractional derivative is $L1$-method, first proposed in [47]. The $L1$-method is described below to approximate the Caputo fractional derivative with order lying in $(0,1)$ under both uniform and non-uniform meshes.

L1-discretization under uniform mesh: The Caputo fractional derivative ${}^{C}D^{\alpha}_{0,x}u(x)$ is discretized utilizing the well-known $L1$-discretization method at a point $x = x_i \in \overline{\Omega}_x^{M_x}$, $i = 1, 2, \ldots, M_x - 1$ as follows

$$\begin{aligned} {}^{C}D^{\alpha}_{0,x_i}u(x) &:= \frac{1}{\Gamma(1-\alpha)}\sum_{k=0}^{i-1}\int_{x_k}^{x_{k+1}}(x_i-\zeta)^{-\alpha}\,u'(\zeta)\,d\zeta \\ &\approx \frac{1}{\Gamma(1-\alpha)}\sum_{k=0}^{i-1}\int_{x_k}^{x_{k+1}}(x_i-\zeta)^{-\alpha}\,\frac{U_{k+1}-U_k}{h_x}\,d\zeta \\ &= \frac{h_x^{-\alpha}}{\Gamma(2-\alpha)}\sum_{k=0}^{i-1}(U_{k+1}-U_k)\,\widehat{b}^{(\alpha)}_{i-k}, \quad i = 1, 2, \ldots, M_x, \end{aligned} \tag{1.2.22}$$

where

$$\widehat{b}^{(\alpha)}_{k} = \begin{cases} k^{1-\alpha} - (k-1)^{1-\alpha}, & \text{for} \quad k = 1, 2, \ldots, M_x, \\ 0, & \text{for} \quad k \leq 0. \end{cases} \tag{1.2.23}$$

L1-discretization under non-uniform mesh: Similar to the above, $L1$-method for Caputo fractional derivative ${}^{C}D^{\alpha}_{0,t}v\,(t)$ at a point $t_n \in \overline{\Omega}_t^N$ under the nonuniform mesh is given as

$$\begin{aligned} {}^{C}D^{\alpha}_{0,t}v\,(t_n) &= \frac{1}{\Gamma(1-\alpha)}\sum_{k=0}^{n-1}\frac{v^{k+1}-v^k}{\tau_{k+1}}\int_{t_k}^{t_{k+1}}(t_n-s)^{-\alpha}\,ds \\ &= \frac{1}{\Gamma(2-\alpha)}\sum_{k=0}^{n-1}\frac{v^{k+1}-v^k}{\tau_{k+1}}\left[(t_n-t_k)^{1-\alpha} - (t_n-t_{k+1})^{1-\alpha}\right] \\ &= \frac{1}{\Gamma(2-\alpha)}\sum_{k=0}^{n-1}\left(v^{k+1}-v^k\right)\mathfrak{b}^{(\alpha)}_{n,n-k}, \end{aligned} \tag{1.2.24}$$

where the coefficient $\mathfrak{b}^{(\alpha)}_{n,n-k}$ is given as

$$\mathfrak{b}^{(\alpha)}_{n,n-k} = \frac{(t_n-t_k)^{1-\alpha} - (t_n-t_{k+1})^{1-\alpha}}{\tau_{k+1}}, \quad k = 0, 1, \ldots, n-1. \tag{1.2.25}$$

1.3 Objective and motivation

In the assessments of FDEs, weakly singular kernels appear as a crucial part. The behavior of these kernels at certain points may exhibit singularities that are weaker than those encountered in classical calculus. In general, most of the FDEs do not have analytical solution and it leads to the search of numerical solutions. When it comes to numerically solving fractional differential equations involving weakly singular kernels, specialized techniques are required to ensure accurate and efficient computations. One common approach is to discretize the fractional derivative using finite difference methods (FDMs) [92, 81, 6, 75], which approximate the derivative operator in terms of finite differences. However, when weakly singular kernels are involved, standard numerical methods may create convergence issues or accuracy problems.

To address these challenges, researchers have developed numerous numerical methods specifically designed to handle weakly singular kernels in FDEs. These methods often involve carefully choosing discretization schemes and integration techniques that take care the peculiar behavior of weakly singular kernels. For instance, numerical techniques such as quadrature rules with adaptive refinement or under the shade of graded meshes, developed for handling weak singularities may be employed. Furthermore, certain regularity assumptions or smoothness conditions can be applied to weaken the effects of weak singularities in numerical computations. The main goal is to design efficient computational methods and perform their theoretical estimates for different kinds of FDE models.

The primary objective of this thesis is to develop and analyze compatible numerical methods within a novel theoretical framework, using FDMs and finite element methods (FEMs) for different FDEs. The motivation for this research originates from the increasing relevance of numerical schemes in the field of FDEs. Presented below is a concise review of recent advancements in this field.

In the past few decades, numerous researchers have delved into exploring solutions for FDEs and have made efforts to establish numerical methods suitable for such equations, employing finite difference and finite element techniques. We first discuss some notable contributions using FDMs. Numerical study of fractional boundary-value problems (FBVPs) has attracted the attention of many scientists from both practical and theoretical points of view in different branches of pure and applied sciences. Few works on FBVPs are discussed in the following paragraph.

Jajarmi and Baleanu [36] has established an efficient iterative method for solving a class of non-linear FBVPs, which is free from perturbation, discretization, linearization, or restrictive

assumptions, and provides the exact solution in the form of a uniformly convergent series. They also provided an iterative algorithm that is computationally efficient to achieve an approximate solution with enough accuracy. Mary and Tamilselvan [58] have applied the FDM to obtain the numerical solution of a non-local FBVP on uniform mesh with the step-size h and proved that the method is convergent with order $O(h^{\gamma-1}), 1 < \gamma < 2$. A novel numerical approach for handling FBVPs is established in [5] by Al-Nana et al. based on the fractional central formula. They also investigated the stability of the proposed approach.

Besides FBVPs, fractional-initial-boundary-value problems (FIBVPs) find applications in numerous fields due to their ability to capture complex behaviours such as non-locality, memory effects, and anomalous diffusion. Its numerical study present unique challenges and opportunities to the researchers and thus it motivates to develop various notable numerical methods. An $L1$-stable scheme has been proposed by Langlands and Henry in [47] to address the fractional-order time diffusion equation. Furthermore, Sun and Wu [74] derived a finite difference method with $L1$-approximation for the fractional-in-time derivative. Similarly, Lin and Xu [55] constructed and analyzed a finite difference scheme for the time discretization of the time-fractional diffusion equations (TFDEs) with order $\alpha, 0 < \alpha < 1$, demonstrating that the time convergence is of order $(2 - \alpha)$. Gracia et.al. [28] have established a finite-difference scheme for an IBVP with a Riemann–Liouville–Caputo (RLC) fractional derivative and established a discrete comparison principle and a discrete barrier function to prove the convergence result.

In the recent days, scientists have also focused on developing various higher-order numerical techniques for FDEs to reduce the computational cost and the requirement of large storage. In [25], Gao et al. developed a new difference scheme to approximate the Caputo fractional derivative with the order of approximation $\mathcal{O}\left(\tau^{3-\alpha}\right)$ called the $L1$-2 formula. This method is valuable for implementing difference schemes for TFDEs in both bounded and unbounded spatial domains. Alikhanov [7] introduced a new scheme, namely the $L2\text{-}1_\sigma$ method, and demonstrated the convergence of the numerical solution with order $\mathcal{O}\left(\tau^{3-\alpha}\right)$ in time. Additionally, in [8], Alikhanov utilized quadratic interpolation to develop a higher-order $L2$-method for TFDEs, and proved stability and convergence for the developed method.

Currently, spline techniques [44, 30, 52] have gained very much interests in numerically solving the FDEs. Sousa [70] has derived a second-order implicit numerical method for a fractional diffusion model with a spatial derivative of fractional order; author used a spline approximation to discretize the Caputo fractional derivative and further discussed the consistency and stability of the proposed method. In [37], Jesus and Sousa have derived a fractional B-splines technique for a sub-diffusion problem including time-fractional RL

derivative of order $0 < \alpha < 1$, and they discussed the von Neumann stability analysis and convergence of the presented numerical method.

In general, the presence of a weakly singular kernel in the solution of FDEs complicates the derivation of higher-order schemes. Particularly when the solution of an FDE lacks smoothness, numerical methods on uniform meshes show poor convergence rates. For these reasons, numerical methods on non-uniform meshes have gained considerable attention among researchers. Zhang et al. [93] proposed a numerical technique in non-uniform mesh to investigate the numerical solution of FDEs, along with a discussion on the stability and error analysis of their developed scheme. In a related work, Li et al. [49] presented FDM utilizing non-uniform meshes to tackle nonlinear fractional differential equations by introducing rectangle and trapezoid formulas and they investigated the error and stability analysis of their proposed scheme. Stynes et al. conducted a new analysis in [72] discussing error analysis of the finite difference method on graded meshes for reaction-diffusion FDEs. More recently, Kedia et al. [42] proposed a generalized $L1$-method for analyzing the numerical solution of a TFDE with generalized memory kernel. Also, the authors proved an optimal convergence order of $(2-\alpha)$ in time on a non-uniform mesh.

Moreover, significant progress has been made in the finite element framework [3, 95, 63, 51] for handling FDEs. Noteworthy contributions are discussed in the next few paragraphs. Ervin and Roop have developed a Galerkin finite element approximation in [20] for the stationary fractional advection-diffusion equation. They have introduced fractional derivative spaces, equivalent to the usual fractional dimension Sobolev spaces $H^s\left(\widehat{\Omega}\right)$ under some domain $\widehat{\Omega}$, and derived the existence and uniqueness results along with the error estimates for the Galerkin approximation. In [23], Fu et al. have derived finite element solution for steady state fractional convection diffusion equation. Furthermore, a rigorous regularity analysis is carried out and error estimates for the finite element approximation are derived by the authors.

In [39], Jin et al. considered standard Galerkin FEM for a 1D fractional-order parabolic equation with a RL type space fractional derivative of order $\gamma \in (1,2)$. Authors have derived error estimates in the $L^2\big(\widehat{\Omega}\big)$- and $H^{\alpha/2}\big(\widehat{\Omega}\big)$-norm for the semidiscrete scheme and in the $L^2\big(\widehat{\Omega}\big)$-norm for the fully discrete schemes under some domain $\widehat{\Omega}$. Huang et al. [33] have studied the optimal error analysis in H^1-norm for a time fractional-initial-boundary-value problem using the FEM on a quasi-uniform mesh. Recently, in the article [90] Yang et al. presented an α-robust stability and error analysis of FEM for space-time fractional diffusion equation (STFDE). Authors have developed finite element approximation to fractional Laplacian and provided a d-dimensional fast Fourier transform-based fast algorithm

to derive spatial discretization and $L1$ scheme on graded temporal meshes to discretize the time-fractional term of the STFDE. Kopteva [46] discussed a non-uniform $L2$-type discretization technique with a convergence order of $(3-\alpha)$ for fractional-order parabolic problems with Caputo time derivative of order $\alpha \in (0,1)$, and established a sharp pointwise-in-time error bounds on quasi-graded temporal meshes with arbitrary degrees of grading.

In the last few years, weak Galerkin finite element method (WGFEM) [82, 61, 84, 83] has attracted many researchers due its flexible discretization scheme that can handle irregular meshes and non-smooth solutions more effectively compared to traditional Galerkin methods. It was developed by Wang and Ye [82] in the year 2011, and after that it started gaining popularity due to its large application on the multi-dimensional problems. Toprakseven [77] has proposed WGFEM for time-fractional reaction-convection diffusion problem. Author has also discussed the related stability and error analysis of the proposed scheme. In [34], Hussein has proved stability analysis and the optimal order error estimate of WGFEM under L^2-norm for a 2D time-fractional coupled Burgers' equations. A stabilizer-free weak Galerkin (SFWG) FEM has been discussed by Ma et al. [57] with the $L2\text{-}1_\sigma$ formula in time for a TFDE. Authors also obtained optimal convergence order of semi-discrete scheme in L^2- and H^1-norm, and of fully-discrete $L2\text{-}1_\sigma$-SFWG scheme in L^2-norm.

For a TFDE type model problems on a multidimensional system, one needs to have a large storage for the numerical computations due to the numbers of time integration steps. An operator-splitting method or dimensional-splitting based on a class of the alternating direction implicit (ADI) method reduces the 2D TFDEs to sets of independent 1D subproblems. The ADI Galerkin FEM for solving the distributed-order time-fractional mobile-immobile equation in 2D has been proposed in [67]. They have used the backward Euler method in the time direction to deal with the temporal first-order derivative, and the weighted and shifted Grünwald formula is applied to discretize the distributed-order time-fractional derivative while the spatial direction is dealt with the Galerkin FEM. In [32], authors studied two-grid ADI finite element approximation for a nonlinear distributed-order fractional sub-diffusion equation. They have used weighted and shifted Grünwald difference operator for solving time distributed-order fractional derivative. They have discussed the stability and optimal error estimates of their scheme.

In conclusion, recent research has showcased significant advancements in numerical methods for FDEs, particularly through the different higher-order schemes. These methodologies offer efficient solutions to FDEs, paving the way for further exploration and application in various scientific and engineering domains.

1.4 Model problems

In this section, we introduce different kinds of fractional differential equations, considered in this thesis and then we briefly discuss the assumptions on the associated functions and the parameters in order to find convergent solution for the same.

1.4.1 1D steady-state FBVP involving fractional convection term with variable coefficients

We consider the following steady-state advection-diffusion-reaction type two-point FBVP:

$$\begin{cases} -D\left({}^{C}D_{0,x}^{\gamma-\alpha}u(x)\right) + a(x)\,{}^{C}D_{0,x}^{\alpha}u(x) + c(x)u(x) = f(x), \quad x \in \Omega_x = (x_l, x_r), \\ {}^{C}D_{0,x}^{\gamma-\alpha}u(x_l) = 0, \quad u(x_r) + \mu\,{}^{C}D_{0,x}^{\gamma-\alpha}u(x_r) = \rho, \end{cases} \tag{1.4.1}$$

where $0 < \gamma - \alpha < \alpha < 1 < \gamma < 2$ and $D = d/dx$ represents the first-order derivative operator with respect to x. Given functions $a, c, f \in \mathfrak{C}(\overline{\Omega})$ and $\mu(\geq 0)$, ρ are constants. Here we consider $x_l = 0$ and $x_r = 1$ for our problem.

1.4.2 1D fractional differential equation with integral boundary equations

Consider the following FBVP with Caputo fractional derivative and with two integral conditions at both the boundary points:

$$\begin{cases} Lu(x) \equiv -{}^{C}D_{0,x}^{\gamma}u(x) + b(x)u'(x) + c(x)u(x) = f(x), \quad x \in \Omega_x = (x_l, x_r), \\ B_0u(x_l) \equiv u(x_l) - \displaystyle\int_{x_l}^{x_r} \phi(x)u(x)dx = \rho_0, \\ B_1u(x_r) \equiv u(x_r) - \displaystyle\int_{x_l}^{x_r} \psi(x)u(x)dx = \rho_1, \end{cases} \tag{1.4.2}$$

where ρ_0, ρ_1 are constants and $1 < \gamma < 2$.

The coefficients $a(x)$, $c(x)(> 0)$ and the source function $f(x)$ are chosen sufficiently smooth over the domain $\overline{\Omega}_x = [x_l, x_r]$ with $x_l = 0$ and $x_r = 1$ for our model problem. The functions $\phi(x)$ and $\psi(x)$ are chosen such that

$$\phi(x),\, \psi(x) \geq 0 \quad \text{and} \quad \int_0^1 \phi(\xi)\,d\xi < 1, \int_0^1 \psi(\xi)\,d\xi < 1.$$

1.4.3 1D nonlinear time-tempered k-Caputo FDE with variable coefficients

Consider the following nonlinear time-tempered **k**-Caputo FDE with variable coefficients:

$$\begin{cases} {}^{C}_{\mathbf{k}}D^{\alpha,\lambda}_{0,t}u(x,t) = \mathcal{L}_{\mathcal{N}}u(x,t) - f(x,t,u), \quad (x,t) \in \mathcal{D} = \Omega_x \times \Omega_t, \\ u(x,0) = \widehat{u}_0(x), \quad x \in \overline{\Omega}_x = [x_l, x_r], \\ u(x_l,t) = 0, \quad u(x_r,t) = 0, \quad t \in \overline{\Omega}_t = [0,T], \end{cases} \tag{1.4.3}$$

where $\mathcal{L}_{\mathcal{N}} \equiv \dfrac{\partial}{\partial x}\left(\Psi(x,t)\dfrac{\partial u}{\partial x}\right)$, $0 < \alpha < 1, \Omega_x = (x_l, x_r), \Omega_t = (0,T]$, $0 < \widehat{\psi}_0 \leq \Psi(x,t) \leq \widehat{\psi}_1$ and $\partial f/\partial u > 0$ for all $(x,t) \in \overline{\mathcal{D}} = \overline{\Omega}_x \times \overline{\Omega}_t$ with $x_l = 0$ and $x_r = 1$. Given functions $\widehat{u}_0$ and f are sufficiently smooth, and the source function $f(x,t,u)$ is nonlinear in the variable $u(x,t)$.

The tempered fractional derivative operator (1.2.11) is coupled with **k**-Caputo fractional derivative operator (1.2.13) to develop a fractional derivative operator, namely tempered **k**-Caputo fractional derivative operator ${}^{C}_{\mathbf{k}}D^{\alpha,\lambda}_{0,t}$, with the parameter $\mathbf{k} \geq 1$ and tempering factor $\lambda \geq 0$, and the operator ${}^{C}_{\mathbf{k}}D^{\alpha,\lambda}_{0,t}$ is defined as

$${}^{C}_{\mathbf{k}}D^{\alpha,\lambda}_{0,t}u(t) = \frac{e^{-\lambda t}}{\mathbf{k}\Gamma_{\mathbf{k}}\left(1-\frac{\alpha}{\mathbf{k}}\right)}\int_0^t (t-\zeta)^{-\alpha/\mathbf{k}}\left(e^{\lambda\zeta}u(\zeta)\right)' d\zeta,$$

where $\Gamma_{\mathbf{k}}(\alpha)$ is the **k**-gamma function. For $\mathbf{k} = 1$, the tempered Caputo fractional derivative operator ${}^{C}D^{\alpha,\lambda}_{0,t}u$ of order α can be achieved.

1.4.4 1D nonlinear time-fractional diffusion equation with generalized memory kernel

Here, we study the following nonlinear TFDE with generalized memory kernel:

$$\begin{cases} {}^{C}D^{\alpha,\omega(t)}_{0,t}u(x,t) = \mathcal{L}_{\mathcal{N}}u(x,t) - f(x,t,u), \ (x,t) \in \mathcal{D} = \Omega_x \times \Omega_t, \\ u(x,0) = \widehat{u}_0(x), \quad x \in \overline{\Omega}_x = [x_l, x_r], \\ u(x_l,t) = 0, \quad u(x_r,t) = 0, \quad t \in \overline{\Omega}_t = [0,T], \end{cases} \tag{1.4.4}$$

where $\mathcal{L}_{\mathcal{N}}u \equiv \dfrac{\partial}{\partial x}\Big(\Psi(x,t)\dfrac{\partial u}{\partial x}\Big)$, $\Omega_x = (x_l, x_r)$ and $\Omega_t = (0,T]$. The functions $\widehat{u}_0$ and f are sufficiently smooth, and the source function $f(x,t,u)$ is nonlinear in the variable $u(x,t)$ with the condition $\dfrac{\partial f}{\partial u} < 0$. The operator ${}^{C}D^{\alpha,\omega(t)}_{0,t}$, defined as

$${}^{C}D^{\alpha,\omega(t)}_{0,t}u(t) = \int_0^t \mathcal{Q}_{1-\alpha}(t-\xi)u'(\xi)\,d\xi,$$

with the generalized memory kernel $\mathcal{Q}_\alpha(t) = \omega(t)t^{\alpha-1}/\Gamma(\alpha)$ is the fractional derivative operator of order α, $0 < \alpha < 1$ in generalized Caputo sense with the weight function $\omega(t) \in \mathcal{C}^2(\overline{\Omega}_t)$, and $0 < \widehat{\psi}_0 \leq \Psi(x,t) \leq \widehat{\psi}_1$. We also consider the following properties of the weight function $\omega(t)$: (i) $0 < \omega(t) \leq 1$ and $\omega'(t) \leq 0\ \forall t \in [0,T]$, and (ii) $\omega(t_1)\,\omega(t_2) = \omega(t_1+t_2)$ and $\omega^{-1}(t) = \omega(-t)\ \forall t \in \overline{\Omega}_t$.

1.4.5 Two-dimensional time-fractional diffusion equation

Here, we focus on the following two-dimensional TFDE:

$$\begin{cases} {}^{C}D^{\alpha}_{0,t}u(\mathbf{x}) - \Delta u(\mathbf{x}) + \mathbf{d}(\mathbf{x}).\nabla u(\mathbf{x}) + c(\mathbf{x})u(\mathbf{x}) = f(\mathbf{x},t), \quad (\mathbf{x},t) \in \mathcal{V} \times \Omega_t, \\ u(\mathbf{x},0) = \widehat{u}_0(\mathbf{x}), \quad \mathbf{x} \in \overline{\mathcal{V}}, \\ u(\mathbf{x},t) = 0, \quad (\mathbf{x},t) \in \partial\mathcal{V} \times \overline{\Omega_t}, \end{cases} \tag{1.4.5}$$

where $u(\mathbf{x}) := u(x,y)$ for any function u, $\Omega_t = (0,T]$, $0 < \alpha < 1$ and $\mathcal{V} = \Omega_x \times \Omega_y$ is the tensor product grids of the x-domain $\Omega_x = (x_l, x_r)$ and the y-domain $\Omega_y = (y_l, y_r)$ with the boundary $\partial\mathcal{V}$. The coefficient functions $\mathbf{d} = (d_1, d_2)$ and $c = c_1 + c_2$ are considered to be smooth and bounded with $d_1 \geq \gamma_x > 0$, $d_2 \geq \gamma_y > 0$, and $c_1, c_2 \geq 0$ in the domain $\overline{\mathcal{V}}$. To confirm the existence of the solution of the model problem (1.4.5), the source function $g(\mathbf{x},t)$ and the initial value $\widehat{u}_0(\mathbf{x})$ are considered to be smooth enough, and we also assume that

$$c - \frac{1}{2}\nabla \cdot \mathbf{d} \geq 0.$$

1.4.6 Two-dimensional nonlinear space-fractional diffusion equation

We consider the following nonlinear two-dimensional (2D) SFDE:

$$\begin{cases} \dfrac{\partial u}{\partial t} - \mathbf{d}(\mathbf{x},t).\,\Delta_\alpha u + \mathbf{a}(\mathbf{x},t).\nabla u + f(\mathbf{x},t,u) = 0, \quad (\mathbf{x},t) \in \mathcal{V} \times \Omega_t, \\ u(\mathbf{x},0) = \widehat{u}_0(\mathbf{x}), \quad \mathbf{x} \in \overline{\mathcal{V}} = \overline{\Omega}_x \times \overline{\Omega}_y, \\ u(\mathbf{x},t) = 0, \quad (\mathbf{x},t) \in \partial\mathcal{V} \times \overline{\Omega}_t, \end{cases} \tag{1.4.6}$$

where the operator Δ_α is defined as $\Delta_\alpha \equiv \left(\dfrac{\partial}{\partial x}{}^{C}D^{\alpha}_{0,x}, \dfrac{\partial}{\partial y}{}^{C}D^{\alpha}_{0,y}\right)$, with $0 < \alpha < 1$, $u(\mathbf{x},t) = u(x,y,t)$, the set $\mathcal{V} = \Omega_x \times \Omega_y$ can be defined as the cartesian product grids of the x-domain $\Omega_x = (x_l, x_r)$ and the y-domain $\Omega_y = (y_l, y_r)$, where the boundary of this grid is denoted as $\partial\mathcal{V}$. The diffusion coefficient function $\mathbf{d} = (d_1, d_2)$ and the coefficient function $\mathbf{a} = (a_1, a_2)$

are considered to be smooth and bounded in the domain $\overline{\mathcal{V}}$ with $0 < m_1 \leq d_1, d_2 \leq m_2 \leq 1$ for some real number m_1, m_2. To validate the presence of a solution to the model problem (1.4.6), the nonlinear source function $f(\mathbf{x}, t, u)$ with $\dfrac{\partial f}{\partial u} > 0$ and the initial value $\widehat{u}_0(\mathbf{x})$, both are assumed to be sufficiently smooth.

1.5 Structure of the thesis

This thesis has been composed of several chapters discussing various efficient computational techniques for the numerical solution of model problems presented in the previous section. We present a brief outline of the works carried out in this thesis as follows:

Chapter 1 describes a comprehensive overview of fractional calculus and fractional differential equations along with the historical context and the evolution of related research. Additionally, it presents the motivations and objectives behind addressing fractional differential equations in both one and two dimensions.

In **Chapter 2** , we begin with a 1D steady-state FBVP with fractional convection term and variable coefficients. First, we derive the existence and uniqueness of the solution of the considered model problem and then apply the well-known $L1$-method to obtain the numerical result. Also, the discrete comparison principle has been proved and later it has been used to study the convergence analysis with a properly chosen discrete barrier function. Some numerical results have been carried out to validate the theoretical result.

Chapter 3 is devoted to study a second-order scheme using the spline technique for a FBVP with integral boundary conditions and its error analysis. We have established the existence and uniqueness theorem for the considered FDE, and then discretized the fractional derivative using second-order spline technique and the convection term has been approximated using the second-order central difference scheme. To discretize the integral terms present in boundary conditions, we have used the trapezoidal rule as it provides second-order approximation. Finally, we carried out the convergence analysis and incorporated the numerical examples in favour of the theoretical estimation.

In **Chapter 4**, we focus on the numerical study of a nonlinear time-tempered **k**-Caputo fractional diffusion equation. At first, we have linearized the considered nonlinear FDE using Newton's quasilinearization technique, and then used ${}_{\mathbf{k}}L2\text{-}1_{\sigma}$-central-difference method to discretize the proposed model problem. Further, we have studied the stability analysis of the proposed scheme and derived second-order convergence result in the L^2-norm. Numerical experiments are carried out to validate the theoretical error bounds.

Chapter 5 deals with the numerical study of a nonlinear TFDE with generalized memory kernel. To study the numerical solution of this model problem, we first linearized the model problem and then used the well-known $L1$-method in a more generalized sense to discretize the generalized Caputo time-fractional derivative term in a graded mesh. Further, we have developed a generalized discrete fractional Grönwall inequality to study the stability analysis and to derive the error estimate result of the fully-discrete method in the discrete L^2-norm. Lastly, few numerical experiments have been addressed to justify the theoretical error estimates.

In **Chapter 6**, we have numerically solved 2D TFDE by the dimensional-splitting $L1$-WGFEM. The proposed scheme alleviates the computational complexity and the high storage requirement for higher-dimensional problems. Initially, the 2D problem has been separated into two 1D problems. Then the WGFEM has been implemented in spatial variable and $L1$-method has been used in discretization of time-fractional derivative term. The stability of the proposed method has been established in each directions and an overall error estimate result is also carried out. Some numerical simulations are incorporated to validate the theoretical error estimate.

Chapter 7 studies a locally one-dimensional (LOD) method for 2D nonlinear space-fractional diffusion equation (SFDE). Initially, the nonlinear problem has been linearized using the Newton's quasilinearization technique, and subsequently it has been decomposed into two 1D problems to reduce the computational cost. This method is based on the combination of the Backward-Euler scheme for the temporal derivative and the $L1$-method for the spatial fractional derivatives. The discrete maximum principle of the present method has been discussed. The convergence of the fully-discrete scheme on a discrete L^∞-norm using is analyzed using discrete barrier function. Lastly, the justification of the theoretical results is done by some numerical experiments.

Finally, **Chapter 8** summarizes the works in this thesis and then conclude with a note on some proposed future works in this direction.

CHAPTER 2

Efficient finite-difference scheme for a steady-state fractional differential equation

In this chapter, we study the finite-difference scheme to obtain numerical solution of the a steady-state FBVP with fractional convection term. We use the well-known $L1$-method to discretize the fractional derivative terms on a uniform mesh. Then we establish a discrete maximum principle and further study the error analysis of the proposed scheme with the help of a properly chosen discrete barrier function. The theoretical error estimates are validated numerically with some test examples.

2.1 Introduction

In this chapter, we consider a steady-state two-point FBVP with fractional convection term:

$$\begin{cases} -D\left({}^{C}D_{0,x}^{\gamma-\alpha}u(x)\right) + a(x){}^{C}D_{0,x}^{\alpha}u(x) + c(x)u(x) = f(x), \quad x \in \Omega_x = (x_l, x_r), \\ {}^{C}D_{0,x}^{\gamma-\alpha}u(x_l) = 0, \quad u(x_r) + \mu\, {}^{C}D_{0,x}^{\gamma-\alpha}u(x_r) = \rho, \end{cases} \tag{2.1.1}$$

where $0 < \gamma - \alpha < \alpha < 1 < \gamma < 2$ and $D = d/dx$ represents the first-order derivative operator with respect to x. Given functions $a, c, f \in \mathcal{C}\left(\overline{\Omega}_x\right)$ and $\mu(\geq 0)$, ρ are constants. Here we consider $x_l = 0$ and $x_r = 1$ for our problem.

The mixed-fractional differential operator $D({}^{C}D_{0,x}^{\gamma-\alpha})$ with order lying in $(1, 2)$, is the combination of the first-order classical derivative operator D and the $(\gamma-\alpha)$-th order Caputo derivative operator ${}^{C}D_{0,x}^{\gamma-\alpha}$ is defined by

$$D\left({}^{C}D_{0,x}^{\gamma-\alpha}\right)\, u(x) = \frac{d}{dx}\frac{1}{\Gamma(1-\gamma+\alpha)}\int_0^x (x-\zeta)^{\alpha-\gamma}u'(\zeta)\, d\zeta,$$

provided $u(x) \in \mathcal{AC}^2(\overline{\Omega}_x)$.

Here, our aim is to solve the FBVP (2.1.1) numerically by applying the $L1$-method based on the uniform mesh. Further, we study the stability of the proposed numerical scheme and derive the error estimate. To validate the theoretical error estimate and order of convergences, some numerical experiments are carried out.

This chapter is organized in the following manner: Section 2.2 discusses some useful results, properties as well as the existence and uniqueness theorem of the given model problem. Section 2.3. starts with the discretization of the model problem followed by the discrete comparison principle. In Section 2.4, the truncation error bound and the convergence analysis are established with the help of properly chosen discrete barrier function. An application of the proposed method for a semilinear FBVP is described in Section 2.5. Some numerical results are included in Section 2.6 and finally some conclusions are drawn in Section 2.7.

2.2 Preliminary results and properties

This section starts with an important lemma which shows the equivalency between the first-order classical derivative and $(\gamma-\alpha)^{th}-$ order Caputo derivative at the point $x = 0$.

Lemma 2.2.1. *Suppose $a, c, f \in \mathcal{C}(\overline{\Omega}_x)$ along with the presence of existence of $D({}^{C}D_{0,x}^{\gamma-\alpha}u(x))$ where $u(x)$ is the solution of (2.1.1). Then $u'(0) = 0$.*

Proof. This can be proved in the similar way as given in [26, Lemma 2.1]. □

Now one may ask the reason behind the choice of the left boundary condition as ${}^{C}D_{0,x}^{\gamma-\alpha}u(0) = 0$ for our problem. This will be discussed in the following subsection.

2.2.1 Necessity of the left boundary condition

We check the requirement of the left boundary condition given in the FBVP (2.1.1) by using the Sumudu transform in the both sides of (2.1.1).

Let us consider a special case of the model problem (2.1.1) such as:

$$-D({}^{C}D_{0,x}^{\gamma-\alpha}u(x)) + aD_{C}^{\alpha}u(x) + cu(x) = f(x), \quad \text{on} \quad \Omega_x, \tag{2.2.1}$$

where the coefficients a and c are considered as constants. The Sumudu transform of the fractional derivative operator ${}^{C}D_{0,x}^{\gamma-\alpha}u(x)$ is given as follows

$$\mathbb{S}\left[{}^{C}D_{0,x}^{\gamma-\alpha}u(x);\vartheta\right] = \vartheta^{-(\gamma-\alpha)}\mathbb{S}[u;\vartheta] - \vartheta^{-(\gamma-\alpha)}u(0).$$

And, the Sumudu transform of the first-order classical derivative of ${}^{C}D_{0,x}^{\gamma-\alpha}u(x)$ is

$$\mathbb{S}\left[D\left({}^{C}D_{0,x}^{\gamma-\alpha}u(x)\right);\vartheta\right] = \frac{\mathbb{S}[u;\vartheta]}{\vartheta^{\gamma-\alpha+1}} - \frac{u(0)}{\vartheta^{\gamma-\alpha+1}} - \frac{{}^{C}D_{0,x}^{\gamma-\alpha}u(0)}{\vartheta}.$$

Applying the Sumudu transform on the both sides of (2.2.1), one gets

$$-\frac{\mathbb{S}[u;\vartheta]}{\vartheta^{\gamma-\alpha+1}} + \frac{u(0)}{\vartheta^{\gamma-\alpha+1}} + \frac{{}^{C}D_{0,x}^{\gamma-\alpha}u(0)}{\vartheta} + a\left[\frac{\mathbb{S}[u;\vartheta]}{\vartheta^{\alpha}} - \frac{u(0)}{\vartheta^{\alpha}}\right] + c\,\mathbb{S}[u;\vartheta] = \mathbb{S}[f;\vartheta],$$

which implies

$$\mathbb{S}[u;\vartheta] = u(0) + \frac{{}^{C}D_{0,x}^{\gamma-\alpha}u(0)}{\vartheta(\vartheta^{-(\gamma-\alpha+1)} - a\vartheta^{-\alpha} - c)} + \frac{c\,u(0)}{\vartheta^{-(\gamma-\alpha+1)} - a\vartheta^{-\alpha} - c} - \frac{\mathbb{S}[f;\vartheta]}{\vartheta^{-(\gamma-\alpha+1)} - a\vartheta^{-\alpha} - c}. \tag{2.2.2}$$

Applying the inverse Sumudu transform [13, Equation 8] on the both sides of (2.2.2) one can obtain

$$u(x) = \psi_1(x)\,{}^{C}D_{0,x}^{\gamma-\alpha}u(0) + u(0)(1 + c\,\psi_2(x)) - f * \psi_2(x), \tag{2.2.3}$$

where

$$\psi_1(x) = \sum_{r=0}^{\infty} a^r x^{(\gamma-2\alpha+1)r+\gamma-\alpha}\, E_{\gamma-\alpha+1,\gamma-\alpha+1+r(\gamma-2\alpha+1)}^{r+1}(cx^{\gamma-\alpha+1}),$$

$$\psi_2(x) = \sum_{r=0}^{\infty} a^r x^{(\gamma-2\alpha+1)r+\gamma-\alpha+1}\, E_{\gamma-\alpha+1,\gamma-\alpha+2+r(\gamma-2\alpha+1)}^{r+1}(cx^{\gamma-\alpha+1}),$$

and $E^{\zeta_3}_{\zeta_1,\zeta_2}$ is the three-parameter Mittag-Leffler function.

From (2.2.3), one can judge that the solution is only continuous and a troublesome singularity exists in the solution u at $x = 0$ when ${}^{C}D^{\gamma-\alpha}_{0,x}u(0) \neq 0$. Thus, for the solution to be in $\mathcal{C}^1(\overline{\Omega}_x)$, the left boundary condition should be ${}^{C}D^{\gamma-\alpha}_{0,x}u(0) = 0$.

Remark 2.2.2. *If we consider the reaction coefficient $c = 0$ and the source function $f(x)$ as constant f in the equation (2.2.1), then the solution will be*

$$\begin{aligned} u(x) &= u(0) + {}^{C}D^{\gamma-\alpha}_{0,x}u(0)x^{\gamma-\alpha}E_{1+\gamma-2\alpha,\,\gamma-\alpha+1}\left(ax^{\gamma+1-2\alpha}\right) \\ &\quad -fx^{\gamma-\alpha+1}E_{1+\gamma-2\alpha,\,\gamma-\alpha+2}\left(ax^{\gamma+1-2\alpha}\right), \end{aligned} \tag{2.2.4}$$

where E_{ζ_1,ζ_2} is the two-parameter Mittag-Leffler function.

Remark 2.2.3. *The solutions given by (2.2.3) and (2.2.4) include $u(0)$, which can be calculated using the right hand boundary condition due to the continuity of the solution in the domain $\overline{\Omega}_x$.*

Remark 2.2.4. *For $\alpha = 1$, the choice of the left boundary condition for the existence of continuously differentiable solution has been shown in [26, Subsecton 2.1] by considering a special case with constant coefficient and constant function f along with use of the Laplace transform in the corresponding model problem.*

The space $\mathcal{C}^{k,\eta}(0,1]$, for each positive integer k and $-\infty < \eta < 1$, contains functions $u \in \mathcal{C}(\overline{\Omega}_x)$ such that the functions $u \in \mathcal{C}^k(0,1]$, and satisfy the bounds

$$|u^{(i)}(x)| \leq \begin{cases} C, & \text{if} \quad i < 1-\eta, \\ C(1+|\ln(x)|), & \text{if} \quad i = 1-\eta, \\ Cx^{1-\eta-i}, & \text{if} \quad i > 1-\eta, \end{cases} \tag{2.2.5}$$

for $x \in (0,1]$ and $i = 1, 2, \ldots, k$.

For the given problem (2.1.1), the result from [65, Theorem 2.1] gives the following assumption and theorem for the existence and uniqueness of the solution.

Assumption 2.2.5. *If $f \equiv 0$ and $\rho \equiv 0$, the FBVP (2.1.1) has the trivial solution $u \equiv 0$.*

Theorem 2.2.6. *Let $a, c, f \in \mathcal{C}^{k,\eta}(0,1]$ for some integer $k \geq 2$ and some $\eta \in (-\infty, 1)$. Then the FBVP (2.1.1) has a unique solution $u \in \mathcal{C}^1(\overline{\Omega}_x)$ with $D({}^{C}D^{\gamma-\alpha}_{0,x}u) \in \mathcal{C}^{k,m}(0,1]$ where $m := \max\{\eta, 2\alpha - \gamma\}$.*

The bound of the derivatives of the solution $u(x)$ to (2.1.1) by summoning the idea from [26, Corollary 2.1] can be given as

Corollary 2.2.7. *Let $a, c, f \in \mathcal{C}^{k,\eta}(0,1]$ for some positive integer k and some $\eta \in (-\infty, 1)$ with $\eta \leq 2\alpha - \gamma$. Then from Theorem 2.2.6, the FBVP (2.1.1) has a unique solution u where $u \in \mathcal{C}^1(\overline{\Omega}_x) \cap \mathcal{C}^{k,\eta}(0,1]$ and there exists a constant C such that the solution u satisfy*

$$\left|u^{(i)}(x)\right| \leq \begin{cases} C, & \text{for} \quad i = 0, \\ Cx^{\gamma-\alpha+1-i}, & \text{for} \quad i = 1, 2, \ldots, k+1, \quad \text{and} \quad x \in (0,1]. \end{cases} \tag{2.2.6}$$

Proof. It can be proved in the same way as given in [26, Corollary 2.1]. □

2.3 Discretization scheme and discrete comparison principle

This section includes the study of the discretization method for the model problem (2.1.1). We apply the well known $L1-$approximation to discretize the fractional derivatives and forward difference formula is used to approximate the first order classical derivative term. Further the discrete comparison principle is also discussed in this section.

2.3.1 Discretization of the fractional derivatives

We consider the uniform mesh $\overline{\Omega}_x^{M_x}$ to employ the $L1-$discretization method to approximate the Caputo fractional derivatives ${}^{C}D_{0,x}^{\gamma-\alpha}u(x)$ and ${}^{C}D_{0,x}^{\alpha}u(x)$ at the point $x = x_i \in \overline{\Omega}_x^{M_x}$, $i = 1, 2, \ldots, M_x - 1$. Using the $L1$-discretization (1.2.22) for the Caputo derivative, we have

$${}^{C}D_{0,x_i}^{\gamma-\alpha}u(x) \approx \frac{h_x^{\alpha-\gamma}}{\Gamma(2-\gamma+\alpha)} \sum_{k=0}^{i-1} (U_{k+1} - U_k)\, \widehat{b}_{i-k}^{(\gamma-\alpha)} := D_{C,L1}^{\gamma-\alpha} U_i, \quad i = 1, 2, \ldots, M_x, \tag{2.3.1}$$

with

$$\widehat{b}_k^{(\gamma-\alpha)} = \begin{cases} k^{1-\gamma+\alpha} - (k-1)^{1-\gamma+\alpha}, & \text{for} \quad k = 1, 2, \ldots, M_x, \\ 0, & \text{for} \quad k \leq 0, \end{cases} \tag{2.3.2}$$

and

$${}^{C}D_{0,x_i}^{\alpha}u(x) \approx \frac{h_x^{-\alpha}}{\Gamma(2-\alpha)} \sum_{k=0}^{i-1} (U_{k+1} - U_k)\, \widehat{b}_{i-k} := D_{C,L1}^{\alpha} U_i, \quad i = 1, 2, \ldots, M_x, \tag{2.3.3}$$

with

$$\widehat{b}_k^{(\alpha)} = \begin{cases} k^{1-\alpha} - (k-1)^{1-\alpha}, & \text{for} \quad k = 1, 2, \ldots, M_x, \\ 0, & \text{for} \quad k \leq 0, \end{cases} \tag{2.3.4}$$

where U_i is the approximate value of the exact solution $u(x)$ at the point $x = x_i$.

Thus, the numerical approximation of the mixed-fractional derivative $D\left({}^{C}D_{0,x}^{\gamma-\alpha}u(x)\right)$ at the point $x = x_i$ can be obtained as

$$\begin{aligned}
-D^{+}(D_{C,L1}^{\gamma-\alpha}U_i) &= -\frac{D_{C,L1}^{\gamma-\alpha}U_{i+1} - D_{C,L1}^{\gamma-\alpha}U_i}{h_x} \\
&= -\frac{h_x^{-(1+\gamma-\alpha)}}{\Gamma(2+\alpha-\gamma)}\left[\sum_{k=0}^{i}(U_{k+1}-U_k)\,\widehat{b}_{i-k+1}^{(\gamma-\alpha)} - \sum_{k=0}^{i-1}(U_{k+1}-U_k)\,\widehat{b}_{i-k}^{(\gamma-\alpha)}\right] \\
&= -\frac{h_x^{-(1+\gamma-\alpha)}}{\Gamma(2+\alpha-\gamma)}\Big[U_0\left(\widehat{b}_i^{(\gamma-\alpha)} - \widehat{b}_{i+1}^{(\gamma-\alpha)}\right) + \sum_{k=1}^{i}\left(\widehat{b}_{i-k+2}^{(\gamma-\alpha)} - 2\widehat{b}_{i-k+1}^{(\gamma-\alpha)} + \widehat{b}_{i-k}^{(\gamma-\alpha)}\right)U_k \\
&\quad + U_{i+1}\widehat{b}_1^{(\gamma-\alpha)}\Big],
\end{aligned}$$

for $i = 1, 2, \ldots\ M_x - 1$ and $D^{+}U_i = (U_{i+1} - U_i)/h_x$ denotes the standard forward difference formula.

Then the discretized version of (2.1.1) takes the following form:

$$\begin{cases}
\text{Find the discretized solution } \{U_i\}_{i=0}^{M_x} \text{ such that} \\
L_{M_x}U_i := -D^{+}(D_{C,L1}^{\gamma-\alpha}U_i) + a_i D_{C,L1}^{\alpha}U_i + c_i U_i = f_i, \quad \text{for } i = 1, 2, \ldots, M_x - 1, \\
-D^{+}U_0 = 0, \quad U_{M_x} + \mu\, D_{C,L1}^{\gamma-\alpha}U_{M_x} = \rho,
\end{cases} \tag{2.3.5}$$

where $a_i := a(x_i)$ and similar expression holds for c_i and f_i.

Lemma 2.3.1. *The following relations for the coefficients $\widehat{b}_i^{(\gamma-\alpha)}$ and $\widehat{b}_i^{(\alpha)}$ follow directly from [26, Section 3],*

$$(i)\quad \widehat{b}_{k+1}^{(\gamma-\alpha)} < \widehat{b}_k^{(\gamma-\alpha)} \quad \text{and} \quad \widehat{b}_{k+1}^{(\alpha)} < \widehat{b}_k^{(\alpha)}, \quad \text{for all integers} \quad k \geq 1, \tag{2.3.6}$$

$$(ii)\quad \widehat{b}_{i-k+2}^{(\gamma-\alpha)} - 2\widehat{b}_{i-k+1}^{(\gamma-\alpha)} + \widehat{b}_{i-k}^{(\gamma-\alpha)} > 0, \quad \text{for} \quad 1 \leq i \leq M_x - 1, \ \text{and} \ \ k \in \{1, \ldots, i-1, i+1\}. \tag{2.3.7}$$

We next discuss the discrete comparison principle that will play an important role to show the convergence of computed solution to the exact solution.

2.3.2 Discrete comparison principle

Lemma 2.3.2. *Assume that the coefficients in our problem (2.1.1) satisfy (i) $a, c, f \in \mathcal{C}^{k,\eta}(0,1] \subset \mathcal{C}(\overline{\Omega}_x)$ and (ii) $c(x) \geq 0$ for $x \in \overline{\Omega}_x$. Let $\{Z_i\}_{i=0}^{M_x}$ be a mesh function that satisfies*

$$-D^{+}Z_0 \geq 0, \quad Z_{M_x} + \mu D_{C,L1}^{\gamma-\alpha}Z_{M_x} \geq 0 \quad \text{and} \quad L_{M_x}Z_i \geq 0, \quad \text{for } i = 1, 2, \ldots, M_x - 1.$$

Let the mesh width h satisfies the condition

$$h_x^{1+\gamma-2\alpha} < E(\gamma,\alpha)\ \min\left\{\left(\frac{\widehat{b}_i^{(\gamma-\alpha)}-\widehat{b}_{i+1}^{(\gamma-\alpha)}}{\widehat{b}_i^{(\alpha)}}\right)_{i=1}^{M_x-1},\left(\frac{\widehat{b}_{i+2}^{(\gamma-\alpha)}-2\widehat{b}_{i+1}^{(\gamma-\alpha)}+\widehat{b}_i^{(\gamma-\alpha)}}{\widehat{b}_i^{(\alpha)}-\widehat{b}_{i+1}^{(\alpha)}}\right)_{i=1}^{M_x-2}\right\}, \tag{2.3.8}$$

where $E(\gamma,\alpha)=\dfrac{\Gamma(2-\alpha)}{\|a\|_\infty\Gamma(2-\gamma+\alpha)}$. *Then* $Z_i\geq 0,\quad$ *for* $i=0,1,\ldots,M_x$.

Proof. It can be observed from (2.3.5) that after some steps one can obtain

$$\begin{aligned} Z_0\left[\frac{\widehat{b}_{i+1}^{(\gamma-\alpha)}-\widehat{b}_i^{(\gamma-\alpha)}}{h_x^{\gamma-\alpha+1}\Gamma(2-\gamma+\alpha)}-\frac{a_i\widehat{b}_i^{(\alpha)}}{h_x^{\alpha}\Gamma(2-\alpha)}\right]+\sum_{k=1}^{i+1}\Bigg[&\frac{-\left(\widehat{b}_{i-k+2}^{(\gamma-\alpha)}-2\widehat{b}_{i-k+1}^{(\gamma-\alpha)}+\widehat{b}_{i-k}^{(\gamma-\alpha)}\right)}{h_x^{\gamma-\alpha+1}\Gamma(2-\gamma+\alpha)}\\ &+\frac{a_i(\widehat{b}_{i-k+1}^{(\alpha)}-\widehat{b}_{i-k}^{(\alpha)})}{h_x^{\alpha}\Gamma(2-\alpha)}\Bigg]Z_k+c_iZ_i=f_i, \end{aligned} \tag{2.3.9}$$

for $i=1,2,\ldots M_x-1$.

Let $P=\left(p_{i,k}\right)_{i,k=0}^{M_x}$ be the $(M_x+1)\times(M_x+1)$ matrix associated to the discretization (2.3.5). Then we have a linear system $P\overrightarrow{Z}=\overrightarrow{f}$ where $\overrightarrow{Z}=(Z_0,Z_1,\ldots,Z_{M_x})^T$ and $\overrightarrow{f}=(f_0,f_1,\ldots,f_{M_x})^T$, with $f_0=0$ and $f_{M_x}=\rho$. By the hypothesis

$$P\overrightarrow{Z}\geq 0. \tag{2.3.10}$$

Entries of the 0^{th} row of the matrix P are

$$p_{0,0}=\frac{1}{h_x},\quad p_{0,1}=-\frac{1}{h_x},\quad p_{0,k}=0,\quad 1<k\leq M_x.$$

For $i=1,2,\ldots M_x-1$, the entries of i^{th} row are

$$p_{i,0}=\frac{\widehat{b}_{j+1}^{(\gamma-\alpha)}-\widehat{b}_j^{(\gamma-\alpha)}}{h_x^{\gamma-\alpha+1}\Gamma(2-\gamma+\alpha)}-\frac{a_i\widehat{b}_i^{(\alpha)}}{h_x^{\alpha}\Gamma(2-\alpha)}, \tag{2.3.11}$$

$$p_{i,k}=\frac{-\left(\widehat{b}_{i-k+2}^{(\gamma-\alpha)}-2\widehat{b}_{i-k+1}^{(\gamma-\alpha)}+\widehat{b}_{i-k}^{(\gamma-\alpha)}\right)}{h_x^{\gamma-\alpha+1}\Gamma(2-\gamma+\alpha)}+\frac{a_i\left(\widehat{b}_{i-k+1}^{(\alpha)}-\widehat{b}_{i-k}^{(\alpha)}\right)}{h_x^{\alpha}\Gamma(2-\alpha)},\quad \text{for}\quad k=1,2,\ldots,i-1,i+1, \tag{2.3.12}$$

$$p_{i,i}=\frac{2\widehat{b}_1^{(\gamma-\alpha)}-\widehat{b}_2^{(\gamma-\alpha)}}{h_x^{\gamma-\alpha+1}\Gamma(2-\gamma+\alpha)}+a_i\frac{\widehat{b}_1^{(\alpha)}}{h_x^{\alpha}\Gamma(2-\alpha)}+c_i, \tag{2.3.13}$$

$$p_{i,k}=0,\quad \text{for}\quad k=i+2,i+3,\ldots,M_x. \tag{2.3.14}$$

The M_x^{th} row of the matrix P is

$$p_{M_x,0} = -\mu\varrho\,\widehat{b}_{M_x}^{(\gamma-\alpha)}, \quad p_{M_x,k} = \mu\varrho\left(\widehat{b}_{M_x-k+1}^{(\gamma-\alpha)} - \widehat{b}_{M_x-k}^{(\gamma-\alpha)}\right), \quad \text{for} \quad k = 1, 2\ldots, M_x-1,$$

$$p_{M_x,M_x} = 1 + \mu\varrho\,\widehat{b}_1^{(\gamma-\alpha)}, \tag{2.3.15}$$

where $\varrho = h_x^{\alpha-\gamma}/\Gamma(2-\gamma+\alpha)$. The entries given in (2.3.15) satisfy $p_{M_x,0} < 0$, $p_{M_x,k} < 0$ and $p_{M_x,M_x} > 0$.

We now prove $P^{-1} > 0$, by considering two cases for the different signs of the coefficient function $a(x)$.

First, considering the case $a \geq 0$ and recalling Lemma 2.3.1, one can easily obtain that the off-diagonal entries of the matrix P are non-positive and the diagonal entries are strictly positive i.e. $p_{i,k} \leq 0$ for $k = 0, 1, \ldots, i-1, i+1, \ldots, M_x$ and $p_{i,i} > 0$ where $0 \leq i \leq M_x$.

Now include the case $a < 0$. Denote $\widehat{\nu} = \Gamma(2-\alpha)/\Gamma(2-\gamma+\alpha)$. For $i = 1, 2, \ldots, M_x-1$, one can rewrite (2.3.11) as

$$\begin{aligned} p_{i,0} &= -\frac{\widehat{b}_i^{(\gamma-\alpha)} - \widehat{b}_{i+1}^{(\gamma-\alpha)}}{h_x^{\gamma-\alpha+1}\Gamma(2-\gamma+\alpha)} + \frac{(-a_i)\widehat{b}_i^{(\alpha)}}{h_x^{\alpha}\Gamma(2-\alpha)} \\ &= \frac{(-a_i)\widehat{b}_i^{(\alpha)}}{h_x^{\gamma-\alpha+1}\Gamma(2-\alpha)}\left[h_x^{\gamma-2\alpha+1} - \widehat{\nu}\,\frac{\widehat{b}_i^{(\gamma-\alpha)} - \widehat{b}_{i+1}^{(\gamma-\alpha)}}{(-a_i)\widehat{b}_i^{(\alpha)}}\right] < 0, \end{aligned}$$

because of the condition (2.3.8) on mesh width h.

From (2.3.12) one can write,

$$\begin{aligned} p_{i,k} &= \frac{-\left(\widehat{b}_{i-k+2}^{(\gamma-\alpha)} - 2\widehat{b}_{i-k+1}^{(\gamma-\alpha)} + \widehat{b}_{i-k}^{(\gamma-\alpha)}\right)}{h_x^{\gamma-\alpha+1}\Gamma(2-\gamma+\alpha)} - \frac{-(a_i)\left(\widehat{b}_{i-k+1}^{(\alpha)} - \widehat{b}_{i-k}^{(\alpha)}\right)}{h_x^{\alpha}\Gamma(2-\alpha)} \\ &= \frac{(-a_i)(\widehat{b}_{i-k}^{(\alpha)} - \widehat{b}_{i-k+1}^{(\alpha)})}{h_x^{\gamma-\alpha+1}\Gamma(2-\alpha)}\left[h_x^{\gamma-2\alpha+1} - \widehat{\nu}\,\frac{\widehat{b}_{i-k+2}^{(\gamma-\alpha)} - 2\widehat{b}_{i-k+1}^{(\gamma-\alpha)} + \widehat{b}_{i-k}^{(\gamma-\alpha)}}{(-a_i)(\widehat{b}_{i-k}^{(\alpha)} - \widehat{b}_{i-k+1}^{(\alpha)})}\right]. \end{aligned} \tag{2.3.16}$$

For $k = 1, 2\ldots, i-1$, one has $1 \leq i-k \leq i-1$ with $i = 2, 3, \ldots, M_x-1$. Thus, using (2.3.8) along with Lemma (2.3.1) it is clear to notice in (2.3.16) that $p_{i,k} < 0$ and for $k = i+1$, we have $p_{i,i+1} = -\widehat{b}_1^{(\gamma-\alpha)}/(h_x^{\gamma-\alpha+1}\Gamma(2-\gamma+\alpha)) < 0$, where $1 \leq i \leq M_x-1$.

It remains to discuss the bound for the diagonal entries. The assumption $c_i > 0$ is already mentioned in the statement of the lemma. The sum of first two terms in (2.3.13) can be rewritten as

$$\frac{2\widehat{b}_1^{(\gamma-\alpha)} - \widehat{b}_2^{(\gamma-\alpha)}}{h_x^{\gamma-\alpha+1}\Gamma(2-\gamma+\alpha)} - (-a_i)\frac{\widehat{b}_1^{(\alpha)}}{h_x^{\alpha}\Gamma(2-\alpha)}, \quad \text{for} \quad i = 1, 2, \ldots, M_x-1,$$

which shows that $p_{i,i} > 0$ owing to the mesh-condition (2.3.8) and the relation $2\widehat{b}_1^{(\gamma-\alpha)} - \widehat{b}_2^{(\gamma-\alpha)} > \widehat{b}_1^{(\gamma-\alpha)} - \widehat{b}_2^{(\gamma-\alpha)}$.

Thus, the matrix P has positive diagonal entries and non-positive off-diagonal entries. Also the entries of P satisfy

$$\sum_{k=1}^{M_x} |p_{0,k}| = \frac{1}{h_x} = |p_{0,0}|, \quad \sum_{k=0}^{M_x-1} |p_{M_x,k}| = \widehat{\nu}\varrho\,\widehat{b}_1^{(\gamma-\alpha)} < |p_{M_x,M_x}| \quad \text{and} \quad \sum_{\substack{k=0 \\ k\neq i}}^{M_x} |p_{i,k}| < |p_{i,i}|.$$

Consequently, P is a irreducibly diagonally dominant matrix, and following [79], we have $P^{-1} > 0$. Thus, from (2.3.10), we get $\overrightarrow{Z} \geq 0$ and hence the result follows. □

In the above lemma, we have discussed discrete comparison principle for L_{M_x}. Proceeding similarly like [26, Lemma 3.2], one can prove the discrete comparison principle for the fractional derivative operator $D_{C,L1}^{\gamma-\alpha}$.

2.4 Error analysis

In this section, we will focus on the error estimation by determining the truncation errors and its related bounds as well as the convergence of the computed solution to the exact solution. Let $u(x_i)$ is the exact solution and U_i is the computed solution of the FBVP (2.1.1) at the point $x_i \in \overline{\Omega}_x^{M_x}, i = 0, 1, \ldots, M_x$.

2.4.1 Truncation error

The truncation errors of the discretization (2.3.5) of the FBVP (2.1.1) are given by

$$\begin{aligned} L_{M_x}(u(x_i) - U_i) &= -D^+ D_{C,L1}^{\gamma-\alpha}(u(x_i) - U_i) + a_i D_{C,L1}^{\alpha}(u(x_i) - U_i) + c_i(u(x_i) - U_i) \\ &= -(D^+ D_{C,L1}^{\gamma-\alpha} - D^C D_{0,x}^{\gamma-\alpha})u(x_i) + a_i(D_{C,L1}^{\alpha} - D_C^{\alpha})u(x_i), \text{ for } 0 < x_i < 1, \end{aligned}$$

and for the boundary conditions we have

$$-D^+ \left(u(x_0 = 0) - U_0\right) = \frac{u(0) - u(h)}{h_x},$$

and

$$[u(x_{M_x}) - U_{M_x}] + \mu \left[{}^C D_{0,x}^{\gamma-\alpha} u(x_{M_x}) - D_{C,L1}^{\gamma-\alpha} U_{M_x}\right] = \mu \left[{}^C D_{0,x}^{\gamma-\alpha} u(x_{M_x}) - D_{C,L1}^{\gamma-\alpha} U_{M_x}\right].$$

In order to get the truncation error bound, we need the following lemma.

Lemma 2.4.1. *For all integers $i \geq 2$, there exists a constant C, independent of i, such that*

$$\sum_{k=1}^{i-1} \left[(i-k)^{1-\alpha} - (i-k-1)^{1-\alpha}\right] k^{\gamma-\alpha-1} \leq C i^{\gamma-2\alpha}. \tag{2.4.1}$$

Proof. For $x \in \mathbb{R}$, we apply the mean-value theorem on the function $m(x) = x^{1-\alpha}$ and proceed like [71, Lemma 4.4] to get

$$\begin{aligned}\sum_{k=1}^{[i/2]-1} \left[(i-k)^{1-\alpha} - (i-k-1)^{1-\alpha}\right] k^{\gamma-\alpha-1} &\leq \sum_{k=1}^{[i/2]-1} (1-\alpha)(i-k-1)^{-\alpha} k^{\gamma-\alpha-1} \\ &\leq C i^{-\alpha} \sum_{k=1}^{[i/2]-1} k^{\gamma-\alpha-1}.\end{aligned}$$

Then, using the convergence-concept given in [72, Equation (5.9)] we get

$$\sum_{k=1}^{[i/2]-1} \left[(i-k)^{1-\alpha} - (i-k-1)^{1-\alpha}\right] k^{\gamma-\alpha-1} \leq C i^{-2} i^{\gamma-2\alpha+2} = C i^{\gamma-2\alpha}, \tag{2.4.2}$$

and for the remaining terms we calculate

$$\begin{aligned}\sum_{k=[i/2]}^{i-1} \left[(i-k)^{1-\alpha} - (i-k-1)^{1-\alpha}\right] k^{\gamma-\alpha-1} &\leq \left[\frac{i}{2}\right]^{\gamma-\alpha-1} \sum_{k=[i/2]}^{i-1} \left[(i-k)^{1-\alpha} - (i-k-1)^{1-\alpha}\right] \\ &\leq C i^{\gamma-2\alpha}. \end{aligned} \tag{2.4.3}$$

Thus, combining (2.4.2) and (2.4.3) we get the required result (2.4.1). □

Lemma 2.4.2. *Let the functions $a, c, f \in \mathcal{C}^{k,\eta}(0,1]$ for some positive integer k with $\eta \leq 2\alpha - \gamma$. Then, we have the following bounds for the truncation errors*

$$(i) \quad |D^+(u(x_0) - U_0)| \leq C h_x^{\gamma-\alpha}, \tag{2.4.4}$$

$$(ii) \quad \left| \left[u(x_{M_x}) - U_{M_x}\right] + \mu \left[{}^{C}D_{0,x}^{\gamma-\alpha} u(x_{M_x}) - D_{C,L1}^{\gamma-\alpha} U_{M_x}\right] \right| \leq C\mu h_x^{\min\{1+\gamma-\alpha, 2-\gamma+\alpha\}} \leq C\mu h_x, \tag{2.4.5}$$

$$(iii) \quad \left| L_{M_x}(u(x_i) - U_i) \right| \leq C h_x \, x_i^{-1}, \quad \text{for} \quad i = 1, 2, \ldots, M_x - 1. \tag{2.4.6}$$

Proof. Our assumption clears that the FBVP (2.1.1) has a unique solution.

(i) Now, using (2.2.6) we have

$$|D^+(u(x_0) - U_0)| \leq \frac{1}{h_x} \left[\int_0^{h_x} \left(\int_0^{\zeta} |u''(s)| \, ds\right) d\zeta\right] \leq C h_x^{-1} \int_0^{h_x} \zeta^{\gamma-\alpha} \, d\zeta = C h_x^{\gamma-\alpha}. \tag{2.4.7}$$

Thus, $|D^+(u(x_0) - U_0)| \leq Ch_x^{\gamma-\alpha}$.

(ii) For the right hand boundary condition, one can write the truncation error term as

$$\begin{aligned} {}^{C}D_{0,x}^{\gamma-\alpha}u(x_{M_x}) - D_{C,L1}^{\gamma-\alpha}U_{M_x} &= \frac{1}{\Gamma(1-\gamma+\alpha)}\sum_{k=0}^{M_x-1}\int_{x_k}^{x_{k+1}}(x_{M_x}-\zeta)^{\alpha-\gamma}\left[u'(\zeta) - \frac{U_{k+1}-U_k}{h_x}\right]d\zeta \\ &= \sum_{k=0}^{M_x-1}\widehat{\mathcal{T}}_{M_x,k}, \end{aligned}$$

where

$$\widehat{\mathcal{T}}_{M_x,k} = \frac{1}{\Gamma(1-\gamma+\alpha)}\int_{x_k}^{x_{k+1}}(x_{M_x}-\zeta)^{\alpha-\gamma}\left[u'(\zeta) - \frac{U_{k+1}-U_k}{h_x}\right]d\zeta.$$

According to the derivation given in [72] and using (2.2.6) one gets

$$|\widehat{\mathcal{T}}_{M_x,0}| \leq Ch_x^{1+\gamma-\alpha} \quad \text{and} \quad |\widehat{\mathcal{T}}_{M_x,M_x-1}| \leq Ch_x^{2-\gamma+\alpha}. \tag{2.4.8}$$

Now, for $k = 1, 2, \ldots, M_x - 2$ and through (2.2.6) we emulate the derivation given in [72] to get

$$\begin{aligned} |\widehat{\mathcal{T}}_{M_x,k}| &\leq Ch_x^2\left(\max_{\zeta\in[x_k,x_{k+1}]}|u''(\zeta)|\right)\int_{x_k}^{x_{k+1}}(x_{M_x}-\zeta)^{\alpha-\gamma-1}\,d\zeta \\ &\leq Ch_x k^{\gamma-\alpha-1}\left[M_x-(k+1)\right]^{\alpha-\gamma-1}. \end{aligned} \tag{2.4.9}$$

Inviting the bounds, given in [72] and using (2.2.6) we get

$$\sum_{k=1}^{[M_x/2]-1}|\widehat{\mathcal{T}}_{M_x,k}| \leq Ch_x^2 \quad \text{and} \quad \sum_{k=[M_x/2]}^{M_x-2}|\widehat{\mathcal{T}}_{M_x,k}| \leq Ch_x^{2+\alpha-\gamma}. \tag{2.4.10}$$

Then calling these bounds all together to get

$$\mu\left|\left[{}^{C}D_{0,x}^{\gamma-\alpha}u(x_{M_x}) - D_{C,L1}^{\gamma-\alpha}U_{M_x}\right]\right| \leq C\mu h_x^{\min\{1+\gamma-\alpha,2-\gamma+\alpha\}} \leq C\mu h_x. \tag{2.4.11}$$

(iii) It remains to find the bound for $x_i \in \Omega_x^{M_x}$. Following the idea given in [26, Lemma 4.1], we disintegrate the truncation error term for the mesh points $x_1, x_2, \ldots, x_{M_x-1}$, into three parts as follows:

$$\begin{aligned} L_{M_x}(u(x_i) - U_i) &= -\left(D^+D_{C,L1}^{\gamma-\alpha} - D({}^{C}D_{0,x}^{\gamma-\alpha})\right)u(x_i) + a_i(D_{C,L1}^{\alpha} - D_C^{\alpha})u(x_i) \\ &= \left(D - D^+\right){}^{C}D_{0,x}^{\gamma-\alpha}u(x_i) + D^+\left({}^{C}D_{0,x}^{\gamma-\alpha} - D_{C,L1}^{\gamma-\alpha}\right)u(x_i) \\ &\quad + a_i\left(D_{C,L1}^{\alpha} - D_C^{\alpha}\right)u(x_i). \end{aligned} \tag{2.4.12}$$

For the first two parts in (2.4.12), one can obtain with the similar derivation same like [26, Lemma 4.1] along with the condition (2.2.6)

$$\left|\left(\frac{d}{dx}-D^{+}\right){}^{C}D_{0,x}^{\gamma-\alpha}u(x_i)\right| \le Ch_x\, x_i^{\gamma-\alpha-1}, \tag{2.4.13}$$

and

$$\left|D^{+}\left({}^{C}D_{0,x}^{\gamma-\alpha}-D_{C,L1}^{\gamma-\alpha}\right)u(x_i)\right| \le Ch_x\, x_i^{-1}. \tag{2.4.14}$$

For the third part in (2.4.12), we follow the derivation of [71, Lemma 4.5].

$$\begin{aligned}\left(D_C^{\alpha}-D_{C,L1}^{\alpha}\right)u(x_i) &= \frac{1}{\Gamma(1-\alpha)}\int_0^{x_i}(x_i-s)^{-\alpha}u'(s)\,ds \\ &\quad -\frac{1}{\Gamma(1-\alpha)}\sum_{k=0}^{i-1}\int_{x_k}^{x_{k+1}}\frac{U_{k+1}-U_k}{h_x}(x_i-s)^{-\alpha}\,ds = \mathcal{T}_{i,0}+\sum_{k=1}^{i-1}\mathcal{T}_{i,k}.\end{aligned} \tag{2.4.15}$$

For $i=2,3,\ldots,M_x-1$, using the mean-value theorem we get

$$\begin{aligned}\mathcal{T}_{i,k} &= \frac{1}{\Gamma(1-\alpha)}\int_{x_k}^{x_{k+1}}(x_i-\zeta)^{-\alpha}u'(\zeta)\,d\zeta-\frac{U_{k+1}-U_k}{h_x^{\alpha}\Gamma(2-\alpha)}\,\widehat{b}_{i-k}^{(\gamma-\alpha)} \\ &= \frac{h_x^{1-\alpha}}{\Gamma(2-\alpha)}\left[u'(\widehat{x})-\frac{U_{k+1}-U_k}{h_x}\right]\widehat{b}_{i-k}^{(\gamma-\alpha)}, \quad \text{for some} \quad \widehat{x}\in(x_k,x_{k+1}).\end{aligned}$$

Thus,

$$\left|u'(\widehat{x})-\frac{U_{k+1}-U_k}{h_x}\right| \le Ch_x\, x_k^{\gamma-\alpha-1}. \tag{2.4.16}$$

Hence, we have

$$|\,\mathcal{T}_{i,k}\,| \le \frac{Ch_x^{1+\gamma-2\alpha}}{\Gamma(2-\alpha)}k^{\gamma-\alpha-1}\widehat{b}_{i-k}^{(\gamma-\alpha)}. \tag{2.4.17}$$

Then, we obtain

$$\left|\sum_{k=1}^{i-1}\mathcal{T}_{i,k}\right| \le \frac{Ch_x^{1+\gamma-2\alpha}}{\Gamma(2-\alpha)}\sum_{k=1}^{i-1}\widehat{b}_{i-k}^{(\gamma-\alpha)}k^{\gamma-\alpha-1}.$$

Using Lemma 2.4.1, we get

$$\left|\sum_{k=1}^{i-1}\mathcal{T}_{i,k}\right| \le \frac{Ch_x^{1+\gamma-2\alpha}}{\Gamma(2-\alpha)}i^{\gamma-2\alpha} \le Ch_x\, x_i^{-(2\alpha-\gamma)}. \tag{2.4.18}$$

Thus, we have

$$\left|\left(D_C^{\alpha}-D_{C,L1}^{\alpha}\right)u(x_i)\right| \le Ch_x\, x_i^{-(2\alpha-\gamma)}, \quad i=2,3,\ldots,M_x-1. \tag{2.4.19}$$

For $k = 0$,

$$\mathcal{T}_{i,0} = \frac{1}{\Gamma(1-\alpha)} \int_{x_0}^{x_1} (x_i - \zeta)^{-\alpha} u'(\zeta)\, d\zeta - \frac{U_1 - U_0}{h_x^{\alpha}\Gamma(2-\alpha)}\, \widehat{b}_i^{(\gamma-\alpha)}.$$

Following accordingly to the derivation of [71, Lemma 4.5], one gets

$$\left| \frac{1}{\Gamma(1-\alpha)} \int_{x_0}^{x_1} (x_i - s)^{-\alpha} u'(\zeta)\, d\zeta \right| \leq C h_x\, x_{i-1}^{-\alpha}, \tag{2.4.20}$$

and thereafter the mean-value theorem gives

$$\left| \frac{U_1 - U_0}{h_x^{\alpha}\Gamma(2-\alpha)}\, \widehat{b}_i^{(\gamma-\alpha)} \right| \leq C h_x\, x_{i-1}^{-\alpha}. \tag{2.4.21}$$

Combining (2.4.20), (2.4.21) and using $x_i \leq 2x_{i-1}$ to obtain

$$|\, \mathcal{T}_{i,0}\, | \leq C x_{i-1}^{-\alpha} h_x^{\gamma-\alpha} \leq C h_x\, x_i^{-\alpha}, \quad i = 2, 3, \ldots, M_x - 1. \tag{2.4.22}$$

Finally the bound for $i = 1$ will complete the bound of $\mathcal{T}_{i,k}$.

Now, for $i = 1$,

$$|\, \mathcal{T}_{1,0}\, | \leq \left| \frac{1}{\Gamma(1-\alpha)} \int_{x_0}^{x_1} (x_1 - \zeta)^{-\alpha} u'(\zeta)\, d\zeta \right| + \left| \frac{U_1 - U_0}{h_x^{\alpha}\Gamma(2-\alpha)}\, \widehat{b}_1^{(\gamma-\alpha)} \right|.$$

Simulating the derivation of [71, Lemma 4.5], we get

$$\begin{aligned} \left| \frac{1}{\Gamma(1-\alpha)} \int_{x_0}^{x_1} (x_1 - s)^{-\alpha} u'(\zeta)\, d\zeta \right| &\leq \frac{C}{\Gamma(1-\alpha)} \int_{x_0}^{x_1} (x_1 - \zeta)^{-\alpha} \zeta^{\gamma-\alpha}\, d\zeta \\ &\leq C h_x\, {x_1}^{-(2\alpha-\gamma)}, \end{aligned} \tag{2.4.23}$$

and

$$\left| \frac{\widehat{b}_1^{(\gamma-\alpha)}}{h_x^{\alpha}\Gamma(2-\alpha)}\, (U_1 - U_0) \right| \leq \frac{C\, \widehat{b}_1^{(\gamma-\alpha)} h_x^{\gamma-\alpha}}{h_x^{\alpha}\Gamma(2-\alpha)} h \leq C h_x\, {x_1}^{-(2\alpha-\gamma)}. \tag{2.4.24}$$

Thus, (2.4.23) and (2.4.24) together yield

$$|\, \mathcal{T}_{1,0}\, | \leq C h {x_1}^{-(2\alpha-\gamma)}. \tag{2.4.25}$$

Putting all these inequalities (2.4.19)-(2.4.25) together, we obtain

$$\left| \left(D_C^{\alpha} - D_{C,L1}^{\alpha} \right) u(x_i) \right| \leq C h_x\, x_i^{-\alpha} \leq C h_x\, x_i^{-1}, \quad i = 1, 2, \ldots, M_x - 1. \tag{2.4.26}$$

We get the required bound (2.4.6) by gathering all the bounds (2.4.13)-(2.4.26). □

The following theorem provides the estimation of the error in discrete maximum norm.

Theorem 2.4.3. *Let the solution $u(x)$ of the problem (2.1.1) satisfies the discrete comparison principle (Lemma 2.3.2) as well as the truncation error bounds (2.4.4-2.4.6). Also assume the coefficients $a(x), c(x)$ are chosen such that $a(x) \leq 0$ and $c(x) \geq 0$ for $x \in \overline{\Omega}_x$. Then there exists a constant C such that*

$$\max_{0\leq i\leq M_x} |e_i| = \max_{0\leq i\leq M_x} |u(x_i) - U_i| \leq Ch_x |\ln h_x|^{\alpha}.$$

Before proceeding towards the proof of above theorem, we enter into the discussion of discrete barrier function that will be used later in the proof of above theorem. We first consider a non-negative mesh function $\{\Theta_i\}_{i=0}^{M_x}$, which satisfies

$$|L_{M_x}(u(x_i) - U_i)| \leq L_{M_x}\Theta_i, \quad \text{for } i = 1, 2, \ldots, M_x - 1, \tag{2.4.27}$$

$$| - D^{+}(u(x_0) - U_0)| \leq -D^{+}\Theta_0, \tag{2.4.28}$$

$$|(u(x_{M_x}) - U_{M_x}) + \mu \left({}^{C}D_{0,x}^{\gamma-\alpha} u(x_{M_x}) - D_{C,L1}^{\gamma-\alpha} U_{M_x}\right)| \leq \Theta_{M_x} + \mu D_{C,L1}^{\gamma-\alpha}\Theta_{M_x}. \tag{2.4.29}$$

Then, using the discrete comparison principle over $\Theta_i \pm (u(x_i) - U_i)$, we have

$$|u(x_i) - U_i| \leq \Theta_i, \quad \text{for all} \quad i \geq 0.$$

This mesh function $\{\Theta_i\}_{i=0}^{M_x}$ is called the discrete barrier function.

Now we call a lemma from [26, Lemma 4.2] which will be useful for the study of barrier function and error estimate. The following lemma is given in the suitable form for our problem.

Lemma 2.4.4. *For a mesh function $\{G_i\}_{i=0}^{M_x}$ along with the condition $G_0 = 0$ and $G_i \leq G_{i+1}$, one has,*

$$D_{C,L1}^{\gamma-\alpha} G_i \geq \frac{G_i}{{x_i}^{\gamma-\alpha}\Gamma(1-\gamma+\alpha)}, \quad \textit{for} \quad 1 \leq i \leq M_x - 1.$$

Proof. The proof follows similarly from [26, Lemma 4.2]. □

We next define a non-negative mesh function [26, Equation (4.11)] $\{B_i\}_{i=0}^{M_x}$ for a smooth construction of the suitable discrete barrier function for our problem, by

$$D_{C,L1}^{\gamma-\alpha} B_i = \frac{e^{|\ln h_x|^{1-\alpha}}}{\Gamma(1-\gamma+\alpha)} {x_i}^{|\ln h_x|^{-\alpha}}, \quad i = 1, 2, \ldots, M_x \quad \text{and} \quad M_0 = 0. \tag{2.4.30}$$

Following the derivation given in [26, Section 4.2] one has

1. $B_1 = (1-\gamma+\alpha)h_x^{\gamma-\alpha}$,
2. B_i is a non-decreasing function for $i \geq 0$,
3. $0 \leq M_i \leq H_i$, $i = 0, 1, \ldots, M_x$, where the mesh function H_i plays the role of discrete barrier function for B_i, defined by

$$H_i = {x_i}^{\gamma-\alpha+|\ln h_x|^{-\alpha}} e^{|\ln h_x|^{1-\alpha}}.$$

Therefore, we have made the path ready to begin the proof of Theorem 2.4.3.

Proof. We start the proof with the consideration of two cases:

$$\mu = 0 \quad \text{and} \quad \mu > 0\,.$$

Case 1 ($\mu = 0$). Define a new mesh function Θ_i with the help of the mesh function B_i as

$$\Theta_i = C_1\, h_x |\ln h_x|^{\alpha} \left(e^{|\ln h_x|^{1-\alpha}} - B_i\right), \quad \text{for} \quad i = 0, 1, \ldots, M_x. \tag{2.4.31}$$

Clearly one can obtain $0 \leq \Theta_i \leq C\, h_x |\ln h_x||^{\alpha}$. Our aim is to show that Θ_i is a discrete barrier function of the error function e_i.

From the upper bound of B_i, it can be said that the mesh function Θ_i attains the non-negative values for all $i = 0, 1, \ldots, M_x$.

Now, at the left end point $x = 0$ we have

$$-D^+\Theta_0 = C_1(1-\gamma+\alpha)h_x^{\gamma-\alpha}|\ln h_x|^{\alpha}.$$

As the mesh function B_i is non-decreasing and the function $c(x) \geq 0$, so using the non-positivity condition over the function $a(x)$ we have

$$a_i\, D^{\alpha}_{C,L1}\Theta_i + c_i\Theta_i = -a_i\, C_1\, h_x |\ln h_x|^{\alpha} D^{\alpha}_{C,L1}B_i + c_i\Theta_i \geq 0\,.$$

Then, for any point x_i, $i = 1, 2, \ldots, M_x - 1$ we have

$$\begin{aligned} L_N\Theta_i &:= -D^+(D^{\gamma-\alpha}_{C,L1}\Theta_i) + a_i D^{\alpha}_{C,L1}\Theta_i + c_i\Theta_i \\ &\geq C_1\, h_x |\ln h_x||^{\alpha} D^+(D^{\gamma-\alpha}_{C,L1}B_i) \\ &\geq \frac{C_1\, h_x}{2\Gamma(1-\gamma+\alpha)}\, x_i^{-1}. \end{aligned} \tag{2.4.32}$$

Also $u(x_{M_x}) - U_{M_x} = 0 \leq \Theta_{M_x}$.

Thus, combination of the above inequalities along with the discrete comparison principle imply that the mesh function Θ_i is a discrete barrier function for the error $|u(x_i) - U_i|$, and hence the result follows for the case $\mu = 0$.

Case 2 ($\mu > 0$)**.** At the point $x = x_{_{M_x}}$, we have

$$\begin{aligned}\Theta_{M_x} + \mu\, D^{\gamma-\alpha}_{C,L1}\Theta_{M_x} &= \Theta_{M_x} - C_1\,\mu\, h_x|\ln h_x|^{\alpha}\frac{e^{|\ln h_x|^{1-\alpha}}}{\Gamma(1-\gamma+\alpha)}\\ &\geq \frac{-C_1\,\mu\, h_x|\ln h_x|^{\alpha}e^{|\ln h_x|^{1-\alpha}}}{\Gamma(1-\gamma+\alpha)}. \end{aligned} \tag{2.4.33}$$

Thus, we can see that Θ_i is not the perfect choice for the case $\mu > 0$ and hence some changes are required in the structure of the discrete barrier function.

We define the modified mesh function as $\widetilde{\Theta}_i = \Theta_i + \Upsilon_i$, where the discrete function Υ_i is defined as

$$\Upsilon_i = \begin{cases} C_2 h_x|\ln h_x|^{\alpha}\left(\dfrac{h_x^{\gamma-\alpha}}{\mu} + \dfrac{2}{\Gamma(2-\gamma+\alpha)}\right)e^{|\ln h_x|^{1-\alpha}}, & \text{for } i = 0, 1, \ldots, M_x - 1,\\ C_2 h_x|\ln h_x|^{\alpha}\dfrac{2e^{|\ln h_x|^{1-\alpha}}}{\Gamma(2-\gamma+\alpha)}, & \text{for} \quad i = M_x. \end{cases} \tag{2.4.34}$$

At the point $x = x_0$,

$$-D^{+}\widetilde{\Theta}_0 = -D^{+}\Theta_0 - D^{+}\Upsilon_0 \geq C_1C_3\Gamma(2-\gamma+\alpha)h_x^{\gamma-\alpha}|\ln h_x|^{\alpha}.$$

It is easy to calculate the following

$$D^{\gamma-\alpha}_{C,L1}\Upsilon_i = 0, \quad \text{for} \quad i = 1, 2, \ldots, M_x - 1, \tag{2.4.35}$$

$$D^{+}(D^{\gamma-\alpha}_{C,L1}\Upsilon_i) = 0, \quad \text{for} \quad i = 1, 2, \ldots, M_x - 2, \tag{2.4.36}$$

$$D^{\alpha}_{C,L1}\Upsilon_i = 0, \quad \text{for} \quad i = 1, 2, \ldots, M_x - 1. \tag{2.4.37}$$

But at the point $x = x_{_{M_x}}$,

$$\begin{aligned} D^{\gamma-\alpha}_{C,L1}\Upsilon_{M_x} &= \frac{1}{h_x^{\gamma-\alpha}\Gamma(2-\gamma+\alpha)}\sum_{k=0}^{M_x-1}(\Upsilon_{k+1} - \Upsilon_k)b_{M_x-k}\\ &= \frac{\Upsilon_{M_x} - \Upsilon_{M_x-1}}{h_x^{\gamma-\alpha}\Gamma(2-\gamma+\alpha)}b_1\\ &= -\frac{C_2h_x|\ln h_x|^{\alpha}h_x^{\gamma-\alpha}}{\mu h_x^{\gamma-\alpha}\Gamma(2-\gamma+\alpha)}e^{|\ln h_x|^{1-\alpha}}\\ &= -\frac{C_2h_x|\ln h_x|^{\alpha}\,e^{|\ln h_x|^{1-\alpha}}}{\mu\Gamma(2-\gamma+\alpha)} \quad \leq 0. \end{aligned}$$

Similarly one can have

$$D^{\alpha}_{C,L1}\Upsilon_{M_x} = -\frac{C_2 h_x^{1+\gamma-2\alpha}|\ln h_x|^{\alpha}}{\mu\Gamma(2-\alpha)} e^{|\ln h_x|^{1-\alpha}} \leq 0.$$

Therefore,

$$-D^{+}(D^{\gamma-\alpha}_{C,L1}\Upsilon_{M_x-1}) \geq 0.$$

We next calculate $L_{M_x}\widetilde{\Theta}_i$, for $1 \leq i \leq M_x - 1$.

For $1 \leq i \leq M_x - 2$,

$$L_{M_x}\widetilde{\Theta}_i = L_{M_x}\Theta_i + L_{M_x}\Upsilon_i = L_{M_x}\Theta_i + c_i\Upsilon_i \geq \frac{C_1\, h_x}{2\Gamma(1-\gamma+\alpha)}\, x_i^{-1}.$$

At the point $x = x_{M_x-1}$,

$$L_{M_x}\widetilde{\Theta}_{M_x-1} = L_{M_x}\Theta_{M_x-1} + L_{M_x}\Upsilon_{M_x-1} \geq L_{M_x}\Theta_{M_x-1} + c_{M_x-1}\Theta_{M_x-1}.$$

Inserting the condition $c(x) \geq 0$, we get

$$L_{M_x}\widetilde{\Theta}_{M_x-1} \geq L_{M_x}\Theta_{M_x-1} \geq \frac{C_1\, h_x}{2\Gamma(1-\gamma+\alpha)}\, x^{-1}_{M_x-1}. \tag{2.4.38}$$

Now,

$$\begin{aligned}\Upsilon_{M_x} + \mu\, D^{\gamma-\alpha}_{C,L1}\Upsilon_{M_x} &= C_2 h_x|\ln h_x|^{\alpha}\frac{2e^{|\ln h_x|^{1-\alpha}}}{\Gamma(2-\gamma+\alpha)} - \frac{\mu\, C_2 h_x|\ln h_x|^{\alpha}e^{|\ln h_x|^{1-\alpha}}}{\mu\,\Gamma(2-\gamma+\alpha)} \\ &= C_2 h_x|\ln h_x|^{\alpha}\frac{e^{|\ln h_x|^{1-\alpha}}}{\Gamma(2-\gamma+\alpha)}.\end{aligned} \tag{2.4.39}$$

Finally at $x = x_{M_x}$,

$$\begin{aligned}\widetilde{\Theta}_{M_x} + \mu\, D^{\gamma-\alpha}_{C,L1}\widetilde{\Theta}_{M_x} &= \left(\Theta_{M_x} + \mu\, D^{\gamma-\alpha}_{C,L1}\Theta_{M_x}\right) + \left(\Upsilon_{M_x} + \mu\, D^{\gamma-\alpha}_{C,L1}\Upsilon_{M_x}\right) \\ &\geq h_x|\ln h_x|^{\alpha}\left[\frac{C_2}{\Gamma(2-\gamma+\alpha)} - \frac{C_1\mu}{\Gamma(1-\gamma+\alpha)}\right]e^{|\ln h_x|^{1-\alpha}} \\ &\geq Ch_x|\ln h_x|^{\alpha}, \quad \text{as} \quad e^{|\ln h_x|^{1-\alpha}} \geq 1,\end{aligned} \tag{2.4.40}$$

where C_2 is chosen such a way that $\dfrac{C_2}{\Gamma(2-\gamma+\alpha)} - \dfrac{C_1\mu}{\Gamma(1-\gamma+\alpha)} > C$.

Thus, $\widetilde{\Theta}_i$ is the discrete barrier function of $|u(x_i) - U_i|$ in case of positive value of μ and hence the result follows. □

2.5 Application on semilinear fractional differential equation

In this section, we show the application of the proposed scheme over a semilinear FBVP with the mixed-fractional derivative. Consider the following semilinear FBVP:

$$\begin{cases} -D({}^{C}D_{0,x}^{\gamma-\alpha}u(x)) + a(x){}^{C}D_{0,x}^{\alpha}u(x) + f(x,u(x)) = 0, \quad x \in (0,1), \\ {}^{C}D_{0,x}^{\gamma-\alpha}u(0) = 0, \quad u(1) + \mu\, {}^{C}D_{0,x}^{\gamma-\alpha}u(1) = \rho, \end{cases} \tag{2.5.1}$$

where $f(x,u(x))$ is a nonlinear source function of $u(x)$. Under sufficient smoothness imposed on the functions $a(x)$ and $f(x,u(x))$, the FBVP (2.5.1), in general, admits a unique solution $u(x)$.

To solve equation (2.5.1) numerically, the Newton method of quasilinearization is applied to obtain a sequence $\left\{u^{(m)}\right\}_0^{\infty}$ of approximations with a proper choice of initial guess $u^{(0)}(x)$.

We define $u^{(m+1)}$ for each fixed non-negative integer m, to be the solution of the following linear FBVP:

$$\begin{cases} -D\left({}^{C}D_{0,x}^{\gamma-\alpha}u^{(m+1)}(x)\right) + a(x){}^{C}D_{0,x}^{\alpha}u^{(m+1)}(x) + c^{(m)}(x)u^{(m+1)}(x) = g^{(m)}(x), \ x \in (0,1), \\ {}^{C}D_{0,x}^{\gamma-\alpha}u^{(m+1)}(0) = 0, \quad u^{(m+1)}(1) + \mu\, {}^{C}D_{0,x}^{\gamma-\alpha}u^{(m+1)}(1) = \rho, \end{cases} \tag{2.5.2}$$

where $c^{(m)}(x)$ and $g^{(m)}(x)$ are given by

$$\begin{cases} c^{(m)}(x) = \dfrac{\partial f}{\partial u}(x,u^{(m)}), \\ g^{(m)}(x) = c^{m}(x)u^{m} - f(x,u^{(m)}). \end{cases} \tag{2.5.3}$$

Hence, for fixed m, we solve (2.5.2) by using the proposed numerical scheme (2.3.5) and then for the above Newton quasilinearization process we use the following convergence criterion for the solution

$$|u^{(m+1)}(x_i) - u^{(m)}(x_i)| \leq \text{tol}, \quad x_i \in \overline{\Omega}_x^{M_x}, \quad m \geq 0. \tag{2.5.4}$$

For computation, we have chosen $\text{tol} = 10^{-8}$.

2.6 Numerical experiments

In this section, numerical examples are presented to affirm the theoretical results. The main motive is to check the error estimates and convergence rates for different values of γ and α.

Example 2.6.1. *Consider the constant-coefficient problem:*

$$\begin{cases} -D({}^{C}D_{0,x}^{\gamma-\alpha}u(x)) - {}^{C}D_{0,x}^{\alpha}u(x) = 1, \quad 0 < \gamma - \alpha < \alpha < 1 < \gamma < 2, \quad x \in (0,1), \\ {}^{C}D_{0,x}^{\gamma-\alpha}u(0) = 0, \quad u(1) = 1. \end{cases} \tag{2.6.1}$$

Exact solution can be found by using the equation (2.2.4).

The maximum error and the corresponding order of convergence are given by,

$$E_{M_x} = \max_{0\le i\le M_x} |U_i - u(x_i)| \quad \text{and} \quad CO_{M_x} = \log_2\left(\frac{E_{M_x}}{E_{2M_x}}\right),$$

respectively.

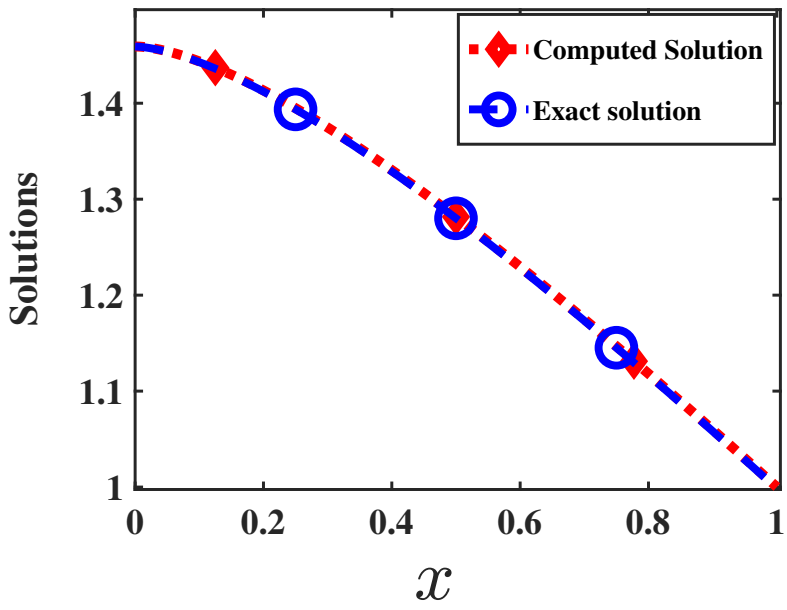

Figure 2.1: Exact vs Computed solution for $\alpha = 0.8$, $\gamma = 1.4$, $M_x = 256$ of Example 2.6.1.

For $\alpha = 0.8$ and $\gamma = 1.4$, Figure 2.1 shows the graph of exact and computed solution with $M_x = 256$ and log-log plots are displayed in Figure 2.2.

The maximum pointwise error and the corresponding first-order convergence of the numerical results for Example 2.6.1 are given in Tables 2.1 and 2.2 for some of those γ and α satisfying the condition given in (2.1.1).

Example 2.6.2. *Consider the following FBVP with variable-coefficient:*

$$\begin{cases} -D\left({}^{C}D_{0,x}^{\gamma-\alpha}u(x)\right) - (1+x^2)\ {}^{C}D_{0,x}^{\alpha}u(x) + e^{-x}u(x) = x, \quad x \in (0,1), \\ {}^{C}D_{0,x}^{\gamma-\alpha}u(0) = 0,\ \ u(1) + {}^{C}D_{0,x}^{\gamma-\alpha}u(1) = 1, \end{cases} \tag{2.6.2}$$

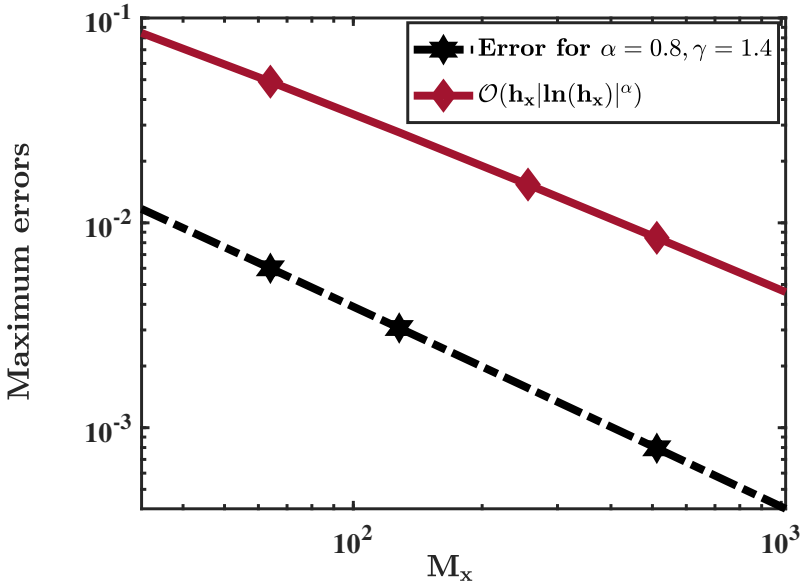

Figure 2.2: Log-log plot for Example 2.6.1 with $\alpha = 0.8$.

Table 2.1: Maximum errors and orders of convergence for $\alpha = 0.8$ of the Example 2.6.1.

$\alpha = 0.8$	$M_x = 32$	$M_x = 64$	$M_x = 128$	$M_x = 256$	$M_x = 512$	$M_x = 1024$
$\gamma = 1.1$	1.1091e-02	5.6327e-03	2.8565e-03	1.4462e-03	7.3100e-04	3.6895e-04
CO_{M_x}	0.97753	0.97956	0.98199	0.98434	0.98645	
$\gamma = 1.2$	1.1175e-02	5.6909e-03	2.8917e-03	1.4661e-03	7.4185e-04	3.7474e-04
CO_{M_x}	0.97353	0.97674	0.97993	0.98278	0.98523	
$\gamma = 1.3$	1.1415e-02	5.8319e-03	2.9706e-03	1.5089e-03	7.6463e-04	3.8669e-04
CO_{M_x}	0.96887	0.97322	0.97722	0.98068	0.98360	
$\gamma = 1.4$	1.1692e-02	5.9989e-03	3.0662e-03	1.5618e-03	7.9319e-04	4.0185e-04
CO_{M_x}	0.96273	0.96826	0.97322	0.97747	0.98103	
$\gamma = 1.5$	1.1891e-02	6.1349e-03	3.1507e-03	1.6114e-03	8.2124e-04	4.1728e-04
CO_{M_x}	0.95469	0.96136	0.96733	0.97246	0.97680	

Table 2.2: Maximum errors and orders of convergence for $\alpha = 0.975$ of the Example 2.6.1.

$\alpha = 0.975$	$M_x = 32$	$M_x = 64$	$M_x = 128$	$M_x = 256$	$M_x = 512$	$M_x = 1024$
$\gamma = 1.1$	1.2335e-02	5.8619e-03	2.7789e-03	1.3143e-03	6.2025e-04	2.9208e-04
CO_{M_x}	1.0734	1.0768	1.0802	1.0834	1.0865	
$\gamma = 1.2$	9.4132e-03	4.2381e-03	2.1333e-03	1.0739e-03	5.4054e-04	2.7207e-04
CO_{M_x}	1.1513	0.99037	0.99026	0.99032	0.99044	
$\gamma = 1.3$	8.5804e-03	4.3212e-03	2.1766e-03	1.0962e-03	5.5199e-04	2.7790e-04
CO_{M_x}	0.98961	0.98936	0.98954	0.98981	0.99008	
$\gamma = 1.4$	8.7758e-03	4.4272e-03	2.2330e-03	1.1257e-03	5.6721e-04	2.8569e-04
CO_{M_x}	0.98712	0.98745	0.98814	0.98884	0.98944	
$\gamma = 1.5$	8.9765e-03	4.5423e-03	2.2967e-03	1.1601e-03	5.8539e-04	2.9516e-04
CO_{M_x}	0.98274	0.98388	0.98534	0.98672	0.98788	
$\gamma = 1.6$	9.1263e-03	4.6396e-03	2.3554e-03	1.1938e-03	6.0413e-04	3.0531e-04
CO_{M_x}	0.97602	0.97803	0.98041	0.98265	0.98458	
$\gamma = 1.7$	9.1236e-03	4.6665e-03	2.3826e-03	1.2139e-03	6.1717e-04	3.1318e-04
CO_{M_x}	0.96726	0.96979	0.97289	0.97594	0.97868	
$\gamma = 1.8$	8.7845e-03	4.5198e-03	2.3223e-03	1.1907e-03	6.0909e-04	3.1091e-04
CO_{M_x}	0.95869	0.96073	0.96378	0.96703	0.97014	
$\gamma = 1.9$	7.7728e-03	3.9938e-03	2.0532e-03	1.0548e-03	5.4122e-04	2.7732e-04
CO_{M_x}	0.96067	0.95989	0.96091	0.96267	0.96468	

where $0 < \gamma - \alpha < \alpha < 1 < \gamma < 2$. The double-mesh principle [26] is used to derive the differences and the order of convergences as exact solution is obscured to us. From the scheme (2.3.5), we obtain two solutions $\{U_i\}_{i=0}^{M_x}$ and $\{\widetilde{U}_i\}_{i=0}^{2M_x}$ using the uniform meshes $\{x_i\}_{i=0}^{M_x}$ and $\{\tilde{x}_i\}_{i=0}^{2M_x}$, where $x_i = \tilde{x}_{2i}$ for $i = 0, 1, \ldots, M_x$.

The differences using double-mesh principle and the corresponding orders of convergence are calculated by

$$\tilde{D}_{M_x} = \max_{0 \le i \le M_x} |U_i - \widetilde{U}_{2i}| \quad \text{and} \quad \widehat{CO}_{M_x} = \log_2 \left(\frac{\tilde{D}_{M_x}}{\tilde{D}_{2M_x}} \right),$$

respectively.

Figure 2.3 depicts the numerical solutions for $\alpha = 0.8$, $\gamma = 1.4$ and $\alpha = 0.975$, $\gamma = 1.8$ with $M_x = 512$. Log-log plots are displayed for the same γ, α in Figures 2.4 and 2.5.

Tables 2.3-2.5 cover the maximum differences and orders of convergence, obtained from double-mesh principle, corresponding to $\alpha = 0.6, 0.8$ and 0.975, respectively. First-order convergence appears from the results given in the tables.

Table 2.3: Double-mesh differences and order of convergences for $\alpha = 0.6$ of the Example 2.6.2.

$\alpha = 0.6$	$M_x = 32$	$M_x = 64$	$M_x = 128$	$M_x = 256$	$M_x = 512$	$M_x = 1024$
$\gamma = 1.1$	2.7964e-03	1.3912e-03	6.8827e-04	3.4023e-04	1.6836e-04	8.3439e-05
$\widehat{CO}_{M_x}$	1.0073	1.0153	1.0164	1.0150	1.0127	

Example 2.6.3. *Consider the following semilinear FBVP:*

$$\begin{cases} -D\left({}^{C}D_{0,x}^{\gamma-\alpha}u(x)\right) - (1+x/2)\,{}^{C}D_{0,x}^{\alpha}u(x) + f(x,u(x)) = 0, \quad x \in (0,1), \\ {}^{C}D_{0,x}^{\gamma-\alpha}u(0) = 0, \;\; u(1) + 0.5\,{}^{C}D_{0,x}^{\gamma-\alpha}u(1) = \rho, \end{cases} \tag{2.6.3}$$

where $\rho = 3 + 1/2\,(\Gamma(2+\gamma-\alpha) + 1/\Gamma(2-\gamma+\alpha))$ and the nonlinear function $f(x,u(x))$ is given by

$$f(x,u(x)) = 2u(x) + u^2(x) + \widehat{s}(x).$$

The function $\widehat{s}(x)$ is chosen in such a way that the exact solution of the FBVP (2.6.3) is $u(x) = x^{\gamma-\alpha+1}$ which belongs to the space $\mathcal{C}^1(\overline{\Omega}_x)$.

Now using the Newton's linearization process given in (2.5.2), we obtain the following

Table 2.4: Maximum differences and order of convergences obtained by double-mesh principle for $\alpha = 0.8$ of the Example 2.6.2.

$\alpha = 0.8$	$M_x = 32$	$M_x = 64$	$M_x = 128$	$M_x = 256$	$M_x = 512$	$M_x = 1024$
$\gamma = 1.1$	4.5118e-03	2.2327e-03	1.1024e-03	5.4419e-04	2.6879e-04	1.3290e-04
$\widehat{CO}_{M_x}$	1.0149	1.0181	1.0185	1.0176	1.0162	
$\gamma = 1.2$	4.2450e-03	2.1064e-03	1.0414e-03	5.1435e-04	2.5410e-04	1.2563e-04
$\widehat{CO}_{M_x}$	1.0110	1.0163	1.0177	1.0174	1.0162	
$\gamma = 1.3$	3.9333e-03	1.9601e-03	9.7124e-04	4.8031e-04	2.3745e-04	1.1744e-04
$\widehat{CO}_{M_x}$	1.0049	1.0130	1.0159	1.0163	1.0157	
$\gamma = 1.4$	3.5660e-03	1.7871e-03	8.8853e-04	4.4037e-04	2.1803e-04	1.0795e-04
$\widehat{CO}_{M_x}$	0.9967	1.0081	1.0127	1.0142	1.0142	
$\gamma = 1.5$	3.1397e-03	1.5829e-03	7.9021e-04	3.9279e-04	1.9492e-04	9.6691e-05
$\widehat{CO}_{M_x}$	0.9880	1.0023	1.0085	1.0109	1.0114	

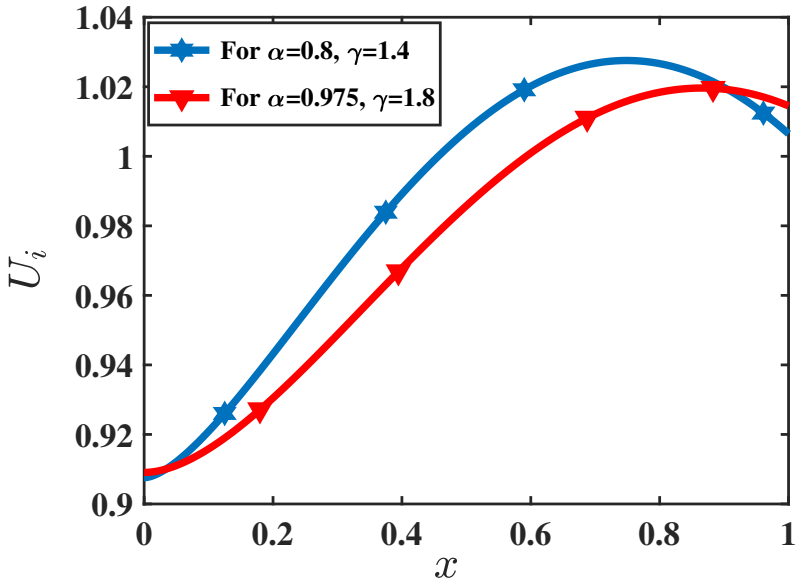

Figure 2.3: Numerical solutions of Example 2.6.2 for $M_x = 512$.

Table 2.5: Maximum differences and orders of convergence obtained by double-mesh principle for $\alpha = 0.975$ of the Example 2.6.2.

$\alpha = 0.975$	$M_x = 32$	$M_x = 64$	$M_x = 128$	$M_x = 256$	$M_x = 512$	$M_x = 1024$
$\gamma = 1.1$	5.6976e-03	2.8506e-03	1.4235e-03	7.1025e-04	3.5423e-04	1.7663e-04
$\widehat{CO}_{M_x}$	0.99908	1.0018	1.0031	1.0037	1.0039	
$\gamma = 1.2$	5.4770e-03	2.7425e-03	1.3701e-03	6.8373e-04	3.4103e-04	1.7006e-04
$\widehat{CO}_{M_x}$	0.99788	1.0012	1.0028	1.0035	1.0038	
$\gamma = 1.3$	5.2450e-03	2.6303e-03	1.3151e-03	6.5658e-04	3.2758e-04	1.6338e-04
$\widehat{CO}_{M_x}$	0.99571	1.0001	1.0021	1.0031	1.0036	
$\gamma = 1.4$	4.9907e-03	2.5091e-03	1.2563e-03	6.2781e-04	3.1340e-04	1.5636e-04
$\widehat{CO}_{M_x}$	0.99207	0.99794	1.0008	1.0023	1.0031	
$\gamma = 1.5$	4.6985e-03	2.3715e-03	1.1904e-03	5.9580e-04	2.9775e-04	1.4867e-04
$\widehat{CO}_{M_x}$	0.98641	0.99440	0.99850	1.0007	1.0020	
$\gamma = 1.6$	4.3490e-03	2.2073e-03	1.1120e-03	5.5806e-04	2.7944e-04	1.3974e-04
$\widehat{CO}_{M_x}$	0.97843	0.98908	0.99469	0.99789	0.99983	
$\gamma = 1.7$	3.9223e-03	2.0039e-03	1.0143e-03	5.1089e-04	2.5658e-04	1.2863e-04
$\widehat{CO}_{M_x}$	0.96892	0.98227	0.98942	0.99360	0.99623	
$\gamma = 1.8$	3.4063e-03	1.7497e-03	8.8937e-04	4.4956e-04	2.2651e-04	1.1389e-04
$\widehat{CO}_{M_x}$	0.96112	0.97623	0.98427	0.98894	0.99188	
$\gamma = 1.9$	2.8070e-03	1.4399e-03	7.3111e-04	3.6933e-04	1.8606e-04	9.3583e-05
$\widehat{CO}_{M_x}$	0.96307	0.97778	0.98518	0.98915	0.99143	

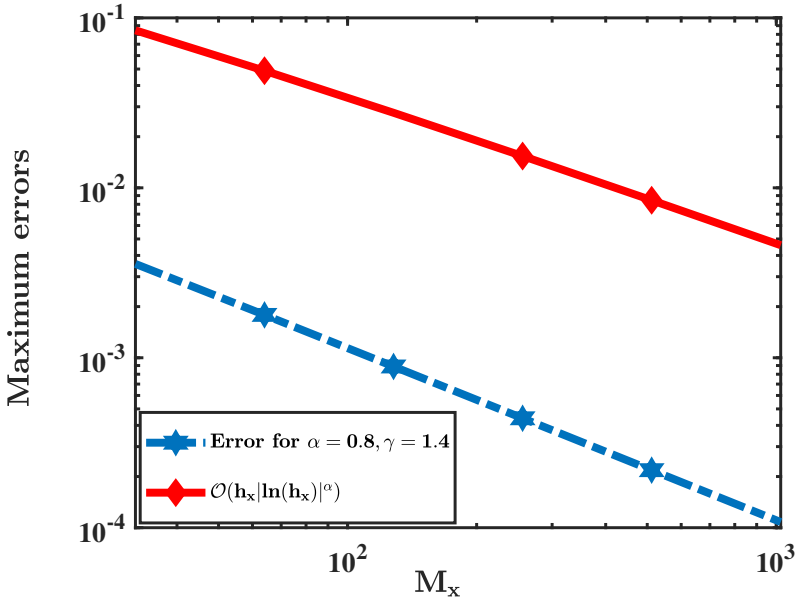

Figure 2.4: Log-log plot for Example 2.6.2 with $\alpha = 0.8$.

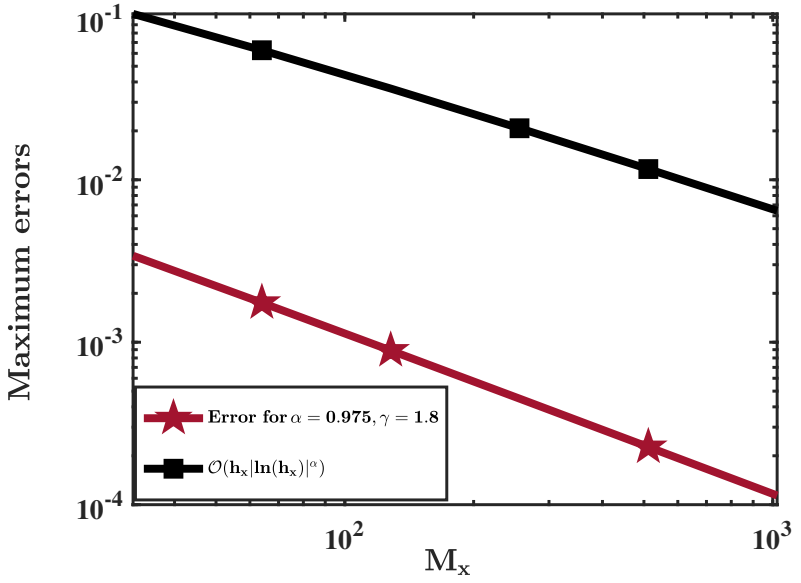

Figure 2.5: Log-log plot for Example 2.6.2 with $\alpha = 0.975$.

sequence of linear FBVPs

$$\begin{cases} -D\left({}^{C}D_{0,x}^{\gamma-\alpha}u^{(m+1)}(x)\right) - (1+x/2)\ {}^{C}D_{0,x}^{\alpha}u^{(m+1)}(x) + (2u^{(m)}+2)u^{(m+1)}(x) = \\ \left(2u^{(m)}+2\right)u^{(m)}(x) - f(x,u^{(m)}), \quad x \in (0,1), \\ {}^{C}D_{0,x}^{\gamma-\alpha}u^{(m+1)}(0) = 0,\ u^{(m+1)}(1) + 0.5\,{}^{C}D_{0,x}^{\gamma-\alpha}u^{(m+1)}(1) = \rho. \end{cases} \tag{2.6.4}$$

Hence, for fixed m, we solve (2.6.4) using the computational method discussed earlier. After reaching the tolerance bound, mentioned in (2.5.4) we break the Newton's sequence and consider that as the solution of our problem.

The maximum point-wise errors and the corresponding order of convergence are found using the same idea as followed in Example 2.6.1.

The numerical results of Example 2.6.3 are given in Table 2.6. The log-log plots for Example 2.6.3 with $\gamma = 1.3$ and $\gamma = 1.5$ are portrayed in Figure 2.6. The graph of the exact and approximate solutions for $M_x = 256$ and $\gamma = 1.5$ is depicted in Figure 2.7.

Table 2.6: Maximum errors and orders of convergence for $\alpha = 0.8$ of the Example 2.6.3.

$\alpha = 0.8$	$M_x = 32$	$M_x = 64$	$M_x = 128$	$M_x = 256$	$M_x = 512$	$M_x = 1024$
$\gamma = 1.1$	1.6477e-02	8.3169e-03	4.2106e-03	2.1331e-03	1.0802e-03	5.4645e-04
CO_{M_x}	0.9863	0.9820	0.9811	0.9817	0.9831	
$\gamma = 1.2$	1.6841e-02	8.5603e-03	4.3577e-03	2.2167e-03	1.1259e-03	5.7081e-04
CO_{M_x}	0.9762	0.9741	0.9751	0.9774	0.9800	
$\gamma = 1.3$	1.7338e-02	8.8741e-03	4.5415e-03	2.3193e-03	1.1813e-03	6.0012e-04
CO_{M_x}	0.9662	0.9664	0.9695	0.9733	0.9771	
$\gamma = 1.4$	1.7850e-02	9.1986e-03	4.7332e-03	2.4276e-03	1.2406e-03	6.3185e-04
CO_{M_x}	0.9565	0.9586	0.9633	0.9685	0.9734	
$\gamma = 1.5$	1.8228e-02	9.4517e-03	4.8906e-03	2.5205e-03	1.2935e-03	6.6114e-04
CO_{M_x}	0.9475	0.9506	0.9563	0.9625	0.9682	

2.7 Conclusions

In this chapter, we have discussed a finite difference scheme based on the uniform $L1-$ method for a steady-state advection-diffusion-reaction type FBVP. The higher-order derivative term of the model problem (2.1.1) contains a mixed-fractional derivative. The discrete

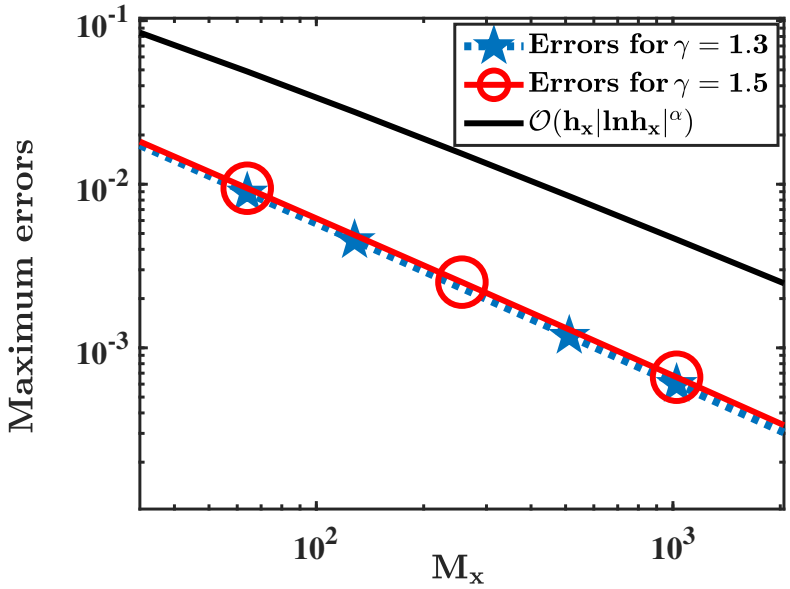

Figure 2.6: Log-log plot for Example 2.6.3 with $\alpha = 0.8$.

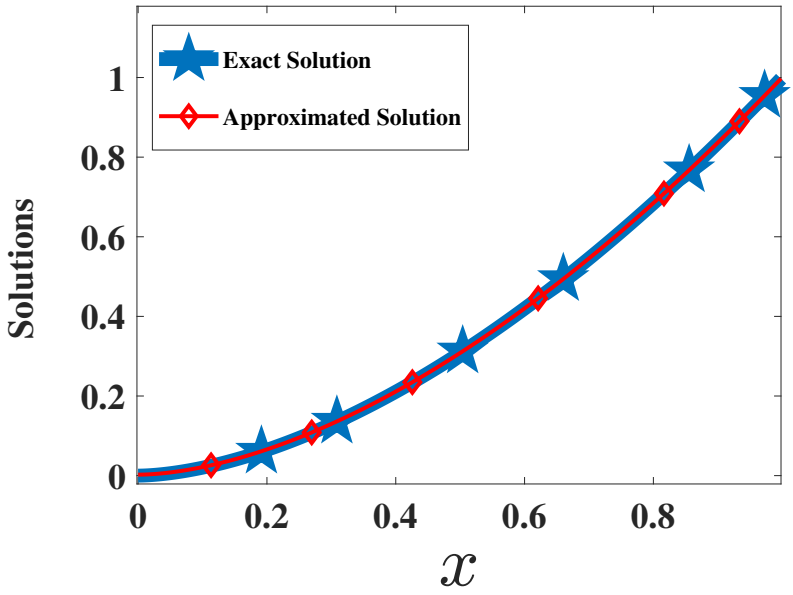

Figure 2.7: Exact vs Approximated solution for $\alpha = 0.8$, $\gamma = 1.5$, $M_x = 256$ of Example 2.6.3.

maximum principle has been addressed here. Further, the related error analysis has also been investigated. The convergence of the scheme was studied with the help of properly chosen discrete barrier function. Semilinear FBVPs have been solved by the proposed method after using the Newton's quasilinearization technique. At last some numerical examples were established to corroborate the theory.

CHAPTER 3

A second-order scheme for fractional differential equation with integral boundary conditions

In this chapter, we address the convergence properties of the second-order scheme for a FBVP with integral type boundary conditions. We firstly prove the existence and uniqueness of solution of the model problem. Then we use a second-order spline technique to discretize the Caputo derivative term, central-difference scheme to discretize the convection term and trapezoidal rule to approximate the integral boundary conditions. Further, we prove the second-order convergence result of the proposed scheme and verify the theoretical result by some numerical experiments.

3.1 Introduction

In this chapter, we consider the following fractional boundary-value problem (FBVP) with Caputo derivative and integral boundary conditions:

$$\begin{cases} Lu(x) \equiv -{}^{C}D^{\gamma}_{0,x}u(x) + a(x)u'(x) + c(x)u(x) = f(x), \quad x \in \Omega_x = (x_l, x_r)\,, \\ B_0u(x_l) \equiv u(x_l) - \displaystyle\int_{x_l}^{x_r} \phi(x)u(x)dx = \rho_0, \\ B_1u(x_r) \equiv u(x_r) - \displaystyle\int_{x_l}^{x_r} \psi(x)u(x)dx = \rho_1, \end{cases} \tag{3.1.1}$$

where ρ_0, ρ_1 are constants, $1 < \gamma < 2$. The coefficients $a(x)$, $c(x)(> 0)$, and the source function $f(x)$ are chosen sufficiently smooth over the domain $\overline{\Omega}_x = [x_l, x_r]$ with $x_l = 0$ and $x_r = 1$ for our model problem. The functions $\phi(x)$ and $\psi(x)$ are chosen such that

$$\phi(x),\, \psi(x) \geq 0, \quad \text{and} \quad \int_0^1 \phi(\zeta)\, d\zeta < 1, \int_0^1 \psi(\zeta)\, d\zeta < 1. \tag{3.1.2}$$

Under these assumptions, the FBVP (3.1.1) will admit a unique solution in $\overline{\Omega}_x$.

Differential equations with integral boundary conditions will occur in many applications, for example, in heat conduction, thermoelasticity, plasma physics, underground water flow, etc. In [86], the author has shown that a second order boundary value problem with integral type boundary conditions is effective for modeling of a thermostat with sensors expressed as linear functionals. Fractional boundary-value problems with integral boundary condition have been studied by several authors, for example, one can refer [24, 58].

Here, we propose a numerical method consists of the second-order spline method [70] for the Caputo derivative and the classical central difference scheme for the advection term. The integral-type boundary conditions are approximated by the trapezoidal rule. Then the truncation error of the proposed scheme is obtained, and the convergence analysis is carried out. In order to demonstrate the effectiveness and accuracy of the suggested approach, numerical examples are included.

The remaining part of the chapter is organized as follows: Existence and Uniqueness theorem of the FBVP (3.1.1) is established in Section 3.2. The discretized form of the model problem (3.1.1) is included in Section 3.3. In Section 3.4, the error analysis is incorporated. Section 3.5 describes the application of proposed method for a semilinear FBVP with integral-type boundary conditions. Some numerical examples are described in Section 3.6 and finally some conclusions have been provided in Section 3.7.

3.2 Existence and uniqueness of solution

Here, in this section, we derive the existence and uniqueness of the solution of the FBVP (3.1.1).

Theorem 3.2.1 (Existence and Uniqueness)**.** *Let the coefficients $a(x)$, $c(x)$ and the source function $f(x)$ be sufficiently smooth in $\overline{\Omega}_x$. Then $u(x)$ is the unique solution of the FBVP (3.1.1), if, and only if, $z(x)$ satisfies the following equation:*

$$z(x) = H_z(x) + \widehat{\mathcal{R}}(x), \tag{3.2.1}$$

where

$$\begin{aligned} H_z(x) &= (a(x)+xc(x))\frac{A_1(M_2 - I^{\gamma}_{0,x}z(1)) + A_2(I^{\gamma}_{0,x}z(0) - M_1)}{B_1A_2 + B_2A_1} \\ &\quad + c(x)\frac{B_1(M_2 - I^{\gamma}_{0,x}z(1)) + B_2(M_1 - I^{\gamma}_{0,x}z(0))}{B_1A_2 + B_2A_1} + a(x)I^{\gamma-1}_{0,x}z(x) + c(x)I^{\gamma}_{0,x}z(x), \end{aligned} \tag{3.2.2}$$

$$\widehat{\mathcal{R}}(x) = (a(x)+xc(x))\frac{\rho_1A_1 - \rho_0A_2}{B_1A_2 + B_2A_1} + c(x)\frac{\rho_1B_1 + \rho_0B_2}{B_1A_2 + B_2A_1} - f(x). \tag{3.2.3}$$

Proof. It is obvious that the FBVP (3.1.1) will admit the trivial solution $u = 0$, when $\rho_0 = 0$, $\rho_1 = 0$ and $f = 0$.

Now let

$${}^{C}D^{\gamma}_{0,x}\,u(x) = z(x), \tag{3.2.4}$$

where $u(x)$ is the solution of (3.1.1).

Then applying $I^{\gamma}_{0,x}$ on both sides of (3.2.4), we get

$$u(x) = \kappa_1 + \kappa_2 x + I^{\gamma}_{0,x}z(x), \tag{3.2.5}$$

where κ_1, κ_2 are constants.

By using (3.2.5) in the boundary conditions of the FBVP (3.1.1), one can obtain

$$\begin{aligned} u(0) - \int_0^1 \phi(x)u(x)\,dx &= \kappa_1 + I^{\gamma}_{0,x}z(0) - \left(\kappa_1\int_0^1 \phi(x)\,dx + \kappa_2\int_0^1 x\phi(x)\,dx \right. \\ &\quad \left. + \int_0^1 \phi(x)I^{\gamma}_{0,x}z(x)\,dx\right), \end{aligned} \tag{3.2.6}$$

$$\begin{aligned} u(1) - \int_0^1 \psi(x)u(x)\,dx &= \kappa_1 + \kappa_2 + I^{\gamma}_{0,x}z(1) - \left(\kappa_1\int_0^1 \psi(x)\,dx + \kappa_2\int_0^1 x\psi(x)\,dx \right. \\ &\quad \left. + \int_0^1 \psi(x)I^{\gamma}_{0,x}z(x)\,dx\right). \end{aligned} \tag{3.2.7}$$

Thus (3.2.6) and (3.2.7) can be rearranged as

$$\kappa_1\left(1-\int_0^1\phi(x)\,dx\right)-\kappa_2\int_0^1 x\phi(x)\,dx+I^{\gamma}_{0,x}z(0)-\int_0^1\phi(x)I^{\gamma}_{0,x}z(x)\,dx=\rho_0, \tag{3.2.8}$$

$$\kappa_1\left(1-\int_0^1\psi(x)\,dx\right)-\kappa_2\left(1-\int_0^1 x\psi(x)\,dx\right)+I^{\gamma}_{0,x}z(1)-\int_0^1\psi(x)I^{\gamma}_{0,x}z(x)\,dx=\rho_1. \tag{3.2.9}$$

From (3.2.8) and (3.2.9), we get

$$\kappa_1=\frac{B_1(\rho_1-I^{\gamma}_{0,x}z(1)+M_2)+B_2(\rho_0-I^{\gamma}_{0,x}z(0)+M_1)}{A_1B_2+A_2B_1},$$

and

$$\kappa_2=\frac{A_1(\rho_1-I^{\gamma}_{0,x}z(1)+M_2)+A_2(I^{\gamma}_{0,x}z(0)-M_1-\rho_0)}{A_1B_2+A_2B_1},$$

where

$$A_1=1-\int_0^1\phi(x)\,dx,\quad A_2=1-\int_0^1\psi(x)\,dx,$$
$$B_1=\int_0^1 x\phi(x)\,dx,\quad B_2=1-\int_0^1 x\psi(x)\,dx,$$
$$M_1=\int_0^1\phi(x)I^{\gamma}_{0,x}z(x)\,dx,\quad M_2=\int_0^1\psi(x)I^{\gamma}_{0,x}z(x)\,dx.$$

Therefore, the solution $u(x)$ of the FBVP (3.1.1) can be expressed as

$$u(x)=\frac{(\rho_1-I^{\gamma}_{0,x}z(1)+M_2)}{A_1B_2+A_2B_1}(B_1+xA_1)+\frac{\rho_0+M_1-I^{\gamma}_{0,x}z(0)}{A_1B_2+A_2B_1}(B_2-xA_2)+I^{\gamma}_{0,x}z(x). \tag{3.2.10}$$

Hence, substituting (3.2.10) in (3.1.1), we finally have

$$z(x)=H_z(x)+\widehat{\mathcal{R}}(x), \tag{3.2.11}$$

Conversely, if, we assume that $z(x)$ satisfies (3.2.1), then one can derive $u(x)$ in the form (3.2.10) which satisfies the FBVP (3.1.1).

In order to prove the uniqueness of the solution of (3.1.1), we assume that the problem (3.1.1) has two solutions $u_1(x)$ and $u_2(x)$. Then, $Y(x):=u_1(x)-u_2(x)$ satisfies the following homogeneous FBVP:

$$\begin{cases}-{}^{C}D^{\gamma}_{0,x}Y(x)+a(x)Y'(x)+c(x)Y(x)=0, \quad x\in\Omega_x=(0,1),\\ Y(0)-\displaystyle\int_0^1\phi(x)Y(x)dx=0,\\ Y(1)-\displaystyle\int_0^1\psi(x)Y(x)dx=0.\end{cases} \tag{3.2.12}$$

It is well-known that the homogeneous FBVP (3.2.12) admits only the trivial solution $Y = 0$. Therefore, $u_1 \equiv u_2$, $\forall x \in \overline{\Omega}_x$, which shows the uniqueness of the solution of the FBVP (3.1.1). □

3.3 Discretization scheme

In this section, we will discuss the discretization scheme for the model problem (3.1.1) by applying the spline method to approximate the Caputo derivative and central difference scheme for the first-order classical derivative term, and the trapezoidal method for the integral-type boundary conditions.

Let M_x be a positive integer. Here, to discretize the domain $\overline{\Omega}_x$, we use uniform mesh with mesh width $h_x = 1/M_x$ and mesh points $x_i = (i-1)h_x$, $i = 1, 2, \ldots, M_x + 1$.

3.3.1 Discretization of Caputo derivative using spline approximation

Following the idea given by Sousa [70], we use a linear spline $s_j(\zeta)$ to approximate the Caputo derivative ${}^{C}D^{\gamma}_{0,x}u(x)$. The knots and nodes of the linear spline $s_i(\zeta)$ are presented at the points x_k, $k = 1, 2, \ldots, i$. Then one can express

$$\begin{aligned} {}^{C}D^{\gamma}_{0,x}u(x_i) &= \frac{1}{\Gamma(2-\gamma)} \int_0^{x_i} (x_i - \zeta)^{1-\gamma} \frac{d^2u(\zeta)}{d\zeta^2}\, d\zeta \\ &= \frac{1}{\Gamma(2-\gamma)} \int_0^{x_i} (x_i - \zeta)^{1-\gamma} s_i(\zeta)\, d\zeta \\ &=: L_S(x_i), \end{aligned} \tag{3.3.1}$$

where $s_j(\zeta) = \sum_{k=1}^{i} \frac{d^2u(x_k)}{d\zeta^2} s_{i,k}(\zeta)$.

The function $s_{i,k}(\zeta)$ at each interval $[x_{k-1}, x_{k+1}]$, for $k = 2, 3, \ldots, i-1$ is given by:

$$s_{i,k}(\zeta) = \begin{cases} \dfrac{\zeta - x_{k-1}}{x_k - x_{k-1}}, & \text{for} \quad x_{k-1} \le \zeta \le x_k, \\ \dfrac{x_{k+1} - \zeta}{x_{k+1} - x_k}, & \text{for} \quad x_k \le \zeta \le x_{k+1}, \\ 0, & \text{otherwise.} \end{cases}$$

For $k = 1$ and $k = i$, we have

$$s_{i,1}(\zeta) = \begin{cases} \dfrac{x_2 - \zeta}{x_2 - x_1}, & \text{for} \quad x_1 \le \zeta \le x_2, \\ 0, & \text{otherwise}, \end{cases}$$

and

$$s_{j,j}(t) = \begin{cases} \dfrac{\zeta - x_{i-1}}{x_i - x_{i-1}}, & \text{for} \quad x_{i-1} \le \zeta \le x_i, \\ 0, & \text{otherwise}. \end{cases}$$

Then, (3.3.1) becomes

$$\begin{aligned} L_S(x_i) &= \frac{1}{\Gamma(2-\gamma)} \sum_{k=1}^{i} \frac{d^2u(x_k)}{d\zeta^2} \int_0^{x_i} (x_i - \zeta)^{1-\gamma} s_{i,k}(\zeta)\, d\zeta \\ &= \frac{h_x^{2-\gamma}}{\Gamma(4-\gamma)} \sum_{k=1}^{i} \frac{d^2u(x_k)}{d\zeta^2} w_{i,k}, \end{aligned} \tag{3.3.2}$$

where

$$w_{i,k} = \begin{cases} (i-1)^{3-\gamma} - i^{2-\gamma}(i-3+\gamma), & k = 1, \\ (i-k+1)^{3-\gamma} - 2(i-k)^{3-\gamma} + (i-k-1)^{3-\gamma}, & 2 \le k \le i-1, \\ 1, & k = i. \end{cases} \tag{3.3.3}$$

The second-order derivative presents in (3.3.2) is approximated by the following second-order central difference scheme:

$$\frac{d^2u(x_i)}{dx^2} = \frac{u(x_{i+1}) - 2u(x_i) + u(x_{i-1})}{h_x^2} + O(h_x^2), \quad i = 2, 3, \ldots, M_x.$$

For $i = 1$, we use the following second-order approximation:

$$\frac{d^2u(x_1)}{dx^2} = \frac{2u(x_1) - 5u(x_2) + 4u(x_3) - u(x_4)}{h_x^2} + O(h_x^2).$$

Thus, we have

$$\begin{aligned} L_S(x_i) &\approx \frac{h_x^{-\gamma}}{\Gamma(4-\gamma)} \left\{ w_{i,1}(2U_1 - 5U_2 + 4U_3 - U_4) + \sum_{k=2}^{i} w_{i,k}(U_{k+1} - 2U_k + U_{k-1}) \right\} \\ &=: D_{C,S}^{\gamma} U_i, \end{aligned} \tag{3.3.4}$$

where U_i is the approximated solution of $u(x)$ at the point $x = x_i$.

Hence, the discretized form of (3.1.1) can be written as:

$$\begin{cases} L_{M_x}U_i \equiv -D^{\gamma}_{C,S}U_i + a_i D^o U_i + c_i U_i = f_i, \quad i = 2,3,\ldots,M_x, \\ B_0U_1 \equiv U_1 - \dfrac{h_x}{2}\displaystyle\sum_{k=1}^{M_x}(\phi_k U_k + \phi_{k+1}U_{k+1}) = \rho_0, \\ B_1U_{M_x} \equiv U_{M_x+1} - \dfrac{h_x}{2}\displaystyle\sum_{k=1}^{M_x}(\psi_k U_k + \psi_{k+1}U_{k+1}) = \rho_1, \end{cases} \tag{3.3.5}$$

where $a_i := a(x_i)$ and similar expression for c_i, f_i, ϕ_i, and ψ_i. The notation $D^oU_i = (U_{i+1} - U_{i-1})/2h_x$ denotes the standard central difference formula and $D^{\gamma}_{C,S}$ is used as the spline approximate operator for the Caputo derivative of order γ. The integral boundary conditions are approximated using the trapezoidal rule.

3.3.2 System of equations

Now, we construct a linear system of equations corresponding to the discretized form (3.3.5). For $i = 2,3,\ldots,M_x$, the difference scheme (3.3.5) can be expressed as

$$\begin{aligned} L_{M_x}U_i \equiv & -\frac{h_x^{-\gamma}}{\Gamma(4-\gamma)}\left\{w_{i,1}(2U_1 - 5U_2 + 4U_3 - U_4) + \sum_{k=2}^{i} w_{i,k}(U_{k+1} - 2U_k + U_{k-1})\right\} \\ & + a_i\frac{U_{i+1} - U_{i-1}}{2h_x} + c_iU_i = f_i, \end{aligned} \tag{3.3.6}$$

and

$$B_0U_1 \equiv \left(1 - \frac{\phi_1 h_x}{2}\right)U_1 + \sum_{k=2}^{M_x}(-h_x\phi_k)U_k + \frac{-h_x\phi_{M_x+1}}{2}U_{M_x+1} = \rho_0, \tag{3.3.7}$$

$$B_1U_{M_x} \equiv -\frac{\psi_1 h_x}{2}U_1 + \sum_{k=2}^{j}(-h_x\psi_k)U_k + \left(1 - \frac{h_x\psi_{M_x+1}}{2}\right)U_{M_x+1} = \rho_1. \tag{3.3.8}$$

Thus, the discrete problem given in (3.3.6)-(3.3.8) makes the following system of linear algebraic equations:

$$[-\varepsilon\,(\mathcal{W} + \mathcal{P}) + \mathcal{S} + \upsilon\, Z + h_x R]\,U = F, \tag{3.3.9}$$

where $\varepsilon = h_x^{-\gamma}/\Gamma(4-\gamma)$, $\upsilon = 1/2h_x$, $U = (U_1, U_2, \ldots, U_{M_x+1})^T$, $F = (\rho_0, f_2, \ldots, f_{M_x}, \rho_1)^T$, and $\mathcal{W}, \mathcal{P}, \mathcal{S}, Z$ and R are the matrices of dimension $(M_x+1)\times(M_x+1)$ associated with the discretization (3.3.5).

Now, we define the matrices as follows:

$$\mathcal{W} = \begin{pmatrix} 0 & 0 & 0 & 0 & 0 & \dots & 0 \\ 2w_{2,1} & -5w_{2,1} & 4w_{2,1} & -w_{2,1} & 0 & \dots & 0 \\ 2w_{3,1} & -5w_{3,1} & 4w_{3,1} & -w_{3,1} & 0 & \dots & 0 \\ \vdots & \vdots & \vdots & \vdots & \vdots & \dots & \vdots \\ 2w_{M_x-1,1} & -5w_{M_x-1,1} & 4w_{M_x-1,1} & -w_{M_x-1,1} & 0 & \dots & 0 \\ 2w_{M_x,1} & -5w_{M_x,1} & 4w_{M_x,1} & -w_{M_x,1} & 0 & \dots & 0 \\ 0 & 0 & 0 & 0 & 0 & \dots & 0 \end{pmatrix},$$

$$\mathcal{P} = \begin{pmatrix} 0 & 0 & 0 & \dots & 0 & 0 & 0 \\ p_{21} & p_{22} & p_{23} & \cdots & p_{2,M_x-1} & p_{2N} & p_{2,N+1} \\ p_{31} & p_{32} & p_{33} & \cdots & p_{3,M_x-1} & p_{3N} & p_{3,N+1} \\ \vdots & \vdots & \vdots & \ddots & \vdots & \vdots & \vdots \\ p_{M_x-1,1} & p_{M_x-1,2} & p_{M_x-1,3} & \cdots & p_{M_x-1,M_x-1} & p_{M_x-1,M_x} & p_{M_x-1,M_x+1} \\ p_{M_x,1} & p_{M_x,2} & p_{M_x,3} & \cdots & p_{M_x,M_x-1} & p_{M_x,M_x} & p_{M_x,M_x+1} \\ 0 & 0 & 0 & \dots & 0 & 0 & 0 \end{pmatrix},$$

where

$$\begin{aligned} &p_{i,1} = w_{i,2},\ i = 2,3,\dots,M_x\,; \quad p_{2,2} = -2w_{2,2}\,; \quad p_{i,2} = -2w_{i,2} + w_{i,3},\ i = 3,4,\dots,M_x\,; \\ &p_{i,i} = w_{i,i-1} - 2w_{i,i},\ i = 3,4,\dots,M_x; p_{i,i+1} = w_{i,i},\ i = 2,3,\dots,M_x \\ &p_{i,k} = w_{i,k+1} - 2w_{i,k} + w_{i,k-1},\ k = 3,4,\dots,i-1,\ i = 4,5,\dots,M_x, \quad \text{and} \\ &p_{i,k} = 0,\ k = i+2, i+3,\dots,M_x+1,\ i = 2,3,\dots,M_x, \end{aligned} \tag{3.3.10}$$

$$\mathcal{S} = \begin{pmatrix} 1 & & & & & & \\ & c_2 & & & & & \\ & & c_3 & & & & \\ & & & \ddots & & & \\ & & & & c_{M_x-1} & & \\ & & & & & c_{M_x} & \\ & & & & & & 1 \end{pmatrix}, \quad Z = \begin{pmatrix} 0 & & & & & & \\ -a_2 & 0 & a_2 & & & & \\ & -a_3 & 0 & a_3 & & & \\ & & & \ddots & & & \\ & & & -a_{M_x-1} & 0 & a_{M_x-1} & \\ & & & & -a_{M_x} & 0 & a_{M_x} \\ & & & & & & 0 \end{pmatrix},$$

and

$$R = \begin{pmatrix} \frac{-\phi_1}{2} & -\phi_2 & \dots & -\phi_{M_x} & \frac{-\phi_{M_x+1}}{2} \\ 0 & 0 & \dots & 0 & 0 \\ \vdots & \vdots & \ddots & \vdots & \vdots \\ 0 & 0 & \dots & 0 & 0 \\ \frac{-\psi_1}{2} & -\psi_2 & \dots & -\psi_{M_x} & \frac{-\psi_{M_x+1}}{2} \end{pmatrix}.$$

Before we study of error analysis of the discretized scheme (3.3.5), we will discuss following two lemmas.

Lemma 3.3.1. *For $0 \le x \le 1$ and $0 \le \mathfrak{n} \le 1$, we have $(1-x)^{\mathfrak{n}} \le 1 - \mathfrak{n}x$.*

Proof. For the given range of x and n, from the binomial expansion we have

$$\begin{aligned} (1-x)^{\mathfrak{n}} &= 1 - \mathfrak{n}x - \frac{\mathfrak{n}(1-\mathfrak{n})}{2!}x^2 - \frac{\mathfrak{n}(1-\mathfrak{n})(2-\mathfrak{n})}{3!}x^3 - \dots \\ &\le 1 - \mathfrak{n}x, \end{aligned} \tag{3.3.11}$$

which is the required result. □

Lemma 3.3.2. *The elements $w_{i,1}$, $i = 2, 3, \dots, M_x$ of the matrix $\mathcal{W}$ are decreasing.*

Proof. From (3.3.3), we have

$$w_{i,1} = (i-1)^{3-\gamma} - i^{2-\gamma}(i-3+\gamma).$$

For $x \ge 1$, let us assume that

$$\mathcal{F}(x) = (x-1)^{3-\gamma} - x^{2-\gamma}(x-3+\gamma). \tag{3.3.12}$$

Differentiating both sides of (3.3.12) with respect to x, we can have

$$\begin{aligned} \mathcal{F}'(x) &= -(3-\gamma)\left[x^{2-\gamma} - (x-1)^{2-\gamma}\right] + (3-\gamma)(2-\gamma)x^{1-\gamma} \\ &= (3-\gamma)(2-\gamma)x^{1-\gamma}\left[1 - \frac{x^{2-\gamma} - (x-1)^{2-\gamma}}{(2-\gamma)x^{1-\gamma}}\right]. \end{aligned} \tag{3.3.13}$$

In order to show that $\mathcal{F}'(x) < 0$, we introduce a new function $g(x)$ given by

$$g(x) = \frac{x^{2-\gamma} - (x-1)^{2-\gamma}}{(2-\gamma)x^{1-\gamma}}.$$

Then proving $g(x) > 1$ for all $x \geq 1$ will be equivalent to $\mathcal{F}'(x) < 0$.

The function $g(x)$ can be rewritten as

$$g(x) = \frac{x}{2-\gamma}\left[1 - \left(1 - \frac{1}{x}\right)^{2-\gamma}\right], \quad \forall\, x \geq 1. \tag{3.3.14}$$

Here, we have $0 < 1/x \leq 1$ and $0 < 2 - \gamma < 1$. Thus using Lemma 3.3.1, we can easily conclude that $g(x) > 1$, directly follows from (3.3.14) and hence it shows that the function $\mathcal{F}(x)$ is decreasing for all $x \geq 1$.

Therefore, $\mathcal{F}(x) > \mathcal{F}(x+1)$ for all $x \geq 1$ and it proves the required result. □

3.4 Error analysis

In this section, we will discuss the truncation error and the convergence of the approximate solution obtained by the proposed numerical scheme.

Theorem 3.4.1. *Let $u(x) \in \mathcal{C}^4(\overline{\Omega}_x)$ and $1 < \gamma < 2$. Consider the discrete operator Δ_γ defined by*

$$\Delta_\gamma u(x_i) = \frac{1}{\Gamma(4-\gamma)}\left(w_{i,1}\Delta_1 u(x_1) + \sum_{k=2}^{i} w_{i,k}\Delta^2 u(x_k)\right),$$

where $\Delta_1 u(x_1) = 2u(x_1) - 5u(x_2) + 4u(x_3) - u(x_4)$ and $\Delta^2 u(x_k) = u(x_{k+1}) - 2u(x_k) + u(x_{k-1})$.

Then, we have

$$h_x^{-\gamma}\Delta_\gamma u(x_i) = {}^{C}D_{0,x}^{\gamma} u(x_i) + \xi_1(x_i) + \xi_2(x_i),$$

with

$$\max_{0 \leq x_i \leq 1} |\xi_p(x_i)| \leq \frac{1}{\Gamma(3-\gamma)} O(h_x^2), \quad p = 1, 2.$$

Proof. The detailed proof can be found in [70, Theorem 1]. □

3.4.1 Truncation error

Let the truncation error be denoted by $\mathcal{T} := (\mathcal{T}_1, \mathcal{T}_2, \ldots, \mathcal{T}_{M_x+1})^T$, where the $\mathcal{T}_i$'s are defined as

$$\mathcal{T}_1 := (Au)_1 - \rho_0 = -\frac{h_x}{2}\sum_{k=1}^{M_x}(\phi_k U_k + \phi_{k+1}U_{k+1}) + \int_0^1 \phi(x)u(x)dx, \tag{3.4.1}$$

$$\mathcal{T}_i := (Au)_i - f_i = (Au)_i - \left[-{}^{C}D^{\gamma}_{0,x}u(x_i) + b_i y'(x_i) + c_i y(x_i)\right], \ i = 2, 3, \ldots, M_x, \tag{3.4.2}$$

$$\mathcal{T}_{M_x+1} := (Au)_{M_x+1} - \rho_1 = -\frac{h_x}{2}\sum_{k=1}^{M_x}(\psi_k U_k + \psi_{k+1}U_{k+1}) + \int_0^1 \psi(x)u(x)dx, \tag{3.4.3}$$

where $u(x_i)$ is the solution of the continuous problem (3.1.1) and U_i is the solution of discretized equation (3.3.5) at the points $x_i,\ i = 1, 2, \ldots, M_x + 1$.

The following lemma will provide the truncation error bound for the discretized scheme (3.3.5).

Lemma 3.4.2. *Let $u(x) \in \mathcal{C}^4(\overline{\Omega}_x)$ be the exact solution of the FBVP (3.1.1). Then the truncation error of the discretized scheme (3.3.5) is of order $\mathcal{O}(h_x^2)$.*

Proof. For the left boundary condition, we have

$$|\mathcal{T}_1| \leq Ch_x^3 |\left[u''(\zeta_1) + u''(\zeta_2) + \ldots + u''(\zeta_N)\right]| \leq Ch_x^2 |u''(\widehat{\zeta})| \leq Ch_x^2, \tag{3.4.4}$$

where $x_i \leq \zeta_i \leq x_{i+1}$ for $1 \leq i \leq M_x$ and assumed the maximum value of $u''(x)$ exists at some $x = \widehat{\zeta}$.

Similarly, one can show for the right boundary condition

$$|\mathcal{T}_{M_x+1}| \leq Ch_x^2. \tag{3.4.5}$$

Following [70] and using the truncation error for the approximation of first-order classical derivative by the central-difference scheme, it can be also shown that

$$|\mathcal{T}_i| \leq Ch_x^2, \quad \text{for} \quad i = 2, 3, \ldots, M_x. \tag{3.4.6}$$

Assembling (3.4.4)-(3.4.6), we get the required result. □

3.4.2 Error bound

In this section, we show that the proposed numerical scheme (3.3.5) is of second-order convergent.

Let $\mathcal{E}_i := u(x_i) - U_i$ represents the error of the numerical scheme (3.3.5) for $1 \leq i \leq M_x+1$, then, one can express the error in the following form:

$$\begin{aligned} \mathcal{E} &= \left[-\varepsilon\left(\mathcal{W}+\mathcal{P}\right)+\mathcal{S}+\upsilon\, Z+h_x R\right]^{-1}\mathcal{T} \\ &= \left[I+\left(-\varepsilon\mathcal{S}^{-1}(\mathcal{W}+P)+\upsilon\,\mathcal{S}^{-1}Z+h_x\mathcal{S}^{-1}R\right)\right]^{-1}\mathcal{S}^{-1}\,\mathcal{T}, \end{aligned} \tag{3.4.7}$$

where $\mathcal{E} = (\mathcal{E}_1, \mathcal{E}_2, \ldots, \mathcal{E}_{M_x+1})^T$.

In order to get the bound of $\mathcal{E}$, we need the following lemmas.

Lemma 3.4.3. *If A is a square matrix of order M_x such that $\|A\|_\infty < 1$, then $(I+A)^{-1}$ exists and $\|\,(I+A)^{-1}\,\|_\infty < 1/\,(1-\|A\|_\infty)$.*

Proof. For the detailed proof one can see [91, Lemma 4]. □

Now, following Lemma 3.4.3, we can have the corollary.

Corollary 3.4.4. *If A and B are two square matrices of order M_x, such that $\left(\|A\|_\infty + \|B\|_\infty\right) < 1$, then $(I+A+B)^{-1}$ exists and $\|\,(I+A+B)^{-1}\,\|_\infty < 1/\,(1-[\|A\|_\infty + \|B\|_\infty])$.*

Remark 3.4.5. *The matrix $\mathcal{S}$ given in Section 3.3.2 is non singular for all $x \in [0,1]$ and $\mathcal{S}^{-1}$ satisfies the following bound:*

$$\|\mathcal{S}^{-1}\|_\infty \leq \max\left\{1, \|1/c\|_\infty\right\}.$$

Now, the following lemma will be used to find the bound for $\mathcal{E}$.

Lemma 3.4.6. *If*

$$\max\left\{1, \left\|c^{-1}\right\|_\infty\right\}\left(\varepsilon\left(12\|w\| + \|\mathcal{P}\|_\infty\right) + 2\upsilon\ \|b\| + h_x\ \max\left\{\|\phi\|_1, \|\psi\|_1\right\}\right) < 1,$$

then the matrix $[-\varepsilon(\mathcal{W}+P)+\mathcal{S}+\upsilon Z+h_x R]$ is non singular.

Proof. For the matrix $\left[-\varepsilon\left(\mathcal{W}+\mathcal{P}\right)+\mathcal{S}+\upsilon\, Z+h_x R\right]$, we have

$$\begin{aligned} &\|\left[-\varepsilon\left(\mathcal{W}+\mathcal{P}\right)+\mathcal{S}+\upsilon\, Z+h_x R\right]^{-1}\|_\infty \\ &\leq \|\left[I+\left(-\varepsilon\mathcal{S}^{-1}(\mathcal{W}+\mathcal{P})+\upsilon\,\mathcal{S}^{-1}Z+h_x\mathcal{S}^{-1}R\right)\right]^{-1}\|_\infty \|\mathcal{S}^{-1}\|_\infty. \end{aligned} \tag{3.4.8}$$

Then, using Corollary 3.4.4, we can write

$$\begin{aligned} &\| \left[-\varepsilon \left(\mathcal{W}+\mathcal{P}\right)+\mathcal{S}+\upsilon\, Z+h_x R\right]^{-1} \|_\infty \\ &\leq \frac{\|\mathcal{S}^{-1}\|_\infty}{1-\|\mathcal{S}^{-1}\|_\infty \left[\varepsilon \left(\|\mathcal{W}\|_\infty+\|\mathcal{P}\|_\infty\right)+\upsilon \|Z\|_\infty+h_x\|R\|_\infty\right]}. \end{aligned} \tag{3.4.9}$$

Now

$$\|Z\|_\infty \leq 2\upsilon\|b\|, \quad \|R\|_\infty \leq \max\left\{\|\phi\|_1, \|\psi\|_1\right\}.$$

Again using Lemma 3.3.2, one can show that

$$\|\mathcal{W}\|_\infty \leq 12\widetilde{w} = 12\left[1-2^{2-\gamma}(\gamma-1)\right],$$

where $\widetilde{w} = \max\left\{w_{2,1}, w_{3,1}, \ldots, w_{M_x,1}\right\}$.

Also,

$$\|\mathcal{P}\|_\infty = \max_{2\leq i\leq M_x}\left\{\sum_{k=1}^{i+1} p_{i,k}\right\}.$$

Then, from (3.4.9), we have

$$\begin{aligned} &\| \left[-\varepsilon \left(\mathcal{W}+\mathcal{P}\right)+\mathcal{S}+\upsilon\, Z+hR\right]^{-1} \|_\infty \\ &\leq \frac{\max\left\{1, \|c^{-1}\|_\infty\right\}}{1-\max\left\{1, \|c^{-1}\|_\infty\right\}\left[\varepsilon\left(12\widetilde{w}+\|\mathcal{P}\|_\infty\right)+2\upsilon\ \|b\|+h_x\ \max\left\{\|\phi\|_1, \|\psi\|_1\right\}\right]}. \end{aligned} \tag{3.4.10}$$

Thus, using the Lemma 3.4.3, one can get the required result. □

The following theorem provides the second-order convergence of the proposed numerical scheme (3.3.5).

Theorem 3.4.7. *Let $u(x)$ be the exact solution of the FBVP (3.1.1) and U_i, for $i = 1, 2, ..., M_x+1$, satisfies the discrete problem given in (3.3.5). Then we have*

$$\|\mathcal{E}\|_\infty \cong \mathcal{O}(h_x^2). \tag{3.4.11}$$

Proof. Using Corollary 3.4.4 and Lemma 3.4.6, we have from relation (3.4.7) that

$$\begin{aligned} \|\mathcal{E}\|_\infty &\leq \frac{\|\mathcal{S}^{-1}\|_\infty \|\mathcal{T}\|_\infty}{1-\|\mathcal{S}^{-1}\|_\infty \left[\varepsilon \left(\|\mathcal{W}\|_\infty+\|\mathcal{P}\|_\infty\right)+\upsilon \|Z\|_\infty+h_x\|R\|_\infty\right]} \\ &\leq \frac{\max\left\{1, \|c^{-1}\|_\infty\right\} Ch_x^2}{1-\max\left\{1, \|c^{-1}\|_\infty\right\}\left[\varepsilon\left(12\widetilde{w}+\|\mathcal{P}\|_\infty\right)+2\upsilon\ \|b\|+h_x\ \max\left\{\|\phi\|_1, \|\psi\|_1\right\}\right]} \\ &\cong \mathcal{O}(h_x^2), \end{aligned}$$

which is the required error bound. □

3.5 Application of semilinear fractional differential equation

In this section, we consider the following semilinear FBVP:

$$\begin{cases} -{}^{C}D^{\gamma}_{0,x}u(x) + a(x)u'(x) + f(x,u(x)) = 0, \quad x \in (0,1), \\ u(0) - \displaystyle\int_0^1 \phi(x)u(x)dx = \rho_0, \\ u(1) - \displaystyle\int_0^1 \psi(x)u(x)dx = \rho_1, \end{cases} \tag{3.5.1}$$

where the source function $f(x,u(x))$ is nonlinear in $u(x)$. Under sufficient smoothness conditions on the functions $a(x)$ and $f(x,u(x))$, the FBVP (3.5.1), in general, admits a unique solution $u(x)$. The conditions on $\phi(x)$ and $\psi(x)$ remain same as given in (3.1.2).

To solve the semilinear FBVP (3.5.1) numerically, the Newton method of quasilinearization is applied to obtain a sequence $\left\{u^{(m)}\right\}_0^{\infty}$ of approximations with a proper choice of initial guess $u^{(0)}(x)$.

We define $u^{(m+1)}$ for each fixed non-negative integer m, to be the solution of the following linear FBVP:

$$\begin{cases} -{}^{C}D^{\gamma}_{0,x}u^{(m+1)}(x) + a(x)(u^{(m+1)}(x))' + c^{(m)}(x)u^{(m+1)}(x) = g^{(m)}(x), \quad x \in (0,1), \\ u^{(m+1)}(0) - \displaystyle\int_0^1 \phi(x)u^{(m+1)}(x)dx = \rho_0, \\ u^{(m+1)}(1) - \displaystyle\int_0^1 \psi(x)u^{(m+1)}(x)dx = \rho_1, \end{cases} \tag{3.5.2}$$

where $c^{(m)}(x)$ and $f^{(m)}(x)$ are given by

$$\begin{cases} c^{(m)}(x) = f_u(x,u^{(m)}), \\ g^{(m)}(x) = c^{(m)}(x)u^{(m)} - f(x,u^{(m)}). \end{cases} \tag{3.5.3}$$

Hence, for each fixed m, we solve (3.5.2) by using the proposed numerical scheme (3.3.5) and then for the above Newton quasilinearization process we use the following convergence criterion for the solution

$$|u^{(m+1)}(x_i) - u^{(m)}(x_i)| \leq \text{tol}, \quad x_i \in \overline{\Omega}_x^{M_x}, \quad m \geq 0. \tag{3.5.4}$$

For computation, we have chosen $\text{tol} = 10^{-8}$.

3.6 Numerical experiments

In this section, first, we provide the numerical algorithm of the discretized scheme (3.3.5) and then perform some numerical examples to illustrate the efficiency of the proposed scheme (3.3.5).

3.6.1 Numerical algorithm for the spline scheme

To establish the proposed numerical scheme given in (3.3.5) and to get the corresponding numerical solution, we use the following algorithm:

Step 1. Discretize the domain $\overline{\Omega}_x = [0, 1]$ using uniform mesh.

Step 2. Use the proposed method given in (3.3.5) to discretize the given FBVP (3.1.1).

Step 3. Generate the matrix $[-\varepsilon(\mathcal{W} + P) + \mathcal{S} + \upsilon Z + h_x R]$ and the right hand side vector F as given in (3.3.9).

Step 4. Solve the system of linear algebraic equations (3.3.9) using any suitable numerical method. Here, we use the Gauss Elimination Method to solve (3.3.9).

3.6.2 Numerical results

Example 3.6.1. *Consider the following FBVP:*

$$\begin{cases} -{}^{C}D^{\gamma}_{0,x}u(x) + (1-x^2)u'(x) + (2+e^x)\,u(x) = f(x), \quad x \in (0,1), \quad 1 < \gamma < 2, \\ u(0) - \displaystyle\int_0^1 x^2 u(x)dx = \rho_0, \quad u(1) - \int_0^1 \frac{x}{3}u(x)dx = \rho_1. \end{cases} \tag{3.6.1}$$

The exact solution of the FBVP (3.6.1) is $u(x) = x^{4+\gamma}(1-x) + 1$ and it clearly belongs to the space $\mathfrak{C}^4(\overline{\Omega}_x)$.

The maximum error and the corresponding order of convergence are given by

$$E_{M_x} = \max_{1 \le i \le M_x+1} |U_i - u(x_i)|, \quad \text{and} \quad CO_{M_x} = \log_2\left(\frac{E_{M_x}}{E_{2M_x}}\right),$$

respectively.

Table 3.1 shows the maximum errors and corresponding of orders of convergence for Example 3.6.1 by the present method (3.3.5) and the FDM given in [69]. Further, one can

notice the second-order convergence of the proposed scheme from the results given in Table 3.1. Figure 3.1 displays the log-log plots for Example 3.6.1 with $\gamma = 1.4$, and the exact and numerical solutions for $M_x = 128$ and $\gamma = 1.4$ are plotted in Figure 3.2.

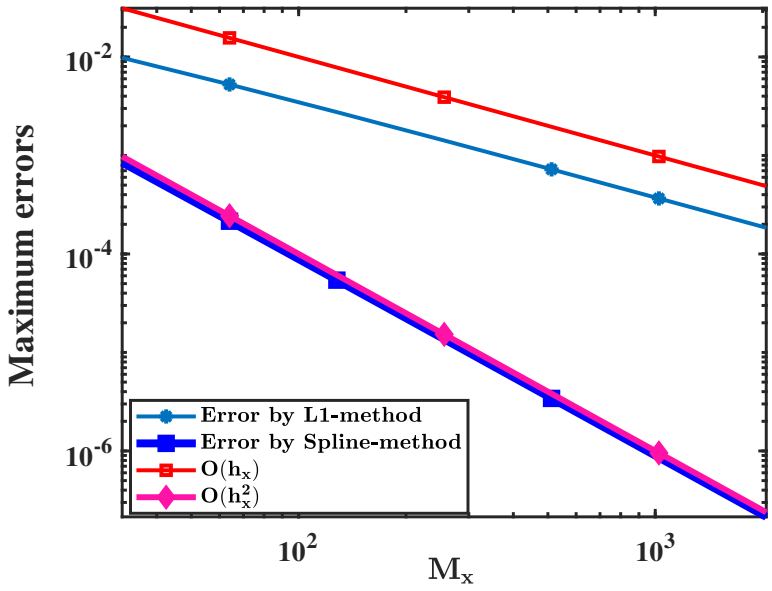

Figure 3.1: Log-log plots for Example 3.6.1 with $\gamma = 1.4$.

Example 3.6.2. *Consider the following semilinear FBVP:*

$$\begin{cases} -{}^{C}D^{\gamma}_{0,x}u(x) + (1-x)u'(x) + f(x,u(x)) = 0, \quad x \in (0,1), \quad 1 < \gamma < 2, \\ u(0) - \displaystyle\int_0^1 xu(x)dx = \rho_0, \quad u(1) - \int_0^1 \frac{x^2}{3}u(x)dx = \rho_1, \end{cases} \tag{3.6.2}$$

where the nonlinear function $f(x,u(x))$ is given by

$$f(x,u(x)) = 2u(x) + u^2(x) + \widehat{s}(x),$$

where $\widehat{s}(x)$ is chosen in such a way that the exact solution of the FBVP (3.6.2) is $u(x) = x^{4\gamma}$ which belongs to the space $\mathcal{C}^4(\overline{\Omega}_x)$.

Now, using the Newton's linearization process given in (3.5.2), we obtain the following sequence of linear FBVPs:

$$\begin{cases} -{}^{C}D^{\gamma}_{0,x}u^{(m+1)}(x) + (1-x)(u^{(m+1)}(x))' + \left(2u^{(m)} + 2\right)u^{(m+1)}(x) = \\ \left(2u^{(m)} + 2\right)u^{(m)}(x) - f\left(x, u^{(m)}\right), \quad x \in (0,1), \quad 1 < \gamma < 2, \\ u^{(m+1)}(0) - \displaystyle\int_0^1 xu^{(m+1)}(x)dx = \rho_0, \quad u^{(m+1)}(1) - \int_0^1 \frac{x^2}{3}u^{(m+1)}(x)dx = \rho_1. \end{cases} \tag{3.6.3}$$

Table 3.1: Maximum errors and order of convergences of Example 3.6.1.

γ	Method	$M_x = 32$	$M_x = 64$	$M_x = 128$	$M_x = 256$	$M_x = 512$	$M_x = 1024$	$M_x = 2048$
1.1	Spline	7.873e-04	1.980e-04	4.962e-05	1.241e-05	3.104e-06	7.762e-07	1.941e-07
	CO_{M_x}	1.9911	1.9968	1.9990	1.9996	1.9998	1.9999	
	FDM	1.084e-02	5.712e-03	2.933e-03	1.487e-03	7.491e-04	3.760e-04	1.884e-04
	CO_{M_x}	0.9239	0.9616	0.9798	0.9894	0.9945	0.9971	
1.2	Spline	8.079e-04	2.035e-04	5.106e-05	1.278e-05	3.198e-06	7.997e-07	1.999e-07
	CO_{M_x}	1.9892	1.9947	1.9981	1.9991	1.9995	1.9997	
	FDM	1.057e-02	5.603e-03	2.888e-03	1.469e-03	7.414e-04	3.727e-04	1.869e-04
	CO_{M_x}	0.9163	0.9562	0.9752	0.9863	0.9924	0.9958	
1.3	Spline	8.272e-04	2.095e-04	5.262e-05	1.319e-05	3.302e-06	8.264e-07	2.067e-07
	CO_{M_x}	1.9816	1.9930	1.9962	1.9978	1.9987	1.9992	
	FDM	1.025e-02	5.456e-03	2.832e-03	1.447e-03	7.333e-04	3.696e-04	1.857e-04
	CO_{M_x}	0.9103	0.9463	0.9681	0.9809	0.9885	0.9931	
1.4	Spline	8.476e-04	2.151e-04	5.422e-05	1.362e-05	3.416e-06	8.558e-07	2.142e-07
	CO_{M_x}	1.9786	1.9878	1.9929	1.9955	1.9971	1.9981	
	FDM	9.807e-03	5.257e-03	2.754e-03	1.419e-03	7.230e-04	3.660e-04	1.845e-04
	CO_{M_x}	0.8994	0.9326	0.9573	0.9723	0.9821	0.9884	
1.5	Spline	8.614e-04	2.199e-04	5.568e-05	1.404e-05	3.530e-06	8.862e-07	2.222e-07
	CO_{M_x}	1.9700	1.9815	1.9877	1.9916	1.9941	1.9959	
	FDM	9.188e-03	4.980e-03	2.639e-03	1.374e-03	7.063e-04	3.601e-04	1.825e-04
	CO_{M_x}	0.8836	0.9163	0.9419	0.9597	0.9720	0.9805	
1.6	Spline	8.639e-04	2.222e-04	5.661e-05	1.435e-05	3.624e-06	9.129e-07	2.295e-07
	CO_{M_x}	1.9593	1.9723	1.9800	1.9854	1.9891	1.9918	
	FDM	8.335e-03	4.574e-03	2.459e-03	1.298e-03	6.755e-04	3.480e-04	1.779e-04
	CO_{M_x}	0.8659	0.8956	0.9217	0.9420	0.9570	0.9680	
1.7	Spline	8.474e-04	2.196e-04	5.642e-05	1.440e-05	3.658e-06	9.262e-07	2.340e-07
	CO_{M_x}	1.9479	1.9610	1.9704	1.9767	1.9815	1.9852	
	FDM	7.164e-03	3.978e-03	2.174e-03	1.168e-03	6.179e-04	3.230e-04	1.673e-04
	CO_{M_x}	0.8488	0.8716	0.8966	0.9184	0.9357	0.9493	
1.8	Spline	8.011e-04	2.089e-04	5.402e-05	1.388e-05	3.551e-06	9.054e-07	2.302e-07
	CO_{M_x}	1.9393	1.9512	1.9604	1.9667	1.9718	1.9759	
	FDM	5.571e-03	3.114e-03	1.731e-03	9.487e-04	5.124e-04	2.732e-04	1.441e-04
	CO_{M_x}	0.8390	0.8473	0.8676	0.8886	0.9072	0.9228	
1.9	Spline	7.102e-04	1.846e-04	4.772e-05	1.229e-05	3.153e-06	8.073e-07	2.063e-07
	CO_{M_x}	1.9436	1.9519	1.9578	1.9621	1.9656	1.9687	
	FDM	3.422e-03	1.879e-03	1.053e-03	5.880e-04	3.252e-04	1.777e-04	9.604e-05
	CO_{M_x}	0.8647	0.8358	0.8402	0.8549	0.8718	0.8876	

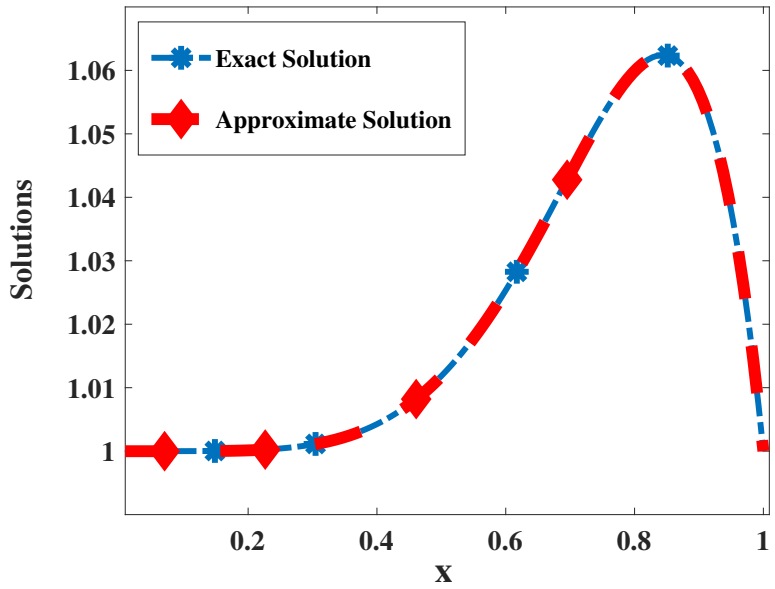

Figure 3.2: Exact vs Approximate solution for Example 3.6.1 with $M_x = 128$ and $\gamma = 1.4$.

Hence, for fixed m we solve (3.6.3) using the computation method given in (3.3.5). We use the stopping criteria given in (3.5.4).

The maximum point-wise error and the corresponding order of convergences are calculated by using the same idea as followed in Example 3.6.1.

The numerical results of Example 3.6.2 are given in Table 3.2, which indicates the second-order convergence of the proposed method to the semilinear FBVP (3.6.2). The log-log plots for Example 3.6.2 with $\gamma = 1.4$ and $\gamma = 1.8$ shown in Figure 3.3 confirm the second-order convergence of the proposed spline method. The graph of the exact and approximate solutions for $M_x = 256$ and $\gamma = 1.8$ is depicted in Figure 3.4.

Example 3.6.3. *Consider the following FBVP:*

$$\begin{cases} -{}^{C}D^{\gamma}_{0,x}u(x) + \dfrac{x^3}{3}u'(x) + \dfrac{1+x}{2}u(x) = x, \quad x \in (0,1), \\ u(0) - \displaystyle\int_0^1 x^2 u(x)dx = 1, \quad u(1) - \int_0^1 xu(x)dx = 2. \end{cases} \tag{3.6.4}$$

The exact solution of (3.6.4) is not known explicitly, therefore, to calculate the errors and the corresponding order of convergences, we use the double-mesh principle given in [27, Test Problem 2].

By using the numerical scheme given in (3.3.6)-(3.3.8), we obtain two solutions $\left\{U_i\right\}_{i=1}^{M_x+1}$

Table 3.2: Maximum errors and orders of convergence of Example 3.6.2.

γ	Method	$M_x = 32$	$M_x = 64$	$M_x = 128$	$M_x = 256$	$M_x = 512$	$M_x = 1024$	$M_x = 2048$
	Spline	1.272e-03	3.184e-04	7.954e-05	1.987e-05	4.966e-06	1.241e-06	3.103e-07
1.1	CO_{M_x}	1.9981	2.0008	2.0009	2.0006	2.0004	2.0002	
	Spline	1.452e-03	3.634e-04	9.083e-05	2.270e-05	5.673e-06	1.418e-06	3.545e-07
1.2	CO_{M_x}	1.9986	2.0003	2.0005	2.0003	2.0002	2.0001	
	Spline	1.701e-03	4.265e-04	1.067e-04	2.670e-05	6.677e-06	1.670e-06	4.175e-07
1.3	CO_{M_x}	1.9958	1.9984	1.9991	1.9995	1.9997	1.9998	
	Spline	1.999e-03	5.033e-04	1.263e-04	3.165e-05	7.924e-06	1.983e-06	4.961e-07
1.4	CO_{M_x}	1.9904	1.9946	1.9966	1.9978	1.9985	1.9990	
	Spline	2.330e-03	5.902e-04	1.487e-04	3.737e-05	9.378e-06	2.351e-06	5.888e-07
1.5	CO_{M_x}	1.9812	1.9888	1.9924	1.9946	1.9962	1.9973	
	Spline	2.672e-03	6.812e-04	1.726e-04	4.358e-05	1.098e-05	2.759e-06	6.927e-07
1.6	CO_{M_x}	1.9718	1.9805	1.9857	1.9894	1.9920	1.9940	
	Spline	2.975e-03	7.652e-04	1.953e-04	4.961e-05	1.256e-05	3.173e-06	7.998e-07
1.7	CO_{M_x}	1.9588	1.9702	1.9768	1.9816	1.9853	1.9881	
	Spline	3.179e-03	8.225e-04	2.114e-04	5.406e-05	1.378e-05	3.501e-06	8.876e-07
1.8	CO_{M_x}	1.9505	1.9604	1.9671	1.9722	1.9763	1.9798	
	Spline	3.172e-03	8.195e-04	2.107e-04	5.402e-05	1.381e-05	3.525e-06	8.979e-07
1.9	CO_{M_x}	1.9527	1.9594	1.9639	1.9674	1.9704	1.9729	

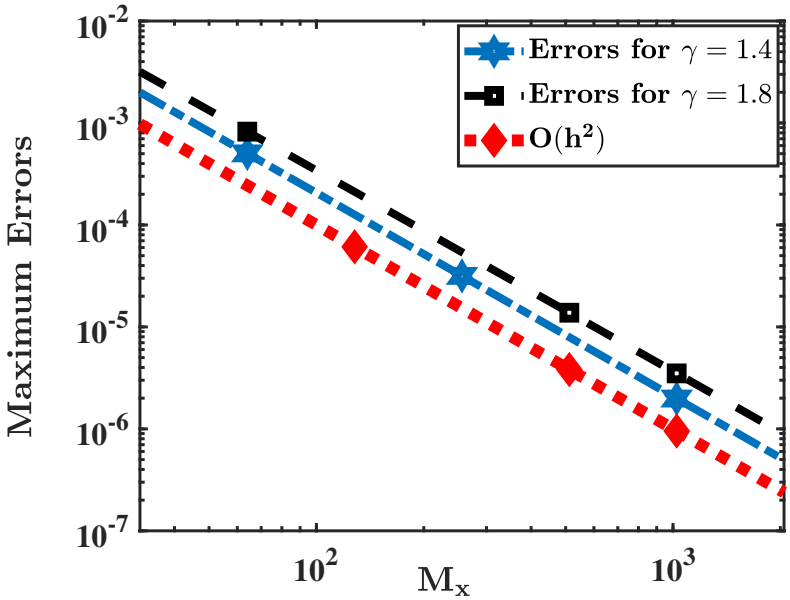

Figure 3.3: Log-log plots for Example 3.6.2 with $\gamma = 1.4$ and $\gamma = 1.8$.

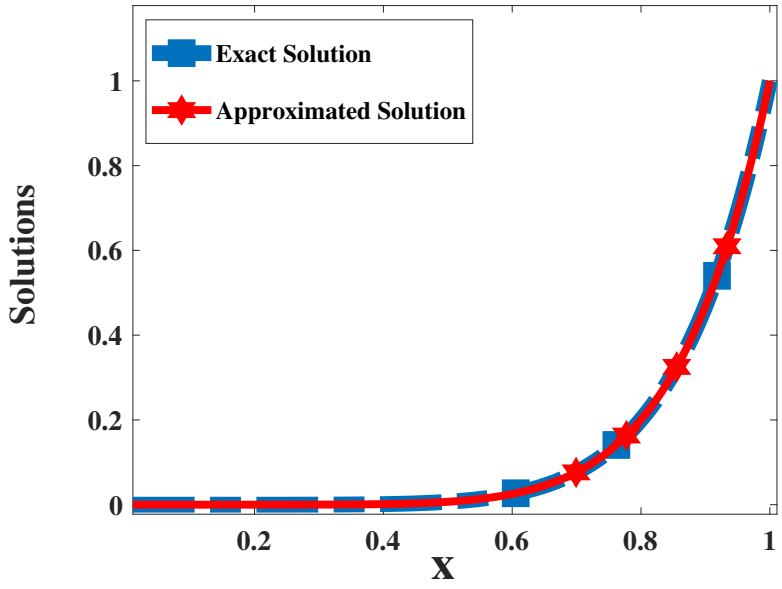

Figure 3.4: Exact vs Approximated solution for Example 3.6.2 with $M_x = 256$ and $\gamma = 1.8$.

and $\left\{\widetilde{U}_i\right\}_{i=1}^{2M_x+2}$ with uniform meshes $\{x_i\}_{i=1}^{M_x+1}$ and $\{\tilde{x}_i\}_{i=1}^{2M_x+2}$, where $x_i = \tilde{x}_{2i}$ for $i = 1, 2, \ldots, M_x + 1$.

Then, the double-mesh differences and the corresponding orders of convergence are calculated by the following double-mesh principle:

$$\widetilde{D}_{M_x} = \max_{1\le i\le M_x+1} |U_i - \widetilde{U}_{2i}|, \quad \text{and} \quad \widehat{CO}_{M_x} = \log_2\left(\frac{\widetilde{D}_{M_x}}{\widetilde{D}_{2M_x}}\right),$$

respectively.

The computed results for Example 3.6.3 are given in Table 3.3, where we compared the results between spline based scheme (3.3.5) and FDM [69]. Here also, we observed that the proposed numerical scheme (3.3.5) is of second-order convergent from the results given in Table 3.3, as well as from the log-log plots shown in Figure 3.5 for the Example 3.6.3 with $\gamma = 1.6$.

3.7 Conclusions

This chapter studies the numerical solution of FBVPs of the form (3.1.1). The numerical scheme consists of the spline approximation for the Caputo derivative, and the second-order

Table 3.3: Double-mesh differences and order of convergences of Example 3.6.3.

γ	Method	$M_x = 32$	$M_x = 64$	$M_x = 128$	$M_x = 256$	$M_x = 512$	$M_x = 1024$	$M_x = 2048$
1.1	Spline	1.177e-03	2.958e-04	7.410e-05	1.854e-05	4.637e-06	1.160e-06	2.900e-07
	$\widehat{CO}_{M_x}$	1.9917	1.9972	1.9988	1.9994	1.9996	1.9997	
	FDM	8.791e-03	4.760e-03	2.472e-03	1.259e-03	6.353e-04	3.191e-04	1.599e-04
	$\widehat{CO}_{M_x}$	0.8849	0.9452	0.9736	0.9870	0.9934	0.9967	
1.2	Spline	9.753e-04	2.451e-04	6.145e-05	1.538e-05	3.850e-06	9.630e-07	2.409e-07
	$\widehat{CO}_{M_x}$	1.9923	1.9960	1.9980	1.9987	1.9991	1.9993	
	FDM	6.157e-03	3.442e-03	1.814e-03	9.310e-04	4.716e-04	2.374e-04	1.191e-04
	$\widehat{CO}_{M_x}$	0.8391	0.9237	0.9627	0.9812	0.9904	0.9951	
1.3	Spline	8.543e-04	2.150e-04	5.392e-05	1.350e-05	3.381e-06	8.459e-07	2.116e-07
	$\widehat{CO}_{M_x}$	1.9904	1.9954	1.9972	1.9982	1.9988	1.9992	
	FDM	4.125e-03	2.415e-03	1.300e-03	6.748e-04	3.439e-04	1.737e-04	8.731e-05
	$\widehat{CO}_{M_x}$	0.7727	0.8927	0.9465	0.9724	0.9855	0.9923	
1.4	Spline	7.776e-04	1.956e-04	4.909e-05	1.230e-05	3.080e-06	7.707e-07	1.928e-07
	$\widehat{CO}_{M_x}$	1.9909	1.9946	1.9967	1.9979	1.9986	1.9990	
	FDM	2.477e-03	1.575e-03	8.794e-04	4.646e-04	2.392e-04	1.215e-04	6.128e-05
	$\widehat{CO}_{M_x}$	0.6536	0.8406	0.9203	0.9581	0.9772	0.9872	
1.5	Spline	7.263e-04	1.827e-04	4.584e-05	1.149e-05	2.877e-06	7.200e-07	1.801e-07
	$\widehat{CO}_{M_x}$	1.9912	1.9945	1.9965	1.9976	1.9984	1.9988	
	FDM	1.565e-03	8.883e-04	5.310e-04	2.898e-04	1.518e-04	7.793e-05	3.957e-05
	$\widehat{CO}_{M_x}$	0.8175	0.7422	0.8738	0.9326	0.9622	0.9778	
1.6	Spline	6.924e-04	1.740e-04	4.364e-05	1.093e-05	2.738e-06	6.854e-07	1.715e-07
	$\widehat{CO}_{M_x}$	1.9926	1.9953	1.9967	1.9976	1.9983	1.9987	
	FDM	1.642e-03	7.273e-04	3.504e-04	1.758e-04	8.949e-05	4.569e-05	2.329e-05
	$\widehat{CO}_{M_x}$	1.1745	1.0534	0.9953	0.9741	0.9699	0.9724	
1.7	Spline	6.698e-04	1.681e-04	4.215e-05	1.056e-05	2.644e-06	6.619e-07	1.656e-07
	$\widehat{CO}_{M_x}$	1.9942	1.9959	1.9970	1.9977	1.9982	1.9985	
	FDM	1.669e-03	7.452e-04	3.627e-04	1.840e-04	9.471e-05	4.887e-05	2.516e-05
	$\widehat{CO}_{M_x}$	1.1632	1.0389	0.9793	0.9579	0.9544	0.9581	
1.8	Spline	6.500e-04	1.631e-04	4.089e-05	1.024e-05	2.566e-06	6.426e-07	1.608e-07
	$\widehat{CO}_{M_x}$	1.9948	1.9959	1.9967	1.9973	1.9977	1.9984	
	FDM	1.570e-03	6.987e-04	3.421e-04	1.756e-04	9.168e-05	4.802e-05	2.508e-05
	$\widehat{CO}_{M_x}$	1.1685	1.0302	0.9624	0.9374	0.9330	0.9371	
1.9	Spline	6.315e-04	1.583e-04	3.965e-05	9.932e-06	2.487e-06	6.228e-07	1.559e-07
	$\widehat{CO}_{M_x}$	1.9965	1.9969	1.9972	1.9975	1.9977	1.9985	
	FDM	1.252e-03	5.274e-04	2.521e-04	1.292e-04	6.828e-05	3.639e-05	1.939e-05
	$\widehat{CO}_{M_x}$	1.2469	1.0649	0.9638	0.9205	0.9078	0.9087	

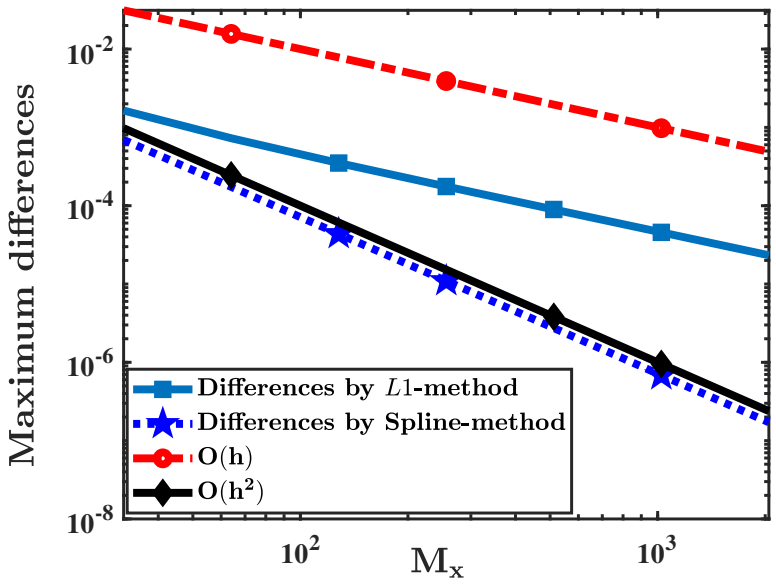

Figure 3.5: Log-log plots for Example 3.6.3 with $\gamma = 1.6$.

classical finite difference for the advection-term and trapezoidal rule for the integral-type boundary conditions. Truncation error of the proposed scheme was obtained, and stability analysis has been carried out. Second-order convergent error estimates were derived for the proposed method. Semilinear FBVPs were also solved by the proposed method after using the Newton's quasilinearization. Some numerical experiments have been carried out to validate the theoretical error estimates and efficiency of the method.

CHAPTER 4

Numerical study of nonlinear time–fractional diffusion equation

In this chapter, we focus on the numerical study of a nonlinear time-tempered **k***-Caputo fractional diffusion equation. Here, we first linearize the considered nonlinear FDE using Newton's quasilinearization technique, and then use* ${}_{\mathbf{k}}L2\text{-}1_{\sigma}$*-central-difference method to discretize the proposed model problem. Further, we study the stability analysis of the proposed scheme and derive second-order convergence result in the* L^2*-norm. Numerical experiments are carried out to validate the theoretical error bounds.*

4.1 Introduction

In this chapter, the following nonlinear time-tempered **k**-Caputo fractional diffusion equation (FDE) with variable coefficients is considered:

$$\begin{cases} {}^{C}_{\mathbf{k}}D^{\alpha,\lambda}_{0,t}u(x,t) = \mathcal{L}_{\mathcal{N}}u(x,t) - f(x,t,u), \quad (x,t) \in \mathcal{D} = \Omega_x \times \Omega_t, \\ u(x,0) = \widehat{u}_0(x), \quad x \in \overline{\Omega}_x = [x_l, x_r], \\ u(x_l,t) = 0, \quad u(x_r,t) = 0, \quad t \in \overline{\Omega}_t = [0,T], \end{cases} \tag{4.1.1}$$

where $\mathcal{L}_{\mathcal{N}} \equiv \dfrac{\partial}{\partial x}\left(\Psi(x,t)\dfrac{\partial u}{\partial x}\right)$, $0 < \alpha < 1, \Omega_x = (x_l, x_r), \Omega_t = (0,T]$, $0 < \widehat{\psi}_0 \leq \Psi(x,t) \leq \widehat{\psi}_1$ and $\partial f/\partial u > 0$ for all $(x,t) \in \overline{\mathcal{D}} = \overline{\Omega}_x \times \overline{\Omega}_t$ with $x_l = 0$ and $x_r = 1$. Given functions $\widehat{u}_0$ and f are sufficiently smooth, and the source function $f(x,t,u)$ is nonlinear in the variable $u(x,t)$.

In this chapter, we first derive the newly developed Elzaki transform of the tempered **k**-Caputo fractional derivative and apply it to find the semi-analytical solution of the given problem (4.1.1) using the Elzaki decomposition method which is a combination of Elzaki transform and Adomian decomposition method [2]. Further, we linearize the nonlinear problem (4.1.1) with the help of Newton's quasilinearization technique, and discretize the temporal term of the quasilinearized problem based on the numerical method, named as tempered ${}_{\mathbf{k}}L2\text{-}1_{\sigma}$ scheme and the spatial term by second-order central difference scheme. By analysing the stability and the error estimation in the L_2-norm, we prove the second order convergence of the proposed numerical scheme both in time and space. Numerical example with smooth solution is provided to support the theory.

The remaining part of this chapter is organized as follows: Semi-analytical solution is established in Section 4.2. The quasilinearization and the discretization technique are included in Section 4.3. Section 4.4 describes the stability and the convergence analysis of the proposed scheme. Numerical example is added in Section 4.5 and finally some conclusions are drawn in Section 4.6.

4.2 Semi-analytical solution using Elzaki decomposition method

In this section, we study the Elzaki decomposition method to find the semi-analytical solution of the nonlinear problem (4.1.1). We first derive the Elzaki transform of the tempered **k**-

Caputo fractional derivative in the following theorem.

Theorem 4.2.1. *The Elzaki transform of the tempered* $\mathbf{k}$*-Caputo fractional derivative* ${}^{C}_{\mathbf{k}}D^{\beta,\lambda}_{0,t}u(t)$ *with* $\lambda \geq 0, \mathbf{k} \geq 1$*, and* $\mathbf{n}-1 \leq \beta < \mathbf{n}$ *for* $\mathbf{n} \in \mathbb{N}$ *is given by*

$$\begin{aligned}\mathbb{E}\left({}^{C}_{\mathbf{k}}D^{\beta,\lambda}_{0,t}u(t);\nu\right) &= \frac{\Gamma\left(\mathbf{n}-\frac{\beta}{\mathbf{k}}\right)}{\mathbf{k}\Gamma_{\mathbf{k}}\left(\mathbf{n}-\frac{\beta}{\mathbf{k}}\right)}\frac{\nu^{\mathbf{n}-\frac{\beta}{\mathbf{k}}}}{(1+\lambda\nu)^{\mathbf{n}-\frac{\beta}{\mathbf{k}}}}\left[\frac{(1+\lambda\nu)^{\mathbf{n}}}{\nu^{\mathbf{n}}}\mathbb{E}\left(u(t);\nu\right)\right.\\ &\left.-\sum_{i=0}^{\mathbf{n}-1}\sum_{j=1}^{\mathbf{n}-i}\binom{\mathbf{n}}{i}\lambda^{i}\nu^{i+j+1-\mathbf{n}}\left.\frac{d^{(j-1)}u(t)}{dt^{(j-1)}}\right|_{t=0}\right],\end{aligned} \tag{4.2.1}$$

where $\binom{\mathbf{n}}{i} = \dfrac{\mathbf{n}!}{i!\,(\mathbf{n}-i)!}$ *is the binomial coefficient.*

Proof. The tempered $\mathbf{k}$-Caputo fractional derivative ${}^{C}_{\mathbf{k}}D^{\beta,\lambda}_{0,t}u(t)$ with $\mathbf{n}-1 \leq \beta < \mathbf{n}$ can be written as

$$\begin{aligned}{}^{C}_{\mathbf{k}}D^{\beta,\lambda}_{0,t}u(t) &= \frac{e^{-\lambda t}}{\mathbf{k}\Gamma_{\mathbf{k}}\left(\mathbf{n}-\frac{\beta}{\mathbf{k}}\right)}\int_0^t (t-\zeta)^{\mathbf{n}-\beta/\mathbf{k}-1}\frac{d^{\mathbf{n}}}{d\zeta^{\mathbf{n}}}\left(e^{\lambda\zeta}u(\zeta)\right)d\zeta\\ &= \frac{1}{\mathbf{k}\Gamma_{\mathbf{k}}\left(\mathbf{n}-\frac{\beta}{\mathbf{k}}\right)}\sum_{i=0}^{\mathbf{n}}\binom{\mathbf{n}}{i}\lambda^{i}\int_0^t e^{-\lambda(t-\zeta)}(t-\zeta)^{\mathbf{n}-\beta/\mathbf{k}-1}\frac{d^{\mathbf{n}-i}u(\zeta)}{d\zeta^{\mathbf{n}-i}}d\zeta\\ &= \frac{1}{\mathbf{k}\Gamma_{\mathbf{k}}\left(\mathbf{n}-\frac{\beta}{\mathbf{k}}\right)}\sum_{i=0}^{\mathbf{n}}\binom{\mathbf{n}}{i}\lambda^{i}\left(e^{-\lambda t}t^{\mathbf{n}-\beta/\mathbf{k}-1}\star u^{(\mathbf{n}-i)}(t)\right),\end{aligned} \tag{4.2.2}$$

where $u^{(r)}(t) = \dfrac{d^{r}u(t)}{dt^{r}}$.

Now applying the Elzaki transform at both sides of (4.2.2) and using the Laplace-Elzaki duality result, stated in Lemma 1.2.17, we get

$$\mathbb{E}\left({}^{C}_{\mathbf{k}}D^{\beta,\lambda}_{0,t}u(t);\nu\right) = \frac{\nu}{\mathbf{k}\Gamma_{\mathbf{k}}\left(\mathbf{n}-\frac{\beta}{\mathbf{k}}\right)}\sum_{i=0}^{\mathbf{n}}\lambda^{i}\binom{\mathbf{n}}{i}\mathbb{L}\left(e^{-\lambda t}t^{\mathbf{n}-\beta/\mathbf{k}-1};\frac{1}{\nu}\right)\mathbb{L}\left(u^{(\mathbf{n}-i)}(t);\frac{1}{\nu}\right).$$

Then, the Laplace transform and [17, Theorem (1-2)] provide the required result. □

Remark 4.2.2. *For* $\mathbf{n}=1$ *and* $0<\alpha<1$*, we have from Theorem 4.2.1*

$$\mathbb{E}\left({}^{C}_{\mathbf{k}}D^{\alpha,\lambda}_{0,t}u(t);\nu\right) = \frac{\Gamma\left(1-\frac{\alpha}{\mathbf{k}}\right)}{\mathbf{k}\Gamma_{\mathbf{k}}\left(1-\frac{\alpha}{\mathbf{k}}\right)}\frac{(1+\lambda\nu)^{\alpha/\mathbf{k}}}{\nu^{\alpha/\mathbf{k}}}\left[\mathbb{E}(u(t);\nu)-\frac{\nu^{2}}{1+\lambda\nu}u(0)\right]. \tag{4.2.3}$$

4.2.1 Elzaki decomposition method for the time-fractional diffusion equation

In this subsection, we investigate the semi-analytical solution of the TFDE (4.1.1) in the form of a series, obtained by using the Elzaki decomposition method.

Applying the Elzaki transform on both sides of the TFDE (4.1.1) with respect to t and, using Remark 4.2.2 and the given initial condition along with the linearity property of the Elzaki transform, we obtain

$$\begin{aligned}\mathbb{E}(u;\nu) &= \frac{\mathbf{k}\Gamma_{\mathbf{k}}\left(1-\frac{\alpha}{\mathbf{k}}\right)}{\Gamma\left(1-\frac{\alpha}{\mathbf{k}}\right)}\frac{\nu^{\alpha/\mathbf{k}}}{(1+\lambda\nu)^{\alpha/\mathbf{k}}}\Bigg[\mathbb{E}\left(\frac{\partial}{\partial x}\left(\Psi(x,t)\frac{\partial u}{\partial x}\right);\nu\right)-\\ &\quad \mathbb{E}\left(f(x,t,u(x,t));\nu\right)\Bigg]+\frac{\nu^2}{1+\lambda\nu}u(x,0). \end{aligned} \tag{4.2.4}$$

Thus, taking the inverse Elzaki transform we get

$$\begin{aligned}u(x,t) &= \frac{\mathbf{k}\Gamma_{\mathbf{k}}\left(1-\frac{\alpha}{\mathbf{k}}\right)}{\Gamma\left(1-\frac{\alpha}{\mathbf{k}}\right)}\mathbb{E}^{-1}\Bigg\{\frac{\nu^{\alpha/\mathbf{k}}}{(1+\lambda\nu)^{\alpha/\mathbf{k}}}\Bigg[\mathbb{E}\left(\frac{\partial}{\partial x}\left(\Psi(x,t)\frac{\partial u}{\partial x}\right);\nu\right)\\ &\quad -\mathbb{E}\left(f(x,t,u(x,t));\nu\right)\Bigg]\Bigg\}+e^{-\lambda t}u(x,0). \end{aligned} \tag{4.2.5}$$

Adomian method consists in writing the solution $u(x,t)$ of (4.1.1) as an infinite series

$$u(x,t)=\sum_{i=0}^{\infty}u_i(x,t), \tag{4.2.6}$$

provided the infinite series is uniformly convergent, and the nonlinear term can be decomposed as

$$f(x,t,u)=\sum_{i=0}^{\infty}\mathbf{H}_i, \tag{4.2.7}$$

where $\mathbf{H}_i$'s are the He's polynomials, which can be calculated by the formula:

$$\mathbf{H}_i=\frac{1}{i!}\frac{\partial^i}{\partial\theta^i}\left[f(x,t,\sum_{j=0}^{i}\theta^j u_j)\right]_{\theta=0},\quad i=0,1,2,\ldots. \tag{4.2.8}$$

Substituting (4.2.6) and (4.2.7) into (4.2.5), we get

$$\begin{aligned}\sum_{i=0}^{\infty}u_i(x,t) &= \frac{\mathbf{k}\Gamma_{\mathbf{k}}\left(1-\frac{\alpha}{\mathbf{k}}\right)}{\Gamma\left(1-\frac{\alpha}{\mathbf{k}}\right)}\mathbb{E}^{-1}\Bigg\{\frac{\nu^{\alpha/\mathbf{k}}}{(1+\lambda\nu)^{\alpha/\mathbf{k}}}\Bigg[\mathbb{E}\left(\frac{\partial}{\partial x}\left(\Psi(x,t)\sum_{i=0}^{\infty}u_{i,x}(x,t)\right);\nu\right)\\ &\quad -\mathbb{E}\left(f(x,t,u(x,t));\nu\right)\Bigg]\Bigg\}+e^{-\lambda t}u(x,0), \end{aligned} \tag{4.2.9}$$

where $u_{i,x} = \dfrac{\partial u_i}{\partial x}$.

Comparison of both sides of the equation (4.2.9) leads to

$$u_0(x,t) = e^{-\lambda t}u(x,0),$$

$$u_1(x,t) = \frac{\mathbf{k}\Gamma_{\mathbf{k}}\left(1-\frac{\alpha}{\mathbf{k}}\right)}{\Gamma\left(1-\frac{\alpha}{\mathbf{k}}\right)}\mathbb{E}^{-1}\left\{\frac{\nu^{\alpha/\mathbf{k}}}{(1+\lambda\nu)^{\alpha/\mathbf{k}}}\left[\mathbb{E}\left(\frac{\partial}{\partial x}\left(\Psi(x,t)u_{0x}(x,t)\right);\nu\right)-\mathbb{E}\left(\mathbf{H}_0;\nu\right)\right]\right\},$$

$$u_2(x,t) = \frac{\mathbf{k}\Gamma_{\mathbf{k}}\left(1-\frac{\alpha}{\mathbf{k}}\right)}{\Gamma\left(1-\frac{\alpha}{\mathbf{k}}\right)}\mathbb{E}^{-1}\left\{\frac{\nu^{\alpha/\mathbf{k}}}{(1+\lambda\nu)^{\alpha/\mathbf{k}}}\left[\mathbb{E}\left(\frac{\partial}{\partial x}\left(\Psi(x,t)u_{1x}(x,t)\right);\nu\right)-\mathbb{E}\left(\mathbf{H}_1;\nu\right)\right]\right\},$$

and so on.

Thus, in general we get the following recursive relation

$$u_{i+1}(x,t) = \frac{\mathbf{k}\Gamma_{\mathbf{k}}\left(1-\frac{\alpha}{\mathbf{k}}\right)}{\Gamma\left(1-\frac{\alpha}{\mathbf{k}}\right)}\mathbb{E}^{-1}\left\{\frac{\nu^{\alpha/\mathbf{k}}}{(1+\lambda\nu)^{\alpha/\mathbf{k}}}\left[\mathbb{E}\left(\frac{\partial}{\partial x}\left(\Psi(x,t)u_{ix}(x,t)\right);\nu\right)-\mathbb{E}\left(\mathbf{H}_i;\nu\right)\right]\right\},$$

for $i = 0, 1, 2, \ldots$.

Finally, the semi-analytical solution can be given by the following truncated series

$$u(x,t) = \lim_{i\to\infty}\left(\sum_{j=0}^{i} u_j(x,t)\right). \tag{4.2.10}$$

Convergence result of the Adomian method can be followed from [31].

4.3 Quasilinearization and discretization

In this section, we discuss the linearization process and the discretization technique of the given nonlinear equation (4.1.1).

In order to solve the model problem (4.1.1), we first use Newton's quasilinearization technique to obtain the sequence $\left\{u^{(m)}\right\}_0^\infty$ with the initial assumption $u^{(0)}$ satisfying the given initial and boundary conditions of the given problem (4.1.1). Therefore, we define $u^{(m+1)}$ for each fixed m, to be the solution of the following linear time-tempered **k**-Caputo FDE:

$$\begin{cases} {}^{C}_{\mathbf{k}}D^{\alpha,\lambda}_{0,t}u^{(m+1)}(x,t) = \mathcal{L}^{(m)}u^{(m+1)}(x,t) + g^{(m)}(x,t),\ (x,t)\in\mathcal{D}, \\ u^{(m+1)}(x,0) = \widehat{u}_0(x), \quad x\in\overline{\Omega}_x, \\ u^{(m+1)}(0,t) = 0, \quad u^{(m+1)}(1,t) = 0, \quad t\in\overline{\Omega}_t, \end{cases} \tag{4.3.1}$$

where $m = 0, 1, 2, \ldots,$

$$\mathcal{L}^{(m)}u^{(m+1)}(x,t) = \frac{\partial}{\partial x}\left(\Psi(x,t)\frac{\partial u}{\partial x}^{(m+1)}\right) - c^{(m)}(x,t)u^{(m+1)}(x,t),$$

and

$$\begin{cases} c^{(m)}(x,t) = \dfrac{\partial f}{\partial u}(x,t,u^{(m)}(x,t)), \\ g^{(m)}(x,t) = u^{(m)}(x,t)c^{(m)}(x,t) - f(x,t,u^{(m)}(x,t)). \end{cases}$$

If the initial assumption $u^{(0)}$ is chosen sufficiently close to the solution $u(x,t)$ of the equation (4.1.1), then the sequence $\left\{u^{(m)}\right\}_0^\infty$ converges quadratically [40] to the solution $u(x,t)$ of (4.1.1).

4.3.1 Time-semi discretization using tempered ${}_{\mathbf{k}}L2\text{-}1_\sigma$ scheme

On the time domain $\overline{\Omega}_t$, we consider the uniform mesh $\overline{\Omega}_t^N$ with time step size $\tau = 1/N$.

Following Alikhanov's work [7], here we have introduced a generalized parameter $\sigma_{\mathbf{k}} = 1 - \alpha/2\mathbf{k}$ that will depend on the value of $\mathbf{k}$. We discretize the tempered $\mathbf{k}$-Caputo fractional derivative ${}_{\mathbf{k}}^{C}D_{0,t}^{\alpha,\lambda}u(t)$ of the function $u(t)$ at the non-integer grid points $t_{n+\sigma_{\mathbf{k}}}$, $n = 0, 1, \ldots, N-1$ using the numerical method, namely the tempered ${}_{\mathbf{k}}L2\text{-}1_\sigma$ scheme. Then, we have

$$\begin{aligned} {}_{\mathbf{k}}^{C}D_{0,t_{n+\sigma_{\mathbf{k}}}}^{\alpha,\lambda}u(t) &= \frac{e^{-\lambda t_{n+\sigma_{\mathbf{k}}}}}{\mathbf{k}\Gamma_{\mathbf{k}}\left(1-\frac{\alpha}{\mathbf{k}}\right)}\int_0^{t_{n+\sigma_{\mathbf{k}}}} \frac{z'(\zeta)}{(t_{n+\sigma_{\mathbf{k}}}-\zeta)^{\alpha/\mathbf{k}}}\,d\zeta \\ &= \frac{e^{-\lambda t_{n+\sigma_{\mathbf{k}}}}}{\mathbf{k}\Gamma_{\mathbf{k}}\left(1-\frac{\alpha}{\mathbf{k}}\right)}\left(\sum_{j=1}^{n}\int_{t_{j-1}}^{t_j}\frac{z'(\zeta)}{(t_{n+\sigma_{\mathbf{k}}}-\zeta)^{\alpha/\mathbf{k}}}\,d\zeta + \int_{t_n}^{t_{n+\sigma_{\mathbf{k}}}}\frac{z'(\zeta)}{(t_{n+\sigma_{\mathbf{k}}}-\zeta)^{\alpha/\mathbf{k}}}\,d\zeta\right), \end{aligned}$$

where $z(\zeta) = e^{\lambda\zeta}u(\zeta)$.

By using the quadratic polynomial $\Pi_{2,j}z(\zeta)$ on each interval $[t_{j-1}, t_j]$ to approximate the function $z(\zeta)$ with the help of three discrete points $(t_{j-1}, z(t_{j-1}))$, $(t_j, z(t_j))$ and $(t_{j+1}, z(t_{j+1}))$, we get

$$\Pi_{2,j}z(\zeta) = z(t_j) - (t_j - \zeta)\left[\frac{z(t_j)-z(t_{j-1})}{\tau} + \frac{z(t_{j+1})-2z(t_j)+z(t_{j-1})}{2\tau^2}(\zeta - t_{j-1})\right],$$

$$(\Pi_{2,j}z(\zeta))' = \delta_t^+ z_{j-1} + (\zeta - t_{j-1/2})\delta_t^+\delta_t^- z_j,$$

and

$$z(\zeta) - \Pi_{2,j}z(\zeta) = \frac{z'''(\widehat{\zeta}_j)}{6}(\zeta - t_{j-1})(\zeta - t_j)(\zeta - t_{j+1}), \quad \text{for} \quad \widehat{\zeta}_j \in (t_{j-1}, t_j),$$

where we have used the following notations

$$\delta_t^+ z_j = \frac{z(t_{j+1}) - z(t_j)}{\tau}, \quad \delta_t^- z_j = \frac{z(t_j) - z(t_{j-1})}{\tau}, \quad \text{and} \quad t_{j-1/2} = t_{j-1} + \tau/2.$$

In the interval $[t_n, t_{n+\sigma_{\mathbf{k}}}]$, the linear interpolation $\Pi_{1,n} z(\zeta)$ is used to approximate the function $z(\zeta)$. Then, the approximation of ${}_{\mathbf{k}}^{C}D_{0,t_{n+\sigma_{\mathbf{k}}}}^{\alpha,\lambda} u(t)$ at the point $t = t_{n+\sigma_{\mathbf{k}}}$ can be written as

$$\begin{aligned}
{}_{\mathbf{k}}^{C}D_{0,t_{n+\sigma_{\mathbf{k}}}}^{\alpha,\lambda} u(\zeta) &\approx {}_{\mathbf{k}}\partial_{0,t_{n+\sigma_{\mathbf{k}}}}^{\alpha,\lambda} u(\zeta) \\
&= \frac{e^{-\lambda t_{n+\sigma_{\mathbf{k}}}}}{\mathbf{k}\Gamma_{\mathbf{k}}\left(1-\frac{\alpha}{\mathbf{k}}\right)} \left(\sum_{j=1}^{n} \int_{t_{j-1}}^{t_j} \frac{(\Pi_{2,j} z(\zeta))'}{(t_{n+\sigma_{\mathbf{k}}} - \zeta)^{\alpha/\mathbf{k}}}\, d\zeta + \int_{t_n}^{t_{n+\sigma_{\mathbf{k}}}} \frac{(\Pi_{1,n} z(\zeta))'}{(t_{n+\sigma_{\mathbf{k}}} - \zeta)^{\alpha/\mathbf{k}}}\, d\zeta \right) \\
&= \frac{e^{-\lambda t_{n+\sigma_{\mathbf{k}}}}}{\mathbf{k}\Gamma_{\mathbf{k}}\left(1-\frac{\alpha}{\mathbf{k}}\right)} \left(\sum_{j=1}^{n} \int_{t_{j-1}}^{t_j} \frac{\delta_t^+ z_{j-1} + (\zeta - t_{j-1/2})\delta_t^+ \delta_t^- z_j}{(t_{n+\sigma_{\mathbf{k}}} - \zeta)^{\alpha/\mathbf{k}}}\, d\zeta \right. \\
&\quad \left. + \delta_t^+ z_n \int_{t_n}^{t_{n+\sigma_{\mathbf{k}}}} \frac{d\zeta}{(t_{n+\sigma_{\mathbf{k}}} - \zeta)^{\alpha/\mathbf{k}}} \right) \\
&= e^{-\lambda t_{n+\sigma_{\mathbf{k}}}} \tau^{1-\alpha/\mathbf{k}} \left\{ \sum_{j=1}^{n} \left(p_{n-j+1}^{(\alpha,\mathbf{k},\sigma_{\mathbf{k}})} \delta_t^+ z_{j-1} + \tau q_{n-j+1}^{(\alpha,\mathbf{k},\sigma_{\mathbf{k}})} \delta_t^+ \delta_t^- z_j \right) + p_0^{(\alpha,\mathbf{k},\sigma_{\mathbf{k}})} \delta_t^+ z_n \right\} \\
&= e^{-\lambda t_{n+\sigma_{\mathbf{k}}}} \tau^{1-\alpha/\mathbf{k}} \sum_{j=0}^{n} r_{n-j}^{(\alpha,\mathbf{k},\sigma_{\mathbf{k}})} \delta_t^+ z_j \\
&= e^{-\lambda t_{n+\sigma_{\mathbf{k}}}} \tau^{-\alpha/\mathbf{k}} \left[r_0^{(\alpha,\mathbf{k},\sigma_{\mathbf{k}})} z_{n+1} - \sum_{j=0}^{n} \left(r_{n-j}^{(\alpha,\mathbf{k},\sigma_{\mathbf{k}})} - r_{n-j+1}^{(\alpha,\mathbf{k},\sigma_{\mathbf{k}})} \right) z_j - r_n^{(\alpha,\mathbf{k},\sigma_{\mathbf{k}})} z_0 \right] \\
&= e^{-\lambda t_{n+\sigma_{\mathbf{k}}}} \tau^{-\alpha/\mathbf{k}} \left[r_0^{(\alpha,\mathbf{k},\sigma_{\mathbf{k}})} e^{\lambda t_{n+1}} u(t_{n+1}) - \right. \\
&\quad \left. \sum_{j=0}^{n} \left(r_{n-j}^{(\alpha,\mathbf{k},\sigma_{\mathbf{k}})} - r_{n-j+1}^{(\alpha,\mathbf{k},\sigma_{\mathbf{k}})} \right) e^{\lambda t_j} u(t_j) - r_n^{(\alpha,\mathbf{k},\sigma_{\mathbf{k}})} e^{\lambda t_0} u(t_0) \right], \qquad (4.3.2)
\end{aligned}$$

where

$$p_0^{(\alpha,\mathbf{k},\sigma_{\mathbf{k}})} = \frac{\sigma_{\mathbf{k}}^{1-\alpha/\mathbf{k}}}{\mathbf{k}\Gamma_{\mathbf{k}}\left(1-\frac{\alpha}{\mathbf{k}}+k\right)}, \quad p_l^{(\alpha,\mathbf{k},\sigma_{\mathbf{k}})} = \frac{(l+\sigma_{\mathbf{k}})^{1-\alpha/\mathbf{k}} - (l+\sigma_{\mathbf{k}}-1)^{1-\alpha/\mathbf{k}}}{\mathbf{k}\Gamma_{\mathbf{k}}\left(1-\frac{\alpha}{\mathbf{k}}+k\right)}, \; l \geq 1,$$

$$\begin{aligned}
q_l^{(\alpha,\mathbf{k},\sigma_{\mathbf{k}})} &= \frac{1}{\mathbf{k}\Gamma_{\mathbf{k}}\left(1-\frac{\alpha}{\mathbf{k}}+k\right)} \left[\frac{(l+\sigma_{\mathbf{k}})^{2-\alpha/\mathbf{k}} - (l+\sigma_{\mathbf{k}}-1)^{2-\alpha/\mathbf{k}}}{2-\frac{\alpha}{\mathbf{k}}} - \right. \\
&\quad \left. \frac{1}{2}\left\{ (l+\sigma_{\mathbf{k}})^{1-\alpha/\mathbf{k}} + (l+\sigma_{\mathbf{k}}-1)^{1-\alpha/\mathbf{k}} \right\} \right]. \qquad (4.3.3)
\end{aligned}$$

For $n=0$, we have $r_0^{(\alpha,\mathbf{k},\sigma_\mathbf{k})}=p_0^{(\alpha,\mathbf{k},\sigma_\mathbf{k})}$, and for $n\geq 1$, we have

$$r_l^{(\alpha,\mathbf{k},\sigma_\mathbf{k})}=\begin{cases} p_0^{(\alpha,\mathbf{k},\sigma_\mathbf{k})}+q_1^{(\alpha,\mathbf{k},\sigma_\mathbf{k})}, & l=0,\\ p_l^{(\alpha,\mathbf{k},\sigma_\mathbf{k})}+q_{l+1}^{(\alpha,\mathbf{k},\sigma_\mathbf{k})}-q_l^{(\alpha,\mathbf{k},\sigma_\mathbf{k})}, & 1\leq l\leq n-1,\\ p_n^{(\alpha,\mathbf{k},\sigma_\mathbf{k})}-q_n^{(\alpha,\mathbf{k},\sigma_\mathbf{k})}, & l=n. \end{cases} \tag{4.3.4}$$

The following lemma gives the truncation error of the tempered ${}_\mathbf{k}L2\text{-}1_\sigma$ scheme.

Lemma 4.3.1. *The truncation error of the tempered ${}_\mathbf{k}L2\text{-}1_\sigma$ scheme (4.3.2) with $u(t)\in \mathcal{C}^3[0,t_{n+1}]$, $0\leq n\leq N-1$, gives*

$$\left|{}_{\mathbf{k}}^{C}D_{0,t_{n+\sigma_\mathbf{k}}}^{\alpha,\lambda}u-{}_\mathbf{k}\partial_{0,t_{n+\sigma_\mathbf{k}}}^{\alpha,\lambda}u\right|\leq\mathcal{O}(\tau^{3-\frac{\alpha}{\mathbf{k}}}).$$

Proof. We estimate the truncation error in the similar way to [7]. Let us first denote the truncation error of the estimate (4.3.2) as follows:

$$\mathcal{T}^{n+\sigma_\mathbf{k}}={}_{\mathbf{k}}^{C}D_{0,t_{n+\sigma_\mathbf{k}}}^{\alpha,\lambda}u-{}_\mathbf{k}\partial_{0,t_{n+\sigma_\mathbf{k}}}^{\alpha,\lambda}u. \tag{4.3.5}$$

Now, we write $\mathcal{T}^{n+\sigma_\mathbf{k}}=\mathcal{T}_1^{n+\sigma_\mathbf{k}}+\mathcal{T}_n^{n+\sigma_\mathbf{k}}$, where

$$\begin{aligned}\mathcal{T}_1^{n+\sigma_\mathbf{k}} &= \frac{e^{-\lambda t_{n+\sigma_\mathbf{k}}}}{\mathbf{k}\Gamma_\mathbf{k}\left(1-\frac{\alpha}{\mathbf{k}}\right)}\sum_{j=1}^{n}\int_{t_{j-1}}^{t_j}\frac{(z(\zeta)-\Pi_{2,j}z(\zeta))'}{(t_{n+\sigma_\mathbf{k}}-\zeta)^{\alpha/\mathbf{k}}}\,d\zeta\\ &= \frac{-\alpha e^{-\lambda t_{n+\sigma_\mathbf{k}}}}{6\mathbf{k}^2\Gamma_\mathbf{k}\left(1-\frac{\alpha}{\mathbf{k}}\right)}\sum_{j=1}^{n}\int_{t_{j-1}}^{t_j}z'''(\widehat{\zeta_j})(\zeta-t_{j-1})(\zeta-t_j)(\zeta-t_{j+1})(t_{n+\sigma_\mathbf{k}}-\zeta)^{-\alpha/\mathbf{k}-1}\,d\zeta,\end{aligned}$$

and thus, we have

$$\begin{aligned}\left|\mathcal{T}_1^{n+\sigma_\mathbf{k}}\right| &\leq \frac{\alpha\left|z'''(t)\right|\tau^3}{3\mathbf{k}^2\Gamma_\mathbf{k}\left(1-\frac{\alpha}{\mathbf{k}}\right)}\int_0^{t_n}(t_{n+\sigma_\mathbf{k}}-\zeta)^{-\alpha/\mathbf{k}-1}\,d\zeta\\ &= \frac{\left|z'''(t)\right|\tau^{3-\frac{\alpha}{\mathbf{k}}}}{3\mathbf{k}\Gamma_\mathbf{k}\left(1-\frac{\alpha}{\mathbf{k}}\right)}\left[\sigma_\mathbf{k}^{-\alpha/\mathbf{k}}-(n+\sigma_\mathbf{k})^{-\alpha/\mathbf{k}}\right]\\ &\leq \frac{\left|z'''(t)\right|\sigma_\mathbf{k}^{-\alpha/\mathbf{k}}}{3\mathbf{k}\Gamma_\mathbf{k}\left(1-\frac{\alpha}{\mathbf{k}}\right)}\tau^{3-\frac{\alpha}{\mathbf{k}}},\quad t\in(0,t_n),\end{aligned} \tag{4.3.6}$$

and

$$\begin{aligned}\mathcal{T}_n^{n+\sigma_\mathbf{k}} &= \frac{e^{-\lambda t_{n+\sigma_\mathbf{k}}}}{\mathbf{k}\Gamma_\mathbf{k}\left(1-\frac{\alpha}{\mathbf{k}}\right)}\int_{t_n}^{t_{n+\sigma_\mathbf{k}}}\frac{(z(\zeta)-\Pi_{1,n}z(\zeta))'}{(t_{n+\sigma_\mathbf{k}}-\zeta)^{\alpha/\mathbf{k}}}\,d\zeta\\ &= \frac{e^{-\lambda t_{n+\sigma_\mathbf{k}}}}{\mathbf{k}\Gamma_\mathbf{k}\left(1-\frac{\alpha}{\mathbf{k}}\right)}\int_{t_n}^{t_{n+\sigma_\mathbf{k}}}\frac{z'(t_{n+1/2})-\delta_t^+z_n}{(t_{n+\sigma_\mathbf{k}}-\zeta)^{\alpha/\mathbf{k}}}\,d\zeta\\ &\quad+\frac{e^{-\lambda t_{n+\sigma_\mathbf{k}}}}{\mathbf{k}\Gamma_\mathbf{k}\left(1-\frac{\alpha}{\mathbf{k}}\right)}z''(t_{n+1/2})\int_{t_n}^{t_{n+\sigma_\mathbf{k}}}\frac{(\zeta-t_{n+1/2})}{(t_{n+\sigma_\mathbf{k}}-\zeta)^{\alpha/\mathbf{k}}}\,d\zeta+\mathcal{O}(\tau^{3-\frac{\alpha}{\mathbf{k}}}).\end{aligned}$$

Then, using $\sigma_{\mathbf{k}} = 1 - \alpha/2\mathbf{k}$, one gets

$$\mathcal{T}_n^{n+\sigma_{\mathbf{k}}} = \mathcal{O}(\tau^{3-\frac{\alpha}{\mathbf{k}}}). \tag{4.3.7}$$

Hence, combining (4.3.6) and (4.3.7), one can obtain the required result. □

4.3.2 Spatial discretization and fully-discrete scheme

We consider the finite difference approximation on a uniform mesh $\overline{\Omega}_x^{M_x}$ at the *n-th* time level.

Then, the discretized form of the domain $\overline{\mathcal{D}}$ is given as

$$\overline{\mathcal{D}}_{M_x}^N = \{(x_i, t_n) : i = 0, 1, \ldots, M_x;\ n = 0, 1, \ldots, N\}.$$

Let $u(x,t) \in \mathcal{C}_{x,t}^{4,3}(\overline{\Omega}_x)$ be the exact solution of the given model problem (4.1.1) and ϑ_i^n be the approximated value of $u_i^n = u(x_i, t_n)$ at the point $(x_i, t_n) \in \overline{\mathcal{D}}_{M_x}^N$, where $\mathcal{C}_{x,t}^{4,3}(\overline{\Omega}_x)$ denotes the space of the function $u(x,t)$ such that $u(x,t) \in \mathcal{C}^4(\overline{\Omega}_x) \cap \mathcal{C}^3(\overline{\Omega}_t)$.

Thus, the fully-discretized form of the quasilinearized problem (4.3.1) at the point $(x_i, t_{n+\sigma_{\mathbf{k}}})$ is

$$ {}_{\mathbf{k}}\partial_{0,t_{n+\sigma_{\mathbf{k}}}}^{\alpha,\lambda} \vartheta_i^{(m+1),n} = \Lambda \vartheta_i^{(m+1),n+\sigma_{\mathbf{k}}} + g_i^{(m),n+\sigma_{\mathbf{k}}}, \tag{4.3.8}$$

where

$$\begin{aligned}
\Lambda\vartheta_i^{(m+1),n+\sigma_{\mathbf{k}}} &= \left(\left(\Psi\vartheta_x^{(m+1)}\right)_x - c^{(m)}\vartheta^{(m+1)}\right)(x_i, t_{n+\sigma_{\mathbf{k}}}) \\
&= \frac{\Psi_{i-1/2}^{n+\sigma_{\mathbf{k}}}\,\vartheta_{i-1}^{(m+1),n+\sigma_{\mathbf{k}}} - \left(\Psi_{i-1/2}^{n+\sigma_{\mathbf{k}}} + \Psi_{i+1/2}^{n+\sigma_{\mathbf{k}}}\right)\vartheta_i^{(m+1),n+\sigma_{\mathbf{k}}} + \Psi_{i+1/2}^{n+\sigma_{\mathbf{k}}}\,\vartheta_{i+1}^{(m+1),n+\sigma_{\mathbf{k}}}}{h_x^2} \\
&\quad - c_i^{(m),n+\sigma_{\mathbf{k}}}\vartheta_i^{(m+1),n+\sigma_{\mathbf{k}}} + \mathcal{O}(h_x^2) \\
&= \frac{\chi_i^{n+\sigma_{\mathbf{k}}}\,\vartheta_{i-1}^{(m+1),n+\sigma_{\mathbf{k}}} - \left(\chi_i^{n+\sigma_{\mathbf{k}}} + \chi_{i+1}^{n+\sigma_{\mathbf{k}}}\right)\vartheta_i^{(m+1),n+\sigma_{\mathbf{k}}} + \chi_{i+1}^{n+\sigma_{\mathbf{k}}}\,\vartheta_{i+1}^{(m+1),n+\sigma_{\mathbf{k}}}}{h_x^2} \\
&\quad - c_i^{(m),n+\sigma_{\mathbf{k}}}\vartheta_i^{(m+1),n+\sigma_{\mathbf{k}}} + \mathcal{O}(h_x^2),
\end{aligned}$$

for $i = 1, 2, \ldots, M_x - 1$, and $\dfrac{\partial^3\Psi}{\partial x^3} \in \mathcal{C}(\overline{\Omega}_x)$, $\Psi_i^{n+\sigma_{\mathbf{k}}} = \Psi(x_i, t_{n+\sigma_{\mathbf{k}}})$, $\chi_i = \Psi_{i-1/2}$, $\vartheta_i^{(m+1),n+\sigma_{\mathbf{k}}} = \sigma_{\mathbf{k}}\vartheta_i^{(m+1),n+1} + (1-\sigma_{\mathbf{k}})\,\vartheta_i^{(m+1),n} + \mathcal{O}(\tau^2)$, $c_i^{(m),n+\sigma_{\mathbf{k}}} = c^{(m)}(x_i, t_{n+\sigma_{\mathbf{k}}})$, and $g_i^{(m),n+\sigma_{\mathbf{k}}} = g^{(m)}(x_i, t_{n+\sigma_{\mathbf{k}}})$.

Hence, considering the Lemma 4.3.1, the truncation error of the difference scheme (4.3.8) can be written as

$$|\mathcal{T}_i^{m,n+\sigma_{\mathbf{k}}}| = \mathcal{O}(h_x^2 + \tau^2). \tag{4.3.9}$$

Lemma 4.3.2. *For $l = 1, 2, 3 \ldots$, the following inequality holds*

$$\frac{1}{2} < \Theta_l < \frac{1}{2 - \alpha/\mathbf{k}},$$

where

$$\Theta_l = \frac{(l+\sigma_\mathbf{k})^{2-\alpha/\mathbf{k}} - (l+\sigma_\mathbf{k}-1)^{2-\alpha/\mathbf{k}} - (2-\alpha/\mathbf{k})\,(l+\sigma_\mathbf{k}-1)^{1-\alpha/\mathbf{k}}}{(2-\alpha/\mathbf{k})\left[(l+\sigma_\mathbf{k})^{1-\alpha/\mathbf{k}} - (l+\sigma_\mathbf{k}-1)^{1-\alpha/\mathbf{k}}\right]}.$$

Proof. The proof can be done in the similar fashion as given in [7]. □

Remark 4.3.3. *The coefficient q_l as defined in (4.3.3) can be reformed as*

$$q_l^{(\alpha,\mathbf{k},\sigma_\mathbf{k})} = \frac{\Theta_l - 1/2}{\mathbf{k}\Gamma_\mathbf{k}\left(1 - \frac{\alpha}{\mathbf{k}} + k\right)}\left[(l+\sigma_\mathbf{k})^{1-\alpha/\mathbf{k}} - (l+\sigma_\mathbf{k}-1)^{1-\alpha/\mathbf{k}}\right]. \tag{4.3.10}$$

In the following lemma, we discuss some properties of the coefficient $r^{(\alpha,\mathbf{k},\sigma_\mathbf{k})}$, defined in (4.3.4).

Lemma 4.3.4. *For any $\alpha \in (0,1)$, $r_l^{(\alpha,\mathbf{k},\sigma_\mathbf{k})}$, for $0 \le l \le i$, satisfies the following relations*

$$(i) \quad r_i^{(\alpha,\mathbf{k},\sigma_\mathbf{k})} > \frac{(i+\sigma_\mathbf{k})^{-\alpha/\mathbf{k}}}{2\mathbf{k}\Gamma_\mathbf{k}\left(1 - \frac{\alpha}{\mathbf{k}}\right)}, \tag{4.3.11}$$

$$(ii) \quad r_0^{(\alpha,\mathbf{k},\sigma_\mathbf{k})} > r_1^{(\alpha,\mathbf{k},\sigma_\mathbf{k})} > \ldots > r_i^{(\alpha,\mathbf{k},\sigma_\mathbf{k})} > 0, \tag{4.3.12}$$

$$(iii) \quad \tau^{-\alpha/\mathbf{k}} r_i^{(\alpha,\mathbf{k},\sigma_\mathbf{k})} > \frac{1}{2T^{\frac{\alpha}{\mathbf{k}}}\mathbf{k}\Gamma_\mathbf{k}\left(1 - \frac{\alpha}{\mathbf{k}}\right)}, \tag{4.3.13}$$

$$(iv) \quad (2\sigma_\mathbf{k} - 1)\,\xi_i^{(\alpha,\mathbf{k},\sigma_\mathbf{k})} - \sigma_\mathbf{k}\xi_{i-1}^{(\alpha,\mathbf{k},\sigma_\mathbf{k})} > 0,\ i = 1, 2, \ldots M_x, \tag{4.3.14}$$

where $\xi_n^{(\alpha,\mathbf{k},\sigma_\mathbf{k})} = r_{i-n}^{(\alpha,\mathbf{k},\sigma_\mathbf{k})},\ 0 \le n \le i.$

Proof. Following the similar path as given in [7], from (4.3.4), we have

$$\begin{aligned} r_i^{(\alpha,\mathbf{k},\sigma_\mathbf{k})} &= p_i^{(\alpha,\mathbf{k},\sigma_\mathbf{k})} - q_i^{(\alpha,\mathbf{k},\sigma_\mathbf{k})} \\ &= \frac{(i+\sigma_\mathbf{k})^{1-\alpha/\mathbf{k}} - (i+\sigma_\mathbf{k}-1)^{1-\alpha/\mathbf{k}}}{\mathbf{k}\Gamma_\mathbf{k}\left(1 - \frac{\alpha}{\mathbf{k}} + k\right)}\left(\frac{3}{2} - \Theta_i\right), \text{ for } i \ge 1. \end{aligned}$$

Then, using Lemma 4.3.2, one has

$$\begin{aligned} r_i^{(\alpha,\mathbf{k},\sigma_\mathbf{k})} &> \frac{(i+\sigma_\mathbf{k})^{1-\alpha/\mathbf{k}} - (i+\sigma_\mathbf{k}-1)^{1-\alpha/\mathbf{k}}}{\mathbf{k}\Gamma_\mathbf{k}\left(1 - \frac{\alpha}{\mathbf{k}} + k\right)}\left(\frac{3}{2} - \frac{1}{2-\alpha/\mathbf{k}}\right) \\ &> \frac{1}{2\mathbf{k}\Gamma_\mathbf{k}\left(1 - \frac{\alpha}{\mathbf{k}}\right)}\int_0^1 (i+\sigma_\mathbf{k}-\zeta)^{-\alpha/\mathbf{k}}\,d\zeta \\ &> \frac{1}{2\mathbf{k}\Gamma_\mathbf{k}\left(1 - \frac{\alpha}{\mathbf{k}}\right)}(i+\sigma_\mathbf{k})^{-\alpha/\mathbf{k}}, \end{aligned} \tag{4.3.15}$$

which is the required result (i).

The bound given in (iii) can be proved directly from (i) since $(i+\sigma_{\mathbf{k}})\tau = t_{i+\sigma_{\mathbf{k}}}$.

For the results (ii) and (iv), one can follow [7]. □

4.4 Stability and convergence analysis

In this section, we will be analysing the stability as well as the convergence of the proposed scheme (4.3.8) for our model problem (4.1.1).

We first denote the space of mesh functions as follows

$$\mathcal{Y}_h^{(m+1)} = \left\{\Theta_h^{(m+1)} = \left\{\Theta_0^{(m+1)}, \Theta_1^{(m+1)}, \ldots, \Theta_{M_x}^{(m+1)}\right\} | \Theta_0^{(m+1)} = 0 = \Theta_{M_x}^{(m+1)}\right\}.$$

For two mesh functions $\Theta_h^{(m+1)}, \varphi_h^{(m+1)} \in \mathcal{Y}_h^{(m+1)}$, we define the discrete inner product as $\langle \Theta_h^{(m+1)}, \varphi_h^{(m+1)} \rangle = h_x \sum_{i=0}^{M_x} \Theta_i^{(m+1)} \varphi_i^{(m+1)}$, the discrete L_2-norm $\|\cdot\|_2$ as $\left\|\Theta_h^{(m+1)}\right\|_2 = \sqrt{\langle \Theta_h^{(m+1)}, \Theta_h^{(m+1)} \rangle}$ and the discrete H^1-semi norm $|\cdot|_1$ as $\left|\Theta_h^{(m+1)}\right|_1 = \sqrt{h_x \sum_{i=0}^{M_x-1} \left(\delta_x^{\frac{1}{2}} \Theta_{i+1/2}^{(m+1)}\right)^2}$, where $\delta_x^{\frac{1}{2}} \Theta_{i+1/2}^{(m+1)} = \dfrac{\Theta_{i+1}^{(m+1)} - \Theta_i^{(m+1)}}{h_x}$.

Before proceeding towards the stability result, we state the following lemmas that will be used later.

Lemma 4.4.1. *([53]) Since $\Psi \geq \widehat{\psi}_0 > 0$ and $c^{(m)}(x,t)$ is positive for all $(x,t) \in \overline{\mathcal{D}}$, then for any mesh function $\vartheta_h^{(m+1)} \in \mathcal{Y}_h^{(m+1)}$, we have*

$$\begin{aligned} -\langle \Lambda \vartheta_h^{(m+1)}, \vartheta_h^{(m+1)} \rangle &= h_x \sum_{i=0}^{M_x-1} \Psi_{i+1/2} \left(\delta_x^{\frac{1}{2}} \vartheta_{i+1/2}^{(m+1)}\right)^2 + h_x \sum_{i=1}^{M_x-1} c_i^{(m)} \left(\vartheta_i^{(m+1)}\right)^2 \\ &\geq \widehat{\psi}_0 \left|\vartheta_h^{(m+1)}\right|_1^2. \end{aligned} \tag{4.4.1}$$

Lemma 4.4.2. *([94]) If the condition (iv), given by equation (4.3.14) of Lemma 4.3.4 holds and a function $u(t)$ is defined in the space $\overline{\Omega}_t^N$, then we have*

$$\langle {}_{\mathbf{k}}\partial_{0,t_{n+\sigma_{\mathbf{k}}}}^{\alpha,\lambda} u^n, u^{n+\sigma_{\mathbf{k}}} \rangle \geq \frac{1}{2} e^{-\lambda t_{n+1}} {}_{\mathbf{k}}\partial_{0,t_{n+\sigma_{\mathbf{k}}}}^{\alpha,\lambda} \left\|u^n\right\|_2^2. \tag{4.4.2}$$

We discuss the stability of the difference scheme (4.3.8) in the following theorem.

Theorem 4.4.3. *The numerical scheme (4.3.8) is unconditionally stable under the L_2-norm and there holds the following a priori bound*

$$\left\|\vartheta^{(m+1),n+1}\right\|_2^2 \leq e^{\lambda T}\left[\left\|\vartheta^{(m+1),0}\right\|_2^2 + \frac{\mathbf{k}\Gamma_{\mathbf{k}}\left(1-\frac{\alpha}{\mathbf{k}}\right)}{4\widehat{\psi}_0}T^{\alpha/\mathbf{k}}\max_{0\leq n\leq N-1}\left\|g^{(m+1),n+\sigma_{\mathbf{k}}}\right\|_2^2\right]. \tag{4.4.3}$$

Proof. We take the inner product at the both sides of (4.3.8) with $\vartheta_i^{(m+1),n+\sigma_{\mathbf{k}}}$ to get

$$\langle {}_{\mathbf{k}}\partial_{0,t_{n+\sigma_{\mathbf{k}}}}^{\alpha,\lambda}\vartheta^{(m+1),n}, \vartheta^{(m+1),n+\sigma_{\mathbf{k}}}\rangle - \langle \Lambda\vartheta^{(m+1),n+\sigma_{\mathbf{k}}}, \vartheta^{(m+1),n+\sigma_{\mathbf{k}}}\rangle = \langle g^{m,n+\sigma_{\mathbf{k}}}, \vartheta^{(m+1),n+\sigma_{\mathbf{k}}}\rangle.$$

Using the Lemma 4.4.1 and Lemma 4.4.2, we get from the above equality

$$\begin{aligned}
&\langle g^{m,n+\sigma_{\mathbf{k}}}, \vartheta^{(m+1),n+\sigma_{\mathbf{k}}}\rangle \\
&\geq \frac{1}{2}e^{-\lambda t_{n+1}}{}_{\mathbf{k}}\partial_{0,t_{n+\sigma_{\mathbf{k}}}}^{\alpha,\lambda}\left\|\vartheta^{(m+1),n}\right\|_2^2 + \widehat{\psi}_0\left|\vartheta^{(m+1),n+\sigma_{\mathbf{k}}}\right|_1^2 \\
&= \frac{\tau^{-\alpha/\mathbf{k}}}{2}e^{-\lambda(t_{n+1}+t_{n+\sigma_{\mathbf{k}}})}\Big[-r_n^{(\alpha,\mathbf{k},\sigma_{\mathbf{k}})}\left\|\vartheta^{(m+1),0}\right\|_2^2 - \sum_{j=1}^{n}\left(r_{n-j}^{(\alpha,\mathbf{k},\sigma_{\mathbf{k}})} - r_{n-j+1}^{(\alpha,\mathbf{k},\sigma_{\mathbf{k}})}\right)e^{\lambda t_n}\left\|\vartheta^{(m+1),n}\right\|_2^2 \\
&+ r_0^{(\alpha,\mathbf{k},\sigma_{\mathbf{k}})}\left\|\vartheta^{(m+1),n+1}\right\|_2^2 e^{\lambda t_{n+1}}\Big] + \widehat{\psi}_0\left|\vartheta^{(m+1),n+\sigma_{\mathbf{k}}}\right|_1^2.
\end{aligned} \tag{4.4.4}$$

Now, using the Young's inequality and [53, Remark 4] with $\widehat{\varepsilon} = 4\widehat{\psi}_0$, we have

$$\begin{aligned}
\langle g^{m,n+\sigma_{\mathbf{k}}}, \vartheta^{(m+1),n+\sigma_{\mathbf{k}}}\rangle &\leq \frac{\left\|g^{m,n+\sigma_{\mathbf{k}}}\right\|_2^2}{4\widehat{\varepsilon}}\widehat{\varepsilon}\left\|\vartheta^{(m+1),n+\sigma_{\mathbf{k}}}\right\|_2^2 \quad \forall\,\widehat{\varepsilon}>0 \\
&\leq \frac{\left\|g^{m,n+\sigma_{\mathbf{k}}}\right\|_2^2}{4\widehat{\varepsilon}} + \frac{\widehat{\varepsilon}\left|\vartheta^{(m+1),n+\sigma_{\mathbf{k}}}\right|_1^2}{4}.
\end{aligned} \tag{4.4.5}$$

Then, we have

$$\begin{aligned}
r_0^{(\alpha,\mathbf{k},\sigma_{\mathbf{k}})}\left\|\vartheta^{(m+1),n+1}\right\|_2^2 e^{\lambda t_{n+1}} &\leq \tau^{\alpha/\mathbf{k}}e^{\lambda(t_{n+1}+t_{n+\sigma_{\mathbf{k}}})}\frac{\left\|g^{m,n+\sigma_{\mathbf{k}}}\right\|_2^2}{8\widehat{\psi}_0} + r_n^{(\alpha,\mathbf{k},\sigma_{\mathbf{k}})}\left\|\vartheta^{(m+1),0}\right\|_2^2 \\
&+ \sum_{j=1}^{n}\left(r_{n-j}^{(\alpha,\mathbf{k},\sigma_{\mathbf{k}})} - r_{n-j+1}^{(\alpha,\mathbf{k},\sigma_{\mathbf{k}})}\right)e^{\lambda t_n}\left\|\vartheta^{(m+1),n}\right\|_2^2 \\
&\leq r_n^{(\alpha,\mathbf{k},\sigma_{\mathbf{k}})}e^{2\lambda t_{n+1}}\left(\left\|\vartheta^{(m+1),0}\right\|_2^2 + \frac{\left\|g^{m,n+\sigma_{\mathbf{k}}}\right\|_2^2}{8\widehat{\psi}_0 r_n^{(\alpha,\mathbf{k},\sigma_{\mathbf{k}})}}\tau^{\alpha/\mathbf{k}}\right) \\
&+ \sum_{j=1}^{n}\left(r_{n-j}^{(\alpha,\mathbf{k},\sigma_{\mathbf{k}})} - r_{n-j+1}^{(\alpha,\mathbf{k},\sigma_{\mathbf{k}})}\right)e^{\lambda t_n}\left\|\vartheta^{(m+1),n}\right\|_2^2.
\end{aligned}$$

The equation (4.3.11) of Lemma 4.3.4 delivers

$$r_0^{(\alpha,\mathbf{k},\sigma_\mathbf{k})}\left\|\vartheta^{(m+1),n+1}\right\|_2^2 e^{\lambda t_{n+1}} \leq r_n^{(\alpha,\mathbf{k},\sigma_\mathbf{k})}e^{2\lambda t_{n+1}}\left(\left\|\vartheta^{(m+1),0}\right\|_2^2+\frac{T^{\alpha/\mathbf{k}}\mathbf{k}\Gamma_\mathbf{k}\left(1-\frac{\alpha}{\mathbf{k}}\right)}{4\widehat{\psi}_0}\left\|g^{m,n+\sigma_\mathbf{k}}\right\|_2^2\right)$$
$$+\sum_{j=1}^{n}\left(r_{n-j}^{(\alpha,\mathbf{k},\sigma_\mathbf{k})}-r_{n-j+1}^{(\alpha,\mathbf{k},\sigma_\mathbf{k})}\right)e^{\lambda t_n}\left\|\vartheta^{(m+1),n}\right\|_2^2.$$

Now, to prove

$$\left\|\vartheta^{(m+1),n+1}\right\|_2^2 \leq e^{\lambda t_{n+1}}\mathcal{W}_\mathbf{k}, \tag{4.4.6}$$

where

$$\mathcal{W}_\mathbf{k}=\left[\left\|\vartheta^{(m+1),0}\right\|_2^2+\frac{\mathbf{k}\Gamma_\mathbf{k}\left(1-\frac{\alpha}{\mathbf{k}}\right)}{4\widehat{\psi}_0}T^{\alpha/\mathbf{k}}\max_{0\leq n\leq N-1}\left\|g^{(m+1),n+\sigma_\mathbf{k}}\right\|_2^2\right],$$

we use the mathematical induction.

For $n=0$ in (4.4.3), we can see the result (4.4.6) is true. Suppose the result (4.4.6) is true up to n. Then, we have

$$r_0^{(\alpha,\mathbf{k},\sigma_\mathbf{k})}\left\|\vartheta^{(m+1),n+1}\right\|_2^2 e^{\lambda t_{n+1}} \leq r_n^{(\alpha,\mathbf{k},\sigma_\mathbf{k})}e^{2\lambda t_{n+1}}\mathcal{W}_\mathbf{k}+\sum_{j=1}^{n}\left(r_{n-j}^{(\alpha,\mathbf{k},\sigma_\mathbf{k})}-r_{n-j+1}^{(\alpha,\mathbf{k},\sigma_\mathbf{k})}\right)e^{\lambda t_n}e^{\lambda t_n}\mathcal{W}_\mathbf{k}$$
$$\leq e^{2\lambda t_{n+1}}\left[r_n^{(\alpha,\mathbf{k},\sigma_\mathbf{k})}+\sum_{j=1}^{n}\left(r_{n-j}^{(\alpha,\mathbf{k},\sigma_\mathbf{k})}-r_{n-j+1}^{(\alpha,\mathbf{k},\sigma_\mathbf{k})}\right)\right]\mathcal{W}_\mathbf{k}, \tag{4.4.7}$$

which yields $r_0^{(\alpha,\mathbf{k},\sigma_\mathbf{k})}\left\|\vartheta^{(m+1),n+1}\right\|_2^2 e^{\lambda t_{n+1}} \leq r_0^{(\alpha,\mathbf{k},\sigma_\mathbf{k})}e^{2\lambda t_{n+1}}\mathcal{W}_\mathbf{k}$, and hence the required result (4.4.3) can be obtained. □

4.4.1 Convergence analysis

In this subsection, we establish the convergence result for the proposed difference scheme (4.3.8). Let us assume that the error term $\mathcal{E}_i^{(m+1),n}=u_i^{(m+1),n}-\vartheta_i^{(m+1),n}$ for $(x_i,t_n)\in\overline{\mathcal{D}}_{M_x}^N$. The following theorem provides the point-wise convergence result for the proposed scheme in the L_2-norm.

Theorem 4.4.4. *If $u_i^{(m+1),n}$ is the solution of (4.3.1) and $\vartheta_i^{(m+1),n}$ is the solution of the difference scheme (4.3.8) at the point $(x_i,t_n), 0\leq i\leq M_x, 0\leq n\leq N$, then we have*

$$\left\|\mathcal{E}^{(m+1),n+1}\right\|_2 \leq \frac{1}{2}\sqrt{\frac{e^{\lambda T}\,\mathbf{k}\Gamma_\mathbf{k}\left(1-\frac{\alpha}{\mathbf{k}}\right)T^{\alpha/\mathbf{k}}}{\widehat{\psi}_0}}\,\mathcal{O}\left(h_x^2+\tau^2\right). \tag{4.4.8}$$

Proof. It is clear that the error term $\mathcal{E}_i^{(m+1),n}$ satisfies the following equation:

$$ {}_{\mathbf{k}}\partial_{0,t_{n+\sigma_{\mathbf{k}}}}^{\alpha,\lambda}\mathcal{E}_i^{(m+1),n} = \Lambda\mathcal{E}_i^{(m+1),n+\sigma_{\mathbf{k}}} + \mathcal{T}_i^{m,n+\sigma_{\mathbf{k}}}, \tag{4.4.9} $$

with the initial error term $\mathcal{E}_i^{(m+1),0} = 0$.

Invoking Theorem 4.4.3, we can arrive at

$$ \left\|\mathcal{E}^{(m+1),n}\right\|_2^2 \leq e^{\lambda T}\,\frac{\mathbf{k}\Gamma_{\mathbf{k}}\left(1-\frac{\alpha}{\mathbf{k}}\right)}{4\widehat{\psi}_0}\,T^{\alpha/\mathbf{k}}\max_{0\leq n\leq N-1}\left\|\mathcal{T}^{(m+1),n+\sigma_{\mathbf{k}}}\right\|_2^2, \tag{4.4.10} $$

and with the help of (4.3.9), the required result can be established. □

4.5 Experimental results

In this section a numerical example is presented to show the efficiency of the proposed scheme and to validate the theoretical analysis for different values of the parameters α, k and λ.

Since the convergence order $\mathcal{O}(h_x^2)$ for the spatial term is standard, so we only examine the errors in the temporal direction due to the tempered ${}_{\mathbf{k}}L2\text{-}1_\sigma$ method of the tempered $\mathbf{k}$-Caputo fractional derivative. We define the discrete error under the L_2-norm $\|.\|_2$ as

$$ E_{M_x}^N = \max_{1\leq n\leq N}\left\|u(t_n) - \vartheta^{(m+1),n}\right\|_2, $$

and the corresponding convergence order is given by

$$ CO_N = \log_2\left(\frac{E_{M_x}^N}{E_{2M_x}^{2N}}\right). $$

Also, for each fixed m, the quasilinearized problem (4.3.1) is first solved by using the proposed scheme (4.3.8) and then for the Newton's quasilinearization technique we use the following convergence criterion

$$ \left|u^{(m+1)}(x,t) - u^{(m)}(x,t)\right| \leq \text{tol}, \quad (x,t)\in\overline{\mathcal{D}}, \quad m\geq 0. \tag{4.5.1} $$

We have chosen tol $= 10^{-8}$ for our computational purposes.

Example 4.5.1. *Consider the time-tempered* $\mathbf{k}$*-Caputo FDE:*

$$ \begin{cases} {}_{\mathbf{k}}^{C}D_{0,t}^{\alpha,\lambda}u(x,t) = \dfrac{\partial}{\partial x}\left(\Psi(x,t)\dfrac{\partial u}{\partial x}\right) - f(x,t,u(x,t)), & (x,t)\in\mathcal{D}, \\ u(x,0) = \sin(\pi x), & x\in\overline{\Omega}_x, \\ u(0,t) = 0, \quad u(1,t) = 0, & t\in\overline{\Omega}_t, \end{cases} \tag{4.5.2} $$

where the coefficient and the nonlinear source term are respectively given by

$$\Psi(x,t) = 2 - \cos(xt), \quad f(x,t,u(x,t)) = \exp(u(x,t)) + \widehat{\xi}(x,t),$$

and the function $\widehat{\xi}(x,t)$ is such that the exact solution of the problem (4.5.2) is $u(x,t) = e^{-\lambda t}\sin(\pi x)(t^{3+\alpha} + 3t^2 + 1)$.

The errors $E^N_{M_x}$ and order of convergences CO_N of Example 4.5.1 are presented in Table 4.1. Figure 4.1 portrays the numerical solutions for $M_x = N = 80$. Figure 4.2 shows the numerical solutions for different values of the tempering parameter λ of the Example 4.5.1 and it can be noticed that the peak of the numerical solutions is higher for the small values of λ. The log-log plots are displayed in Figure 4.3.

Table 4.1: L_2 error and order of convergences of Example 4.5.1 with $M_x = N$.

k = 4												
	$\lambda = 3$						$\lambda = 6$					
	$\alpha = 0.3$		$\alpha = 0.6$		$\alpha = 0.9$		$\alpha = 0.3$		$\alpha = 0.6$		$\alpha = 0.9$	
N	$E^N_{M_x}$	CO_N	$E^N_{M_x}$	CO_N	$E^N_{M_x}$	CO_N	$E^N_{M_x}$	CO_N	$E^N_{M_x}$	CO_N	$E^N_{M_x}$	CO_N
10	2.430e-03	– –	1.781e-03	– –	1.610e-03	– –	4.412e-04	– –	3.672e-03	– –	6.900e-03	–
20	6.517e-04	1.899	4.534e-04	1.974	4.077e-04	1.981	1.314e-04	1.748	1.151e-03	1.674	2.159e-03	1.676
40	1.693e-04	1.944	1.1467e-04	1.983	1.029e-03	1.987	3.679e-05	1.837	3.241e-04	1.829	6.055e-04	1.834
80	4.316e-05	1.972	2.884e-05	1.991	2.584e-05	1.993	9.831e-06	1.904	8.603e-05	1.913	1.600e-04	1.920
160	1.089e-05	1.987	7.231e-06	1.996	6.474e-06	1.997	2.548e-06	1.948	2.213e-05	1.959	4.097e-05	1.965
k = 7												
	$\lambda = 3$						$\lambda = 6$					
	$\alpha = 0.3$		$\alpha = 0.6$		$\alpha = 0.9$		$\alpha = 0.3$		$\alpha = 0.6$		$\alpha = 0.9$	
N	$E^N_{M_x}$	CO_N	$E^N_{M_x}$	CO_N	$E^N_{M_x}$	CO_N	$E^N_{M_x}$	CO_N	$E^N_{M_x}$	CO_N	$E^N_{M_x}$	CO_N
10	2.981e-03	– –	2.282e-03	– –	1.852e-03	– –	9.512e-04	– –	9.064e-04	– –	2.770e-03	– –
20	8.165e-04	1.868	6.057e-04	1.914	4.758e-04	1.961	3.109e-04	1.613	2.791e-04	1.699	8.686e-04	1.673
40	2.145e-04	1.928	1.565e-04	1.952	1.207e-04	1.979	8.836e-05	1.815	7.869e-05	1.827	2.450e-04	1.826
80	5.502e-05	1.963	3.978e-05	1.976	3.040e-05	1.989	2.348e-05	1.912	2.100e-05	1.905	6.520e-05	1.910
160	1.393e-05	1.982	1.002e-05	1.988	7.630e-06	1.994	6.045e-06	1.958	5.432e-06	1.951	1.681e-05	1.955

4.6 Conclusions

This chapter focuses on the semi-analytical and numerical solutions of a nonlinear time-tempered **k**-Caputo FDE. The Elzaki decomposition method was considered to find the semi-analytical solution of the model problem (4.1.1). The model problem (4.1.1) has been linearized using Newton's quasilinearization method and to discretize the quasilinearized problem (4.3.1), a numerical scheme namely tempered ${}_{\mathbf{k}}L2\text{-}1_\sigma$ method has been proposed. The stability and convergence analysis of the fully discretized problem (4.3.8) have been

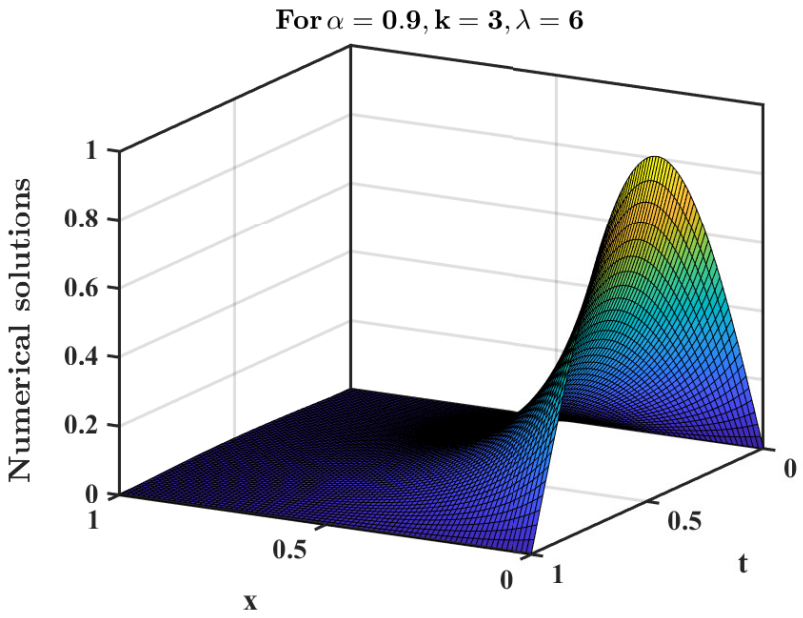

Figure 4.1: Numerical solutions of Example 4.5.1 for $M_x = N = 80$.

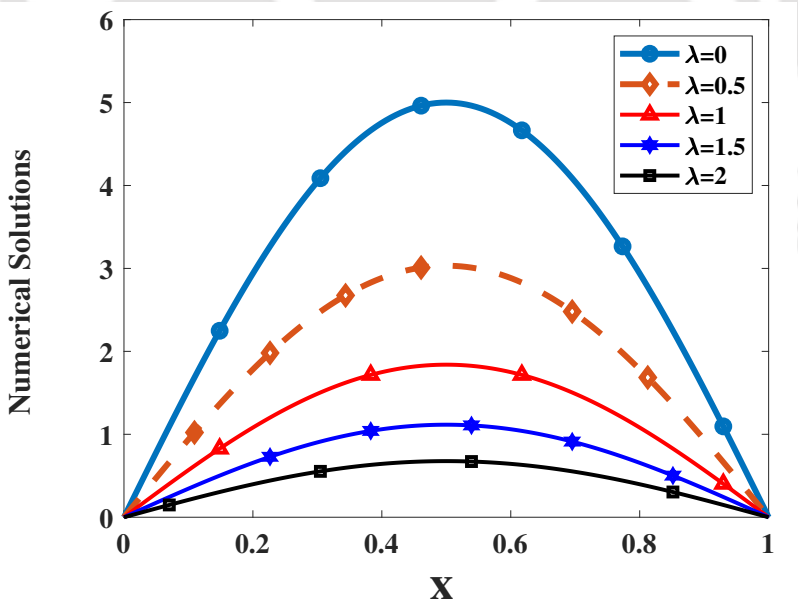

Figure 4.2: Numerical solutions for different values of the tempering parameter λ of Example 4.5.1 at $T = 1, \alpha = 0.6$, and $\mathbf{k} = 7$.

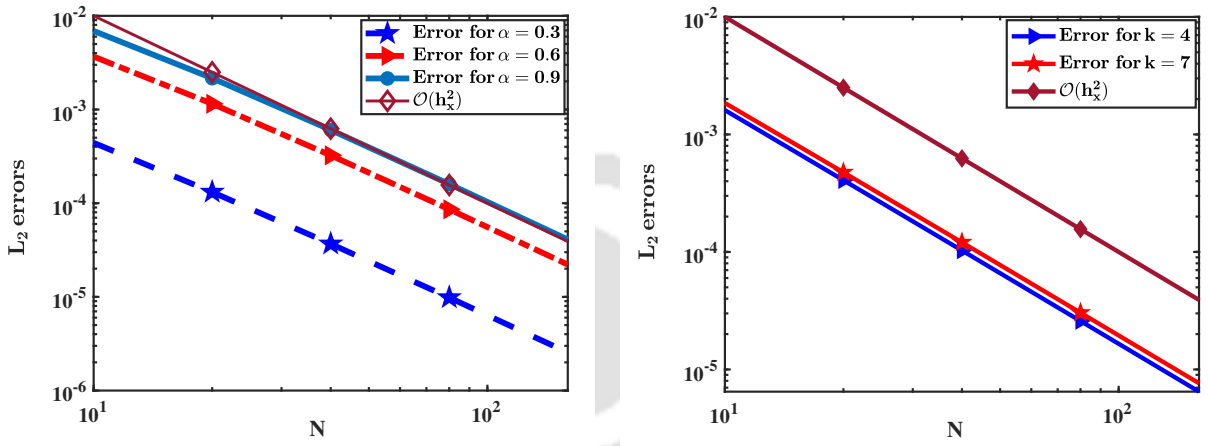

(a) $\mathbf{k} = 4, \lambda = 6$ (b) $\alpha = 0.9, \lambda = 3$

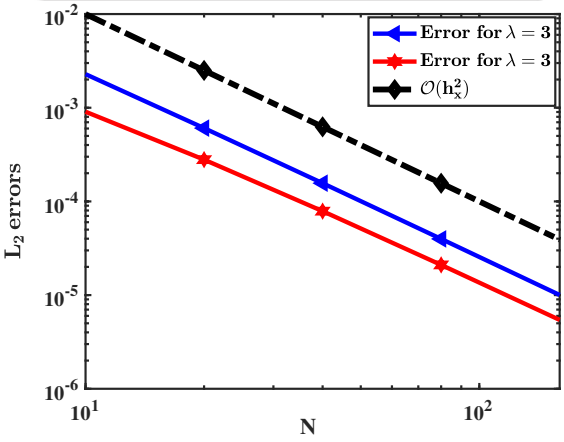

(c) $\alpha = 0.6, \mathbf{k} = 7$

Figure 4.3: Log-log plots corresponding to Table 4.1.

carried out in the L_2-norm using the energy method, and the second-order convergence in both time and space has been substantiated in the theoretical analysis. In support of the theoretical results, a numerical experiment has been appended.

CHAPTER 5

Error estimate for nonlinear time-fractional diffusion equation with generalized memory kernel

In this chapter, we focus on the numerical study of a nonlinear TFDE with generalized memory kernel. To study the numerical solution of this model problem, we first linearize the model problem and then use the well-known L1-method to discretize the generalized Caputo time-fractional derivative term in graded mesh. Further, we develop a generalized discrete fractional Grönwall inequality to study the stability analysis and to derive the error estimate result for the fully-discrete scheme in the discrete L^2-norm. Lastly, a few numerical experiments are addressed to justify the theoretical error estimates.

5.1 Introduction

In this chapter, we consider the following nonlinear time-fractional diffusion equations with generalized memory kernel:

$$\begin{cases} {}^{C}D_{0,t}^{\alpha,\omega(t)}u(x,t) = \mathcal{L}_{\mathcal{N}}u(x,t) - f(x,t,u),\ (x,t) \in \mathcal{D} = \Omega_x \times \Omega_t, \\ u(x,0) = \widehat{u}_0(x), \quad x \in \overline{\Omega}_x = [x_l, x_r], \\ u(x_l,t) = 0, \quad u(x_r,t) = 0, \quad t \in \overline{\Omega}_t = [0,T], \end{cases} \tag{5.1.1}$$

where $\mathcal{L}_{\mathcal{N}}u \equiv \dfrac{\partial}{\partial x}\Big(\Psi(x,t)\dfrac{\partial u}{\partial x}\Big)$, $\Omega_x = (x_l, x_r)$ and $\Omega_t = (0,T]$, $0 < \widehat{\psi}_0 \leq \Psi(x,t) \leq \widehat{\psi}_1$. The functions $\widehat{u}_0(x)$ and f are sufficiently smooth, and the source function $f(x,t,u)$ is nonlinear in the variable $u(x,t)$ with the condition $\dfrac{\partial f}{\partial u} < 0$.

Memory is defined as a output at current time that also depends on the history of change of input on a finite or infinite time interval. Memory is described by the functions that are called memory functions and these are the kernel of an integro-differential operator. These are also known as power-law memory in the study of fractional calculus. The fractional derivatives are preferable over the derivatives of positive integer orders in describing processes with memory, and for this reason various works based on memory type kernel are being taken into consideration in the recent days.

The main result of this chapter is to comprise the generalized discrete fractional Grönwall inequality for non-uniform generalized $L1$-scheme. Further, this inequality is taken into account to establish the stability for the fully discrete scheme, and under the following regularity condition on the solution $u(x,t)$

$$\left\|\frac{\partial^4 u}{\partial x^4}\right\|_{L^2(\overline{\Omega}_x)} \leq C, \quad \text{and} \quad \left\|\frac{\partial^l u}{\partial t^l}\right\|_{L^2(\overline{\Omega}_x)} \leq C\left(1 + t^{\alpha-l}\right), \quad l = 0,1,2, \tag{5.1.2}$$

an optimal time accuracy is proved in non-uniform mesh with order $\mathcal{O}\left(N^{\alpha-2}\right)$, where N is an integer to be used in discretization of the time interval $\overline{\Omega}_t$. Some numerical calculations are put in to corroborate the theoretical aspects.

The remaining part of this chapter is decorated as follows: in Section 5.2, we include the quasilinearization technique and the discretization process by $L1$-method, and also we introduce the complementary discrete generalized memory kernel to develop the generalized discrete fractional Grönwall inequality in this section. The fully discrete scheme is incorporated in Section 5.3, and further the stability and the error analysis are studied. Section 5.4 contains some numerical experiments in support of the theoretical estimation. Finally some conclusions are drawn in Section 5.5.

5.2 Discretization method and discrete inequality

This section is devoted to address the quasilinearization technique and discretization method for the given nonlinear equation (5.1.1). Therewith, the generalized discrete fractional Grönwall inequality will also be vindicated at the end of this section.

5.2.1 Quasilinearization technique

To deal with the given nonlinear problem (5.1.1), the use of Newton's quasilinearization process is taken into account to obtain a sequence $\left\{u^{(m)}\right\}_0^\infty$ with the initial assumption $u^{(0)}$ satisfying the given initial and boundary conditions of the given equation (5.1.1). Thus we can define $u^{(m+1)}$ for each fixed non-negative integer m, to be the solution of the following quasilinearized problem:

$$\begin{cases} {}^{C}D_{0,t}^{\alpha,\omega(t)}\vartheta(x,t) = \mathcal{L}^{(m)}\vartheta(x,t) + g^{(m)}(x,t),\ (x,t)\in\mathcal{D}, \\ \vartheta(x,0) = \widehat{u_0}(x), \quad x\in\overline{\Omega}_x, \\ \vartheta(x_l,t) = 0, \quad \vartheta(x_r,t) = 0, \quad t\in\overline{\Omega}_t, \end{cases} \tag{5.2.1}$$

where $\vartheta(x,t) = u^{(m+1)}(x,t)$,

$$\mathcal{L}^{(m)}\vartheta(x,t) = \frac{\partial}{\partial x}\left(\Psi(x,t)\frac{\partial\vartheta(x,t)}{\partial x}\right) + c^{(m)}(x,t)\vartheta(x,t),$$

and

$$\begin{cases} c^{(m)}(x,t) = -\dfrac{\partial f}{\partial u}(x,t,u^{(m)}(x,t)) > 0, \\ g^{(m)}(x,t) = -u^{(m)}(x,t)c^{(m)}(x,t) - f(x,t,u^{(m)}(x,t)). \end{cases}$$

Convergence of the quasilinearized problem

If the initial assumption $u^{(0)}$ is chosen sufficiently close to the solution $u(x,t)$ of the equation (5.1.1), then the sequence $\left\{u^{(m)}\right\}_0^\infty$ converges quadratically [40] to the solution $u(x,t)$ of (5.1.1).

Also for each fixed $m \geq 0$, the quasilinearized problem will converge under the Newton's quasilinearization technique with following convergence criterion

$$\left|\vartheta(x,t) - u^{(m)}(x,t)\right| \leq \text{tol}, \quad (x,t)\in\overline{\mathcal{D}}, \quad m\geq 0. \tag{5.2.2}$$

We will choose tol $= 10^{-8}$ for our computational purposes.

5.2.2 Time semi-discretization

We use graded mesh for temporal discretization to deal with the non-smoothness of the solution at the point $t = 0$. The graded mesh has the advantage in the analysis of non-smooth solution as it helps to concentrate the grid points near $t = 0$. To this end, let $N > 0$ be an integer. On the time domain $\overline{\Omega}_t$, we consider the partition $\overline{\Omega}_t^N$ of the time-interval with the non-uniform time-step size $\tau_n = t_n - t_{n-1}$. Define $t_n = T\,(n/N)^r$ for $n = 1, \ldots, N$, with a user-chosen mesh grading parameter $r \geq 1$. Note that if $r = 1$, then the mesh is uniform. Observe that

$$\tau_{n+1} = T\left(\frac{n+1}{N}\right)^r - T\left(\frac{n}{N}\right)^r \leq CTN^{-r}n^{r-1} \text{ for } n = 0, 1, \ldots, N-1, \tag{5.2.3}$$

with the following assumption

$$\frac{\tau_k}{\tau_{k+1}} \leq 1, \ k = 1, 2, \ldots, N-1. \tag{5.2.4}$$

Now, we follow [42] to approximate the generalized Caputo derivative ${}^{C}D_{0,t_n}^{\alpha,\omega(t)}\vartheta(t)$ at the point $t = t_n$ by using a generalized version of the popular $L1-$method on the graded time-domain $\overline{\Omega}_t^N$ as follows

$$\begin{aligned}
{}^{C}D_{0,t_n}^{\alpha,\omega(t)}\vartheta(t) &= \frac{1}{\Gamma(1-\alpha)}\int_0^{t_n}\frac{\omega(t_n-\zeta)}{(t_n-\zeta)^\alpha}\vartheta'(\zeta)\,d\zeta \\
&= \frac{1}{\Gamma(1-\alpha)}\left[\sum_{k=1}^{n}\int_{t_{k-1}}^{t_k}\frac{\omega(t_n-\zeta)}{(t_n-\zeta)^\alpha}\frac{\vartheta(t_k)-\vartheta(t_{k-1})}{\tau_k}\,d\zeta\right. \\
&\quad \left.+\sum_{k=1}^{n}\int_{t_{k-1}}^{t_k}\frac{\omega(t_n-\zeta)\big(\vartheta(\zeta)-\Pi_{1,k}\vartheta(\zeta)\big)'}{(t_n-\zeta)^\alpha}\,d\zeta\right].
\end{aligned}$$

Now, using the transformation $\zeta \to t_{k-1} + z\,\tau_k$, we get

$$d\zeta = z\tau_k \quad \text{and} \quad \omega(t_n-\zeta) = \widehat{\Psi} + \big(\omega(t_n - t_{k-1} - z\tau_k) - \widehat{\Psi}\big),$$

where

$$\widehat{\Psi} = \omega\left(t_n - t_{k-1} - \frac{\tau_k}{2}\right) + \Big[\omega(t_n - t_k) - \omega(t_n - t_{k-1})\Big](z - 1/2).$$

Thus, we have

$$\begin{aligned} {}^{C}D^{\alpha,\omega(t)}_{0,t_n}\vartheta(t) &= \frac{1}{\Gamma(2-\alpha)}\sum_{k=1}^{n}\big(\vartheta(t_k)-\vartheta(t_{k-1})\big)\Big[\omega\Big(t_n-t_{k-1}-\frac{\tau_k}{2}\Big)q^{(n)}_{n-k} \\ &\quad +\big(\omega(t_n-t_k)-\omega(t_n-t_{k-1})\big)r^{(n)}_{n-k}\Big]+\mathcal{T}^n_d+\mathcal{T}^n_\omega \\ &= \sum_{k=1}^{n}s^{(n)}_{n-k}\big(\vartheta(t_k)-\vartheta(t_{k-1})\big)+\mathcal{T}^n_d+\mathcal{T}^n_\omega, \end{aligned} \tag{5.2.5}$$

where

$$\Pi_{1,k}\vartheta(\zeta) = \vartheta(t_k)\frac{\zeta-t_{k-1}}{\tau_k}-\vartheta(t_{k-1})\frac{\zeta-t_k}{\tau_k}, \tag{5.2.6}$$

$$q^{(n)}_{n-k} = \frac{(t_n-t_{k-1})^{1-\alpha}-(t_n-t_k)^{1-\alpha}}{\tau_k}, \tag{5.2.7}$$

$$r^{(n)}_{n-k} = \frac{1}{\tau_k^2}\left(\frac{1}{2-\alpha}\big[(t_n-t_{k-1})^{2-\alpha}-(t_n-t_k)^{2-\alpha}\big]-\frac{\tau_k}{2}\big[(t_n-t_{k-1})^{1-\alpha}+(t_n-t_k)^{1-\alpha}\big]\right), \tag{5.2.8}$$

$$\mathcal{T}^n_d = \frac{1}{\Gamma(1-\alpha)}\sum_{k=1}^{n}\int_{t_{k-1}}^{t_k}\frac{\omega(t_n-\zeta)(\vartheta(\zeta)-\Pi_{1,k}\vartheta(\zeta))'}{(t_n-\zeta)^\alpha}\,d\zeta, \tag{5.2.9}$$

$$\mathcal{T}^n_\omega = \frac{1}{\Gamma(1-\alpha)}\sum_{k=1}^{n}(\vartheta(t_k)-\vartheta(t_{k-1}))\int_0^1\frac{\omega\big(t_n-t_{k-1}-z\tau_k\big)-\widehat{\Psi}}{(t_n-t_{k-1}-z\tau_k)^\alpha}\,dz, \tag{5.2.10}$$

and

$$s^{(n)}_{n-k} = \frac{1}{\Gamma(2-\alpha)}\left[\omega\Big(t_n-t_{k-1}-\frac{\tau_k}{2}\Big)q^{(n)}_{n-k}+\big(\omega(t_n-t_k)-\omega(t_n-t_{k-1})\big)r^{(n)}_{n-k}\right]. \tag{5.2.11}$$

Therefore, the numerical approximation by using $L1$ formula on non-uniform mesh is

$$\triangle^{\alpha,\omega(t)}_{0,t_n}\vartheta(t) = \sum_{k=1}^{n}s^{(n)}_{n-k}\big(\vartheta(t_k)-\vartheta(t_{k-1})\big). \tag{5.2.12}$$

5.2.3 Some properties

In this subsection, we discuss some properties of the coefficients $q^{(n)}, r^{(n)}$ and $s^{(n)}$:

Lemma 5.2.1. *[42] For any $n = 1, 2, \ldots, N$, the coefficients $q_{n-k}^{(n)}$ and $r_{n-k}^{(n)}$ with $\alpha \in (0,1)$ satisfy the following inequalities*

$$q_0^{(n)} > q_1^{(n)} > \ldots > q_{n-1}^{(n)} > \frac{1-\alpha}{(t_n - t_0)^\alpha},$$

and

$$r_0^{(n)} > r_1^{(n)} > \ldots > r_{n-1}^{(n)} > 0.$$

Lemma 5.2.2. *[42] For any $n = 1, 2, \ldots, N$, the coefficient $s_{n-k}^{(n)}$, $\alpha \in (0,1)$ and $\omega(t) \in \mathcal{C}^2(\overline{\Omega}_t)$ where $\omega(t) > 0$, $\omega'(t) \leq 0$ for all $t \in \overline{\Omega}_t$, the following inequality holds*

$$s_0^{(n)} > s_1^{(n)} > \ldots > s_{n-1}^{(n)} > \frac{\omega(t_n - t_0 - \frac{\tau_1}{2})}{\Gamma(1-\alpha)(t_n - t_0)^\alpha} > 0.$$

5.2.4 Complementary discrete kernel and discrete fractional Grönwall inequality

We first introduce the complementary discrete generalized memory kernels in this subsection. The following property of the generalized memory kernel $\mathcal{Q}_{1-\alpha}(t-\xi)$ says that

$$\sum_{j=k}^{n} \int_{t_{j-1}}^{t_j} \mathcal{Q}_\alpha(t_n - \zeta)\, \mathcal{Q}_{1-\alpha}(\zeta - t_{k-1})\, d\zeta = \mathcal{Q}_1(t_n - t_{k-1}) = \omega(t_n - t_{k-1}), \tag{5.2.13}$$

and it inspires us to define the discrete generalized memory kernels (DGMKs) $\mathcal{H}_{n-j}^{(n)}$ with the following identical property:

$$\sum_{j=k}^{n} \mathcal{H}_{n-j}^{(n)}\, s_{j-k}^{(j)} \equiv \omega(t_n - t_{k-1}), \tag{5.2.14}$$

which can be rewritten in the recursion relation such as

$$\mathcal{H}_0^{(n)} = \frac{\omega(\tau_n)}{s_0^{(n)}}, \quad \mathcal{H}_{n-k}^{(n)} = \frac{\omega(t_n - t_{k-1})}{s_0^{(k)}} \sum_{j=k+1}^{n} \mathcal{H}_{n-j}^{(n)} \left(\frac{s_{j-k-1}^{(j)}}{\omega(t_n - t_k)} - \frac{s_{j-k}^{(j)}}{\omega(t_n - t_{k-1})} \right), \quad \text{for } 1 \leq k \leq n-1. \tag{5.2.15}$$

Corollary 5.2.3. *In the similar way to the relation* (5.2.13)*, we can find that*

$$\int_0^{t_n} \mathcal{Q}_\alpha(t_n - \zeta) \left({}^C D_{0,t}^{\alpha,\omega(t)} \psi \right)(\zeta)\, d\zeta = \sum_{k=1}^{n} \int_{t_{k-1}}^{t_k} \psi'(\zeta) \omega(t_n - \zeta) d\zeta. \tag{5.2.16}$$

We next study some properties of the DGMKs $\mathcal{H}_{n-j}^{(n)}$ in the following lemma.

Lemma 5.2.4. *The DGMKs $\mathcal{H}_{n-j}^{(n)}$, defined in (5.2.15) satisfy the following bounds*

$$0 \le \mathcal{H}_{n-j}^{(n)} \le \frac{\tau_j^{\alpha}\Gamma(2-\alpha)\omega(\tau_j)}{\omega\left(\frac{\tau_j}{2}\right) + \frac{\alpha}{2(2-\alpha)}(1-\omega(\tau_j))}, \quad 1 \le j \le n, \tag{5.2.17}$$

and

$$\sum_{j=1}^{n} \mathcal{H}_{n-j}^{(n)} \mathcal{Q}_{1-\alpha}(t_j) \le \omega(\tau_n)\,\omega\left(\frac{\tau_1}{2}\right). \tag{5.2.18}$$

Proof. We start with the proof of (5.2.17). The definition (5.2.15) of $\mathcal{H}_{n-j}^{(n)}$ implies that $\mathcal{H}_0^{(n)} = \omega(\tau_n)/s_0^{(n)}$.

Now, from the expression of $s_0^{(n)}$ in (5.2.11) we have

$$s_0^{(n)} = \frac{1}{\Gamma(2-\alpha)}\left[\omega(\tau_n/2)q_0^{(n)} + (\omega(0)-\omega(\tau_n))r_0^{(n)}\right]. \tag{5.2.19}$$

The equations (5.2.7) and (5.2.8) give

$$q_0^{(n)} = \tau_n^{-\alpha} \quad \text{and} \quad r_0^{(n)} = \frac{\alpha}{2(2-\alpha)}\tau_n^{-\alpha}. \tag{5.2.20}$$

Hence, (5.2.19) and (5.2.20) combinedly imply

$$\mathcal{H}_0^{(n)} = \frac{\tau_n^{\alpha}\Gamma(2-\alpha)\omega(\tau_n)}{\omega(\frac{\tau_n}{2}) + \frac{\alpha}{2(2-\alpha)}(\omega(0)-\omega(\tau_n))}, \tag{5.2.21}$$

where the equality holds for $j = n$.

For $j \neq n$, the non-negative property of the DGMKs $\mathcal{H}_{n-j}^{(n)}$ says

$$\mathcal{H}_{n-j}^{(n)} \ge 0, \quad \text{and} \quad \frac{\mathcal{H}_{n-k}^{(n)} s_0^{(k)}}{\omega(t_n - t_{k-1})} \le \sum_{j=k}^{n} \mathcal{H}_{n-j}^{(n)}\, s_{j-k}^{(j)} \frac{1}{\omega(t_n - t_{k-1})} = 1, \tag{5.2.22}$$

and, thus by using (5.2.19) and the decreasing property of the weight function $\omega(t)$, the required result (5.2.17) is obtained.

Now, the expressions (5.2.7) and (5.2.11) together imply

$$s_{n-k}^{(n)} \ge \omega(t_n - t_{k-1} - \tau_k/2)\frac{(t_n - t_{k-1})^{-\alpha}}{\Gamma(1-\alpha)} = \omega(-\tau_k/2)\mathcal{Q}_{1-\alpha}(t_n - t_{k-1}). \tag{5.2.23}$$

Then, changing the index n to j and taking $k = 1$ we get

$$\mathcal{Q}_{1-\alpha}(t_j) \le s_{j-1}^{(j)}\omega\left(\frac{\tau_1}{2}\right). \tag{5.2.24}$$

Taking a multiplication of the above inequality with the DGMKs $\mathcal{H}_{n-j}^{(n)}$ and summing over the index j we have

$$\sum_{j=1}^{n} \mathcal{H}_{n-j}^{(n)} \mathcal{Q}_{1-\alpha}(t_j) \leq \sum_{j=1}^{n} \mathcal{H}_{n-j}^{(n)} s_{j-1}^{(j)} \omega\left(\frac{\tau_1}{2}\right) \leq \omega\left(\tau_n\right) \omega\left(\frac{\tau_1}{2}\right), \tag{5.2.25}$$

and hence the result (5.2.18) is obtained. □

In the following lemma, we discuss the Chebyshev's sorting inequality [29] that will be used in Lemma 5.2.6.

Lemma 5.2.5 (Chebyshev's sorting inequality)**.** *If $\mathcal{F}$ and $\mathcal{G}$ are two integrable functions such that $\mathcal{F}$ is monotone increasing and $\mathcal{G}$ is monotone decreasing on the interval $[l_1, l_2]$, then*

$$(l_2 - l_1) \int_{l_1}^{l_2} \mathcal{F}(\zeta)\mathcal{G}(\zeta)d\zeta \leq \int_{l_1}^{l_2} \mathcal{F}(t)dt \int_{l_1}^{l_2} \mathcal{G}(\zeta)d\zeta. \tag{5.2.26}$$

Now, we prove the following property of the generalized Caputo derivative (1.4.4).

Lemma 5.2.6. *If $\Phi_c : \overline{\Omega}_t \to \mathbb{R}$ is any continuous, piecewise $\mathcal{C}^1$ function such that Φ_c' is non-negative and monotone then*

$$\sum_{j=1}^{n-1} \mathcal{H}_{n-j}^{(n)} \left({}^{C}D_{0,t}^{\alpha,\omega(t)}\Phi_c\right)(t_j) \leq \omega(\tau_n) \int_0^{t_n} \Phi_c'(\zeta)\, d\zeta, \quad \text{for } 1 \leq n \leq N.$$

Proof. We will start the proof by considering two cases: (i) the function Φ_c' is monotone decreasing, and (ii) the function Φ_c' is monotone increasing.

Case (i). We first write the generalized memory kernel $\mathcal{Q}_\alpha(t)$ in the form

$$\mathcal{Q}_\alpha(t) = \omega(t)\mathcal{B}_\alpha(t), \quad \text{where } \mathcal{B}_\alpha(t) = \frac{t^{\alpha-1}}{\Gamma(\alpha)}.$$

From the definition (1.4.4), one can write

$$\left({}^{C}D_{0,t}^{\alpha,\omega(t)}\Phi_c\right)(t_j) = \int_0^{t_j} \omega(t_j-\zeta)\mathcal{B}_{1-\alpha}(t_j-\zeta)\Phi_c'(\zeta)d\zeta \leq \sum_{k=1}^{j} \omega(t_j-t_k) \int_{t_{k-1}}^{t_k} \mathcal{B}_{1-\alpha}(t_j-\zeta)\Phi_c'(\zeta)d\zeta.$$

Now, considering $[l_1, l_2] = [t_{k-1}, t_k]$, $\mathcal{F}(\zeta) = \mathcal{B}_{1-\alpha}(t_j - \zeta)$, and $\mathcal{G}(\zeta) = \Phi_c'(\zeta)$ in Lemma 5.2.5, we get

$$\begin{aligned}\left({}^{C}D_{0,t}^{\alpha,\omega(t)}\Phi_c\right)(t_j) &\leq \sum_{k=1}^{j}\frac{1}{\tau_k}\omega(t_j-t_k)\int_{t_{k-1}}^{t_k}\mathcal{B}_{1-\alpha}(t_j-t)dt\int_{t_{k-1}}^{t_k}\Phi_c'(\zeta)d\zeta\\ &\leq \sum_{k=1}^{j}\frac{1}{\tau_k}\frac{\omega(t_j-t_k)}{\omega(t_j-t_{k-1})}\int_{t_{k-1}}^{t_k}\mathcal{Q}_{1-\alpha}(t_j-t)dt\int_{t_{k-1}}^{t_k}\Phi_c'(\zeta)d\zeta\\ &\approx \sum_{k=1}^{j}\omega(t_{k-1}-t_k)\,s_{j-k}^{(j)}\int_{t_{k-1}}^{t_k}\Phi_c'(\zeta)d\zeta. \qquad (5.2.27)\end{aligned}$$

Then, multiplying both sides of (5.2.27) by the DGMKs $\mathcal{H}_{n-j}^{(n)}$ and summing over the index j from 1 to $n-1$ we have

$$\begin{aligned}\sum_{j=1}^{n-1}\mathcal{H}_{n-j}^{(n)}\left({}^{C}D_{0,t}^{\alpha,\omega(t)}\Phi_c\right)(t_j) &\leq \sum_{j=1}^{n-1}\mathcal{H}_{n-j}^{(n)}\sum_{k=1}^{j}\omega(t_{k-1}-t_k)\,s_{j-k}^{(j)}\int_{t_{k-1}}^{t_k}\Phi_c'(\zeta)d\zeta\\ &= \sum_{k=1}^{n-1}\omega(t_{k-1}-t_k)\int_{t_{k-1}}^{t_k}\Phi_c'(\zeta)d\zeta\sum_{j=k}^{n-1}\mathcal{H}_{n-j}^{(n)}s_{j-k}^{(j)}\\ &\leq \sum_{k=1}^{n-1}\omega(t_n-t_k)\int_{t_{k-1}}^{t_k}\Phi_c'(\zeta)d\zeta\\ &\leq \omega(\tau_n)\sum_{k=1}^{n}\int_{t_{k-1}}^{t_k}\Phi_c'(\zeta)d\zeta, \qquad (5.2.28)\end{aligned}$$

as the function Φ_c is non-negative.

Case (ii). If the function Φ_c' is monotonically increasing, then we have

$$\begin{aligned}\sum_{j=1}^{n-1}\mathcal{H}_{n-j}^{(n)}\left({}^{C}D_{0,t}^{\alpha,\omega(t)}\Phi_c\right)(t_j) &\leq \sum_{j=1}^{n-1}\mathcal{H}_{n-j}^{(n)}\sum_{k=1}^{j}\Phi_c'(t_k)\int_{t_{k-1}}^{t_k}\mathcal{Q}_{1-\alpha}(t_j-\zeta)d\zeta\\ &\approx \sum_{j=1}^{n-1}\mathcal{H}_{n-j}^{(n)}\sum_{k=1}^{j}\tau_k\Phi_c'(t_k)s_{j-k}^{(j)}\\ &= \sum_{k=1}^{n-1}\tau_k\Phi_c'(t_k)\sum_{j=k}^{n-1}\mathcal{H}_{n-j}^{(n)}s_{j-k}^{(j)}\\ &\leq \sum_{k=1}^{n-1}\tau_{k+1}\Phi_c'(t_k)\omega(t_n-t_{k-1})\\ &\leq \omega(\tau_n+\tau_{n-1})\int_{0}^{t_n}\Phi_c'(\zeta)d\zeta, \qquad (5.2.29)\end{aligned}$$

where we have used the condition (5.2.4).

Hence, by combining the results (5.2.28) and (5.2.29), the required result holds. □

Next in the following lemma, we will study the property of Mittag-Leffler function $E_\alpha(z)$ when it is combined with the DGMKs $\mathcal{H}^{(n)}_{n-j}$.

Lemma 5.2.7. *For any real $\nu > 0$, we have*

$$\nu \sum_{j=1}^{n-1} \mathcal{H}^{(n)}_{n-j} \omega(t_j) E_\alpha(\nu t_j^\alpha) \le \omega(\tau_n) \left[E_\alpha(\nu t_n^\alpha) - 1\right].$$

Proof. From the definition of the Mittag-Leffler function $E_\alpha(z)$, we have

$$E_\alpha(\nu t^\alpha) = \sum_{k=0}^{\infty} \frac{\nu^k t^{\alpha k}}{\Gamma(1+k\alpha)} = \sum_{k=0}^{\infty} \nu^k \mathcal{B}_{1+k\alpha}(t), \tag{5.2.30}$$

where the derivative $\mathcal{B}'_{1+k\alpha}(t) = \mathcal{B}_{k\alpha}(t)$ is positive for all $k \ge 1$. It can be easily shown that the function $\mathcal{B}_{k\alpha}(t)$ is monotonically increasing for $k \in [1, 1/\alpha]$ and monotonically decreasing for $k \in (1/\alpha, \infty)$.

Now, we have

$$\begin{aligned}
\sum_{j=1}^{n-1} \mathcal{H}^{(n)}_{n-j} \left({}^C D^{\alpha,\omega(t)}_{0,t} \mathcal{B}_{1+k\alpha}\right)(t_j) &= \sum_{j=1}^{n-1} \mathcal{H}^{(n)}_{n-j} \int_0^{t_j} \mathcal{Q}_{1-\alpha}(t_j - \zeta) \mathcal{B}_{k\alpha}(\zeta)\, d\zeta \\
&= \sum_{j=1}^{n-1} \mathcal{H}^{(n)}_{n-j} \int_0^{t_j} \omega(t_j - \zeta) \mathcal{B}_{1-\alpha}(t_j - \zeta) \mathcal{B}_{k\alpha}(\zeta)\, d\zeta \\
&\ge \sum_{j=1}^{n-1} \mathcal{H}^{(n)}_{n-j} \omega(t_j) \int_0^{t_j} \mathcal{B}_{1-\alpha}(t_j - \zeta) \mathcal{B}_{k\alpha}(\zeta)\, d\zeta \\
&= \sum_{j=1}^{n-1} \mathcal{H}^{(n)}_{n-j} \omega(t_j) \mathcal{B}_{1+(k-1)\alpha}(t_j).
\end{aligned} \tag{5.2.31}$$

Then, by applying the Lemma 5.2.6, we have

$$\sum_{j=1}^{n-1} \mathcal{H}^{(n)}_{n-j} \omega(t_j) \mathcal{B}_{1+(k-1)\alpha}(t_j) \le \omega(\tau_n) \mathcal{B}_{1+k\alpha}(t_n). \tag{5.2.32}$$

Multiplying both sides of (5.2.32) by ν^k and summing over the index k, we have

$$\begin{aligned}\sum_{k=1}^{m}\nu^k\sum_{j=1}^{n-1}\mathcal{H}_{n-j}^{(n)}\omega(t_j)\mathcal{B}_{1+(k-1)\alpha}(t_j) &= \sum_{j=1}^{n-1}\omega(t_j)\mathcal{H}_{n-j}^{(n)}\sum_{k=1}^{m}\nu^k\mathcal{B}_{1+(k-1)\alpha}(t_j)\\ &\leq \sum_{k=1}^{m}\nu^k\omega(\tau_n)\mathcal{B}_{1+k\alpha}(t_n). \qquad (5.2.33)\end{aligned}$$

Using the absolutely convergent property of the series $\sum_{k=1}^{\infty}\nu^k\mathcal{B}_{1+k\alpha}(t)$ and taking the limit $m\to\infty$, the required result can be obtained. □

Now, it is worthy to point out that in [42], authors have discussed the stability of the model problem (1.1) with linear term $-f(x,t,u) = -p(x,t)u+\phi(x,t)$. The stability analysis, in their work requires the condition $p(x,t)\geq 0$, and thus this technique for analyzing the $L1$-formula (5.2.12) can not be applied directly to the linearized problem (5.2.1) with $c^{(m)}(x,t) > 0$. Therefore to overcome this difficulty, we will develop the generalized discrete fractional Grönwall inequality in the next theorem that will help us to analyze the stability and error estimate of the fully discrete scheme (see (5.3.1)) in the next section.

Theorem 5.2.8 (Generalized discrete fractional Grönwall inequality)**.** *Let, for a given non-negative sequence* $\{\Upsilon_d\}_{d=0}^{N-1}$, $\exists$ *a constant* Υ, *independent of time-steps such that* $\sum_{d=0}^{N-1}\Upsilon_d\leq\Upsilon$. *Assume further that for any grid function* $\{z^n|\, n\geq 0\}$ *such that*

$$\triangle_{0,t_n}^{\alpha,\omega(t)}(z^n)^2 \leq \omega(2t_n)\sum_{d=1}^{n}\Upsilon_{n-d}(z^d)^2 + z^n\left(\sum_{i=1}^{3}\Theta_i^n\right), \quad n\geq 1, \qquad (5.2.34)$$

where $\{\Theta_i^n|\, 1\leq i\leq 3,\, 1\leq n\leq N\}$ *are non-negative sequences. If the maximum time-step size satisfies*

$$\tau_N \leq \left(\frac{\omega(0)+\frac{\alpha}{2(2-\alpha)}[\omega(0)-\omega(T)]}{2\Upsilon\,\Gamma(2-\alpha)}\right)^{1/\alpha}, \qquad (5.2.35)$$

then it holds that

$$z^n \leq \left\{2\omega(-t_n)E_\alpha(2\Upsilon t_n^\alpha)\right\}\times\left\{z^0+\omega\left(-t_n-t_{n-1}\right)\omega\left(\frac{\tau_1}{2}\right)\Gamma(1-\alpha)\max_{1\leq j\leq n}\left(t_j^\alpha\sum_{i=1}^{3}\Theta_i^j\right)\right\}. \qquad (5.2.36)$$

Proof. By using the $L1-$formula (5.2.12), we have

$$\triangle_{0,t_n}^{\alpha,\omega(t)}(z^n)^2 = \sum_{k=1}^{n}s_{n-k}^{(n)}\big((z^k)^2-(z^{k-1})^2\big). \qquad (5.2.37)$$

Thus, from (5.2.34), we get

$$\sum_{k=1}^{n} s_{n-k}^{(n)}\big((z^k)^2-(z^{k-1})^2\big) \le \omega(2t_n)\sum_{d=1}^{n}\Upsilon_{n-d}(z^d)^2 + z^n\left(\sum_{i=1}^{3}\Theta_i^n\right). \tag{5.2.38}$$

After changing the index n to j, we multiply both sides of (5.2.38) by the DGMKS $\mathcal{H}_{n-j}^{(n)}$ and take the sum over j to obtain

$$\sum_{j=1}^{n}\mathcal{H}_{n-j}^{(n)}\sum_{k=1}^{j} s_{j-k}^{(j)}\big((z^k)^2-(z^{k-1})^2\big) \le \sum_{j=1}^{n}\mathcal{H}_{n-j}^{(n)}\omega(2t_j)\left[\sum_{d=1}^{j}\Upsilon_{j-d}(z^d)^2 + z^j\left(\sum_{i=1}^{3}\Theta_i^j\right)\right]. \tag{5.2.39}$$

Interchanging the order of the summation in the left hand side of (5.2.39) and using the identity (5.2.14), we obtain

$$\begin{aligned}\sum_{k=1}^{n}\big((z^k)^2-(z^{k-1})^2\big)\sum_{j=k}^{n}\mathcal{H}_{n-j}^{(n)}s_{j-k}^{(j)} &= \sum_{k=1}^{n}\big((z^k)^2-(z^{k-1})^2\big)\omega(t_n-t_{k-1})\\ &\ge \omega(t_n)\sum_{k=1}^{n}\big((z^k)^2-(z^{k-1})^2\big)\\ &= \omega(t_n)\big((z^n)^2-(z^0)^2\big).\end{aligned} \tag{5.2.40}$$

Thus, (5.2.39) gives

$$(z^n)^2 \le (z^0)^2 + \omega(-t_n)\sum_{j=1}^{n}\mathcal{H}_{n-j}^{(n)}\omega(2t_j)\left[\sum_{d=1}^{j}\Upsilon_{j-d}(z^d)^2 + z^j\left(\sum_{i=1}^{3}\Theta_i^j\right)\right]. \tag{5.2.41}$$

For the term $\sum_{j=1}^{n}\mathcal{H}_{n-j}^{(n)}\left(\sum_{i=1}^{3}\Theta_i^j\right)$, we apply Lemma 5.2.4 (ii) to receive

$$\begin{aligned}\sum_{j=1}^{n}\mathcal{H}_{n-j}^{(n)}\left(\sum_{i=1}^{3}\Theta_i^j\right) &\le \max_{1\le j\le n}\left[\frac{\sum_{i=1}^{3}\Theta_i^j}{\mathcal{Q}_{1-\alpha}(t_j)}\right]\sum_{j=1}^{n}\mathcal{H}_{n-j}^{(n)}\mathcal{Q}_{1-\alpha}(t_j)\\ &\le \omega(\tau_n)\,\omega\left(\frac{\tau_1}{2}\right)\max_{1\le j\le n}\left[\frac{\left(\sum_{i=1}^{3}\Theta_i^j\right)t_j^{\alpha}\Gamma(1-\alpha)}{\omega(t_j)}\right]\\ &\le \omega(-t_{n-1})\,\omega\left(\frac{\tau_1}{2}\right)\Gamma(1-\alpha)\max_{1\le j\le n}\left[\left(\sum_{i=1}^{3}\Theta_i^j\right)t_j^{\alpha}\right].\end{aligned} \tag{5.2.42}$$

To proceed further, let us define a non-decreasing sequence $\{\chi_n\}_{n\geq 1}$ by

$$\chi_n = z^0 + \omega\left(-t_n - t_{n-1}\right)\omega\left(\frac{\tau_1}{2}\right)\Gamma(1-\alpha)\max_{1\leq j\leq n}\left[\left(\sum_{i=1}^{3}\Theta_i^j\right)t_j^{\alpha}\right]. \tag{5.2.43}$$

and assume $\Xi_n = \{2\omega(-t_n)E_\alpha(2\Upsilon t_n^\alpha)\}$ which is an increasing function as $\Xi_n \geq \Xi_{n-1} \geq 2\omega(0)$ for $n \geq 2$.

We will apply the mathematical induction to evaluate the claimed inequality (5.2.36) in the form of $z^n \leq \Xi_n\,\chi_n$.

Now, we first inspect for $n = 1$. If $z^1 \leq z^0$, then $z^1 \leq \chi_1 \leq \Xi_1\chi_1$ and the result (5.2.36) holds for $n = 1$. Apart from that, if $z^1 \geq z^0$, then for $n = 1$ we have from (5.2.41)

$$(z^1)^2 \leq (z^0)^2 + \omega(-t_1)\mathcal{H}_0^{(1)}\omega(2t_1)\Big[\Upsilon_0(z^1)^2 + z^1(\Theta_1^1 + \Theta_2^j + \Theta_3^j)\Big]. \tag{5.2.44}$$

Applying (5.2.42) and using the representation (5.2.43) to get

$$\begin{aligned}(z^1)^2 &\leq z^1\left(z^0 + \omega(-t_1)\omega\left(\frac{\tau_1}{2}\right)\Gamma(1-\alpha)\Big[(\Theta_1^1 + \Theta_2^1 + \Theta_3^1)t_1^{\alpha}\Big]\right) + \omega(-t_1)\mathcal{H}_0^{(1)}\Upsilon_0(z^1)^2\\ &= z^1\chi_1 + \omega(-t_1)\mathcal{H}_0^{(1)}\Upsilon_0(z^1)^2.\end{aligned}$$

Lemma (5.2.17)(i) yields

$$\begin{aligned}(z^1)^2 &\leq z^1\chi_1 + \omega(-t_1)\Upsilon(z^1)^2\frac{\tau_1^{\alpha}\Gamma(2-\alpha)\omega(\tau_1)}{\omega\left(\frac{\tau_1}{2}\right) + \frac{\alpha}{2(2-\alpha)}[\omega(0) - \omega(\tau_1)]}\\ &\leq z^1\chi_1 + \frac{1}{2}(z^1)^2,\end{aligned} \tag{5.2.45}$$

where the limitation $\tau_1 \leq \left(\dfrac{\omega(0) + \frac{\alpha}{2(2-\alpha)}[\omega(0) - \omega(T)]}{2\Upsilon\,\Gamma(2-\alpha)}\right)^{1/\alpha}$ over the time-step size τ_1 has been implemented, and thus the result $z^1 \leq 2\chi_1 \leq \Xi_1\chi_1$ arrives and the desired result holds for $n = 1$.

Now, we consider that the expected result (5.2.36) holds for $k = 1, 2\ldots n-1$ *i.e.*,

$$z^k \leq \Xi_k\chi_k,\ k = 1, 2\ldots n-1, \tag{5.2.46}$$

where $2 \leq n \leq N$.

Let us take some integer $i_0, 0 \leq i_0 \leq n-1$ such that $z^{i_0} = \max\limits_{0\leq j\leq n-1} z^j$. Now for $k = n$, we take two cases into consideration:

Case(a). If $z^n \leq z^{i_0}$, then

$$z^n \leq z^{i_0} \leq \Xi_{i_0}\chi_{i_0} \leq \Xi_n\chi_n, \tag{5.2.47}$$

and thus the inequality (5.2.36) holds for $k = n$.

Case(b). If $z^n \geq z^{i_0}$, then from (5.2.41) we have

$$\begin{aligned}
(z^n)^2 &\leq z^n z^0 + \omega(-t_n)(z^n)^2\mathcal{H}_0^{(n)}\omega(2t_n)\sum_{d=1}^{j}\Upsilon_{j-d} \\
&\quad +\omega(-t_n)z^n\sum_{j=1}^{n-1}\mathcal{H}_{n-j}^{(n)}\omega(2t_j)\sum_{d=1}^{j}\Upsilon_{j-d}z^d + \omega(-t_n)z^n\sum_{j=1}^{n}\mathcal{H}_{n-j}^{(n)}\left(\sum_{i=1}^{3}\Theta_i^j\right) \\
&\leq z^n\left(z^0 + \omega(-t_n)\sum_{j=1}^{n}\mathcal{H}_{n-j}^{(n)}\left(\sum_{i=1}^{3}\Theta_i^j\right)\right) + (z^n)^2\omega(-t_n)\mathcal{H}_0^{(n)}\Upsilon \\
&\quad +\omega(-t_n)z^n\sum_{j=1}^{n-1}\mathcal{H}_{n-j}^{(n)}\omega(2t_j)\sum_{d=1}^{j}\Upsilon_{j-d}z^d.
\end{aligned} \tag{5.2.48}$$

Then, recalling the step size condition (5.2.35) and the induction hypothesis (5.2.46), we can rewrite the inequality (5.2.48) as

$$\begin{aligned}
z^n &\leq \chi_n + \omega(-t_n)\sum_{j=1}^{n-1}\mathcal{H}_{n-j}^{(n)}\omega(2t_j)\sum_{d=1}^{j}\Upsilon_{j-d}\Xi_d\chi_d + \frac{1}{2}z^n \\
&= 2\chi_n + 2\omega(-t_n)\sum_{j=1}^{n-1}\mathcal{H}_{n-j}^{(n)}\omega(2t_j)\sum_{d=1}^{j}\Upsilon_{j-d}2\omega(-t_d)E_\alpha(2\Upsilon t_d^\alpha)\chi_d \\
&\leq 2\chi_n + 4\omega(-t_n)\sum_{j=1}^{n-1}\mathcal{H}_{n-j}^{(n)}\omega(t_j)E_\alpha(2\Upsilon t_j^\alpha)\chi_j\sum_{d=1}^{j}\Upsilon_{j-d} \\
&\leq 2\chi_n + 4\omega(-t_n)chi_{n-1}\Upsilon\sum_{j=1}^{n-1}\mathcal{H}_{n-j}^{(n)}\omega(t_j)E_\alpha(2\Upsilon t_j^\alpha) \\
&\leq 2\chi_n + 2\omega(-t_n)\chi_n\omega(\tau_n)\left[E_\alpha(2\Upsilon t_n^\alpha) - 1\right] \leq 2\chi_n\omega(-t_n)E_\alpha(2\Upsilon t_n^\alpha),
\end{aligned}$$

and hence it completes the proof. □

5.3 Fully discrete scheme and theoretical results

In this section, we focus to study the fully discrete scheme of the linearized problem (5.2.1) as well as the error analysis of the proposed scheme with help of the DGMKs $\mathcal{H}_{n-j}^{(n)}$.

5.3.1 Spatial discretization and fully-discrete scheme

We consider a uniform mesh $\overline{\Omega}_x^{M_x}$ to further study the numerical solution of the given model problem (5.1.1). Then the discretized mesh of the domain $\overline{\mathcal{D}}$ is given as

$$\overline{\mathcal{D}}_{M_x}^N = \{(x_i, t_n) : i = 0, 1, \ldots, M_x;\, n = 0, 1, \ldots, N\}.$$

Let ρ_i^n be the approximation of the solution $\vartheta_i^n = \vartheta(x_i, t_n)$ for $x_i \in \overline{\Omega}_x^M$, $0 \le n \le N$. Then the fully discrete scheme of the quasilinearized problem (5.2.1) at the point (x_i, t_n) is

$$\begin{cases} \triangle_{0,t_n}^{\alpha,\omega(t)} \rho_i = \Lambda \rho_i^n + g_i^{(m),n}, \quad x_i \in \Omega_x^{M_x},\ 1 \le n \le N, \\ \rho_i^0 = \phi(x_i), \quad x_i \in \overline{\Omega}_x^{M_x}, \\ \rho_0^n = 0, \quad \rho_{M_x}^n = 0, \quad 1 \le n \le N, \end{cases} \tag{5.3.1}$$

where

$$\begin{aligned} \Lambda\rho_i^n &= \left((\Psi\rho_x)_x + c^{(m)}\rho\right)(x_i, t_n) \\ &= \frac{\Psi_{i-1/2}^n \rho_{i-1}^n - \left(\Psi_{i-1/2}^n + \Psi_{i+1/2}^n\right)\rho_i^n + \Psi_{i+1/2}^n \rho_{i+1}^n}{h_x^2} + c_i^{(m),n}\rho_i^n + \mathcal{O}(h_x^2) \\ &= \frac{\chi_i^n \rho_{i-1}^n - \left(\chi_i^n + \chi_{i+1}^n\right)\rho_i^n + \chi_{i+1}^n \rho_{i+1}^n}{h_x^2} + c_i^{(m),n}\rho_i^n + \mathcal{O}(h_x^2) \\ &= \triangle_h \rho_i^n + c_i^{(m),n}\rho_i^n + \mathcal{O}(h_x^2), \end{aligned} \tag{5.3.2}$$

and $\triangle_h \rho_i = \left[\chi_i\, \rho_{i-1} - (\chi_i + \chi_{i+1})\, \rho_i + \chi_{i+1}\, \rho_{i+1}\right]/h_x^2$ for $i = 1, 2, \ldots, M_x - 1$. Also, we have $\dfrac{\partial^3 \Psi}{\partial x^3} \in \mathcal{C}(\overline{\Omega}_x)$, $\Psi_i^n = \Psi(x_i, t_n)$, $\chi_i^n = \Psi_{i-1/2}^n$, $c_i^{(m),n} = c^{(m)}(x_i, t_n)$, and $g_i^{(m),n} = g^{(m)}(x_i, t_n)$.

Next, we denote a space of mesh functions as follows

$$\mathcal{Y}_h = \{\Theta_h = \{\Theta_0, \Theta_1, \ldots, \Theta_M\} \,|\Theta_0 = 0 = \Theta_M\}.$$

For any two mesh functions $\Theta_h, \Phi_h \in \mathcal{Y}_h$, define the discrete inner product as $\langle \Theta_h, \Phi_h \rangle = h_x \sum_{i=0}^{M_x} \Theta_i \Phi_i$ and the discrete L^2-norm as $\left\|\Theta_h\right\|_2 = \sqrt{\langle \Theta_h, \Theta_h \rangle}$.

5.3.2 A priori estimate

We will establish the a priori estimate for the fully discrete scheme (5.3.1) in the following theorem and later this result will be used in the analysis of the error estimate.

Theorem 5.3.1. *Let us consider that the non-uniform temporal grid size satisfies the condition* (5.2.4)*. Then the following result will hold for the fully discrete scheme* (5.3.1)

$$\begin{aligned}\|\rho^n\|_2 \;\leq\; & \left\{2\omega(-t_n)E_\alpha\left(4\omega(-2t_n)\left\|c^{(m),n}\right\|_\infty t_n^\alpha\right)\right\}\times \\ & \left\{\|\phi\|_2+2\omega(-t_n-t_{n-1})\omega\left(\frac{\tau_1}{2}\right)\Gamma(1-\alpha)\max_{1\leq j\leq n}\left(t_j^\alpha\left\|g^{(m),j}\right\|_2\right)\right\}, \quad n=1,2,\ldots,N,\end{aligned} \tag{5.3.3}$$

if the maximum temporal step size satisfies the condition

$$\tau_N \leq \left(\frac{\omega(0)+\frac{\alpha}{2(2-\alpha)}[\omega(0)-\omega(T)]}{4\left\|c^{(m),n}\right\|_\infty\Gamma(2-\alpha)}\right)^{1/\alpha}. \tag{5.3.4}$$

Proof. The approximation of the time fractional derivative term $\triangle_{0,t_n}^{\alpha,\omega(t)}\rho_i$ can be explicitly rewritten in the form

$$\triangle_{0,t_n}^{\alpha,\omega(t)}\rho_i = \rho_i^n s_0^{(n)} - \sum_{k=1}^{n-1}\left(s_{n-k-1}^{(n)}-s_{n-k}^{(n)}\right)\rho_i^k - \rho_i^0 s_{n-1}^{(n)}. \tag{5.3.5}$$

Thus, the fully discrete scheme (5.3.1) takes the form

$$\rho_i^n s_0^{(n)} - \triangle_h\rho_i^n - c_i^{(m),n}\rho_i^n = \sum_{k=1}^{n-1}\left(s_{n-k-1}^{(n)}-s_{n-k}^{(n)}\right)\rho_i^k + \rho_i^0 s_{n-1}^{(n)} + g_i^{(m),n}. \tag{5.3.6}$$

Then, taking the inner product at both sides of (5.3.6) by $2\rho^n$ and using the monotonicity property of the coefficient s_n, one can have

$$\begin{aligned}2s_0^{(n)}\langle\rho^n,\rho^n\rangle - 2\langle\triangle_h\rho^n,\rho^n\rangle \;=\; & \langle c_i^{(m),n}\rho^n,\rho^n\rangle + \sum_{k=1}^{n-1}\left(s_{n-k-1}^{(n)}-s_{n-k}^{(n)}\right)\langle\rho^k,\rho^n\rangle \\ & + s_{n-1}^{(n)}\langle\rho^0,\rho^n\rangle + \langle g^{(m),n},\rho^n\rangle.\end{aligned} \tag{5.3.7}$$

The Young's inequality, Cauchy-Schwarz inequality and the positive semi-definite property $\langle-\triangle_h\rho^n,\rho^n\rangle \geq 0$ give

$$s_0^{(n)}\|\rho^n\|_2^2 - \sum_{k=1}^{n-1}\left(s_{n-k-1}^{(n)}-s_{n-k}^{(n)}\right)\|\rho^k\|_2^2 - s_{n-1}^{(n)}\|\rho^0\|_2^2 \leq 2\left\|c^{(m),n}\right\|_\infty\|\rho^n\|_2^2 + 2\left\|g^{(m),n}\right\|_2\|\rho^n\|_2^2.$$

Then, the representation (5.3.5) gives

$$\triangle_{0,t_n}^{\alpha,\omega(t)}\|\rho^n\|_2^2 \leq 2\left\|c^{(m),n}\right\|_\infty\|\rho^n\|_2^2 + 2\left\|g^{(m),n}\right\|_2\|\rho^n\|_2^2, \text{ for } n\geq 1. \tag{5.3.8}$$

Now, comparing above inequality with the relation (5.2.34) one gets

$$z^n = \|\rho^n\|_2\,,\ \omega(2t_n)\Upsilon_0 = 2\left\|c^{(m),n}\right\|_\infty,\ \Upsilon_l = 0,\ \text{for } l \geq 1,\ \text{and } \sum_{i=1}^{3}\Theta_i^n = 2\left\|g^{(m),n}\right\|_2,$$

and thus replacement of the above equalities in the Theorem 5.2.8 gives the required result. □

5.3.3 Truncation error estimate

In this subsection, we will state the truncation error of the temporal discretization (5.2.5). The truncation error of the temporal discretization (5.2.5) can be written as

$$\begin{aligned}\mathcal{T}^n &= {}^{C}D_{0,t_n}^{\alpha,\omega(t)}u(t_n) - \triangle_{0,t_n}^{\alpha,\omega(t)}u(t_n),\\ &= \mathcal{T}_d^n + \mathcal{T}_\omega^n,\ \text{for } n \geq 1,\end{aligned} \tag{5.3.9}$$

where $\mathcal{T}_d^n$ and $\mathcal{T}_\omega^n$ are defined in (5.2.9) and (5.2.10) respectively.

The following lemma exhibits the truncation error estimate for the temporal approximation by the non-uniform $L1$-method in (5.2.12).

Lemma 5.3.2. *For all $(x_i, t_n) \in \overline{\mathcal{D}}_{M_x}^N$, there is a constant C such that there holds*

$$|\mathcal{T}_d^n + \mathcal{T}_\omega^n| \leq Cn^{-\min\{2-\alpha, r\alpha\}}. \tag{5.3.10}$$

Proof. The detailed proof can be found in [42]. □

5.3.4 Error analysis

The convergence of the solution $\vartheta(x,t)$ of the quasilinearized problem (5.2.1) will be studied in this subsection. Let us denote the error function $\mathcal{E}_i^n = \vartheta_i^n - \rho_i^n$ for $(x_i, t_n) \in \overline{\mathcal{D}}_{M_x}^N$. Then the error term $\mathcal{E}_i^n$ satisfies the following governing equation

$$\begin{cases}\triangle_{0,t_n}^{\alpha,\omega(t)}\mathcal{E}_i = \Lambda\mathcal{E}_i^n + \mathcal{T}_{d,i}^n + \mathcal{T}_{\omega,i}^n + \mathcal{T}_{s,i}^n, \quad x_i \in \Omega_x^M,\ 1 \leq n \leq N,\\ \mathcal{E}_i^0 = 0, \quad x_i \in \overline{\Omega}_x^M,\\ \mathcal{E}_0^n = 0, \quad \mathcal{E}_M^n = 0, \quad 1 \leq n \leq N,\end{cases} \tag{5.3.11}$$

where $\mathcal{T}_{d,i}^n, \mathcal{T}_{\omega,i}^n$ are the temporal truncation error and $\mathcal{T}_{s,i}^n$ is spatial truncation error term at the point $(x_i, t_n) \in \overline{\mathcal{D}}_{M_x}^N$. By plugging the regularity condition (5.1.2) we can get the second order approximation in the spatial direction $\left\|\mathcal{T}_{s,i}^n\right\| \leq Ch_x^2$. The following theorem gives the error bound for the fully discrete scheme (5.3.1).

Theorem 5.3.3. *Let $\vartheta(x_i, t_n)$ be the solution of the quasilinearized problem (5.2.1) and ρ_i^n be the solution of the fully discrete scheme (5.3.1) at the point $(x_i, t_n) \in \overline{\mathcal{D}}_{M_x}^N$ with $\alpha \in (0,1)$. Also, consider that the non-uniform time step size satisfies the bound (5.2.4) along with the condition (5.3.4), then under the graded mesh $t_n = T(n/N)^r$, $n = 1, 2, \ldots, N$ with grading parameter $r \geq 1$, the error $\mathcal{E}_i^n$ attains the following bound with respect to the L^2-norm*

$$\begin{aligned} \left\|\mathcal{E}^n\right\|_2 \;\leq\; & C\omega(-t_n)E_\alpha\Big(4\omega(-2t_n)\left\|c^{(m),n}\right\|_\infty t_n^\alpha\Big) \times \\ & \left\{\omega(-t_n - t_{n-1})\omega\left(\frac{\tau_1}{2}\right)\Gamma(1-\alpha)\left(T^\alpha N^{-\min(r\alpha,2-\alpha)} + t_n^\alpha h_x^2\right)\right\}, \end{aligned} \tag{5.3.12}$$

for $n = 1, 2, \ldots, N$.

Proof. Under the given condition on the mesh size and imposing the Theorem 5.3.1, the solution $\mathcal{E}_i^n$ of the error equation (5.3.11) satisfies the following inequality for $n = 1, 2, \ldots, N$

$$\begin{aligned} &\left\|\mathcal{E}^n\right\|_2 \leq \left\{4\omega(-t_n)E_\alpha\Big(4\omega(-2t_n)\left\|c^{(m),n}\right\|_\infty t_n^\alpha\Big)\right\} \times \\ &\left\{\omega(-t_n - t_{n-1})\omega\left(\frac{\tau_1}{2}\right)\Gamma(1-\alpha)\max_{1\leq j\leq n}\left(t_j^\alpha\left\|(\mathcal{R}_1^t)^j + (\mathcal{R}_2^t)^j\right\|_2 + t_j^\alpha\left\|(\mathcal{R}_3^s)^j\right\|_2\right)\right\}. \end{aligned}$$

Thus, recalling Lemma 6.3.2 and the truncation error in the spatial direction to get

$$\begin{aligned} \left\|\mathcal{E}^n\right\|_2 \;\leq\; & C\omega(-t_n)E_\alpha\Big(4\omega(-2t_n)\left\|c^{(m),n}\right\|_\infty t_n^\alpha\Big) \times \\ & \left\{\omega(-t_n - t_{n-1})\omega\left(\frac{\tau_1}{2}\right)\Gamma(1-\alpha)\left(\max_{1\leq j\leq n} t_j^\alpha j^{-\min(r\alpha,2-\alpha)} + t_n^\alpha h_x^2\right)\right\}, \end{aligned} \tag{5.3.13}$$

for $n = 1, 2, \ldots, N$.

Now, under the graded mesh $t_n = T(n/N)^r$, $n = 1, 2, \ldots, N$ with grading parameter $r \geq 1$, one can write

$$\begin{aligned} t_n^\alpha n^{-\min(r\alpha,2-\alpha)} &= T^\alpha\left(\frac{n}{N}\right)^{r\alpha} n^{-\min(r\alpha,2-\alpha)} \\ &= T^\alpha\left(\frac{n}{N}\right)^{r\alpha-\min(r\alpha,2-\alpha)} N^{-\min(r\alpha,2-\alpha)} \\ &\leq T^\alpha N^{-\min(r\alpha,2-\alpha)}. \end{aligned} \tag{5.3.14}$$

Hence, using the bound (5.3.14) in the inequality (5.3.13), one can receive the required result (5.3.12). □

Remark 5.3.4. *To obtain an optimal convergence rate* $\mathcal{O}\left(N^{-(2-\alpha)}\right)$ *in time, we choose the optimal grading parameter* $r_{opt} = \frac{2-\alpha}{\alpha}$. *Also, we can note that the uniform mesh under the case* $r = 1$ *will produce the convergence order near to* $\mathcal{O}\left(N^{-\alpha}\right)$ *in time.*

Remark 5.3.5. *We also note that one can replace the regularity condition* (5.1.2) *with the following assumption*

$$\left\| \frac{\partial^l u}{\partial t^l} \right\|_{L^2(\overline{\Omega})} \leq C\left(1 + t^{\sigma-l}\right), \quad l = 0, 1, 2, \tag{5.3.15}$$

where σ *is the regularity parameter such as* $\sigma \in (0,1) \cup (1,2)$. *Then under the regularity condition* (5.3.15), *the temporal convergence rate* $\mathcal{O}\left(N^{-\min(r\sigma, 2-\alpha)}\right)$ *can be obtained with respect to the graded meshes* $t_n = T\left(n/N\right)^r, n = 0, 1, \ldots, N$, *and by choosing the optimal grid parameter* $r_{opt_\sigma} = \max\left\{1, \frac{2-\alpha}{\sigma}\right\}$, *one can achieve the optimal convergence rate* $\mathcal{O}\left(N^{-(2-\alpha)}\right)$ *in time. We will validate this result with an example in the next section for different values of* σ.

5.4 Numerical experiments

In this section, some numerical examples will be performed in favor of the theoretical analysis. We will establish the numerical results for different values of the fractional order α and of the grading parameter r such as $r = 1, r_{opt}, 5/4r_{opt}$ in Example 5.4.1. Also, for different values of the regularity parameter σ and grid parameter r such that $r = 1, r_{opt_\sigma}, 5/4r_{opt_\sigma}$ the errors and convergence order will be investigated in Example 5.4.2. In both the examples, we will choose $M_x = 2N$ to discretize the spatial domain.

Since the convergence order $\mathcal{O}(h_x^2)$ for the spatial term is standard, so we only examine the errors of the quasilinearized problem (5.2.1) in the temporal direction due to the non-uniform $L1$-scheme of the generalized Caputo derivative. We define the discrete error under the norm $\|.\|_2$ and the corresponding convergence order as

$$E_{M_x}^N = \max_{1 \leq n \leq N} \left\| u(t_n) - \rho^n \right\|_2, \quad \text{and} \quad CO_N = \log_2\left(\frac{E_{M_x}^N}{E_{2M_x}^{2N}}\right),$$

respectively.

Example 5.4.1. *We demonstrate an example with a nonlinear source term* $f(x,t,u) = e^{-u} + \widehat{\xi}(x,t)$, *where the function* $\widehat{\xi}(x,t)$ *is chosen such a way that the exact solution of the problem* (5.1.1) *is* $u(x,t) = \mathcal{Q}_{1+\alpha}(t)\sin(\pi x)$ *by considering the coefficient function* $\Psi(x,t) = 2 - \cos(x,t)$, *the domain* $\mathcal{D} = (0,1) \times (0,1)$, *and the weight function* $\omega(t) = e^{-5t}$ *in the model problem* (5.1.1).

It is clear that the solution has a singularity at the point $t = 0$ and henceforth the graded mesh is suitable to experience the better rate of convergence.

The numerical solution plot is drawn in Figure 5.1 with $N = 100$ and $\alpha = 0.6$. The errors and orders of the Example 5.4.1 are shown in Tables 5.1-5.3. Table 5.1 shows the errors $E^N_{M_x}$ and confirms the orders around $\mathcal{O}\left(N^{-\alpha}\right)$ under the uniform mesh for different values of α and N. In Tables 5.2-5.3, the errors $E^N_{M_x}$ and the related optimal orders around $\mathcal{O}\left(N^{-(2-\alpha)}\right)$ are observed in temporal direction. Figure 5.2 displays the log-log plots for different values of the grid parameter r, given in Tables 5.1-5.3.

Table 5.1: L^2 errors and CO_N of the Example 5.4.1 with $r = 1$ for different values of N and α.

N	$\alpha = 0.4$		$\alpha = 0.6$		$\alpha = 0.8$	
	$E^N_{M_x}$	CO_N	$E^N_{M_x}$	CO_N	$E^N_{M_x}$	CO_N
50	1.4197e-02	–	1.0212e-02	–	4.7801e-03	–
100	1.2158e-02	0.2237	7.4390e-03	0.4571	2.7971e-03	0.7731
200	1.0405e-02	0.2246	5.3455e-03	0.4768	1.6333e-03	0.7761
400	8.8336e-03	0.2362	3.7785e-03	0.5005	9.5181e-04	0.7790
800	7.4057e-03	0.2544	2.6274e-03	0.5242	5.5559e-04	0.7766
1600	6.1198e-03	0.2752	1.8011e-03	0.5448	3.2425e-04	0.7769
$\min\{r\alpha, 2-\alpha\}$		0.40		0.60		0.80

Example 5.4.2. *We consider the next example with the similar inputs as taken in Example 5.4.1 such that the problem* (5.1.1) *has an exact solution* $u(x,t) = \mathcal{Q}_{1+\sigma}(t)\sin(\pi x)$.

This solution also has a singularity at the point $t = 0$ with the regularity condition (5.3.15) and therefore the graded mesh is the better choice to gain optimal convergence rate.

Figure 5.3 depicts the numerical solutions plot with $N = 100, \alpha = 0.4$ and $\sigma = 0.75$. The errors $E^N_{M_x}$ of the Example 5.4.2 are revealed in Table 5.4 for $r = 1$ as well as the convergence orders, near about $\mathcal{O}\left(N^{-\sigma}\right)$ are also exhibited in this table. Tables 5.5-5.6 represent the errors $E^N_{M_x}$ of the Example 5.4.2 and the time accuracy which is closed upon the optimal rate $\mathcal{O}\left(N^{-(2-\alpha)}\right)$ is also illustrated in the same table. The corresponding log-log plots are portrayed in Figure 5.4 for different values of the grid parameter r.

Table 5.2: L^2 errors and CO_N of the Example 5.4.1 with $r = r_{opt}$ for different values of N and α.

N	$\alpha = 0.4$		$\alpha = 0.6$		$\alpha = 0.8$	
	$E^N_{M_x}$	CO_N	$E^N_{M_x}$	CO_N	$E^N_{M_x}$	CO_N
50	6.1852e-04	–	1.0405e-03	–	1.6862e-03	–
100	2.2957e-04	1.4299	4.5129e-04	1.2051	7.9956e-04	1.0765
200	8.1850e-05	1.4879	1.8770e-04	1.2656	3.7382e-04	1.0969
400	2.8457e-05	1.5242	7.5870e-05	1.3068	1.7340e-04	1.1082
800	9.7691e-06	1.5425	3.0039e-05	1.3367	7.9948e-05	1.1170
1600	3.3281e-06	1.5535	1.1727e-05	1.3570	3.6631e-05	1.1260
$\min\{r\alpha, 2-\alpha\}$		1.60		1.40		1.20

Table 5.3: L^2 errors and CO_N of the Example 5.4.1 with $r = \frac{5}{4}r_{opt}$ for different values of N and α.

N	$\alpha = 0.4$		$\alpha = 0.6$		$\alpha = 0.8$	
	$E^N_{M_x}$	CO_N	$E^N_{M_x}$	CO_N	$E^N_{M_x}$	CO_N
50	3.8922e-04	–	6.4266e-04	–	1.1929e-03	–
100	1.3631e-04	1.5137	2.5362e-04	1.3414	5.3668e-04	1.1523
200	4.7010e-05	1.5358	9.8263e-05	1.3679	2.3821e-04	1.1718
400	1.6045e-05	1.5509	3.7715e-05	1.3815	1.0486e-04	1.1837
800	5.4337e-06	1.5621	1.4405e-05	1.3886	4.5955e-05	1.1903
1600	1.8290e-06	1.5709	5.4863e-06	1.3927	2.0084e-05	1.1942
$\min\{r\alpha, 2-\alpha\}$		1.60		1.40		1.20

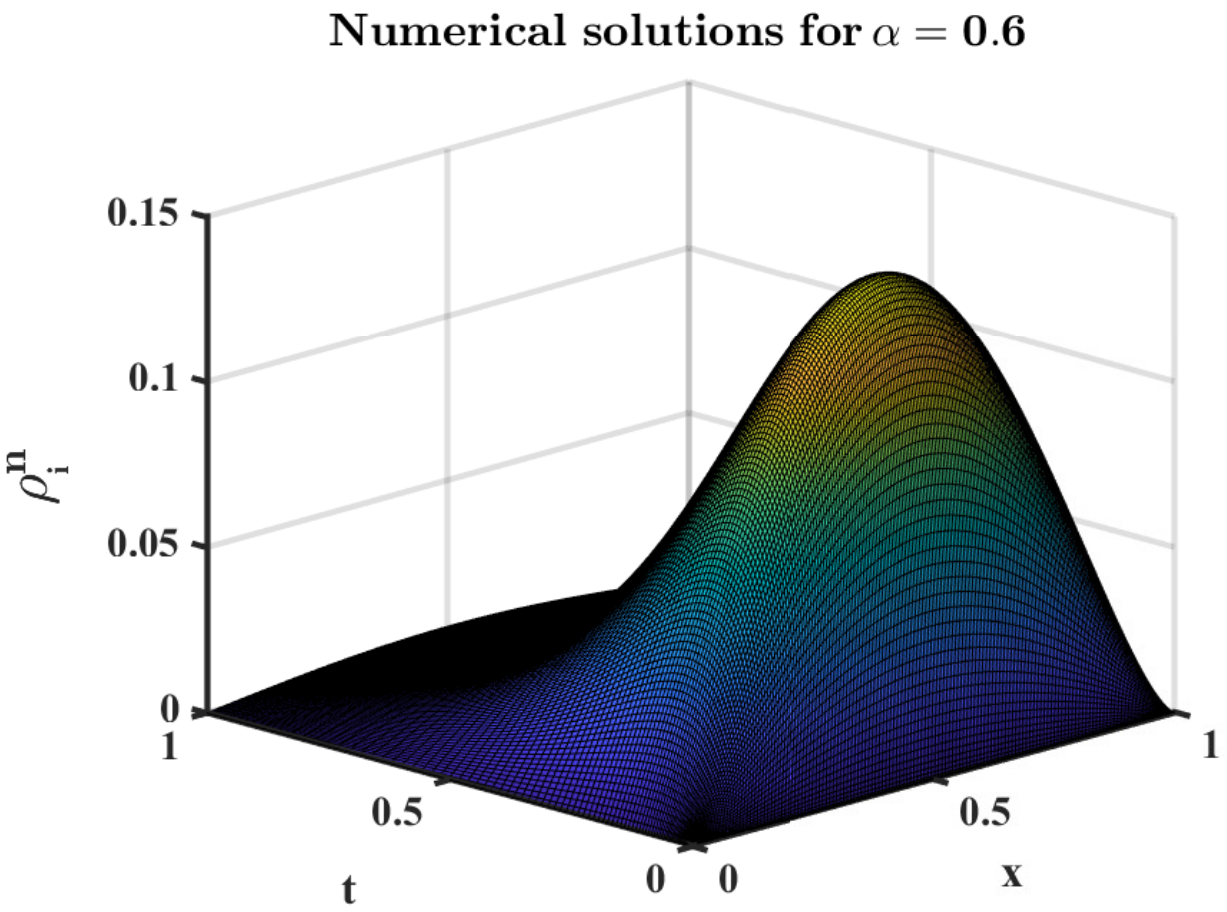

Figure 5.1: Numerical solutions plot for $N = 100$ with $r = \frac{5}{4}r_{opt}$.

Table 5.4: L^2 errors and CO_N of the Example 5.4.1 with $r = 1$ and $\alpha = 0.6$ for different values of N and σ.

N	$\sigma = 0.75$		$\sigma = 1.25$	
	$E^N_{M_x}$	CO_N	$E^N_{M_x}$	CO_N
50	3.7196e-03	–	1.9107e-04	–
100	2.3362e-03	0.6710	1.2313e-04	0.6339
200	1.4728e-03	0.6656	6.5600e-05	0.9085
400	9.2431e-04	0.6721	3.1805e-05	1.0444
800	5.7468e-04	0.6856	1.5200e-05	1.0652
1600	3.5362e-04	0.7006	7.0078e-06	1.1171
$\min\{r\sigma, 2-\alpha\}$	0.75		1.25	

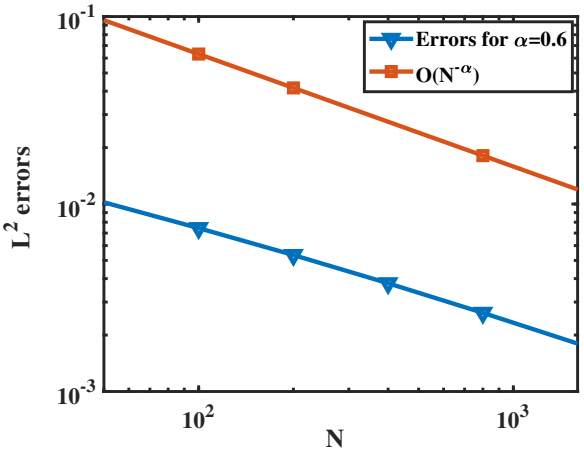

(a) Log-log plot for $r = 1$

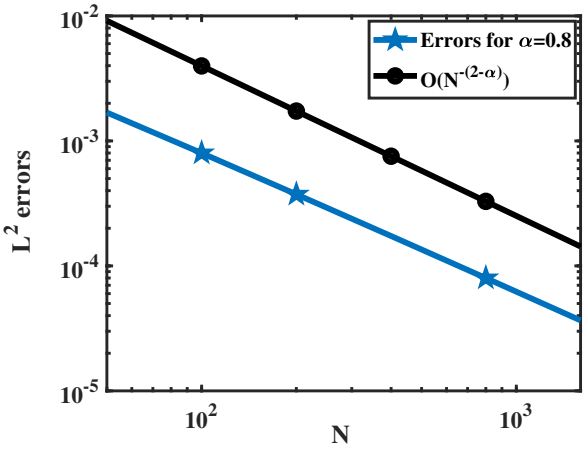

(b) Log-log plot for $r = r_{opt}$

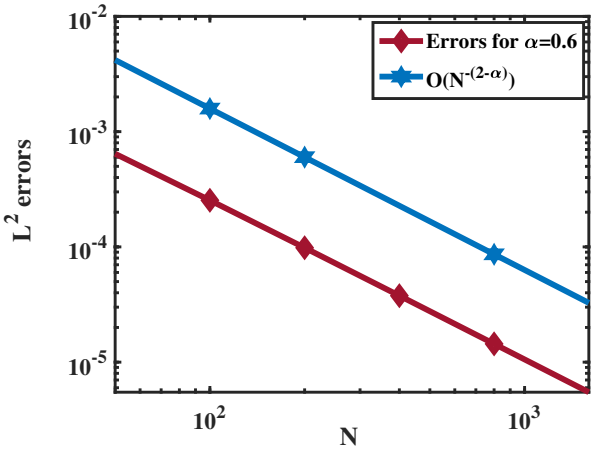

(c) Log-log plot for $r = \frac{5}{4}r_{opt}$

Figure 5.2: Log-log plots corresponding to Tables 5.1-5.3.

Table 5.5: L^2 errors and CO_N of the Example 5.4.1 with $r = r_{opt_\sigma}$ and $\alpha = 0.6$ for different values of N and σ.

N	$\sigma = 0.75$		$\sigma = 1.50$	
	$E^N_{M_x}$	CO_N	$E^N_{M_x}$	CO_N
50	5.1387e-04	–	1.5021e-04	–
100	2.2171e-04	1.2127	7.1116e-05	1.0787
200	9.3446e-05	1.2465	3.2213e-05	1.1425
400	3.8427e-05	1.2820	1.3905e-05	1.2121
800	1.5481e-05	1.3116	5.8348e-06	1.2528
1600	6.1401e-06	1.3342	2.3807e-06	1.2933
$\min\{r\sigma, 2-\alpha\}$		1.40		1.40

Table 5.6: L^2 errors and CO_N of the Example 5.4.1 with $r = \frac{5}{4} r_{opt_\sigma}$ and $\alpha = 0.6$ for different values of N and σ.

N	$\sigma = 0.75$		$\sigma = 1.50$	
	$E^N_{M_x}$	CO_N	$E^N_{M_x}$	CO_N
50	3.6114e-04	–	6.1805e-05	–
100	1.4057e-04	1.3613	2.5977e-05	1.2505
200	5.4160e-05	1.3760	1.0600e-05	1.2932
400	2.0741e-05	1.3847	4.1803e-06	1.3423
800	7.9134e-06	1.3901	1.6221e-06	1.3657
1600	3.0121e-06	1.3935	6.2352e-07	1.3794
$\min\{r\sigma, 2-\alpha\}$		1.40		1.40

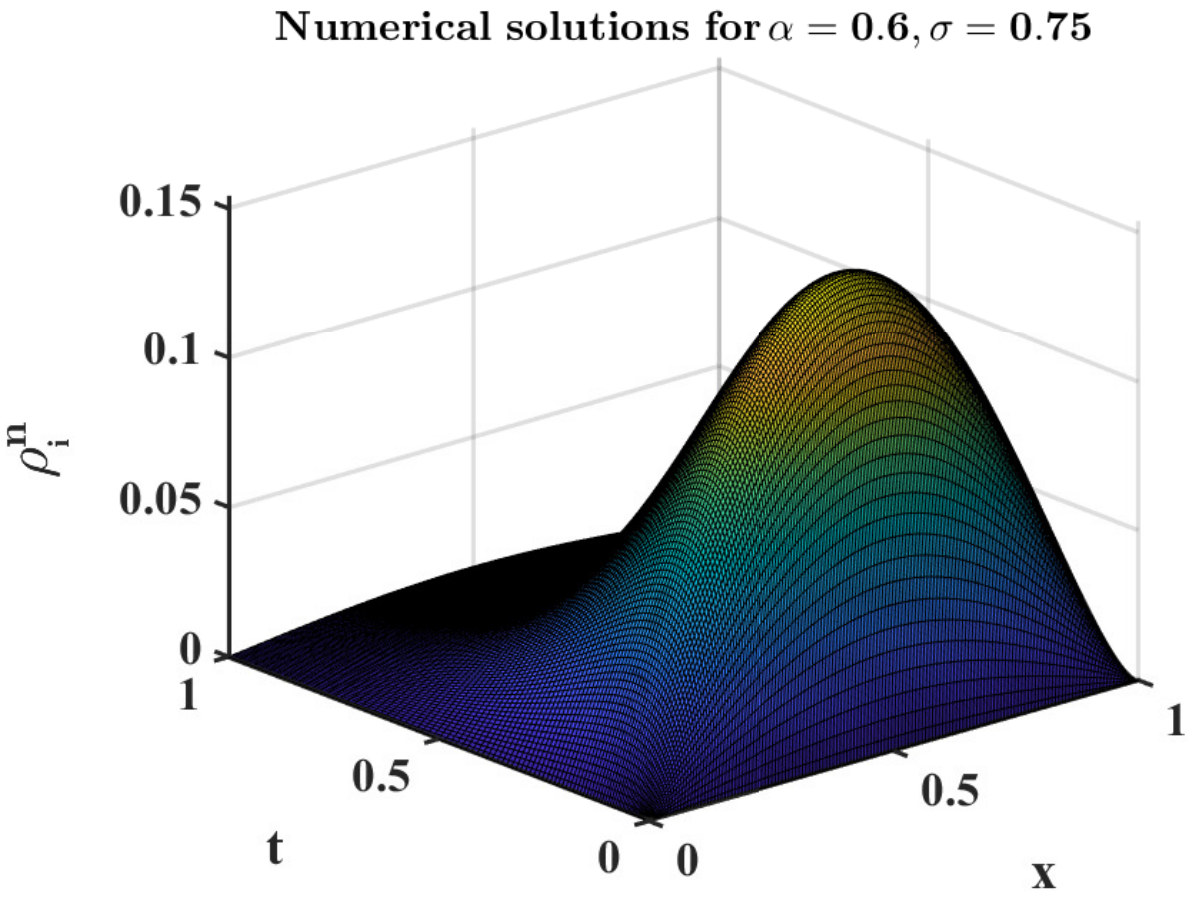

Figure 5.3: Numerical solutions plot for $N = 100$ with $r = r_{opt_\sigma}$.

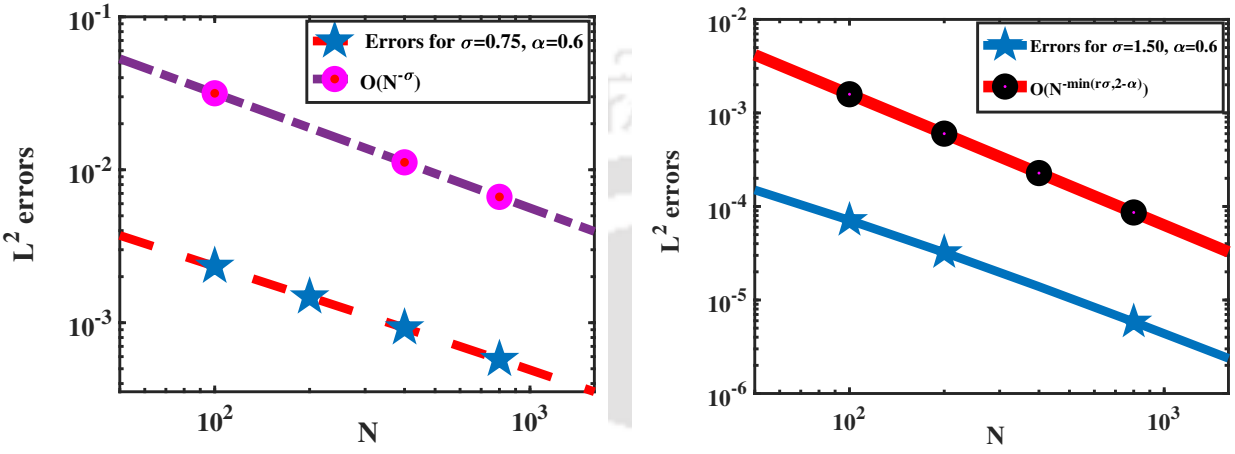

(a) Log-log plot for $r = 1$

(b) Log-log plot for $r = r_{opt_\sigma}$

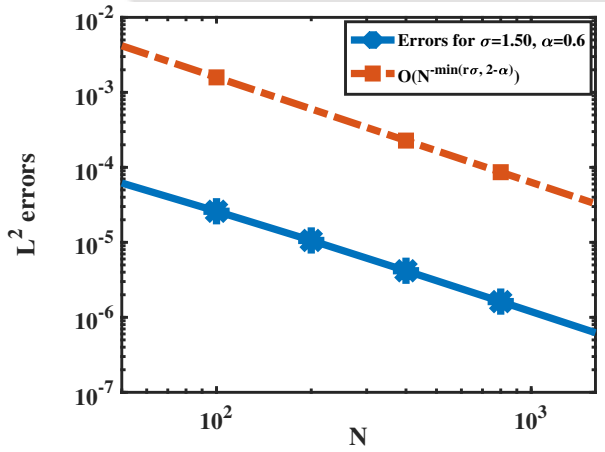

(c) Log-log plot for $r = \frac{5}{4} r_{opt_\sigma}$

Figure 5.4: Log-log plots corresponding to Tables 5.4-5.6.

5.5 Conclusions

The study in this chapter investigated an analysis of the non-uniform $L1$-method to find the numerical solution of a nonlinear time-fractional diffusion equation (5.1.1) with generalized memory kernel. To overcome the difficulty due to the presence of singularity in the solution at $t = 0$, the graded meshes $t_n = T\,(n/N)^r$, $n = 0, 1, 2 \ldots, N$ have been conducted as it has advantage to concentrate the mesh points near $t = 0$. Complementary discrete generalized memory kernel has been introduced to develop a generalized discrete fractional Grönwall inequality for the non-uniform $L1$-formula (5.2.12). Stability and the error estimate of the proposed scheme with convergence order $\mathcal{O}\left(N^{-\min(r\alpha, 2-\alpha)}\right)$ were carried out in the L^2-norm. Also, a regularity parameter $\sigma \in (0, 1) \cup (1, 2)$ has been taken into account and the convergence rates $\mathcal{O}\left(N^{-\min(r\sigma, 2-\alpha)}\right)$ have been enumerated in temporal direction under the regularity condition (5.3.15). Some numerical simulations have been comprehended in support of the performance of theoretical aspects and the computed results have shown good agreement with the presented analysis.

CHAPTER 6

An efficient dimensional-splitting $L1$-WGFEM for 2D time-fractional diffusion equation

In this chapter, 2D TFDE is numerically solved by the dimensional-splitting WGFEM. The proposed scheme alleviates the computational complexity and the high storage requirement for higher-dimensional problems. Initially, the 2D problem is separated into two 1D problems. Then the WGFEM is implemented in spatial variable and L1-method is used in time-fractional derivative term. The stability of the proposed method is established in each directions and an overall error estimate result is carried out. Some numerical simulations are incorporated to validate the theoretical error estimate.

6.1 Introduction

In this chapter, we study the following two-dimensional time-fractional diffusion equation (TFDE):

$$\begin{cases} {}^{C}D^{\alpha}_{0,t}u - \Delta u + \mathbf{d}(\mathbf{x}).\nabla u + c(\mathbf{x})u = f(\mathbf{x},t), \quad (\mathbf{x},t) \in \mathcal{V}\times\Omega_t, \\ u(\mathbf{x},0) = \widehat{u}_0(\mathbf{x}), \quad \mathbf{x}\in\overline{\mathcal{V}}, \\ u(\mathbf{x},t) = 0, \quad (\mathbf{x},t) \in \partial\mathcal{V}\times\overline{\Omega}_t, \end{cases} \tag{6.1.1}$$

where $u(\mathbf{x}) := u(x,y)$ for any function u, $\Omega_t = (0,T]$ and $\mathcal{V} = \Omega_x \times \Omega_y$ is the tensor product grids of the x-domain $\Omega_x = (x_l, x_r)$ and the y-domain $\Omega_y = (y_l, y_r)$ with the boundary $\partial\mathcal{V}$. The coefficient functions $\mathbf{d} = (d_1, d_2)$ and $c = c_1 + c_2$ are considered to be smooth and bounded with $d_1 \geq \gamma_x > 0$, $d_2 \geq \gamma_y > 0$, and $c_1, c_2 \geq 0$ in the domain $\overline{\mathcal{V}}$. To confirm the existence of the solution of the model problem (6.1.1), the source function $f(\mathbf{x},t)$ and the initial value $u_0\mathbf{x}$ are considered to be smooth enough, and we also assume that $c - 1/2\nabla\cdot\mathbf{d} \geq 0$.

The main motive of this chapter is to study the numerical solution of the time-fractional diffusion equation using the WGFEM along with the ADI-type dimensional-splitting technique to approximate the spatial derivatives and the $L1$-method to approximate the Caputo fractional time derivative to discretize the TFDE (6.1.1). Initially, we disintegrate the 2D TFDE (6.1.1) into two one-dimensional sub-problems with the help of dimensional-splitting and then apply the non-uniform $L1$-scheme in time, and thereafter the WGFEM is implemented separately over each of the sub-problems. Finally, the stability and optimal error analysis of the proposed method are studied in $L^{\infty}\left(L^2(\mathcal{V})\right)$-norm.

The rest of the chapter is constructed as follows: in Section 6.2, the subproblems are introduced with the help of dimensional-splitting technique. The fully discrete scheme, time-discretization and the stability analysis are incorporated in Section 6.3. The error estimate is analyzed in Section 6.4. Section 6.5 contains numerical experiment in favor of the theoretical estimation. Finally some conclusions are drawn in Section 6.6.

6.2 ADI-type dimensional-splitting technique

In this section, we establish the idea of ADI-type dimensional-splitting technique for the model problem (6.1.1). Let us propose two operators defined as:

$$\begin{cases} \mathcal{L}_x \equiv -\dfrac{\partial^2}{\partial x^2} + d_1(\mathbf{x})\dfrac{\partial}{\partial x} + c_1(\mathbf{x}), \quad \forall\ y\in\Omega_y, \\ \mathcal{L}_y \equiv -\dfrac{\partial^2}{\partial y^2} + d_2(\mathbf{x})\dfrac{\partial}{\partial y} + c_2(\mathbf{x}), \quad \forall\ x\in\Omega_x, \end{cases} \tag{6.2.1}$$

in the both spatial discretization, and the force function f is decomposed as $f = f_1 + f_2$ in such a way that it fulfils the following compatibility condition that is an essential assumption in the asymptotic study of the semi-discrete formulation of the problem:

$$f_1(x,0,t) = f_2(0,y,t) = f_1(x,1,t) = f_2(1,y,t) = 0. \tag{6.2.2}$$

Now, we can rewrite the model problem (6.1.1) as follows:

$${}^{C}D^{\alpha}_{0,t}u + (\mathcal{L}_x + \mathcal{L}_y)\, u = f_1(\mathbf{x},t) + f_2(\mathbf{x},t) \quad \text{in} \quad \mathcal{V} \times \Omega_t. \tag{6.2.3}$$

We use the non-uniform temporal mesh $\overline{\Omega}_t^N$ for time discretization of the interval $\overline{\Omega}_t$ with the non-uniform time-step length $\tau_n = t_n - t_{n-1}$, $n = 1, 2, \ldots, N$, where $N \in \mathbb{N}$ is the number of mesh intervals of $\overline{\Omega}_t^N$.

Now, we represent the following sub-problems in each time subinterval $(t_n, t_{n+1}]$ for $n = 0, 1, \ldots, N-1$ as

Step 1.

Seek a solution $u^{(+)} : \mathcal{V} \times (t_n, t_{n+1}] \to \mathbb{R}$ such that $\forall\, y \in \Omega_y$

$$\begin{cases} {}^{C}D^{\alpha}_{0,t}u^{(+)} + \mathcal{L}_x u^{(+)} = f_1(\mathbf{x}, t_{n+1}) \quad \text{in} \quad \mathcal{V} \times (t_n, t_{n+1}], \\ u^{(+)}(\mathbf{x},t) = 0, \quad (\mathbf{x},t) \in \partial\Omega_x \times \Omega_y \times (t_n, t_{n+1}], \\ u^{(+)}(\mathbf{x},t_n) = u(\mathbf{x},t_n), \quad \mathbf{x} \in \mathcal{V}, \end{cases} \tag{6.2.4}$$

and

Step 2.

Seek a solution $u : \mathcal{V} \times (t_n, t_{n+1}] \to \mathbb{R}$ such that $\forall\, x \in \Omega_x$

$$\begin{cases} {}^{C}D^{\alpha}_{0,t}u + \mathcal{L}_y u = f_2(\mathbf{x}, t_{n+1}) \quad \text{in} \quad \mathcal{V} \times (t_n, t_{n+1}], \\ u(\mathbf{x},t) = 0, \quad (\mathbf{x},t) \in \Omega_x \times \partial\Omega_y \times (t_n, t_{n+1}], \\ u(\mathbf{x},t_n) = u^{(+)}(\mathbf{x}, t_{n+1}), \quad \mathbf{x} \in \mathcal{V}. \end{cases} \tag{6.2.5}$$

In Step 1, we first solve the time-fractional initial-boundary value problem (FIBVP) (6.2.4) along the $x-$ axis by considering y as a parameter, and after solving for each $y \in \Omega_y$, the solution $u^{(+)}(\mathbf{x}, t_{n+1})$ will be the initial step for the second step (6.2.5). In Step 2, we next consider $y-$ axis and in a similar fashion we solve the problem (6.2.5) $\forall\ x \in \Omega_x$. In other words, we have used their initial conditions to couple the above two subproblems.

We define the standard Sobolev space

$$H^m(\mathcal{V}) = \left\{ v \in L^2(\mathcal{V}) : D^q v \in L^2(\mathcal{V}),\ |q| \leq m \right\},$$

where, $\mathcal{V} = \Omega_x \times \Omega_y \in \mathbb{R}^2$.

Also, we recall the following Sobolev spaces in the both spatial variables

$$H_0^1(\Omega_x) := \left\{ v(x) \in L^2(\Omega_x) : \frac{dv}{dx} \in L^2(\Omega_x),\ v|_{\partial\Omega_x} = 0 \right\}, \tag{6.2.6}$$

and

$$H_0^1(\Omega_y) := \left\{ v(y) \in L^2(\Omega_y) : \frac{dv}{dy} \in L^2(\Omega_y),\ v|_{\partial\Omega_y} = 0 \right\}. \tag{6.2.7}$$

The standard weak form of the subproblems (6.2.4) and (6.2.5) can be obtained after multiplying by the functions $v_1 \in H_0^1(\Omega_x)$ and $v_2 \in H_0^1(\Omega_y)$ respectively and integration by parts, as follows

Weak form: ($x-$direction)

$$\begin{cases} \left({}^C D_{0,t}^{\alpha} u^{(+)}, v_1\right) + \left(\mathcal{L}_x u^{(+)}, v_1\right) = (f_1, v_1), \quad \forall v_1 \in H_0^1(\Omega_x), t \in (t_n, t_{n+1}], \\ u^{(+)}(\mathbf{x}, t_n) = u(\mathbf{x}, t_n), \quad \mathbf{x} \in \overline{\mathcal{V}}, \end{cases} \tag{6.2.8}$$

and

Weak form: ($y-$direction)

$$\begin{cases} \left({}^C D_{0,t}^{\alpha} u, v_2\right) + \left(\mathcal{L}_y u, v_2\right) = (f_2, v_2), \quad \forall v_2 \in H_0^1(\Omega_y), t \in (t_n, t_{n+1}], \\ u(\mathbf{x}, t_n) = u^{(+)}(\mathbf{x}, t_{n+1}), \quad \mathbf{x} \in \overline{\mathcal{V}}. \end{cases} \tag{6.2.9}$$

6.3 Weak Galerkin finite element discretization and stability analysis

In this section, discretization technique of the model problem (6.1.1) will be addressed in both spatial and temporal direction. The stability result of the fully discrete scheme will also be established in this section. Let M_x and M_y be two positive integers in the x- and y-directions respectively. In our problem, we consider $M = M_x = M_y$ in both the directions.

(Along $x-$direction)

Let $\overline{\Omega}_x^M = \{x_i : 0 = x_0 < x_1 < \ldots < x_{M-1} < x_M = 1,\ i = 0, 1, \ldots, M\}$ be a partition of the interval Ω_x, $I_{x_i} = [x_{i-1}, x_i]$ be mesh, triangulation $\mathcal{K}_x^M = \{I_{x_i},\ i = 1, 2, \ldots, M\}$ and $h_x = x_i - x_{i-1},\ i = 1, 2, \ldots, M$ is the uniform step-size.

Let k be a positive integer. The weak function space $W(I_{x_i}, k)$ on $I_{x_i} \in \mathcal{K}_x^M$ is defined as

$$W(I_{x_i}, k) = \{u_h^{(+)} = \{u_0^{(+)}, u_b^{(+)}\} : u_0^{(+)}|_{I_{x_i}} \in \mathbb{P}_k(I_{x_i}), u_b^{(+)}|_{\partial I_{x_i}} \in \mathbb{P}_0(\partial I_{x_i})\}, \tag{6.3.1}$$

where $\mathbb{P}_k(I_{x_i})$ is the set of polynomials defined on I_{x_i} of degree at most k and $\mathbb{P}_0(\partial I_{x_i})$ denotes the constant polynomials on ∂I_{x_i}.

A global weak Galerkin finite element space S_{h_x} can be defined as putting together the weak function space $W(I_{x_i}, k)$ that has a single value on the mesh points of the triangulation $\mathcal{K}_x^M$. That is, $w_h = \{w_0, w_b\} \in S_{h_x}$ means that $w_0 \in \mathbb{P}_k(I_{x_i})$ for $i = 1, \ldots, M$, and w_b is a single-valued on the nodes of the partition $\mathcal{K}_x^M$.

We next define $S_{h_x}^0$ as the subspace of S_{h_x} with zero boundary values, given by

$$S_{h_x}^0 = \left\{u_h^{(+)} = \{u_0^{(+)}, u_b^{(+)}\} : u^{(+)} \in S_{h_x},\ u_b^{(+)}(0) = u_b^{(+)}(1) = 0\right\}. \tag{6.3.2}$$

(Along $y-$direction)

In a similar fashion, we can define the following for $y-$direction:

Let $\overline{\Omega}_y^M = \{y_j : 0 = y_0 < y_1 < \ldots < y_{M-1} < y_M = 1,\ j = 0, 1, \ldots, M\}$ be a partition of the interval Ω_y, $I_{y_j} = [y_{j-1}, y_j]$ be mesh, triangulation $\mathcal{K}_y^M = \left\{I_{y_j},\ j = 1, 2, \ldots, M\right\}$ and $h_y = y_j - y_{j-1}, j = 1, 2, \ldots, M$ be the uniform step-size.

Let k be a positive integer. The weak function space $W\left(I_{y_j}, k\right)$ on $I_{y_j} \in \mathcal{K}_y^M$ is defined as

$$W\left(I_{y_j}, k\right) = \{u_h = \{u_0, u_b\} : u_0|_{I_{y_j}} \in \mathbb{P}_k(I_{y_j}), u_b|_{\partial I_{y_j}} \in \mathbb{P}_0(\partial I_{y_j})\}, \tag{6.3.3}$$

where $\mathbb{P}_k(I_{y_j})$ is the set of polynomials defined on I_{y_j} of degree at most k and $\mathbb{P}_0(\partial I_{y_j})$ denotes the constant polynomials on ∂I_{y_j}.

A global weak Galerkin finite element space S_{h_y} can be defined as putting together the weak function space $W\left(I_{y_j}, k\right)$ that has a single value on the mesh points of the triangulation $\mathcal{K}_y^M$. That is, $v_h = \{v_0, v_b\} \in S_{h_y}$ means that $v_0 \in \mathbb{P}_k(I_{y_j})$ for $j = 1, \ldots, M$, and v_b is a single-valued on the nodes of the partition $\mathcal{K}_y^M$.

We next define $S_{h_y}^0$ as the subspace of S_{h_y} with zero boundary values, given by

$$S_{h_y}^0 = \left\{ u_h = \{u_0, u_b\} : u_h \in S_{h_y},\ u_b(0) = u_b(1) = 0 \right\}. \tag{6.3.4}$$

We define weak derivative $d_{w,I_{x_i}} v_h^{(+)} \in \mathbb{P}_{k-1}(I_{x_i})$ of a weak function $v_h^{(+)} = \{v_0^{(+)}, v_b^{(+)}\} \in W(I_{x_i}, k)$ as the unique polynomial such that the following equation holds

$$(d_{w,I_{x_i}} v_h^{(+)}, q)_{I_{x_i}} = -(v_0^{(+)}, q')_{I_{x_i}} + \langle v_b^{(+)}, q\bar{n}\rangle_{\partial I_{x_i}}, \quad \forall q \in \mathbb{P}_{k-1}(I_{x_i}), \tag{6.3.5}$$

where $(\varphi, \psi)_{I_{x_i}} := \int_{I_{x_i}} \varphi(x)\psi(x)\mathrm{d}x$ and $\langle \varphi, \psi n\rangle_{\partial I_{x_i}} := \varphi(x_i)\psi(x_i) - \varphi(x_{i-1})\psi(x_{i-1})$.

The weak derivative $d_{w,I_{y_j}} v_h \in \mathbb{P}_{k-1}\left(I_{y_j}\right)$ can be defined similarly.

The convection parts $d_1 u_x$ and $d_2 u_y$ can be approximated by a weak convection derivative defined as follows.

For any weak function $v_h^{(+)} = \{v_0^{(+)}, v_b^{(+)}\} \in W(I_{x_i}, k)$, the weak convection derivative of $v_h^{(+)}$ is the unique polynomial $d_{w,I_{x_i}}^{d_1} v_h^{(+)} \in \mathbb{P}_k(I_{x_i})$ satisfying

$$(d_{w,I_{x_i}}^{d_1} v_h^{(+)}, q)_{I_{x_i}} = -(v_0^{(+)}, (d_1 q)')_{I_{x_i}} + \langle v_b^{(+)}, d_1 q\bar{n}\rangle_{\partial I_{x_i}}, \quad \forall q \in \mathbb{P}_k(I_{x_i}). \tag{6.3.6}$$

Similarly, we can define the weak convection derivative $d_{w,I_{y_j}}^{d_2} v_h \in \mathbb{P}_k(I_{y_j})$ of v_h in the y-direction.

The weak derivatives d_w and $d_w^{d_1}$ on the WG finite element space S_{h_x} are computed on each interval I_{x_i} for $i = 1, \ldots, M$, respectively. That is,

$$(d_w v_h^{(+)})|_{I_{x_i}} = d_{w,I_{x_i}}((v_h^{(+)})|_{I_{x_i}}), \quad (d_w^{d_1} v_h^{(+)})|_{I_{x_i}} = d_{w,I_{x_i}}^{d_1}((v_h^{(+)})|_{I_{x_i}}),\ \forall v_h^{(+)} \in S_{h_x}.$$

Similarly, the weak derivatives d_w and $d_w^{d_2}$ on the WG finite element space S_{h_y} can be computed.

For simplicity, we adopt the following notations

$$(\phi, \psi)_{\mathcal{K}_x^M} = \sum_{i=1}^{M} (\phi, \psi)_{I_{x_i}}, \quad \langle \phi, \psi\rangle_{\partial\mathcal{K}_x^M} = \sum_{i=1}^{M} \langle \phi, \psi\rangle_{\partial I_{x_i}},$$

and the corresponding L^2-norm is defined as $\|\phi\|_{\mathcal{K}_x^M} = \sum_{i=1}^{M} \|\phi\|_{I_{x_i}}$. Similarly, the notations can be defined in the y-direction.

We introduce the following bilinear forms on S_{h_x} for our formulation of the WG-FEM.

For any $u_h^{(+)} = \{u_0^{(+)}, u_b^{(+)}\},\ v_h^{(+)} = \{v_0^{(+)}, v_b^{(+)}\} \in S_{h_x}$, we define

$$a^{(+)}\left(u_h^{(+)}, v_h^{(+)}\right) = \left(d_w u_h^{(+)}(t), d_w v_h^{(+)}\right)_{\mathcal{K}_x^M} + \left(d_w^{d_1} u_h^{(+)}(t) + c_1 u_0^{(+)}, v_0^{(+)}\right)_{\mathcal{K}_x^M},$$

$$s_c^{(+)}(u_h^{(+)}, v_h^{(+)}) = \sum_{i=1}^{M} \langle d_1 \bar{n}(u_0^{(+)} - u_b^{(+)}), v_0^{(+)} - v_b^{(+)} \rangle_{\partial_+ I_{x_i}},$$

$$s_d^{(+)}(u_h^{(+)}, v_h^{(+)}) = \sum_{i=1}^{M} \langle h_x^{-1}(u_0^{(+)} - u_b^{(+)}), v_0^{(+)} - v_b^{(+)} \rangle_{\partial I_{x_i}},$$

where $\partial_+ I_{x_i} = \{x \in \partial I_{x_i} : d_1(x)\bar{n}_{I_{x_i}}(x) \geq 0\}$. Similarly, we define the bilinear forms on S_{h_y} for our formulation of the WG-FEM. For any $u_h = \{u_0, u_b\},\ v_h = \{v_0, v_b\} \in S_{h_y}$, we define

$$a\left(u_h, v_h\right) = \left(d_w u_h(t), d_w v_h\right)_{\mathcal{K}_y^M} + \left(d_w^{d_2} u_h(t) + c_2 u_0, v_0\right)_{\mathcal{K}_y^M},$$

$$s_c(u_h, v_h) = \sum_{j=1}^{M} \langle d_2 \bar{n}(u_0 - u_b), v_0 - v_b \rangle_{\partial_+ I_{y_j}},$$

$$s_d(u_h, v_h) = \sum_{j=1}^{M} \langle h_y^{-1}(u_0 - u_b), v_0 - v_b \rangle_{\partial I_{y_j}}.$$

We introduce an energy norm $\|\cdot\|_W^{(+)}$ in the WG finite element space S_{h_x}. For any $v_h^{(+)} = \{v_0^{(+)}, v_b^{(+)}\} \in S_{h_x}$, define

$$\|v_h^{(+)}\|_W^{(+)} := |v_h^{(+)}|_1^{(+)} + \|\sqrt{c_1} v_0^{(+)}\|_{\mathcal{K}_x^M}^2 + |v_h^{(+)}|_C^{(+)}, \tag{6.3.7}$$

where

$$|v_h^{(+)}|_1^{(+)} := \|d_w v_h^{(+)}\|_{\mathcal{K}_x^M}^2 + s_d^{(+)}(v_h^{(+)}, v_h^{(+)}),$$

$$|v_h^{(+)}|_C^{(+)} := \sum_{i=1}^{M} \varsigma_i^{(+)} |\sqrt{d_1}(v_0^{(+)} - v_b^{(+)})|^2(x_i^-),$$

with

$$\varsigma_i^{(+)} = \begin{cases} \frac{1}{2}, & i = M, \\ 1, & i = 1, \ldots, M-1. \end{cases}$$

Similarly, one can define the norm $\|\cdot\|_W$ in the y-direction.

From [96, Lemma 3.2], we have the following coercivity of the bilinear forms $A^{(+)}(\cdot,\cdot)$ and $A(\cdot,\cdot)$ on $S_{h_x}^0$ and $S_{h_y}^0$ with respect to the norm $\|\cdot\|_W^{(+)}$ and $\|\cdot\|_W$, respectively.

Lemma 6.3.1. *[96] The bilinear forms $A^{(+)}(\cdot,\cdot)$ and $A(\cdot,\cdot)$ is coercive on $S^0_{h_x}$ and $S^0_{h_y}$ with respect to the norm $\|\cdot\|^{(+)}_W$ and $\|\cdot\|_W$, respectively, that is,*

$$A^{(+)}(v_h^{(+)}, v_h^{(+)}) \geq (\|v_h^{(+)}\|_W^{(+)})^2, \quad \forall v_h^{(+)} \in S^0_{h_x}, \tag{6.3.8}$$

$$A(v_h, v_h) \geq \|v_h\|_W^2, \quad \forall v_h \in S^0_{h_y}, \tag{6.3.9}$$

where

$$A^{(+)}\left(u_h^{(+)}(t), v_h\right) := a^{(+)}(u_h^{(+)}(t), v_h) + s_c^{(+)}(u_h^{(+)}, v_h) + s_d^{(+)}(u_h^{(+)}, v_h), \tag{6.3.10}$$

$$A\left(u_h(t), w_h\right) := a(u_h(t), w_h) + s_c(u_h, w_h) + s_d(u_h, w_h). \tag{6.3.11}$$

The semidiscrete continuous time WGFEM for the problem (6.2.8) and (6.2.9) can be formulated by replacing the derivative by weak derivative operators as follows: Find $u_h^{(+)}(t) = \{u_0^{(+)}(t), u_b^{(+)}(t)\} \in S^0_{h_x}$ for $t > 0$ such that

$$\left({}^C D^{\alpha}_{0,t} u_0^{(+)}(t), v_0\right)_{\mathcal{K}_x^M} + A^{(+)}\left(u_h^{(+)}(t), v_h\right) = (f_1, v_0)_{\mathcal{K}_x^M}, \ \forall v_h = \{v_0, v_b\} \in S^0_{h_x}, \ t \in (0, T], \tag{6.3.12}$$

and

$$\left({}^C D^{\alpha}_{0,t} u_0(t), w_0\right)_{\mathcal{K}_y^M} + A\left(u_h(t), w_h\right) = (f_2, w_0)_{\mathcal{K}_y^M}, \quad \forall w_h = \{w_0, w_b\} \in S^0_{h_y}, \ t \in (0, T]. \tag{6.3.13}$$

6.3.1 Time discretization

We use the following graded mesh for temporal discretization to deal with the singularity of the solution at $t = 0$. To this end, let $N > 0$ be an integer. Define $t_n = T\,(n/N)^r$ for $n = 1, \ldots, N$, with a user-chosen mesh grading constant $r \geq 1$. Note that if $r = 1$, then the mesh is uniform. Let $\tau_n = t_n - t_{n-1}$ for $n = 1, \ldots, N$ be the time step. Observe that

$$\tau_{n+1} = T\left(\frac{n+1}{N}\right)^r - T\left(\frac{n}{N}\right)^r \leq CTN^{-r}n^{r-1} \text{ for } n = 0, 1, \ldots, N-1. \tag{6.3.14}$$

To approximate the Caputo derivative ${}^C D^{\alpha}_{0,t} v$ of a function $v(\cdot, t)$ at the point $t = t_n$, we use the $L1$-scheme, described in (1.2.24) of Chapter 1 on the graded time-domain $\overline{\Omega}_t^N$ as follows:

$$\begin{aligned} {}^C D^{\alpha}_{0,t} v\left(\mathbf{x}, t_n\right) &= \frac{\mathfrak{b}_{n,1}^{(\alpha)}}{\Gamma(2-\alpha)} v^n - \frac{\mathfrak{b}_{n,n}^{(\alpha)}}{\Gamma(2-\alpha)} v^0 + \frac{1}{\Gamma(2-\alpha)} \sum_{k=1}^{n-1} v^{n-k}\left(\mathfrak{b}_{n,k+1}^{(\alpha)} - \mathfrak{b}_{n,k}^{(\alpha)}\right) + \widehat{\mathcal{T}}^n(x) \\ &= \triangle_N^{\alpha} v^n + \widehat{\mathcal{T}}^n(x), \end{aligned} \tag{6.3.15}$$

where $v^n := v(\cdot, t_n)$ and the temporal truncation error $\widehat{\mathcal{T}}^n(\mathbf{x})$ has the following expression. When $k = 1$, we have $\mathfrak{b}_{n,1}^{(\alpha)} = \tau_n^{-\alpha}$. Using the mean value theorem, one can show that

$$\mathfrak{b}_{n,k+1}^{(\alpha)} < \mathfrak{b}_{n,k}^{(\alpha)} \text{ for } 0 \leq k \leq n-1 \leq N-1. \tag{6.3.16}$$

The temporal truncation error $\widehat{\mathcal{T}}^n(\mathbf{x})$ is given as:

$$\begin{aligned}\widehat{\mathcal{T}}^n(\mathbf{x}) &:= {}^C D_{0,t}^{\alpha} v(\mathbf{x}, t_n) - \Delta_N^{\alpha} v(\mathbf{x}, t_n) \\ &= \sum_{k=1}^{n-1} \frac{1}{\Gamma(1-\alpha)} \int_{t_k}^{t_{k+1}} (t_n - \zeta)^{-\alpha} \left(\frac{\partial v(\mathbf{x}, \zeta)}{\partial \zeta} - \frac{v(\mathbf{x}, t_{k+1}) - v(\mathbf{x}, t_k)}{\tau_{k+1}} \right) d\zeta.\end{aligned}$$

The following lemma shows the convergence rate of the L1-WG-FEM.

Lemma 6.3.2. *For all $(\boldsymbol{x}, t_n) \in \mathcal{V} \times \Omega_t$, there is a constant C such that there holds*

$$|\widehat{\mathcal{T}}^n| \leq C n^{-\min\{2-\alpha, r\alpha\}}.$$

Proof. The proof can be found in [72, Lemma 5.2] in details. □

6.3.2 Fully-discrete scheme

Using the $L1-$method (6.3.15), we discretize the semi-discrete problems (6.3.12) and (6.3.13) in time. The fully discrete WG scheme can be formulated as follows:

(Along x-direction)

Find $u_h^{(+),n+1}(x, y_j) = \left\{ u_{h,0}^{(+),n+1}, u_{h,b}^{(+),n+1} \right\} \in S_{h_x}^0$ for given $u_h^{(+),n}(x, y_j)$ with $y_j \in I_{h_y}$ such that

$$\begin{aligned}\left(\triangle_N^{\alpha} u_{h,0}^{(+),n+1}(x, y_j), v_0 \right)_{\mathcal{K}_x^M} + A^{(+)} \left(u_h^{(+),n+1}(x, y_j), v \right)_{\mathcal{K}_x^M} &= \left(f_1^{n+1}(x, y_j), v_0 \right)_{\mathcal{K}_x^M}, \\ &\forall v = \{v_0, v_b\} \in S_{h_x}^0,\end{aligned} \tag{6.3.17}$$

and

(Along y-direction)

Find $u_h^{n+1}(x_i, y) \in S_{h_y}^0$ for given $u_h^n(x_i, y)$ and for all $x_i \in \overline{\Omega}_x^M$ such that

$$\begin{aligned}\left(\triangle_N^{\alpha} u_{h,0}^{n+1}(x_i, y), w_0 \right)_{\mathcal{K}_y^M} + A \left(u_h^{n+1}(x_i, y), w \right) &= \left(f_2^{n+1}(x_i, y), w_0 \right)_{\mathcal{K}_y^M}, \\ &\forall w = \{w_0, w_b\} \in S_{h_y}^0,\end{aligned} \tag{6.3.18}$$

where $f_l^{n+1}(x,y) := f_l(x,y,t_{n+1})$ for each $l = 1,2$ and $u_h^{(+),0}(x,y_j) = u_h^0(x,y_j)$ $\forall j = 0,\ldots,M$ and $u_h^0(x,y_j) = \pi_y u_0(\mathbf{x})$ is the L^2 projection of the initial condition $u_0(\mathbf{x})$ on the WG-FEM space.

6.3.3 Stability analysis

In this subsection we will study the stability of the proposed dimensional-splitting WG method. The results will be studied for each sub-problem to establish the stability theorem in each x and y directions.

Theorem 6.3.3. *Let $u_h^{(+),n+1}$ and u_h^{n+1} be the numerical solutions computed by the fully discrete WG schemes* (6.3.17) *and* (6.3.18) *respectively. Then we have the following stability bounds*

$$\left\|u_{h,0}^{(+),n+1}\right\|_{\mathcal{K}_x^M} \leq \tau_n^\alpha \Big[\Gamma(2-\alpha)\left\|f_1^{n+1}\right\|_{\mathcal{K}_x^M} + \mathfrak{b}_{n,n}^{(\alpha)}\left\|u_{h,0}^{(+),0}\right\|_{\mathcal{K}_x^M} + \sum_{i=1}^{n-1}\left(\mathfrak{b}_{n,i}^{(\alpha)} - \mathfrak{b}_{n,i+1}^{(\alpha)}\right)\left\|u_{h,0}^{(+),i+1}\right\|_{\mathcal{K}_x^M}\Big],$$

and

$$\left\|u_{h,0}^{n+1}\right\|_{\mathcal{K}_y^M} \leq \tau_n^\alpha \Big[\Gamma(2-\alpha)\left\|f_2^{n+1}\right\|_{\mathcal{K}_y^M} + \mathfrak{b}_{n,n}^{(\alpha)}\left\|u_{h,0}^{(+),0}\right\|_{\mathcal{K}_y^M} + \sum_{i=1}^{n-1}\left(\mathfrak{b}_{n,i}^{(\alpha)} - \mathfrak{b}_{n,i+1}^{(\alpha)}\right)\left\|u_{h,0}^{i+1}\right\|_{\mathcal{K}_y^M}\Big],$$

for each $n = 0,1,\ldots,N-1$.

Proof. From now onwards, we will denote $u_h^{(+),n+1}(x,y_j) = u_h^{(+),n+1}$, $u_h^{n+1}(x_i,y) = u_h^{n+1}$, $f_1^{n+1}(x,y_j) = f_1^{n+1}$ and $f_2^{n+1}(x,y_j) = f_2^{n+1}$ for the simplicity. We set $v = u_h^{(+),n+1}$ in the equation (6.3.17) to obtain

$$\left(\triangle_N^\alpha u_{h,0}^{(+),n+1}, u_{h,0}^{(+),n+1}\right)_{\mathcal{K}_x^M} + A^{(+)}\left(u_h^{(+),n+1}, u_h^{(+),n+1}\right) = \left(f_1^{n+1}, u_{h,0}^{(+),n+1}\right)_{\mathcal{K}_x^M}, \forall v \in S_{h_x}^0.$$

Now, using the Cauchy-Schwarz inequality, we get

$$\left(f_1^{n+1}, u_{h,0}^{(+),n+1}\right)_{\mathcal{K}_x^M} \leq \left\|f_1^{n+1}\right\|_{\mathcal{K}_x^M}\left\|u_{h,0}^{(+),n+1}\right\|_{\mathcal{K}_x^M}.$$

Now, recalling the coercivity of the bilinear form $A^{(+)}(\cdot,\cdot)$ given by (6.3.8), we have

$$A^{(+)}\left(u_h^{(+),n+1}, u_h^{(+),n+1}\right) \geq C(\|u_h^{(+),n+1}\|_W^{(+)})^2.$$

Thus, we have

$$\left\|f_1^{n+1}\right\|_{\mathcal{K}_x^M}\left\|u_{h,0}^{(+),n+1}\right\|_{\mathcal{K}_x^M} \geq \left(\triangle_N^\alpha u_{h,0}^{(+),n+1}, u_{h,0}^{(+),n+1}\right)_{\mathcal{K}_x^M}. \tag{6.3.19}$$

We will prove that the $L1$ method is coercive. It follows from the Cauchy-Schwarz inequality and the fact that $\mathfrak{b}_{n,i}^{(\alpha)} - \mathfrak{b}_{n,i+1}^{(\alpha)} > 0$ that

$$\begin{aligned}
\left(\triangle_N^{\alpha} u_{h,0}^{(+),n+1}, u_{h,0}^{(+),n+1}\right)_{\mathcal{K}_x^M} &= \frac{\mathfrak{b}_{n,1}^{(\alpha)}}{\Gamma(2-\alpha)}\left(u_{h,0}^{(+),n+1}, u_{h,0}^{(+),n+1}\right)_{\mathcal{K}_x^M} - \frac{\mathfrak{b}_{n,n}^{(\alpha)}}{\Gamma(2-\alpha)}\left(u_{h,0}^{(+),0}, u_{h,0}^{(+),n+1}\right)_{\mathcal{K}_x^M} \\
&\quad - \frac{1}{\Gamma(2-\alpha)}\sum_{i=1}^{n-1}\left(\mathfrak{b}_{n,i}^{(\alpha)} - \mathfrak{b}_{n,i+1}^{(\alpha)}\right)\left(u_{h,0}^{(+),n-i}, u_{h,0}^{(+),n+1}\right)_{\mathcal{K}_x^M} \\
&\geq \frac{\mathfrak{b}_{n,1}^{(\alpha)}}{\Gamma(2-\alpha)}\left\|u_{h,0}^{(+),n+1}\right\|_{\mathcal{K}_x^M}^2 - \frac{\mathfrak{b}_{n,n}^{(\alpha)}}{\Gamma(2-\alpha)}\left\|u_{h,0}^{(+),0}\right\|_{\mathcal{K}_x^M}\left\|u_{h,0}^{(+),n+1}\right\|_{\mathcal{K}_x^M} \\
&\quad - \frac{1}{\Gamma(2-\alpha)}\sum_{i=1}^{n-1}\left(\mathfrak{b}_{n,i}^{(\alpha)} - \mathfrak{b}_{n,i+1}^{(\alpha)}\right)\left\|u_{h,0}^{(+),n-i}\right\|_{\mathcal{K}_x^M}\left\|u_{h,0}^{(+),n+1}\right\|_{\mathcal{K}_x^M} \\
&= \left(\triangle_N^{\alpha}\left\|u_{h,0}^{(+),n+1}\right\|_{\mathcal{K}_x^M}\right)\left\|u_{h,0}^{(+),n+1}\right\|_{\mathcal{K}_x^M}.
\end{aligned}$$

Therefore, from (6.3.19), we obtain

$$\left\|f_1^{n+1}\right\|_{\mathcal{K}_x^M}\left\|u_{h,0}^{(+),n+1}\right\|_{\mathcal{K}_x^M} \geq \left(\triangle_N^{\alpha}\left\|u_{h,0}^{(+),n+1}\right\|_{\mathcal{K}_x^M}\right)\left\|u_{h,0}^{(+),n+1}\right\|_{\mathcal{K}_x^M}.$$

Cancelling $\left\|u_{h,0}^{(+),n+1}\right\|_{\mathcal{K}_x^M}$, we get

$$\triangle_N^{\alpha}\left\|u_{h,0}^{(+),n+1}\right\|_{\mathcal{K}_x^M} \leq \left\|f_1^{n+1}\right\|_{\mathcal{K}_x^M}.$$

Now, using (6.3.15) to expand $\triangle_N^{\alpha}\left\|u_{h,0}^{(+),n+1}\right\|_{\mathcal{K}_x^M}$ yields

$$\begin{aligned}
\frac{\mathfrak{b}_{n,1}^{(\alpha)}}{\Gamma(2-\alpha)}\left\|u_{h,0}^{(+),n+1}\right\|_{\mathcal{K}_x^M} &\leq \left\|f_1^{n+1}\right\|_{\mathcal{K}_x^M} + \frac{1}{\Gamma(2-\alpha)}\Bigg[\mathfrak{b}_{n,n}^{(\alpha)}\left\|u_{h,0}^{(+),0}\right\|_{\mathcal{K}_x^M} \\
&\quad + \sum_{i=1}^{n-1}\left(\mathfrak{b}_{n,i}^{(\alpha)} - \mathfrak{b}_{n,i+1}^{(\alpha)}\right)\left\|u_{h,0}^{(+),i+1}\right\|_{\mathcal{K}_x^M}\Bigg],
\end{aligned}$$

which gives the desired result and we complete the proof for the stability estimate in the $x-$direction.

Similar to the above calculation, one can establish the stability result in the $y-$direction. □

6.4 Error analysis

In this section, we will study the convergence of the above discretized scheme. We first introduce the local L^2-projections in each direction as follows. For each $I_{x_i} \in \mathcal{K}_x^M$, $\pi_{x,0} : v \in L^2(I_{x_i}) \to \pi_{0,x}v \in \mathbb{P}_k(I_{x_i})$ is defined by $\left(\pi_{x,0}v - v, \phi\right) = 0, \quad \forall \phi \in \mathbb{P}_k(I_{x_i}), \quad i = 1, \ldots, M.$

The Bramble–Hilbert lemma implies that

$$\|v-\pi_{x,0}v\|_{L^2(I_{x_i})}+h_x\|v-\pi_{x,0}v\|_{H^1(I_{x_i})}\leq C(h_x)^s\|v\|_{H^s(I_{x_i})},\quad 0\leq s\leq k+1. \tag{6.4.1}$$

We define a projection operator $\pi_x : H^1(I_{x_i}) \to W(I_{x_i},k)$ such that

$$\pi_x v|_{I_{x_i}}=\{\pi_{x,0}v,\pi_{x,b}v\}=\{\pi_{x,0}v,\{v(x_{i-1}),v(x_i)\}\},\quad i=1,\ldots,M.$$

We emphasize that $\pi_x v\in S^0_{h_x}$ when $v\in H^1_0(\overline{\Omega}^M_x)$.

Similarly, we define a projection $\pi_y : H^1(I_{y_j}) \to W(I_{y_j},k)$ with $\pi_y v|_{I_{y_j}}=\{\pi_{y,0}v,\pi_{y,b}v\}$ and that

$$\|v-\pi_{y,0}v\|_{L^2(I_{y_j})}+h_y\|v-\pi_{y,0}v\|_{H^1(I_{y_j})}\leq C(h_y)^s\|v\|_{H^s(I_{y_j})},\quad 0\leq s\leq k+1. \tag{6.4.2}$$

For any function $\varphi\in H^1(I)$, the following trace inequality holds true (see [82] for details):

$$\|\varphi\|^2_{L^2(\partial I)}\leq C\left(h_I^{-1}\|\varphi\|^2_{L^2(I)}+h_I\|\varphi'\|^2_{L^2(I)}\right), \tag{6.4.3}$$

where h_I is the mesh size of the interval I.

In order to derive an optimal order convergence rate, we follow the Wheeler's projection technique in defining an elliptic (Ritz) projection $P_x : H^1_0(\Omega_x)\to S^0_{h_x}$ given by

$$A^{(+)}(P_x u^{(+)},v_h^{(+)})=(\mathcal{L}_x u^{(+)},v_0^{(+)}),\quad \forall v_h^{(+)}=\{v_0^+,v_b^+\}\in S^0_{h_x}. \tag{6.4.4}$$

For the sake of notation, we denote $P_x u^{(+)}=\{P_{x,0}u^{(+)},P_{x,b}u^{(+)}\}$, where $P_{0,x}u^{(+)}$ represents the value in the interior of elements, and $P_{0,b}u^{(+)}$ represents the value on the end points of I_{x_i}.

Similarly, we define the Ritz operator $P_y u=\{P_{y,0}u,P_{y,b}u\}$ of $u\in H^1_0(\Omega_y)$ in the y-direction as follows.

$$A(P_y u,v_h)=(\mathcal{L}_y u,v_0),\quad \forall v_h=\{v_0,v_b\}\in S^0_{h_y}. \tag{6.4.5}$$

Lemma 6.4.1. *Assume that $u^{(+)}$ and u be the solution of (6.2.4) and (6.2.5) respectively, and $u^{(+)}\in H^{k+1}(\Omega_x)$, $u\in H^{k+1}(\Omega_y)$, we have*

$$(i)\quad \left\|u^{(+)}-P_{x,0}u^{(+)}\right\|_{L^2(\Omega_x)}+h_x\left\|u^{(+)}-P_x u^{(+)}\right\|^{(+)}_W\leq Ch_x^{k+1}\|u^{(+)}\|_{k+1},$$

$$(ii)\quad \|u-P_{y,0}u\|_{L^2(\Omega_y)}+h_y\|u-P_y u\|_W\leq Ch_y^{k+1}\|u\|_{k+1},$$

$$(iii)\quad \left\|{}^C D^\alpha_{0,t}\left(u^{(+)}-P_{x,0}u^{(+)}\right)\right\|_{L^2(\Omega_x)}\leq Ch_x^{k+1}\left\|{}^C D^\alpha_{0,t}u^{(+)}\right\|_{k+1},$$

$$(iv)\quad \left\|{}^C D^\alpha_{0,t}\left(u-P_{y,0}u\right)\right\|_{L^2(\Omega_y)}\leq Ch_y^{k+1}\left\|{}^C D^\alpha_{0,t}u\right\|_{k+1}.$$

Proof. [96, Lemma 3.1] implies that there exist positive constants C_1 and C_2 such that for any $v_h^+ \in S_{h_x}^0$

$$C_1\|v_h^+\|_{\mathcal{M}} \leq \|v_h^+\|_W \leq C_2\|v_h^+\|_{\mathcal{M}}, \tag{6.4.6}$$

where $\left\|v_h^+\right\|_{\mathcal{M}}^2 := \left\|\dfrac{dv_h^{(+)}}{dx}\right\|_{L^2(\Omega_x)}^2 + \left\|\sqrt{c_1}v_0^{(+)}\right\|_{L^2(\Omega_x)}^2 + \|v_h^{(+)}\|_C^{(+)}$.

From [54, Lemma 3.6], we obtain, for $0 \leq s \leq k$

$$\sum_{I_{x_i}\in\mathcal{K}_M}\left(\left\|u^{(+)} - \pi_{x,0}u^{(+)}\right\|_{L^2(I_{x_i})}^2 + h_x^2\left\|\frac{d(u^{(+)} - \pi_{x,0}u^{(+)})}{dx}\right\|_{L^2(I_{x_i})}^2\right) \leq Ch_x^{2(s+1)}\|u\|_{s+1}^2. \tag{6.4.7}$$

On the other hand, we have from [54, Theorem 3.8] that

$$\|\pi_x u^{(+)} - P_x u^{(+)}\|_W \leq Ch_x^k\|u^{(+)}\|_{k+1}. \tag{6.4.8}$$

Combining (6.4.6) -(6.4.8) yields

$$\|u^{(+)} - P_x u^{(+)}\|_W \leq Ch_x^k\|u^{(+)}\|_{k+1}. \tag{6.4.9}$$

Now, we proceed with the following dual problem that seeks $\Phi \in H_0^1(\Omega_x) \cap H^2(\Omega_x)$ such that

$$-\frac{d^2\Phi}{dx^2} - \frac{d(d_1\Phi)}{dx} + c_1\Phi = e_0 := u^{(+)} - P_{x,0}u^{(+)}. \tag{6.4.10}$$

We assume that the dual problem (6.4.10) has the following H^2-regularity. That is,

$$\|\Phi\|_2 \leq C\|e_0\|. \tag{6.4.11}$$

By testing (6.4.10) with e_0 yields

$$\|e_0\|^2 = -\left(\frac{d^2\Phi}{dx^2}, e_0\right) - \left(\frac{d(d_1\Phi)}{dx}, e_0\right) + \left(c_1\Phi, e_0\right). \tag{6.4.12}$$

Using [Lemma 3.3, Lemma 3.4 and Lemma 3.5 from [54]], we have

$$\begin{aligned}
\|e_0\|^2 &= \ell_a(u^{(+)}, \pi_x\Phi) + \ell_b(u^{(+)}, \pi_x\Phi) + \ell_c(u^{(+)}, \pi_x\Phi) + s_d^{(+)}(\pi_x u^{(+)}, \pi_x\Phi) \\
&+ s_c^{(+)}(\pi_x u^{(+)}, \pi_x\Phi) - \ell_a(\Phi, e_h) - \ell_b(\Phi, e_h) - \ell_c(\Phi, e_h) \\
&- s_d^{(+)}(e_h, \pi_x\Phi) - s_c^{(+)}(e_h, \pi_x\Phi),
\end{aligned}$$

where

$$\begin{aligned}
\ell_a(u^{(+)}, \pi_x\Phi) &= \sum_{i=1}^{M} \langle \frac{d(u^{(+)} - \pi_{x,0}u^{(+)})}{dx} n, \pi_{x,0}\Phi - \pi_{x,b}\Phi\rangle_{\partial I_{x_i}}, \\
\ell_b(u^{(+)}, \pi_x\Phi) &= \left(u^{(+)} - \pi_{x,0}u^{(+)}, d_1 \frac{d(\pi_{x,0}\Phi)}{dx}\right) + \sum_{i=1}^{M} \langle u^{(+)} - \pi_{x,b}u^{(+)}, d_1 n(\pi_{x,0}\Phi - \pi_{x,b}\Phi)\rangle_{\partial I_{x_i}}, \\
\ell_c(u^{(+)}, \pi_x\Phi) &= -\big(c_1(u^{(+)} - \pi_{x,0}u^{(+)}), \pi_{x,0}\Phi\big).
\end{aligned}$$

From [50, Theorem 6.4, (6.26)-(6.29)], we have the following error estimates:

$$\begin{aligned}
&\left|\ell_a(u^{(+)}, \pi_x\Phi)\right| \le Ch_x^{k+1}\|u^{(+)}\|_{k+1}\|\Phi\|_2, \\
&\left|s_d^{(+)}\left(\pi_x u^{(+)}, \pi_x\Phi\right)\right| \le Ch_x^{k+1}\|u^{(+)}\|_{k+1}\|\Phi\|_2, \\
&\left|s_d^{(+)}\left(e_h, \pi_x\Phi\right)\right| \le Ch_x^{k+1}\|u^{(+)}\|_{k+1}\|\Phi\|_2, \\
&\left|\ell_a\left(\Phi, e_h\right)\right| \le Ch_x^{k+1}\|u^{(+)}\|_{k+1}\|\Phi\|_2.
\end{aligned} \tag{6.4.13}$$

It follows from (6.4.3), the Cauchy–Schwarz inequality, and (6.4.7) that,

$$\begin{aligned}
&\left|s_c^{(+)}\left(\pi_x u^{(+)}, \pi_x\Phi\right)\right| \\
&\le C\left(\sum_{i=1}^{M}\left\||d_1 n|^{1/2}\left(\pi_{x,0}u^{(+)} - u^{(+)} + u^{(+)} - \pi_{x,b}u^{(+)}\right)\right\|_{\partial I_{x_i}}\right)^{1/2} \times \\
&\quad\left(\sum_{i=1}^{M}\left\||d_1 n|^{1/2}\left(\pi_{x,0}\Phi - \Phi + \Phi - \pi_{x,b}\Phi\right)\right\|_{\partial I_{x_i}}^2\right)^{1/2} \\
&\le \frac{C}{2}\left(\sum_{i=1}^{M}\|d_1\|_{L^\infty(I_{x_i})}\right)\left(\sum_{i=1}^{M}\left\|\left(\pi_{x,0}u^{(+)} - u^{(+)}\right)\right\|_{\partial I_{x_i}}^2\right)^{1/2}\left(\sum_{i=1}^{M}\|(\pi_{x,0}\Phi - \Phi)\|_{\partial I_{x_i}}^2\right)^{1/2} \\
&\le Ch_x^{k+2}\|u^{(+)}\|_{k+1}\|\Phi\|_2,
\end{aligned}$$

where we have used that $\|u^{(+)} - \pi_{x,b}u^{(+)}\|_{L^2(\partial I_{x_i})} \le \|u^{(+)} - \pi_{x,0}u^{(+)}\|_{L^2(\partial I_{x_i})}$ and $\|\Phi - \pi_{x,b}\Phi\|_{L^2(\partial I_{x_i})} \le \|\Phi - \pi_{x,0}\Phi\|_{L^2(\partial I_{x_i})}$ The estimates (3.13) with $k = 1$ and (3.15) from [54] yield that

$$|s_c^{(+)}(e_h, \pi_x\Phi)| \le Ch_x^{3/2}\|\Phi\|_2\|e_h\|_W \le Ch_x^{k+3/2}\|u^{(+)}\|_{k+1}\|\Phi\|_2.$$

We next derive the error bound for the term $\ell_b(u^{(+)}, \pi_x\Phi)$. Let $\overline{d_1}_{I_{x_i}}$ be the constant value of the average of d_1 over the element I_{x_i}. Using the Cauchy-Schwarz inequality, (6.4.7) and

the Poincare inequality, we have

$$\begin{aligned}
&\sum_{i=1}^{M}\left(u^{(+)}-\pi_{x,0}u^{(+)},d_1\frac{d(\pi_{x,0}\Phi)}{dx}\right)_{L^2(I_{x_i})}\\
&=\sum_{i=1}^{M}\left(u^{(+)}-\pi_{x,0}u^{(+)},\left(d_1-\overline{d_1}_{I_{x_i}}\right)\frac{d(\pi_{x,0}\Phi)}{dx}\right)_{L^2(I_{x_i})}\\
&\quad-\sum_{i=1}^{M}\left(u^{(+)}-\pi_{x,0}u^{(+)},\left(d_1-\overline{d_1}_{I_{x_i}}\right)\frac{d(\Phi-\pi_{x,0}\Phi)}{dx}\right)_{L^2(I_{x_i})}\\
\leq\quad&\sum_{i=1}^{M}\left\|u^{(+)}-\pi_{x,0}u^{(+)}\right\|_{L^2(I_{x_i})}\left\|d_1-\overline{d_1}_{I_{x_i}}\right\|_{L^\infty(I_{x_i})}\|\frac{d(\pi_{x,0}\Phi)}{dx}\|_{L^2(I_{x_i})}\\
&\quad+\sum_{i=1}^{M}\left\|u^{(+)}-\pi_{x,0}u^{(+)}\right\|_{L^2(I_{x_i})}\left\|d_1-\overline{d_1}_{I_{x_i}}\right\|_{L^\infty(I_{x_i})}\left\|\frac{d(\Phi-\pi_{x,0}\Phi)}{dx}\right\|_{L^2(I_{x_i})}\\
&\leq Ch_x^{k+1}\|u^{(+)}\|_{k+1}\|\Phi\|_1+Ch_x^{k+2}\|u^{(+)}\|_{k+1}\|\Phi\|_2\\
&\leq Ch_x^{k+1}\|u^{(+)}\|_{k+1}\|\Phi\|_2.
\end{aligned}$$

Moreover, using the Cauchy-Schwartz inequality, the trace inequality (6.4.3) and (6.4.8), one can obtain

$$\begin{aligned}
&\left\langle u^{(+)}-\pi_{x,b}u^{(+)},d_1n(\pi_{x,0}\Phi-\pi_{x,b}\Phi)\right\rangle\\
&=\left\langle u^{(+)}-\pi_{x,b}u^{(+)},d_1n(\pi_{x,0}\Phi-\Phi+\Phi-\pi_{x,b}\Phi)\right\rangle\\
&\leq C\sum_{i=1}^{M}\left\|u^{(+)}-\pi_{x,b}u^{(+)}\right\|_{L^2(\partial I_{x_i})}\|d_1\|_{L^\infty(I_{x_i})}\|\pi_{x,0}\Phi-\Phi\|_{L^2(\partial I_{x_i})}\\
&\leq Ch_x^{k+1}\|u^{(+)}\|_{k+1}\|\Phi\|_2,
\end{aligned}$$

where we have again used the facts that $\|\Phi-\pi_{x,b}\Phi\|_{L^2(\partial I_{x_i})}\leq\|\Phi-\pi_{x,0}\Phi\|_{L^2(\partial I_{x_i})}$. As a result, we have

$$|\ell_b(u^{(+)},\pi_x\Phi)|\leq Ch_x^{k+1}\|u^{(+)}\|_{k+1}\|\Phi\|_2. \tag{6.4.14}$$

Similar arguments show that

$$\begin{aligned}
&|\ell_b(\Phi,e_h)|\leq Ch_x^{k+1}\|u^{(+)}\|_{k+1}\|\Phi\|_2,\\
&|\ell_c(u^{(+)},\pi_x\Phi)|\leq Ch_x^{k+1}\|u^{(+)}\|_{k+1}\|\Phi\|_2,\\
&|\ell_c(\Phi,e_h)|\leq Ch_x^{k+1}\|u^{(+)}\|_{k+1}\|\Phi\|_2.
\end{aligned} \tag{6.4.15}$$

Combining (6.4.13)- (6.4.15) yield

$$\|e_0\|^2 \leq Ch_x^{k+1}\|u^{(+)}\|_{k+1}\|\Phi\|_2,$$

which together with the H^2 regularity (6.4.11) and (6.4.8) completes the proof of (i). One can prove the rest of the results using similar arguments. Thus, we have finished the proof. □

By considering [77, Lemma 4.1], we state the error estimate for $P_x u^{(+)}$ and $P_y u$ in the following lemma.

Lemma 6.4.2. *Let $u^{(+)} \in H^{k+1}(\Omega_x)$ and $u \in H^{k+1}(\Omega_y)$ be the solutions of the equations* (6.2.4) *and* (6.2.5) *respectively. Also assume that $P_x u^{(+)}$ and $P_y u$ are the elliptic projections defined in* (6.4.4) *and* (6.4.5) *respectively. If $\pi_x u^{(+)} = \left\{\pi_{x,0}u^{(+)}, \pi_{x,b}u^{(+)}\right\}$ and $\pi_y u = \{\pi_{y,0}u, \pi_{y,b}u\}$, then there exists a constant C such that*

$$\begin{aligned}
&(i)\ \left\|\pi_{x,0}u^{(+)} - P_{x,0}u^{(+)}\right\|_{L^2(\Omega_x)} \leq Ch_x^{k+1}\left\|u^{(+)}\right\|_{k+1},\\
&(ii)\ \left\|\pi_{y,0}u - P_{y,0}u\right\|_{L^2(\Omega_y)} \leq Ch_y^{k+1}\left\|u\right\|_{k+1},\\
&(iii)\ \left\|d_w(\pi_x u^{(+)} - P_x u^{(+)})\right\|_{L^2(\Omega_x)} \leq Ch_x^{k}\left\|u^{(+)}\right\|_{k+1},\\
&(iv)\ \left\|d_w(\pi_y u - P_y u)\right\|_{L^2(\Omega_y)} \leq Ch_y^{k}\left\|u\right\|_{k+1}.
\end{aligned}$$

We now split the overall error term into two parts given as follows:

$$\begin{aligned}
\mathcal{E}_{h,i,j}^{n+1} &= \left(u^{(+)}(x, y_j, t_{n+1}) - u_h^{(+),n+1}(x, y_j)\right) + \left(u(x_i, y, t_{n+1}) - u_h^{n+1}(x_i, y)\right)\\
&=: e_{h,j}^{(+),n+1} + e_{h,i}^{n+1}, \quad i = 0, 1, \ldots, M, \quad j = 0, 1, \ldots, M,
\end{aligned} \tag{6.4.16}$$

where $e_{h,j}^{(+),n+1}$ and $e_{h,i}^{n+1}$ are the errors between the numerical solutions of problems (6.3.17) and (6.3.18) and the solutions of (6.2.4) and (6.2.5) ate time level t_{n+1}, respectively.

We will use the following error splitting.

$$\begin{aligned}
e_{h,j}^{(+),n+1} &= \left(u^{(+)}(x, y_j, t_{n+1}) - \pi_x u^{(+)}(x, y_j, t_{n+1})\right) + \left(\pi_x u^{(+)}(x, y_j, t_{n+1})\right.\\
&\quad \left. - P_x u^{(+)}(x, y_j, t_{n+1})\right) + \left(P_x u^{(+)}(x, y_j, t_{n+1}) - u_h^{(+),n+1}(x, y_j)\right)\\
&=: \theta_{h,j}^{(+),n+1} + \nu_{h,j}^{(+),n+1} + \eta_{h,j}^{(+),n+1}, \quad j = 0, \ldots, M, \text{ and,}
\end{aligned} \tag{6.4.17}$$

$$\begin{aligned}
e_{h,i}^{n+1} &= \left(u(x_i, y, t_{n+1}) - \pi_y u(x_i, y, t_{n+1})\right) + \left(\pi_y u(x_i, y, t_{n+1})\right.\\
&\quad \left. - P_y u(x_i, y, t_{n+1})\right) + \left(P_y u(x_i, y, t_{n+1}) - u_h^{n+1}(x_i, y)\right)\\
&=: \theta_{h,i}^{n+1} + \nu_{h,i}^{n+1} + \eta_{h,i}^{n+1}, \quad i = 0, \ldots, M.
\end{aligned} \tag{6.4.18}$$

The interpolation error estimates $\theta_{h,j}^{(+),n+1} = \left\{\theta_{0,j}^{(+),n+1}, \theta_{b,j}^{(+),n+1}\right\}$ and $\theta_{h,i}^{n+1} = \{\theta_{0,i}^{n+1}, \theta_{b,i}^{n+1}\}$ follow from (6.4.1) and (6.4.2). Also the error estimates $\nu_{h,j}^{(+),n+1} = \left\{\nu_{0,j}^{(+),n+1}, \nu_{b,j}^{(+),n+1}\right\}$ and $\nu_{h,i}^{n+1} = \{\nu_{0,i}^{n+1}, \nu_{b,i}^{n+1}\}$ can be estimated by using Lemma 6.4.2 (i) and (ii). We will estimate the discretization errors $\eta_{h,i}^{n+1}$ and $\eta_{h,j}^{(+),n+1}$. To this end, we need the following error equations in the error analysis.

Lemma 6.4.3. *Let $u^{(+)}$ and u be the solutions of (6.2.4) and (6.2.5), respectively. Then, we have for any $v_h^{(+)} = \{v_0^{(+)}, v_b^{(+)}\} \in S_{h_x}^0$*

$$-\left(u_{xx}^{(+)}, v_0^{(+)}\right)_{\mathcal{K}_x^M} = \left(d_w \pi_x u^{(+)}, d_w v_h^{(+)}\right)_{\mathcal{K}_x^M} - Z_d^{(+)}(u^{(+)}, v_h^{(+)}), \tag{6.4.19}$$

where $Z_d^{(+)}(u^{(+)}, v_h^{(+)}) = \sum_{i=1}^{M} \left\langle u_x^{(+)} - \pi_{x,0} u_x^{(+)}, (v_0^{(+)} - v_b^{(+)})n \right\rangle_{\partial I_{x_i}}$, and for any $v_h = \{v_0, v_b\} \in S_{h_y}^0$

$$-\left(u_{yy}, v_0\right)_{\mathcal{K}_y^M} = \left(d_w \pi_y u, d_w v_h\right)_{\mathcal{K}_y^M} - Z_d(u, v_h), \tag{6.4.20}$$

where $Z_d(u, v_h) = \sum_{j=1}^{M} \left\langle u_y - \pi_{y,0} u_y, (v_0 - v_b)n \right\rangle_{\partial I_{y_j}}$.

Proof. Using the definition of the weak derivative (6.3.5), integration by parts and the definition of π_x, we have that for any $\widetilde{v} \in \mathbb{P}_{k-1}(I_{x_i})$

$$\begin{aligned}
\left(d_w \pi_x u^{(+)}, \widetilde{v}\right)_{I_{x_i}} &= -\left(\pi_{x,0} u^{(+)}, \widetilde{v}_x\right)_{I_{x_i}} + \left\langle \pi_{x,b} u^{(+)} n, \widetilde{v} \right\rangle_{\partial I_{x_i}} \\
&= \left(u^{(+)}, \widetilde{v}_x\right)_{I_{x_i}} + \left\langle u^{(+)} n, \widetilde{v} \right\rangle_{\partial I_{x_i}} \\
&= \left(u_x^{(+)}, \widetilde{v}\right)_{I_{x_i}} = \left(\pi_{x,0} u_x^{(+)}, \widetilde{v}\right)_{I_{x_i}},
\end{aligned}$$

which implies that

$$d_w \pi_x u^{(+)} = \pi_{x,0} u_x^{(+)}, \quad \forall u^{(+)} \in H^1(\Omega). \tag{6.4.21}$$

It follows from (6.4.21), the definition of the weak derivative (6.3.5), and integration by parts that

$$\begin{aligned}
\left(d_w \pi_x u^{(+)}, d_w v_h^{(+)}\right)_{I_{x_i}} &= \left(\pi_{x,0} u_x^{(+)}, d_w v_h^{(+)}\right)_{I_{x_i}} \\
&= -\left(v_0^{(+)}, (\pi_{x,0} u_x^{(+)})_x\right)_{I_{x_i}} + \left\langle v_b^{(+)} n, \pi_{x,0} u_x^{(+)} \right\rangle_{\partial I_{x_i}} \\
&= \left((v_0^{(+)})_x, \pi_{x,0} u_x^{(+)}\right)_{I_{x_i}} - \left\langle (v_0^{(+)} - v_b^{(+)})n, \pi_{x,0} u_x^{(+)} \right\rangle_{\partial I_{x_i}} \\
&= \left((v_0^{(+)})_x, u_x^{(+)}\right)_{I_{x_i}} - \left\langle (v_0^{(+)} - v_b^{(+)})n, \pi_{x,0} u_x^{(+)} \right\rangle_{\partial I_{x_i}}.
\end{aligned} \tag{6.4.22}$$

On the other hand, we have

$$-\left(u_{xx}^{(+)}, v_0^{(+)}\right)_{I_{x_i}} = \left(u_x^{(+)}, (v_0^{(+)})_x\right)_{I_{x_i}} - \left\langle u_x^{(+)}, (v_0^{(+)} - v_b^{(+)})n\right\rangle_{\partial I_{x_i}}, \tag{6.4.23}$$

where we have used the fact that $\sum_{i=1}^{M}\langle u_x^{(+)}, v_b^{(+)}n\rangle_{\partial I_{x_i}} = 0$. The desired result (6.4.19) follows from substituting (6.4.23) into (6.4.22).

Similarly, we can prove (6.4.20). The proof is now completed. □

Lemma 6.4.4. *Let $u^{(+)}$ and u be the solutions of (6.2.4) and (6.2.5), respectively. Then, we have for any $v_h^{(+)} = \{v_0^{(+)}, v_b^{(+)}\} \in S_{h_x}^0$*

$$\left(d_1 u_x^{(+)}, v_0^{(+)}\right)_{\mathcal{K}_x^M} = \left(d_w^{d_1}\left(\pi_x u^{(+)}\right), v_0^{(+)}\right)_{\mathcal{K}_x^M} - Z_c^{(+)}\left(u^{(+)}, v_h^{(+)}\right), \tag{6.4.24}$$

where $Z_c^{(+)}\left(u^{(+)}, v_h^{(+)}\right) = \left(u^{(+)} - \pi_{x,0}u^{(+)}, (d_1 v_0^{(+)})_x\right)_{\mathcal{K}_x^M} + \left\langle u^{(+)} - \pi_{x,b}u^{(+)}, d_1 v_0^{(+)}n\right\rangle_{\partial\mathcal{K}_x^M}$, and for any $v_h = \{v_0, v_b\} \in S_{h_y}^0$

$$(d_2 u_x, v_0)_{\mathcal{K}_y^M} = \left(d_w^{d_2}(\pi_y u), v_0\right)_{\mathcal{K}_y^M} - Z_c(u, v_h), \tag{6.4.25}$$

where $Z_c(u, v_h) = (u - \pi_{y,0}u, (d_2 v_0)_y)_{\mathcal{K}_y^M} + \left\langle u - \pi_{y,b}u, d_2 v_0 n\right\rangle_{\partial\mathcal{K}_y^M}$.

Proof. It follows from the weak convectional derivative (6.3.6) that

$$(d_w^{d_1}(\pi_x u^{(+)}), v_0^{(+)})_{\mathcal{K}_x^M} = -(\pi_{x,0}u^{(+)}, (d_1 v_0^{(+)})_x)_{\mathcal{K}_x^M} + \left\langle \pi_{x,b}u^{(+)}, d_1 v_0^{(+)}n\right\rangle_{\partial\mathcal{K}_x^M}. \tag{6.4.26}$$

Integration by parts leads to

$$(d_1 u_x^{(+)}, v_0^{(+)})_{\mathcal{K}_x^M} = -(u^{(+)}, (d_1 v_0^{(+)})_x)_{\mathcal{K}_x^M} + \left\langle u^{(+)}, d_1 v_0^{(+)}n\right\rangle_{\partial\mathcal{K}_x^M}. \tag{6.4.27}$$

Combining (6.4.26) and (6.4.27) gives the desired conclusion (6.4.24). Similar reason shows that the equation (6.4.25) holds true. Thus we complete the proof. □

Lemma 6.4.5. *Let $\pi_x u^{(+)}$ be the projection of the solution $u^{(+)}$ of (6.2.4) and $u_h^{(+)}$ be the numerical solution computed by (6.3.12), respectively. Then, for any $v_h^{(+)} = \{v_0^{(+)}, v_b^{(+)}\} \in S_{h_x}^0$, we have*

$$\begin{aligned}&\left({}^C D_{0,t}^{\alpha}\left(\pi_{x,0}u^{(+)} - u_0^{(+)}\right), v_h^{(+)}\right)_{\mathcal{K}_x^M} + A^{(+)}\left(\pi_x u^{(+)} - u_h^{(+)}, v_h^{(+)}\right)\\ &= Z^{(+)}\left(u^{(+)}, v_h^{(+)}\right) + s_c^{(+)}\left(\pi_x u^{(+)}, v_h^{(+)}\right) + s_d^{(+)}\left(\pi_x u^{(+)}, v_h^{(+)}\right),\end{aligned} \tag{6.4.28}$$

where

$$Z^{(+)}(u^{(+)}, v_h^{(+)}) = Z_d^{(+)}(u^{(+)}, v_h^{(+)}) + Z_c^{(+)}(u^{(+)}, v_h^{(+)}) + Z_r^{(+)}(u^{(+)}, v_h^{(+)}), \tag{6.4.29}$$

where $Z_r^{(+)}(u^{(+)}, v_h^{(+)}) = (c_1(\pi_{x,0}u^{(+)} - u^{(+)}), v_0^{(+)})_{\mathcal{K}_x^M}$.

Proof. Multiplying (6.2.4) by $v_h^{(+)} = \{v_0^{(+)}, v_b^{(+)}\} \in S_{h_x}^0$, we arrive at

$$\left({}^C D_{0,t}^{\alpha} u^{(+)}, v_h^{(+)}\right)_{\mathcal{K}_x^M} + \left(\mathcal{L}_x u^{(+)}, v_h^{(+)}\right)_{\mathcal{K}_x^M} = \left(f_1, v_h^{(+)}\right)_{\mathcal{K}_x^M}.$$

Substituting (6.4.19) and (6.4.24) into the above equation and using the definition of the projection π_x give

$$\left({}^C D_{0,t}^{\alpha} \pi_{x,0} u^{(+)}, v_h^{(+)}\right)_{\mathcal{K}_x^M} + a^{(+)}\left(\pi_x u^{(+)}, v_h^{(+)}\right) = \left(f_1, v_h^{(+)}\right)_{\mathcal{K}_x^M} + Z^{(+)}\left(u^{(+)}, v_h^{(+)}\right).$$

Adding $s_c^{(+)}(\pi_x u^{(+)}, v_h^{(+)})$ and $s_d^{(+)}(\pi_x u^{(+)}, v_h^{(+)})$ on the both sides of the equation yields

$$\begin{aligned}&\left({}^C D_{0,t}^{\alpha} \pi_{x,0} u^{(+)}, v_h^{(+)}\right)_{\mathcal{K}_x^M} + A^{(+)}\left(\pi_x u^{(+)}, v_h^{(+)}\right)\\ &= \left(f_1, v_h^{(+)}\right)_{\mathcal{K}_x^M} + Z^{(+)}\left(u^{(+)}, v_h^{(+)}\right) + s_c^{(+)}\left(\pi_x u^{(+)}, v_h^{(+)}\right) + s_d^{(+)}\left(\pi_x u^{(+)}, v_h^{(+)}\right).\end{aligned} \tag{6.4.30}$$

Subtracting (6.3.12) from (6.4.30) gives the error equation (6.4.28). Thus, we complete the proof. □

Similar argument can be used for the proof of the following lemma.

Lemma 6.4.6. *Let $\pi_x u$ be the projection of the solution u of (6.2.5) and u_h be the numerical solution computed by (6.3.13), respectively. Then, for any $v_h = \{v_0, v_b\} \in S_{h_y}^0$, we have*

$$\left({}^C D_{0,t}^{\alpha} \pi_{x,0} u - u_0, v_h\right)_{\mathcal{K}_y^M} + A(\pi_x u - u_h, v_h) = Z(u, v_h) + s_c(\pi_{y,0} u, v_h) + s_d(\pi_{y,0} u, v_h), \tag{6.4.31}$$

where $Z(u, v_h) = Z_d(u, v_h) + Z_c(u, v_h) + Z_r(u, v_h)$.

Lemma 6.4.7. *Suppose that $w \in H^{k+1}(\Omega)$. Then for $v_h \in S_{h_y}^0$, there holds*

$$|Z(w, v_h)| \le C h_y^k |||v_h|||_W.$$

Proof. The Cauchy-Schwarz inequality, the trace inequality and (6.4.2) imply that

$$\begin{aligned}|Z_d(u, v_h)| &\le \sum_{j=1}^{M} \|u_y - \pi_{y,0} u_y\|_{L^2(\partial I_{y_j})} \|v_0 - v_b\|_{L^2(\partial I_{y_j})}\\ &\le \Big(\sum_{j=1}^{M} h_y \|u_y - \pi_{y,0} u_y\|_{L^2(\partial I_{y_j})}^2\Big)^{1/2} \Big(\sum_{j=1}^{M} (h_y^{-1}) \|v_0 - v_b\|_{L^2(\partial I_{y_j})}^2\Big)^{1/2}\\ &\le \Big(\sum_{j=1}^{M} (\|u_y - \pi_{y,0} u_y\|_{L^2(I_{y_j})}^2 + h_y^2 \|u_y - \pi_{y,0} u_y\|_{H^1(I_{y_j})}^2)\Big)^{1/2} \|v_h\|_W\\ &\le C h_y^k \|u_y\|_{H^{k+1}(\Omega)} \|v_h\|_W.\end{aligned} \tag{6.4.32}$$

We now estimate $Z_c(u, v_h) + Z_r(u, v_h)$ as follows:

$$\begin{aligned} Z_c(u, v_h) + Z_r(u, v_h) &= \big(u - \pi_{y,0}u, d_2(v_0)_y\big) + \big(((d_2)_y + c)(\pi_{y,0}u - u), v_0\big) \\ &\quad + \big\langle u - \pi_{y,b}u, d_2 v_0 n\big\rangle \\ &=: T_1 + T_2 + T_3. \end{aligned} \tag{6.4.33}$$

We estimate each term in (6.4.33) separately. Let $\hat{d}_2$ be a piecewise constant function whose value is the average of d_2 over the element. It follows from the projection error (6.4.2) and an inverse inequality that

$$|T_1| \leq \big(u - \pi_{y,0}u, d_2(v_0)_y\big) = \big(u - \pi_{y,0}u, (d_2 - \hat{d}_2)(v_0)_y\big) \leq C h_y^{k+1} \|u\|_{H^{k+1}(\Omega)} \|v_0\|.$$

The Cauchy-Schwarz inequality and (6.4.2) gives that

$$|T_2| \leq C h_y^{k+1} \|u_y\|_{H^{k+1}(\Omega)} \|v_0\|.$$

Finally, it follows from the definition of $\pi_{y,b}$, the trace inequality (6.4.3), the projection error (6.4.2), and the Cauchy-Schwarz inequality that

$$\begin{aligned} |T_3| &= |\big\langle u - \pi_{y,b}u, d_2(v_0 - v_b)n\big\rangle| \\ &\leq \Big(\sum_{j=1}^{M} \|u - \pi_{y,b}u\|^2_{L^2(\partial I_{y_j})}\Big)^{1/2} \|v_h\|_W \\ &\leq C\left(h_y^{-1}\|u - \pi_{y,0}u\|^2_{L^2(I_{y_j})} + h_y \|(u - \pi_{y,0}u)'\|^2_{L^2(I_{y_j})}\right)^{1/2} \|v_h\|_W \\ &\leq C h_y^{k+1/2} \|u_y\|_{H^{k+1}(\Omega)} \|v_h\|_W, \end{aligned}$$

where we have used that $\|u - \pi_{y,b}u\|_{L^2(\partial I_{y_j})} \leq \|u - \pi_{y,0}u\|_{L^2(\partial I_{y_j})}$.

It follows from the trace inequality (6.4.3), Cauchy-Schwarz inequality, and the projection error estimates (6.4.2) that

$$\begin{aligned} &| \, s_c\left(\pi_y u, v_h\right) \, | \\ &\leq \sum_{j=1}^{M} \left| \left\langle bn\left(\pi_{y,0}u - \pi_{y,b}u\right), v_0 - v_b \right\rangle_{L^2(\partial_+ I_{y_j})} \right| \\ &\leq \left(\sum_{j=1}^{M} \left\| |bn|^{1/2}\left(\pi_{y,0}u - u + u - \pi_{y,b}u\right)\right\|^2_{L^2(\partial I_{y_j})}\right)^{1/2} \left(\sum_{j=1}^{M} \left\| |bn|^{1/2}\left(v_0 - v_b\right)\right\|^2_{L^2(\partial I_{y_j})}\right)^{1/2} \\ &\leq C\left(\sum_{j=1}^{M} \left\| |bn|^{1/2}\left(\pi_{y,0}u - u\right)\right\|^2_{L^2(\partial I_{y_j})}\right)^{1/2} \left(\sum_{j=1}^{M} \left\| |bn|^{1/2}\left(v_0 - v_b\right)\right\|^2_{L^2(\partial I_{y_j})}\right)^{1/2} \\ &\leq C h_y^{k+\frac{1}{2}} \|u_y\|_{H^{k+1}(\Omega)} \|v\|_W. \end{aligned}$$

Similar argument shows that

$$| s_d(\pi_y u, v_h) | \leq C h_y^k \|u_y\|_{H^{k+1}(\Omega)} \|v\|_W.$$

Therefore, we complete the proof. □

Similar estimates holds for x-direction as well.

Lemma 6.4.8. *Suppose that $w \in H^{k+1}(\Omega)$. Then for $v_h^{(+)} \in S_{h_x}^0$, there holds*

$$|Z^{(+)}(w, v_h^{(+)})| \leq C h_x^k \|v_h^{(+)}\|_W^{(+)}.$$

We now establish the theorem for optimal error estimate. Let $u^{(+),n+1} = u^{(+)}(x, y_j, t_{n+1})$ be the exact solution of the problem (6.1.1) at the time level $t = t_{n+1}$ and $u_h^{(+),n+1}$ be the approximated solution of the fully discrete scheme be the solution of the fully discrete scheme given in (6.3.17).

We resume to estimate the error $\eta_{h,j}^{(+),n+1} = \left\{\eta_{0,j}^{(+),n+1}, \eta_{b,j}^{(+),n+1}\right\}$ for $j = 0, 1, \ldots, M$ in the following theorem.

Theorem 6.4.9. *Let $P_x u^{(+)}$ be the elliptic projection defined by (6.4.4) of the solution $u^{(+)}$ of the problem (6.2.4) and $u_h^{(+),n}$ be the solution of the problem (6.3.17). Then, for $n = 1, 2, \ldots, N$ there holds*

$$\|\eta_{0,j}^{(+),n}\|_{\mathcal{K}_x^M} \leq C\Big(h_x^{k+1} + N^{-\min\{2-\alpha, r\alpha\}}\Big),\ j = 0, 1, \ldots, M.$$

Proof. The error term $\eta_{0,j}^{(+),n+1}$ satisfies the following equation for any $v_h^{(+)} \in S_{h_x}^0$

$$\begin{aligned}
&\big(\Delta_N^\alpha \eta_{0,j}^{(+),n}, v_0^{(+)}\big)_{\mathcal{K}_x^M} + A^{(+)}(\eta_{h,j}^{(+),n}, v_h^{(+)}) \\
&= \big(P_{x,0}\Delta_N^\alpha u^{(+)}, v_0^{(+)}\big)_{\mathcal{K}_x^M} + A^{(+)}(P_x u^{(+),n}, v_h^{(+)}) - \big(\Delta_N^\alpha u_{h,0}^{(+)}, v_0^{(+)}\big)_{\mathcal{K}_x^M} - A^{(+)}(u_h^{(+)}, v_h^{(+)}) \\
&= \big((P_{x,0} - \pi_{x,0})\Delta_N^\alpha u^{(+)}, v_0^{(+)}\big)_{\mathcal{K}_x^M} + \big(\pi_{x,0}\Delta_N^\alpha u^{(+)}, v_0^{(+)}\big)_{\mathcal{K}_x^M} \\
&\quad + \big(\mathcal{L}u^{(+),n}, v_0^{(+)}\big)_{\mathcal{K}_x^M} - \big(f_1^n, v_0^{(+)}\big)_{\mathcal{K}_x^M} \\
&= \big((P_{x,0} - \pi_{x,0})\Delta_N^\alpha u^{(+)}, v_0^{(+)}\big)_{\mathcal{K}_x^M} + \big(\pi_{x,0}\Delta_N^\alpha u^{(+)}, v_0^{(+)}\big)_{\mathcal{K}_x^M} \\
&\quad + \big(\pi_{x,0}(\mathcal{L}u^{(+),n}), v_0^{(+)}\big)_{\mathcal{K}_x^M} - \big(\pi_{x,0} f_1^n, v_0^{(+)}\big)_{\mathcal{K}_x^M} \\
&= -\big(\Delta_N^\alpha \nu_{0,j}^{(+),n}, v_0^{(+)}\big)_{\mathcal{K}_x^M} + \big(\pi_{x,0}(f_1^n + \Phi^n), v_0^{(+)}\big)_{\mathcal{K}_x^M} - \big(\pi_{x,0} f_1^{n+1}, v_0^{(+)}\big)_{\mathcal{K}_x^M} \\
&= -\big(\Delta_N^\alpha \nu_{0,j}^{(+),n}, v_0^{(+)}\big)_{\mathcal{K}_x^M} + \big(\pi_{x,0}(\Phi^n), v_0^{(+)}\big)_{\mathcal{K}_x^M},
\end{aligned} \tag{6.4.34}$$

where we have used the definitions of Φ^n, $\nu_{0,j}^{(+),n}$ and the projection π_x.

Now, taking $v_h^{(+)} = \eta_{h,j}^{(+),n}$ in (6.4.34) yield

$$\left(\Delta_N^\alpha \eta_{0,j}^{(+),n}, \eta_{0,j}^{(+),n}\right)_{\mathcal{K}_x^M} + A^{(+)}(\eta_{h,j}^{(+),n}, \eta_{h,j}^{(+),n}) = -\left(\Delta_N^\alpha \nu_{0,j}^{(+),n}, \eta_{0,j}^{(+),n}\right)_{\mathcal{K}_x^M} + \left(\pi_{x,0}(\Phi^n), \eta_{0,j}^{(+),n}\right)_{\mathcal{K}_x^M}.$$

Using the coercivity of the L1 method [45, Lemma 2.1] stating that $\left(\Delta_N^\alpha \eta_{0,j}^{(+),n}, \eta_{0,j}^{(+),n}\right)_{\mathcal{K}_x^M} \geq (\Delta_N^\alpha \|\eta_{0,j}^{(+),n}\|_{\mathcal{K}_x^M})\|\eta_{0,j}^{(+),n}\|_{\mathcal{K}_x^M}$

and the coercivity of the bilinear form $A^{(+)}(\cdot,\cdot)$ and Cauchy-Schwarz inequality, we have

$$\left(\Delta_N^\alpha \|\eta_{0,j}^{(+),n}\|_{\mathcal{K}_x^M}\right) \|\eta_{0,j}^{(+),n}\|_{\mathcal{K}_x^M} \leq C \left(\|\Delta_N^\alpha \nu_{0,j}^{(+),n}\|_{\mathcal{K}_x^M} + \|\Phi^n\|_{\mathcal{K}_x^M}\right) \|\eta_{0,j}^{(+),n}\|_{\mathcal{K}_x^M},$$

where we have used the fact that $\|\pi_{x,0}\Phi_{\mathcal{K}_x^M}^n\| \leq \|\Phi^n\|_{\mathcal{K}_x^M}$. Cancelling out the term $\|\eta_{0,j}^{(+),n}\|_{\mathcal{K}_x^M}$, we get

$$\Delta_N^\alpha \|\eta_{0,j}^{(+),n}\|_{\mathcal{K}_x^M} \leq C R^n,$$

where

$$R^n := \|\Delta_N^\alpha \nu_{0,j}^{(+),n}\|_{\mathcal{K}_x^M} + \|\Phi^n\|_{\mathcal{K}_x^M}. \tag{6.4.35}$$

Now using (6.3.15) to expand fully out $\Delta_N^\alpha \|\eta_{0,j}^{(+),n}\|_{\mathcal{K}_x^M}$ gives

$$\begin{aligned}\frac{\mathfrak{b}_{n,1}^{(\alpha)}}{\Gamma(2-\alpha)} \left\|\eta_{0,j}^{(+),n}\right\|_{\mathcal{K}_x^M} \leq\ & C\,\|R^n\|_{\mathcal{K}_x^M} + \frac{1}{\Gamma(2-\alpha)}\left[\mathfrak{b}_{n,n}^{(\alpha)} \left\|\eta_{0,j}^{(+),0}\right\|_{\mathcal{K}_x^M}\right. \\ & \left. + \sum_{i=1}^{n-1}\left(\mathfrak{b}_{n,i}^{(\alpha)} - \mathfrak{b}_{n,i+1}^{(\alpha)}\right) \left\|\eta_{0,j}^{(+),i}\right\|_{\mathcal{K}_x^M}\right].\end{aligned}$$

Following [72, (4.6)], we define the positive real numbers $\theta_{n,\mathfrak{r}}$, for $n = 1, 2, \ldots, M$ and $\mathfrak{r} = 1, 2, \ldots, n-1$ by

$$\theta_{n,n} = 1, \quad \theta_{n,\mathfrak{r}} = \sum_{i=1}^{n-\mathfrak{r}} \tau_{n-i}^\alpha \left(\mathfrak{b}_{n,i}^{(\alpha)} - \mathfrak{b}_{n,i+1}^{(\alpha)}\right) \theta_{n-i,\mathfrak{r}}.$$

As in [72, Lemma 4.2], one can deduce the following stability estimate

$$\left\|\eta_{0,j}^{(+),n}\right\|_{\mathcal{K}_x^M} \leq \left\|\eta_{0,j}^{(+),0}\right\|_{\mathcal{K}_x^M} + C\tau_n^\alpha \Gamma(2-\alpha) \sum_{j=1}^{n} \theta_{n,j} \left\|R^j\right\|_{\mathcal{K}_x^M} \text{ for } n = 1, 2, \ldots, M. \tag{6.4.36}$$

Now, plugging R^j in (6.4.35) into (6.4.36) yields

$$\|\eta_{0,j}^{(+),n}\|_{\mathcal{K}_x^M} \leq \|\eta_{0,j}^{(+),0}\|_{\mathcal{K}_x^M} + C\tau_n^\alpha \Gamma(2-\alpha) \sum_{\mathfrak{r}=1}^{n} \theta_{n,\mathfrak{r}} (\|\Delta_N^\alpha \nu_{0,j}^{(+),\mathfrak{r}}\|_{\mathcal{K}_x^M} + \|\Phi^{\mathfrak{r}}\|_{\mathcal{K}_x^M}) \tag{6.4.37}$$

for $n = 1, 2, \ldots, M$. Thus, we get

$$\begin{aligned}
\left\|\Delta_N^{\alpha}\nu_{0,j}^{(+),\mathfrak{r}}\right\|_{\mathcal{K}_x^M} &= \left\|\Delta_N^{\alpha}\nu_{0,j}^{(+),\mathfrak{r}} - {}^{C}D_{0,t}^{\alpha}\nu_{0,j}^{(+),\mathfrak{r}} + {}^{C}D_{0,t}^{\alpha}\nu_{0,j}^{(+),\mathfrak{r}}\right\|_{\mathcal{K}_x^M} \\
&\leq \|P_{x,0}({}^{C}D_{0,t}^{\alpha}u^{(+),\mathfrak{r}} - \Delta_N^{\alpha}u^{(+),\mathfrak{r}}) - \pi_{x,0}\left({}^{C}D_{0,t}^{\alpha}u^{(+),\mathfrak{r}} - \Delta_N^{\alpha}u^{(+),\mathfrak{r}}\right)\|_{\mathcal{K}_x^M} \\
&\quad + \left\|{}^{C}D_{0,t}^{\alpha}\nu_{0,j}^{(+),\mathfrak{r}}\right\|_{\mathcal{K}_x^M} \\
&\leq \|P_{x,0}\Phi^{\mathfrak{r}}\|_{\mathcal{K}_x^M} + \|\pi_{x,0}\Phi^{\mathfrak{r}}\|_{\mathcal{K}_x^M} + Ch_x^{k+1}\left|{}^{C}D_{0,t}^{\alpha}u^{(+),\mathfrak{r}}\right|_{k+1} \\
&\leq 2\|\Phi^{\mathfrak{r}}\|_{\mathcal{K}_x^M} + Ch_x^{k+1}\left|{}^{C}D_{0,t}^{\alpha}u^{(+),\mathfrak{r}}\right|_{k+1},
\end{aligned}$$

where we have used $\|P_{x,0}\Phi^{\mathfrak{r}}\|_{\mathcal{K}_x^M} \leq \|\Phi^{\mathfrak{r}}\|_{\mathcal{K}_x^M}$, $\|\pi_{x,0}\Phi^{\mathfrak{r}}\|_{\mathcal{K}_x^M} \leq \|\Phi^{\mathfrak{r}}\|_{\mathcal{K}_x^M}$, Lemma 6.4.1 and Lemma 6.4.2. As a result, we have $\left\|\Delta_N^{\alpha}\nu_{0,j}^{(+),\mathfrak{r}}\right\|_{\mathcal{K}_x^M} + \|\Phi^{\mathfrak{r}}\|_{\mathcal{K}_x^M} \leq 3\|\Phi^{\mathfrak{r}}\|_{\mathcal{K}_x^M} + Ch_x^{k+1}\left|{}^{C}D_{0,t}^{\alpha}u^{(+),\mathfrak{r}}\right|_{k+1}$. Plugging this estimate into (6.4.37) and recalling Lemma 6.3.2 gives

$$\begin{aligned}
\left\|\eta_{0,j}^{(+),n}\right\|_{\mathcal{K}_x^M} &\leq \left\|\eta_{0,j}^{(+),0}\right\|_{\mathcal{K}_x^M} + C\tau_n^{\alpha}\Gamma(2-\alpha)\sum_{\mathfrak{r}=1}^{n}\theta_{n,\mathfrak{r}}\left(Ch_x^{k+1}\left|{}^{C}D_{0,t}^{\alpha}u^{(+),\mathfrak{r}}\right|_{k+1} + 3\|\Phi^{\mathfrak{r}}\|_{\mathcal{K}_x^M}\right) \\
&\leq \left\|\eta_{0,j}^{(+),0}\right\|_{\mathcal{K}_x^M} + C\tau_n^{\alpha}\Gamma(2-\alpha)\sum_{\mathfrak{r}=1}^{n}\theta_{n,\mathfrak{r}}\left[h_x^{k+1}\left|{}^{C}D_{0,t}^{\alpha}u^{(+),\mathfrak{r}}\right|_{k+1} + \mathfrak{r}^{-\min\{2-\alpha,r\alpha\}}\right] \\
&\leq Ch_x^{k+1} + C\tau_n^{\alpha}\sum_{\mathfrak{r}=1}^{n}\theta_{n,\mathfrak{r}}\left[h_x^{k+1} + \mathfrak{r}^{-\min\{2-\alpha,r\alpha\}}\right] \qquad (6.4.38) \\
&\leq C\left(h_x^{k+1} + N^{-\min\{2-\alpha,r\alpha\}}\right),
\end{aligned}$$

where we have used the fact that $\|{}^{C}D_{0,t}^{\alpha}u^{(+)}(\cdot,t)\|_{k+1} \leq C$ from [45], and by Lemma 6.4.2

$$\left\|\eta_{0,j}^{(+),0}\right\|_{\mathcal{K}_x^M} = \|P_{x,0}u^{(+),0} - \pi_{x,0}u^{(+),0}\|_{\mathcal{K}_x^M} = \left\|\nu_{0,j}^{(+),0}\right\|_{\mathcal{K}_x^M} \leq Ch_x^{k+1}\|u^{(+),0}\|_{k+1} \leq Ch_x^{k+1},$$

and the inequality $\tau_n^{\alpha}\sum_{\mathfrak{r}=1}^{n}\mathfrak{r}^{-s}\theta_{n,\mathfrak{r}} \leq \frac{T^{\alpha}N^{-s}}{1-\alpha}$, provided that $s \leq r\alpha$, from [72, Lemma 4.3] is used in (6.4.38) with $s = 0$ for the h_x^{k+1} factor and $s = \min\{2-\alpha, r\alpha\}$ for the $\mathfrak{r}^{-\min\{2-\alpha,r\alpha\}}$ factor. Thus, we complete the proof. □

Theorem 6.4.10. *Let $u^{(+)}$ be the solution of the problem (6.2.4) and $u_h^{(+),n}$ be the solution of the problem (6.3.17). Then, for $n = 1, 2, \ldots, N$ there holds*

$$\|e_{0,j}^{(+),n}\|_{\mathcal{K}_x^M} \leq C\left(h_x^{k+1} + N^{-\min\{2-\alpha,r\alpha\}}\right),\ j = 0, 1, \ldots, M.$$

Proof. By using the triangle inequality one can write

$$\left\|e_{0,j}^{(+),n}\right\|_{\mathcal{K}_x^M} \leq \left\|\theta_{0,j}^{(+),n}\right\|_{\mathcal{K}_x^M} + \left\|\nu_{0,j}^{(+),n}\right\|_{\mathcal{K}_x^M} + \left\|\eta_{0,j}^{(+),n}\right\|_{\mathcal{K}_x^M}, \quad j = 0, \ldots, M.$$

Then applying (6.4.1), Lemma 6.4.2(i) and Theorem 6.4.9, the desired result holds. □

Similar to Theorem 6.4.9 and Theorem 6.4.10, one can establish the following error estimates in the $y-$direction.

Theorem 6.4.11. *Let $P_y u$ be the elliptic projection defined by (6.4.5) of the solution u of the problem (6.2.5) and u_h^n be the solution of the problem (6.3.18). Then, for $n = 1, 2, \ldots, M$ there holds*

$$\|\eta_{0,i}^n\|_{\mathcal{K}_y^M} \leq C\Big(h_y^{k+1} + N^{-\min\{2-\alpha, r\alpha\}}\Big),\ i = 0, 1, \ldots, M.$$

Theorem 6.4.12. *Let u be the solution of the problem (6.2.5) and u_h^n be the solution of the problem (6.3.18). Then, for $n = 1, 2, \ldots, M$ there holds*

$$\|e_{0,i}^n\|_{\mathcal{K}_y^M} \leq C\Big(h_y^{k+1} + N^{-\min\{2-\alpha, r\alpha\}}\Big),\ i = 0, 1, \ldots, M.$$

Now the error estimate result of the proposed WG method can be proved under the $L^\infty(L^2(\mathcal{V}))$ norm in the following theorem.

Theorem 6.4.13. *Let $\mathcal{E}_{h,i,j}^n = \{\mathcal{E}_{0,i,j}^n, \mathcal{E}_{b,i,j}^n\}$ be the error defined by (6.4.16). Then, for $n = 1, 2, \ldots, M$ there holds*

$$\max_{1\leq n\leq N} \|\mathcal{E}_{0,i,j}^n\|_{L^2(\mathcal{V})} \leq C\Big(h^{k+1} + N^{-\min\{2-\alpha, r\alpha\}}\Big),\ \forall\, i, j = 0, 1, \ldots, M,$$

where $h := \max\{h_x, h_y\}$.

Proof. The proof follows from Theorem 6.4.10 and Theorem 6.4.12. Thus, we have completed the proof. □

6.5 Numerical experiments

In this section, we present a numerical example that will be solved with the help of proposed scheme in support of the theoretical results. The dimensional-splitting weak Galerkin methods (6.3.17) and (6.3.18) are implemented over the polynomial spaces $\mathbb{P}_1$ and $\mathbb{P}_2$. To obtain the optimal convergence rate $\mathcal{O}(N^{-(2-\alpha)})$ in time, we have chosen the mesh grading parameter $r = (2-\alpha)/\alpha$. We define the error as

$$E_M^N = \max_{1\leq n\leq N} \|u^n - u_{h,0}^n\|, \tag{6.5.1}$$

and the convergence rates are calculated as

$$CO_N = \log_2\left(\frac{E_M^N}{E_M^{2N}}\right), \text{ and } CO_M = \log_2\left(\frac{E_M^N}{E_{2M}^N}\right), \tag{6.5.2}$$

in time and space respectively.

To calculate the error E_M^N, defined in (5.1) we have taken supremum over all time step τ_n, $n = 1, 2, \ldots, N$ and the space step h.

Example 6.5.1. *Consider the following two-dimensional TFDE:*

$$\begin{cases} {}^{C}D_{0,t}^{\alpha} u - \Delta u + \boldsymbol{d}(\boldsymbol{x}).\nabla u + u = f(\boldsymbol{x}, t), \ (\boldsymbol{x}, t) \in \mathcal{V} \times \Omega_t, \\ u(\boldsymbol{x}, 0) = \widehat{u}_0(\boldsymbol{x}), \quad \boldsymbol{x} \in \overline{\mathcal{V}}, \\ u(\boldsymbol{x}, t) = 0, \quad (\boldsymbol{x}, t) \in \ \partial\mathcal{V} \times \overline{\Omega_t}, \end{cases} \tag{6.5.3}$$

where $\boldsymbol{d}(\mathbf{x}) = (x(1-x)+1, \, y(1-y)+1)$, $\Omega_t = (0, 1]$ and the domain $\mathcal{V} = (0, 1) \times (0, 1)$. The functions $\widehat{u}_0$ and f are chosen such a way that the exact solution of the equation (6.5.3) is $u(\mathbf{x}, t) = \sin(\pi x)\sin(\pi y)(t^{\alpha} + 2t^3 + 2)$.

Numerical solution at the time level $t = 1$ is portrayed in the Figure 6.1 with $N = 256$ and order $\alpha = 0.7$. In Table 6.1, the errors E_M^N in time and orders CO_N for the Example 6.5.1 have been included for different values of N and α. To discretize the spatial domain, we have considered the M number of mesh points with $M = [N^{(2-\alpha)/k+1}]$ in the x and y direction, where $[X]$ represents the greatest integer less than or equal to any given real number X. For better understand of the orders, log-log plots, related to the errors are depicted in Figure 6.2. These results are in good agreement with the theoretical findings obtained in Theorem 6.4.13.

Table 6.1: L^2 errors and CO_N of the Example 6.5.1 for different values of N and α using the $\mathbb{P}_1$ element.

N	$\alpha = 0.3$		$\alpha = 0.5$		$\alpha = 0.7$	
	E_M^N	CO_N	E_M^N	CO_N	E_M^N	CO_N
64	1.6336e-02	–	4.0869e-02	–	1.0151e-01	–
128	5.3840e-03	1.6013	1.4349e-02	1.5101	3.9229e-02	1.3716
256	1.6757e-03	1.6839	5.1940e-03	1.4660	1.6430e-02	1.2556
512	5.2404e-04	1.6771	1.8866e-03	1.4611	6.6602e-03	1.3027
1024	1.6079e-04	1.7045	6.6470e-04	1.5050	2.6984e-03	1.3034

We next fix the number of intervals $N = 2000$ along the temporal direction that is sufficiently large to neglect the errors in time. Table 6.2 represents the errors E_M^N in space and

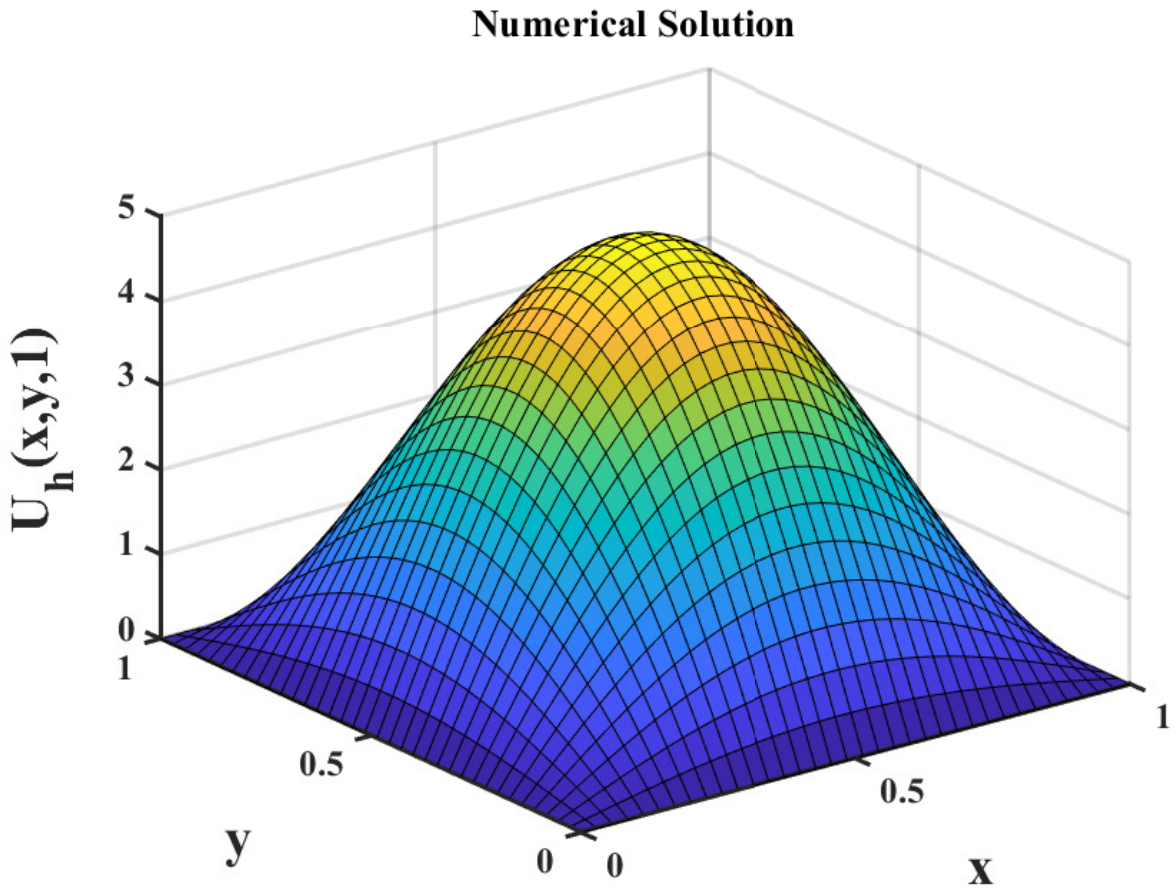

Figure 6.1: Numerical solution of the Example 6.5.1 at the time $t = 1$ using the $\mathbb{P}_1$ element.

Table 6.2: L^2 errors and CO_M of the Example 6.5.1 with $\alpha = 0.5$ using the $\mathbb{P}_1$ and $\mathbb{P}_2$ elements.

M	$\mathbb{P}_1$		$\mathbb{P}_2$	
	E_M^N	CO_M	E_M^N	CO_M
16	8.2428e-02	–	1.6397e-02	–
32	2.1218e-02	1.9584	2.0667e-03	2.9880
64	5.3929e-03	1.9786	2.5717e-04	3.0069
128	1.3563e-03	2.0008	3.0914e-05	3.0564
256	3.2725e-04	2.0512	3.8017e-06	3.0235

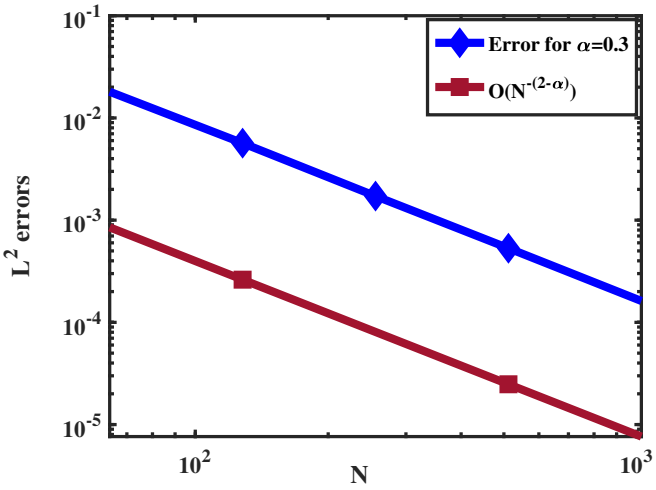

(a) Log-log plot for $\alpha = 0.3$

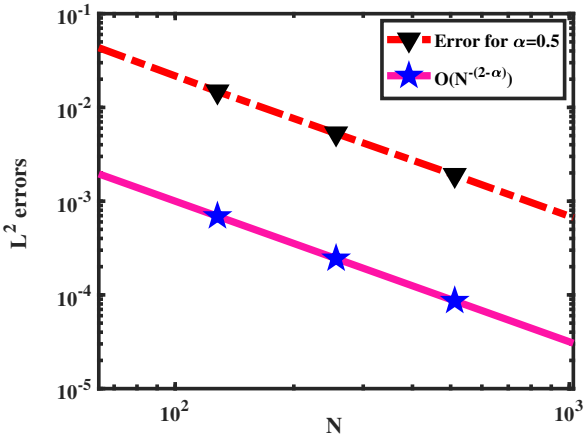

(b) Log-log plot for $\alpha = 0.5$

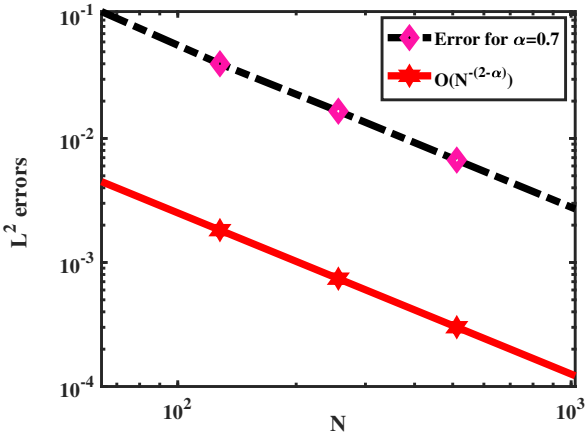

(c) Log-log plot for $\alpha = 0.7$

Figure 6.2: Log-log plots corresponding to the Table 6.1.

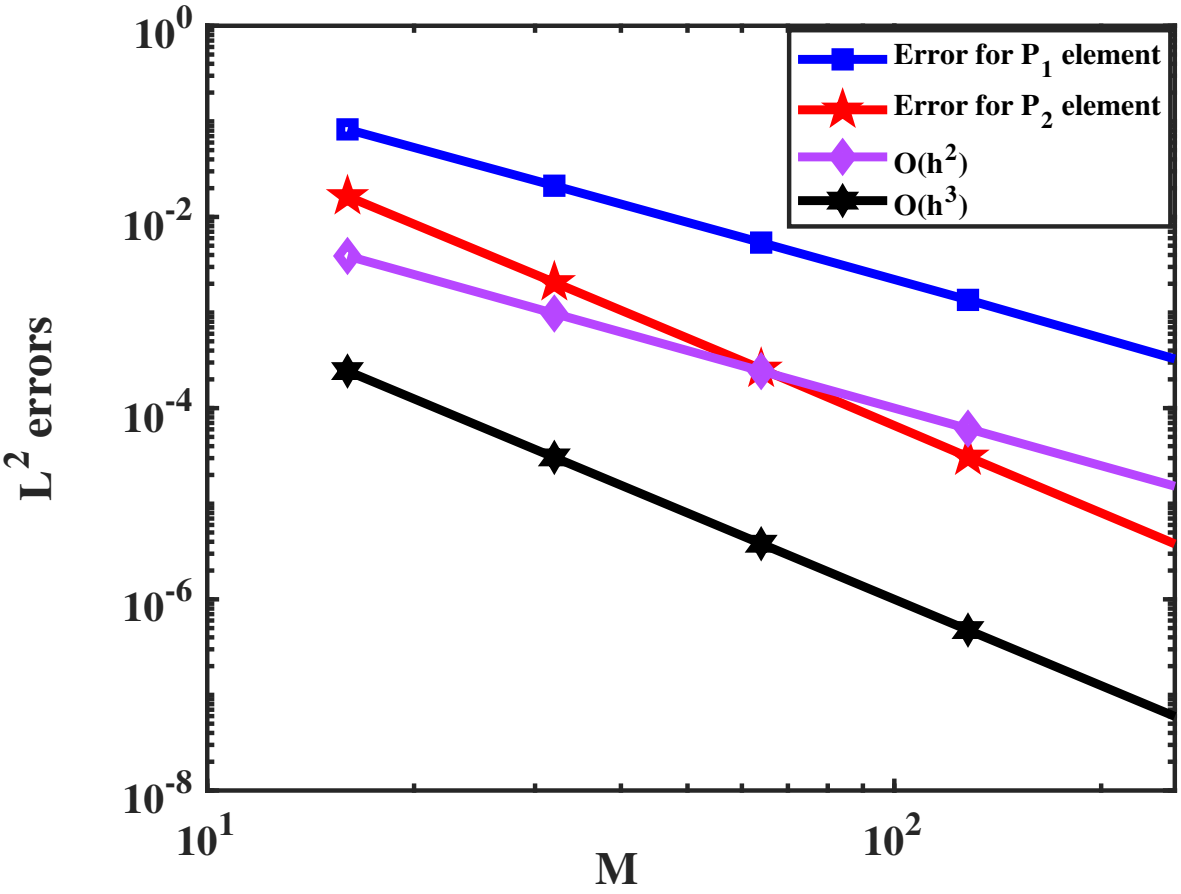

Figure 6.3: Log-log plot of the convergence rates in the spatial direction using the $\mathbb{P}_1$ element.

orders CO_M for the different values of M along the spatial direction, and it gives the $(k+1)$-th order convergence when $\mathbb{P}_k$ is employed, *i.e.*, the second order and third order convergence are obtained using the $\mathbb{P}_1$ and $\mathbb{P}_2$ element respectively in the approximation space. Again, these results show that the proposed method has the optimal order of convergence in space as stated in Theorem 6.4.13. The log-log plot corresponding to the $\mathbb{P}_1$ element is sketched in Figure 6.3.

6.6 Conclusions

In this chapter, we investigated the WGFEM, coupled with the ADI–type dimensional-splitting technique to find the numerical solution of a class of time-factional diffusion equation. It helped us to easily deal with the 2D time-fractional diffusion problem. This dimensional-splitting technique assists to reduce the computational cost in solving the 2D time-fractional problem (6.1.1). The well known $L1$-method has been used to approximate the time-fractional derivative term over a non-uniform mesh and the uniform dimensional-splitting WGFEM was used for the space discretization. We have analyzed the stability and the error estimate of the proposed scheme. In support of the theoretical estimate, a numerical example has been proposed.

CHAPTER 7

Novel LOD technique for 2D nonlinear space-fractional diffusion equation

In this chapter, we deal with a locally one-dimensional (LOD) method for 2D nonlinear space-fractional diffusion equation (SFDE). Initially, the nonlinear problem is linearized using the Newton's quasilinearization technique, and subsequently it has been decomposed into two 1D problems to reduce the computational cost. This method is based on the combination of the Backward-Euler scheme for the temporal derivative and the L1-method for the spatial fractional derivatives. The discrete maximum principle of the present method is also discussed. The convergence of the fully-discrete scheme on a discrete L^∞-norm is analyzed using discrete barrier function. Lastly, the justification of the theoretical results is done by some numerical experiments.

7.1 Introduction

In this chapter, we consider the following nonlinear two-dimensional (2D) SFDE:

$$\begin{cases} \dfrac{\partial u}{\partial t} - \mathbf{d}(\mathbf{x},t).\,\Delta_\alpha u + \mathbf{a}(\mathbf{x},t).\nabla u + f(\mathbf{x},t,u) = 0, \quad \mathbf{x} \in \mathcal{V}, t \in \Omega_t, \\ u(\mathbf{x},0) = \widehat{u}_0(\mathbf{x}), \quad \mathbf{x} \in \overline{\mathcal{V}} = \overline{\Omega}_x \times \overline{\Omega}_y, \\ u(\mathbf{x},t) = 0, \quad (\mathbf{x},t) \in \partial\mathcal{V} \times \overline{\Omega}_t, \end{cases} \tag{7.1.1}$$

where the operator Δ_α is defined as $\Delta_\alpha \equiv \left(\dfrac{\partial}{\partial x} {}^C D^\alpha_{0,x}, \dfrac{\partial}{\partial y} {}^C D^\alpha_{0,y} \right)$, with $0 < \alpha < 1$, $u(\mathbf{x},t) = u(x,y,t)$, the set $\mathcal{V} = \Omega_x \times \Omega_y \subset \mathbb{R}^2$ can be defined as the cartesian product grids of the x-domain $\Omega_x = (x_l, x_r)$ and the y-domain $\Omega_y = (y_l, y_r)$, where the boundary of this grid is denoted as $\partial\mathcal{V}$. The diffusion coefficient function $\mathbf{d} = (d_1, d_2)$ and the coefficient function $\mathbf{a} = (a_1, a_2)$ are considered to be smooth and bounded in the domain $\overline{\mathcal{V}}$ with $0 < \mathfrak{m}_1 \leq d_1, d_2 \leq \mathfrak{m}_2 \leq 1$ for some real number $\mathfrak{m}_1, \mathfrak{m}_2$. To validate the presence of a solution to the model problem (7.1.1), the nonlinear source function $f(\mathbf{x},t,u)$ with $\partial f/\partial u > 0$ and the initial value $\widehat{u}_0(\mathbf{x})$, both are assumed to be sufficiently smooth. ${}^C D^\alpha_{0,x}$ and ${}^C D^\alpha_{0,y}$ are the Caputo derivative operators in the x- and y-directions respectively..

Initially, we linearize the model problem (7.1.1) using the Newton's quasilinearization method. Subsequently, we partition it into two one-dimensional subproblems by employing the LOD approach to handle the linearized SFDE. We then use the well-known $L1$-discretization technique to approximate the fractional derivative term, while the convection term is taken care of by the standard central difference scheme. Furthermore, we establish an error estimate using a discrete maximum principle, aided by a suitably chosen discrete barrier function, under the following regularity condition on the solution $u(\mathbf{x},t)$

$$\left| \frac{\partial^k u}{\partial t^k}(\mathbf{x},t) \right| \leq C, \text{ for } k = 0,1,2, \text{ and } \left| \frac{\partial^l u}{\partial z^l}(\mathbf{x},t) \right| \leq C z^{\alpha+1-l}, \text{ for } l = 1,2,3, \tag{7.1.2}$$

where $z = x, y$.

The rest of the chapter is structured as follows: Section 7.2 describes the quasilinearization and LOD method applied to the given model problem (7.1.1). In Section 7.3, we implement the renowned $L1$-discretization method into the linearized subproblems and conduct an error analysis. Section 7.4 showcases some computational results in favour of the theoretical aspects. Finally, a brief summary is incorporated in Section 7.5.

7.2 Quasilinearization and LOD technique

In this section, we will set up the linearization process that will be followed by the splitting process of the model problem (7.1.1) in a set of one-dimensional problems. The simplified linearized version of the model problem (7.1.1) enables us to use the numerical schemes in a comfort way.

7.2.1 Newton's quasilinearization process

To streamline the nonlinear problem outlined in (7.1.1), we employ Newton's quasilinearization technique, yielding a sequence $\left\{u^{(m)}\right\}_0^\infty$. We initiate this sequence with the initial guess $u^{(0)}$ adhering to the initial and boundary conditions provided by the equation (7.1.1). Henceforth, we establish $u^{(m+1)}$ for every non-negative integer m as the solution of the following quasilinearized problem:

$$\begin{cases} \dfrac{\partial \mathfrak{v}}{\partial t} - \mathbf{d}(\mathbf{x},t).\,\Delta_\alpha \mathfrak{v} + \mathbf{a}(\mathbf{x},t).\nabla \mathfrak{v} + c^{(m)}(\mathbf{x},t)\mathfrak{v} = g^{(m)}(\mathbf{x},t), \quad \mathbf{x} \in \mathcal{V}, t \in \Omega_t, \\ \mathfrak{v}(\mathbf{x},0) = \widehat{u}_0(\mathbf{x}), \quad \mathbf{x} \in \overline{\mathcal{V}}, \\ \mathfrak{v}(\mathbf{x},t) = 0, \quad (\mathbf{x},t) \in \partial\mathcal{V} \times \overline{\Omega}_t, \end{cases} \tag{7.2.1}$$

where $\mathfrak{v}(\mathbf{x},t) = u^{(m+1)}(\mathbf{x},t)$,

$$\begin{cases} c^{(m)}(\mathbf{x},t) = \dfrac{\partial f}{\partial u}(\mathbf{x},t,u^{(m)}(\mathbf{x},t)) > 0, \\ g^{(m)}(\mathbf{x},t) = u^{(m)}(\mathbf{x},t)c^{(m)}(\mathbf{x},t) - f(\mathbf{x},t,u^{(m)}(\mathbf{x},t)). \end{cases}$$

Convergence of the quasilinearized problem

If the initial guess $u^{(0)}$ is selected to be adequately near to the solution $u(\mathbf{x},t)$ of the equation (7.1.1), then the sequence $\left\{u^{(m)}\right\}_0^\infty$ will exhibit quadratic convergence [40] to the solution $u(\mathbf{x},t)$ of the equation (7.1.1).

Further, for every fixed $m \geq 0$, employing Newton's quasilinearization technique to achieve the convergence of the quasilinearized problem, subject to the following convergence criterion

$$\left|\mathfrak{v}(\mathbf{x},t) - u^{(m)}(\mathbf{x},t)\right| \leq \text{tol}, \quad \forall (\mathbf{x},t) \in \overline{\mathcal{V}}, \quad m \geq 0. \tag{7.2.2}$$

For our computational requirements, we will select $\text{tol} = 10^{-8}$.

7.2.2 LOD method

Let us propose two operators defined as:

$$\begin{cases} \mathcal{L}_{x,\alpha} \equiv -d_1(\mathbf{x},t)\dfrac{\partial}{\partial x}{}^{C}D^{\alpha}_{0,x} + a_1(\mathbf{x},t)\dfrac{\partial}{\partial x} + c_1^{(m)}(\mathbf{x},t), \quad \forall\ y \in \Omega_y, \\ \mathcal{L}_{y,\alpha} \equiv -d_2(\mathbf{x},t)\dfrac{\partial}{\partial y}{}^{C}D^{\alpha}_{0,y} + a_2(\mathbf{x},t)\dfrac{\partial}{\partial y} + c_2^{(m)}(\mathbf{x},t), \quad \forall\ x \in \Omega_x, \end{cases} \tag{7.2.3}$$

in the both spatial discretization such that $c^{(m)} = c_1^{(m)} + c_2^{(m)}$ with $c_1^{(m)}, c_2^{(m)} > 0$ and the function $g^{(m)}$ can be partitioned as $g^{(m)} = g_1^{(m)} + g_2^{(m)}$, ensuring it satisfies the subsequent compatibility condition, serving as a fundamental assumption in the asymptotic study of the semi-discrete formulation of the problem.

$$g_1^{(m)}(x,0,t) = g_2^{(m)}(0,y,t) = g_1^{(m)}(x,1,t) = g_2^{(m)}(1,y,t) = 0. \tag{7.2.4}$$

Then, the model problem (7.1.1) can be rephrased in the following manner:

$$\frac{\partial \mathfrak{v}}{\partial t} + (\mathcal{L}_{x,\alpha} + \mathcal{L}_{y,\alpha})\,\mathfrak{v} = g_1^{(m)}(\mathbf{x},t) + g_2^{(m)}(\mathbf{x},t), \quad (\mathbf{x},t) \in \mathcal{V} \times \Omega_t. \tag{7.2.5}$$

For the temporal discretization of the time interval $\overline{\Omega}_t$, we have considered the uniform mesh $\overline{\Omega}_t^N$ with the time-step length $\tau = T/N$.

Next, we delineate the subsequent sub-problems within each time sub-interval $(t_{n-1}, t_n]$ for $n = 1, \ldots, N$ as:

Sub-problem 1 $(x-$ direction$)$

Find a solution $\mathfrak{v}^{\otimes} : \mathcal{V} \times (t_{n-1}, t_n] \to \mathbb{R}$ such that $\forall y \in \Omega_y$

$$\begin{cases} \dfrac{\partial \mathfrak{v}^{\otimes}}{\partial t} + \mathcal{L}_{x,\alpha}\mathfrak{v}^{\otimes} = g_1^{(m)}(x,y,t_n), \quad \text{in } \mathcal{V} \times (t_{n-1}, t_n], \\ \mathfrak{v}^{\otimes}(\mathbf{x},t) = 0, \quad (\mathbf{x},t) \in \partial\Omega_x \times \Omega_y \times (t_{n-1}, t_n], \\ \mathfrak{v}^{\otimes}(\mathbf{x}, t_{n-1}) = \mathfrak{v}(\mathbf{x}, t_{n-1}), \quad \mathbf{x} \in \mathcal{V}, \end{cases} \tag{7.2.6}$$

Sub-problem 2 $(y-$ direction$)$

Find a solution $\mathfrak{v} : \mathcal{V} \times (t_{n-1}, t_n] \to \mathbb{R}$ such that $\forall x \in \Omega_x$

$$\begin{cases} \dfrac{\partial \mathfrak{v}}{\partial t} + \mathcal{L}_{y,\alpha}\mathfrak{v} = g_2^{(m)}(\mathbf{x},t_n), \quad \text{in } \mathcal{V} \times (t_{n-1}, t_n], \\ \mathfrak{v}(\mathbf{x},t) = 0, \quad (\mathbf{x},t) \in \Omega_x \times \partial\Omega_y \times (t_{n-1}, t_n], \\ \mathfrak{v}(\mathbf{x}, t_{n-1}) = \mathfrak{v}^{\otimes}(\mathbf{x}, t_n), \quad \mathbf{x} \in \mathcal{V}, \end{cases} \tag{7.2.7}$$

for every non-negative integer m.

To initiate the process, we initially tackle the equation (7.2.6) along the x-axis, treating y as a parameter. After solving for each $y \in \Omega_y$, the solution $\mathfrak{v}^{\otimes}(\mathbf{x}, t_n)$ serves as the initial step for the subsequent Step-2 (7.2.7). In Step-2, we then address along the y-axis similarly, solving the problem (7.2.7) for all $x \in \Omega_x$. In essence, we utilize their initial conditions to interconnect the aforementioned two sub-problems.

7.3 Discretization technique and theoretical analysis

In this section, we will delineate the discretization process of the linearized problem (7.2.1) and analyze the theoretical estimation of the error associated with the discretized version of the problem (7.2.1).

7.3.1 Fully-discrete scheme

To derive the fully-discrete scheme of the model problem (7.2.1), we consider the uniform meshes $\overline{\Omega}_x^{M_x}$ with the uniform step size h_x and $\overline{\Omega}_y^{M_y}$ the uniform step size h_y in the $x-$ and $y-$ direction respectively.

Therefore, the discretized grid across the domain $\overline{\mathcal{V}} \times \overline{\Omega}_t$ is established as follows:

$$\overline{\Omega}_{M_x,M_y}^{N} = \{(x_i, y_j, t_n) : 0 \leq i \leq M_x, 0 \leq j \leq M_y, 0 \leq n \leq N\}. \tag{7.3.1}$$

We first employ the well-known $L1$-method to discretize the Caputo derivative operator ${}^{C}D_{0,x}^{\alpha}$ at the point $x = x_i, 0 < i < M_x$. The first-order classical derivative operator, presented in the convection term will be discretized using the well known second-order central difference formula and the classical time derivative in (7.1.1) will be approximated using the backward Euler method at a point $t = t_n, n = 1, 2, \ldots, N$.

Using the $L1$-scheme (1.2.22), the Caputo derivative ${}^{C}D_{0,x}^{\alpha}u(x)$ at the point $x = x_i$ is written as

$${}^{C}D_{0,x}^{\alpha}u(x_i) \approx \frac{h_x^{-\alpha}}{\Gamma(2-\alpha)} \sum_{k=0}^{i-1} \left(u(x_{k+1}) - u(x_k)\right) \widehat{b}_{i-k}^{(\alpha)} = \delta_x^{\alpha} u_i, \ i = 1, 2, \ldots, M_x - 1. \tag{7.3.2}$$

Similarly, in the y-direction one can obtain

$$\delta_y^{\alpha} u_j = \frac{h_y^{-\alpha}}{\Gamma(2-\alpha)} \sum_{k=0}^{j-1} \left(u(y_{k+1}) - u(y_k)\right) \widehat{b}_{j-k}^{(\alpha)}, \ j = 1, 2, \ldots, M_y - 1. \tag{7.3.3}$$

We define the following operators for the convenience of the representation

$$\delta_x^+ \mathfrak{w}_{i,j} = \frac{\mathfrak{w}_{i+1,j} - \mathfrak{w}_{i,j}}{h_x}, \delta_y^+ \mathfrak{w}_{i,j} = \frac{\mathfrak{w}_{i,j+1} - \mathfrak{w}_{i,j}}{h_y},$$
$$\delta_x^0 \mathfrak{w}_{i,j} = \frac{\mathfrak{w}_{i+1,j} - \mathfrak{w}_{i-1,j}}{2h_x}, \delta_y^0 \mathfrak{w}_{i,j} = \frac{\mathfrak{w}_{i,j+1} - \mathfrak{w}_{i,j-1}}{2h_y}, \tag{7.3.4}$$

Then, the fully-discrete scheme for the problem (7.2.6) and (7.2.7) can be written as:

x-direction

$$\begin{cases} \mathcal{L}_{M_x}^N \mathfrak{v}_{i,j}^{\otimes,n} := \delta_t \mathfrak{v}_{i,j}^{\otimes,n} - d_{1,ij}^n \delta_x^+ \delta_x^\alpha \mathfrak{v}_{i,j}^{\otimes,n} + a_{1,ij}^n \delta_x^0 \mathfrak{v}_{i,j}^{\otimes,n} + c_{1,ij}^{(m),n} \mathfrak{v}_{i,j}^{\otimes,n} = g_{1,ij}^{(m),n}, \quad 0 \le j \le M_y, \\ \mathfrak{v}_{i,j}^{\otimes,n-1} = \mathfrak{v}_{i,j}^{n-1}, \quad 0 \le i \le M_x, 0 \le j \le M_y, \\ \mathfrak{v}_{0,j}^{\otimes,n} = \mathfrak{v}_{M_x,j}^{\otimes,n}, \quad 0 \le j \le M_y, \end{cases} \tag{7.3.5}$$

and

y-direction

$$\begin{cases} \mathcal{L}_{M_y}^N \mathfrak{v}_{i,j}^{\otimes,n} := \delta_t \mathfrak{v}_{i,j}^{n} - d_{2,ij}^n \delta_y^+ \delta_y^\alpha \mathfrak{v}_{i,j}^{n} + a_{2,ij}^n \delta_y^0 \mathfrak{v}_{i,j}^{n} + c_{2,ij}^{(m),n} \mathfrak{v}_{i,j}^{n} = g_{2,ij}^{(m),n}, \quad 0 \le i \le M_x, \\ \mathfrak{v}_{i,j}^{n-1} = \mathfrak{v}_{i,j}^{\otimes,n}, \quad 0 \le i \le M_x, 0 \le j \le M_y, \\ \mathfrak{v}_{i,0}^{n} = \mathfrak{v}_{i,M_y}^{n}, \quad 0 \le i \le M_x, \end{cases} \tag{7.3.6}$$

where $\delta_t w^n = \frac{w^n - w^{n-1}}{\tau}$ for some function w^n, the notations $\mathfrak{v}_{i,j}^{\otimes,n}$ and $\mathfrak{v}_{i,j}^n$ are the approximation of $\mathfrak{v}^\otimes(x_i, y_j, t_n)$ and $\mathfrak{v}(x_i, y_j, t_n)$ respectively, at the point $(x_i, y_j, t_n) \in \overline{\Omega}_{M_x,M_y}^N$, $a_{ij}^n = a(x_i, y_j, t_n)$, and similar expressions hold for c, d and g also.

7.3.2 Discrete maximum principle

Lemma 7.3.1. *Suppose the mesh function $\mathfrak{v}_{i,j}^{\otimes,n}$ with $0 \le i \le M_x, 0 \le j \le M_y, 0 \le n \le N$ satisfies the following conditions:*

$$\mathfrak{v}_{i,j}^{\otimes,0} \ge 0, \quad \textit{for} \quad 0 \le i \le M_x, 0 \le j \le M_y,$$
$$\mathfrak{v}_{0,j}^{\otimes,n} \ge 0, \quad \mathfrak{v}_{M_x,j}^{\otimes,n} \ge 0, \quad \textit{for} \quad 0 \le j \le M_y, 0 \le n \le N,$$
$$\textit{and} \quad \mathcal{L}_{M_x}^N \mathfrak{v}_{i,j}^{\otimes,n} \ge 0, \quad \textit{for} \quad 0 \le i \le M_x, 0 \le j \le M_y, \quad 0 \le n \le N.$$

If the step size h_x maintains the following bound

$$h_x < \left(\frac{2\mathfrak{m}_2(\widehat{b}_3^{(\alpha)} - 2\widehat{b}_2^{(\alpha)} + \widehat{b}_1^{(\alpha)})}{\|a_1^n\|_\infty \Gamma(2-\alpha)} \right)^{1/\alpha}, \tag{7.3.7}$$

then $\mathfrak{v}_{i,j}^{\otimes,n} \geq 0$ for $0 \leq i \leq M_x, 0 \leq j \leq M_y$ and $0 \leq n \leq N$.

Proof. Let us consider a matrix $\mathcal{P}_j = \left(p_{l,k}\right)_{l,k=0}^{M_x}$ associated with the fully-discrete scheme (7.3.5) for all $j = 0, 1, \ldots, M_y$. Then, we have a linear system $\mathcal{P}_j \overrightarrow{\mathfrak{v}}_j^{\otimes,n} = \overrightarrow{g}_j^n$ where $\overrightarrow{\mathfrak{v}}_j^{\otimes,n} = \left(\mathfrak{v}_{0,j}^{\otimes,n}, \mathfrak{v}_{1,j}^{\otimes,n}, \ldots, \mathfrak{v}_{M_x,j}^{\otimes,n}\right)^T$ and $\overrightarrow{g}_j^n = \left(g_{0,j}^n, g_{0,j}^n, \ldots, g_{0,j}^n\right)^T$ for all $j = 0, 1, \ldots, M_y$. Then $\mathcal{P}_j \overrightarrow{\mathfrak{v}}_j^{\otimes,n} \geq 0$ holds as hypothesized.

The entries of the matrix $\mathcal{P}_j$ related to the boundary conditions at $x = x_l$ and $x = x_r$ are specified as follows:

$$\begin{aligned} &\mathfrak{p}_{j,00} = 1, \quad \mathfrak{p}_{j,0k} = 0, \text{ for } 1 \leq k \leq M_x, \\ &\mathfrak{p}_{j,(M_x,M_x)} = 1, \quad \mathfrak{p}_{j,(M_x,k)} = 0, \text{ for } 0 \leq k \leq M_x - 1, \end{aligned}$$

and for $0 < l < M_x$, the entries of the l-th row of the matrix $\mathcal{P}_j$ are expressed as:

$$\begin{aligned} \mathfrak{p}_{j,l0} &= d_{1,1j}^n \frac{\widehat{b}_{l+1}^{(\alpha)} - \widehat{b}_l^{(\alpha)}}{h_x^{\alpha+1}\Gamma(2-\alpha)} - \frac{a_{1,1j}^n}{2h_x}\delta_{l,1}, \quad 1 \leq l \leq M_x - 1, \\ \mathfrak{p}_{j,lk} &= d_{1,lj}^n \frac{-\widehat{b}_{l-k+2}^{(\alpha)} + 2\widehat{b}_{l-k+1}^{(\alpha)} - \widehat{b}_{l-k}^{(\alpha)}}{h_x^{\alpha+1}\Gamma(2-\alpha)} - \frac{a_{1,lj}^n}{2h_x}\delta_{l-1,k}, \quad 1 \leq k \leq l-1, \\ \mathfrak{p}_{j,ll} &= \frac{1}{\tau} + d_{1,lj}^n \frac{2\widehat{b}_1^{(\alpha)} - \widehat{b}_2^{(\alpha)}}{h_x^{\alpha+1}\Gamma(2-\alpha)} + c_{1,lj}^{(m),n} > 0, \\ \mathfrak{p}_{j,(l,l-1)} &= d_{1,lj}^n \frac{-\widehat{b}_3^{(\alpha)} + 2\widehat{b}_2^{(\alpha)} - \widehat{b}_1^{(\alpha)}}{h_x^{\alpha+1}\Gamma(2-\alpha)} - \frac{a_{1,lj}^n}{2h_x}, \quad l = 2, 3, \ldots, M_x - 1, \\ \mathfrak{p}_{j,(l,l+1)} &= -d_{1,lj}^n \frac{\widehat{b}_1^{(\alpha)}}{h_x^{\alpha+1}\Gamma(2-\alpha)} + \frac{a_{1,lj}^n}{2h_x}, \end{aligned}$$

for all $j = 0, 1, \ldots, M_y$.

Then, it is clear that the matrix $\mathcal{P}_j$ is a lower Hessenberg matrix, with the above entries and also suppose $\mathcal{Q}$ is another diagonal matrix with the following entries

$$\mathfrak{q}_{l,l} = \begin{cases} \dfrac{1}{\tau}, & \text{for } l = 1, 2, \ldots, M_x - 1, \\ 0, & \text{for } l = 0, M_x. \end{cases} \tag{7.3.8}$$

We will now use the induction on n to prove $\overrightarrow{\mathfrak{v}}_j^{\otimes,n} \geq 0$ for all $j = 0, 1, \ldots, M_y$. From the given conditions, $\overrightarrow{\mathfrak{v}}_j^{\otimes,0} \geq 0$ and also suppose $\overrightarrow{\mathfrak{v}}_j^{\otimes,n} \geq 0$ for $n = 0, 1, \ldots, N-1$.

Our aim is to prove $\overrightarrow{\mathfrak{v}}_j^{\otimes,n+1} \geq 0$, which is equivalent to prove $\mathcal{P}_j^{-1} > 0$ in the relation $\mathcal{P}_j \overrightarrow{\mathfrak{v}}_j^{\otimes,n+1} \geq 0$.

Following the steps outlined in [26, Lemma 3.1], it is shown that the matrix $\mathcal{P}_j$ is an irreducibly diagonally dominant matrix, and hence $\mathcal{P}_j^{-1} > 0$. Consequently, the required result is proved. □

Similar to the Lemma 7.3.1, one can prove in the y-direction:

Lemma 7.3.2. *Suppose that the mesh function $\mathfrak{v}_{i,j}^n$ with $0 \leq i \leq M_x, 0 \leq j \leq M_y, 0 \leq n \leq N$ satisfies the following conditions:*

$$\mathfrak{v}_{i,j}^0 \geq 0, \quad \text{for} \quad 0 \leq i \leq M_x,\ 0 \leq j \leq M_y,$$

$$\mathfrak{v}_{i,0}^n \geq 0, \quad \mathfrak{v}_{i,M_y}^n \geq 0, \quad \text{for} \quad 0 \leq i \leq M_x,\ 0 \leq n \leq N, \quad \text{and}$$

$$\mathcal{L}_{M_y}^N \mathfrak{v}_{i,j}^n \geq 0, \quad \text{for} \quad 0 \leq i \leq M_x,\ 0 \leq j \leq M_y, \quad 0 \leq n \leq N.$$

If the step size h_y maintains the following bound

$$h_y < \left(\frac{2\mathfrak{m}_2 \left(\widehat{b}_3^{(\alpha)} - 2\widehat{b}_2^{(\alpha)} + \widehat{b}_1^{(\alpha)} \right)}{\|a_2^n\|_\infty \Gamma(2-\alpha)} \right)^{1/\alpha}, \tag{7.3.9}$$

then $\mathfrak{v}_{i,j}^n \geq 0$ for $0 \leq i \leq M_x, 0 \leq j \leq M_y$ and $0 \leq n \leq N$.

Truncation error estimates

The temporal truncation error $\mathcal{T}_{i,j}^n$ is given as

$$\mathcal{T}_{i,j}^n = \frac{\partial u}{\partial t}(x_i, y_j, t_n) - \delta_t u(x_i, y_j, t_n),$$

and it is easy to see that

$$\left|\mathcal{T}_{i,j}^n\right| \leq C\tau. \tag{7.3.10}$$

Then, for $n = 1, 2, \ldots, N$, (7.3.10) and [26, Lemma 4.1] combinedly give

$$\left| \mathcal{L}_{M_x}^N \left(\mathfrak{v}^\otimes(x_i, y_j, t_n) - \mathfrak{v}_{i,j}^{\otimes,n} \right) \right| \leq C(h_x x_i^{-1} + \tau), \quad \text{for } 0 < i < M_x,\ 0 \leq j \leq M_y,$$

and

$$\left| \mathcal{L}_{M_y}^N \left(\mathfrak{v}(x_i, y_j, t_n) - \mathfrak{v}_{i,j}^n \right) \right| \leq C(h_y y_j^{-1} + \tau), \quad \text{for } 0 < j < M_y,\ 0 \leq i \leq M_x.$$

7.3.3 Convergence result

This subsection will explore the error analysis of the presented method. Initially, to proceed, we divide the overall error into two parts as follows:

$$E^n_{h,ij} = \left(\mathfrak{v}^{\otimes}(x_i, y_j, t_n) - \mathfrak{v}^{\otimes,n}_{i,j}\right) + \left(\mathfrak{v}(x_i, y_j, t_n) - \mathfrak{v}^n_{i,j}\right) \tag{7.3.11}$$

$$= E^n_{h_x,ij} + E^n_{h_y,ij}, \quad 0 \le i \le M_x, 0 \le j \le M_y, \tag{7.3.12}$$

where $\mathfrak{v}^{\otimes}(x_i, y_j, t_n)$ and $\mathfrak{v}(x_i, y_j, t_n)$ are the exact solution of the equations (7.2.6) and (7.2.7) respectively, and $\mathfrak{v}^{\otimes,n}_{i,j}$ and $\mathfrak{v}^n_{i,j}$ are the solutions of the fully-discrete schemes (7.3.5) and (7.3.6) respectively at the point $(x_i, y_j, t_n), 0 \le n \le N$. Now to bound the error parts $E^n_{h_x,ij}$ and $E^n_{h_y,ij}$, we will take the help of barrier function.

Discrete barrier function

We start the analysis in the x-direction for the error term $E^n_{h_x,ij}$. Let, $B^n_{i,j}$ be a non-negative grid function in the computational domain $\overline{\Omega}^N_{M_x,M_y}$ satisfying

$$\begin{cases} \left|\mathcal{L}^N_{M_x} E^n_{h_x,ij}\right| \le \mathcal{L}^N_{M_x} B^n_{i,j}, \quad 0 < i \le M_x, 0 \le j \le M_y, 0 < n \le N, \\ \left|E^n_{h_x,0j}\right| \le B^n_{0,j}, \quad 0 \le j \le M_y,\ 0 < n \le N, \\ \left|E^n_{h_x,M_xj}\right| \le B^n_{M_x,j}, \quad 0 \le j \le M_y,\ 0 < n \le N. \end{cases} \tag{7.3.13}$$

Then, we can obtain $\left|E^n_{h_x,ij}\right| \le B^n_{i,j}$ for $i = 0, 1, \ldots, M_x, j = 0, 1, \ldots, M_y$, and $n = 0, 1, \ldots, N$ by importing the Lemma 7.3.1 to the grid functions $B^n_{i,j} \pm E^n_{h_x,ij}$. Then the non-negative function $B^n_{i,j}$ is called the discrete barrier function. We next construct a suitable discrete barrier function $B^n_{i,j}$ for the error function $E^n_{h_x,ij}$ and then this barrier function will be used in establishing the theoretical estimate of the error term.

We follow [26, Section 4] to define the discrete barrier function

$$\mathcal{B}_i = Ch_x \left|\ln h_x\right| \left((x_r - x_l)^{|\ln h_x|^{-1}+\alpha} - \widehat{Q}_i\right), \quad 0 \le i \le M_x, \tag{7.3.14}$$

where the function $\left\{\widehat{Q}_i\right\}_{i=0}^{M_x}$ is defined as follows:

$$\delta^{\alpha}_x \widehat{Q}_i = \frac{1}{\Gamma(1-\alpha)} x_i^{|\ln h_x|^{-1}}, \quad i \ge 1, \quad \text{and} \quad \widehat{Q}_0 = 0. \tag{7.3.15}$$

Also, following [26, equation 4.14], the bound $0 \leq \widehat{Q}_i \leq x_i^{|\ln h_x|^{-1}+\alpha}$, $i = 0, 1, \ldots, M_x$ can be shown. In the next theorem, the error estimate for the computed solution result will be addressed.

Theorem 7.3.3. *Let the solution $\mathfrak{v}^{\otimes}$ of the subproblem (7.2.6) satisfying the condition (7.1.2). Then there exist a constant C such that the following error estimation holds*

$$\max \left| E^n_{h_x,ij} \right| \leq C \left(\tau + h_x \left| \ln h_x \right| \right), \quad 0 \leq i \leq M_x,\, 0 \leq j \leq M_y, \text{ and } \quad 0 \leq n \leq N. \tag{7.3.16}$$

Proof. In order to establish the error estimate result in the x-direction for all $y_j \in \overline{\Omega}_y^{M_y}$, we now consider a suitable barrier function $\mathcal{G}_i^n$, defined by

$$\mathcal{G}_i^n = C \left(\tau t_n + \mathcal{B}_i \right), \quad \text{for} \quad 0 \leq i \leq M_x,\, 0 \leq n \leq N. \tag{7.3.17}$$

Following the idea given in [26], we can also show that

$$\mathcal{L}^N_{M_x} \mathcal{B}_i \geq \frac{C_1 h_x e^{-1}}{2\Gamma(1-\alpha)} x_i^{-1}, \quad \text{for some constant } C_1, \tag{7.3.18}$$

considering the coefficient $a_1(x, y, t) \leq 0$ for all $(x, y, t) \in \overline{\mathcal{V}} \times \overline{\Omega}_t$.

Then, from (7.3.17) and (7.3.18), we have

$$\begin{aligned} \mathcal{L}^N_{M_x} \mathcal{G}_i^n &\geq C \left(\tau \frac{t_n - t_{n-1}}{\tau} + \frac{C_1 h_x e^{-1}}{2\Gamma(1-\alpha)} x_i^{-1} \right) \\ &= C \left(\tau + \frac{C_1 h_x e^{-1}}{2\Gamma(1-\alpha)} x_i^{-1} \right). \end{aligned} \tag{7.3.19}$$

Therefore, the mesh function $\mathcal{G}_i^n$ is a discrete barrier function of the error function $E^n_{h_x,ij}$ for all $j = 0, 1, \ldots, M_y$, and accordingly the result follows from the Lemma 7.3.1. □

Likewise, in the y-direction it can be proved that

Theorem 7.3.4. *Let the solution $\mathfrak{v}$ of the subproblem (7.2.7) satisfying the condition (7.1.2). Then there exist a constant $\mathfrak{C}$ such that the following error estimation holds*

$$\max \left| E^n_{h_y,ij} \right| \leq C \left(\tau + h_y \left| \ln h_y \right| \right), \quad 0 \leq i \leq M_x,\, 0 \leq j \leq M_y, \text{ and } \quad 0 \leq n \leq N. \tag{7.3.20}$$

Therefore, the overall error estimate of the proposed LOD-$L1$-method can be proved under the maximum norm as follows:

Theorem 7.3.5. *Let $E_{h,ij}^n$ be the error term as mentioned in (7.3.11). Then, for $n = 0, 1, \ldots, N, \exists$ a constant C such that*

$$\max \left| E_{h,ij}^n \right| \leq C \left(\tau + h \left| \ln h \right| \right), \quad \text{for} \quad 0 \leq i \leq M_x, 0 \leq j \leq M_y, \tag{7.3.21}$$

where $h = \max \{h_x, h_y\}$.

Proof. The proof can be done directly by combining the Theorems 7.3.3 and 7.3.4, and hence the result follows. □

Remark 7.3.6. *In the given model problem (7.1.1), one can replace the classical convection term ∇u with a fractional convection term of the form $\Delta_{\varpi}^{1/2} u$, where $\Delta_{\varpi}^{1/2} \equiv \left(D_x^{\varpi}, D_y^{\varpi} \right)$ and the fractional order $\varpi \in (0, 1)$. This concept has found applications in various fields such as porous media flow, where non-local transport phenomena are prevalent, and in biological systems, where anomalous diffusion behaviour is observed. The fractional convection term allows for a more accurate description of these complex transport processes.*

In numerical studies, the fractional convection term can be computed using the well-known L1-method, as demonstrated in Section 7.3. If the proposed method is extended to a SFDE with fractional derivatives in both diffusion and convection terms, it is anticipated that first-order accuracy can be achieved in both spatial and temporal directions. The validation of this assertion will be presented in the subsequent section through a numerical example.

7.4 Numerical experiment

In this section, we will demonstrate some numerical examples to validate our theoretical findings. We compute the maximum discrete error E_M^N and the corresponding convergence rate CO_M^N as

$$E_M^N = \sup_{0 \leq n \leq N} \sup_{\substack{0 \leq i \leq M_x \\ 0 \leq j \leq M_y}} \left| u(x_i, y_j, t_n) - \mathfrak{v}_{i,j}^n \right|, \text{ and } CO_M^N = \log_2 \left(\frac{E_M^N}{E_{2M}^{2N}} \right), \tag{7.4.1}$$

respectively, with the same number of grid points in the spatial directions as well as in the temporal direction.

Example 7.4.1. *Consider the following 2D SFDE:*

$$\begin{cases} \dfrac{\partial u}{\partial t} - \mathbf{d}(\boldsymbol{x}, t). \Delta_{\alpha} u - \left(1 - \dfrac{xy}{2} + t, 1 + \dfrac{xy}{2} - t \right). \nabla u + f(\boldsymbol{x}, t, u) = 0, \ \boldsymbol{x} \in \mathcal{V}, t \in \Omega_t, \\ u(\boldsymbol{x}, 0) = (x^{\alpha+1} - x^2)(y^{\alpha+1} - y^2), \quad \boldsymbol{x} \in \overline{\mathcal{V}}, \\ u(\boldsymbol{x}, t) = 0, \quad (\boldsymbol{x}, t) \in \partial\mathcal{V} \times \overline{\Omega}_t, \end{cases} \tag{7.4.2}$$

with the domain $\mathcal{V} = (0,1)^2, \Omega_t = (0,1)$ and with the diffusion coefficient $\mathbf{d}(\mathbf{x},t) = e^{-t}(x^\alpha, y^\alpha)$ and nonlinear source term $f(\mathbf{x},t,u) = e^u + \widehat{\xi}(\mathbf{x},t)$, where the function $\widehat{\xi}(\mathbf{x},t)$ is selected in such a manner that the exact solution of equation (7.4.2) is $u(\mathbf{x},t) = (t^2+1)(x^{\alpha+1}-x^2)(y^{\alpha+1}-y^2)$.

Implementing the Newton's quasilinearization technique as discussed in (7.2.1), we can obtain the following sequence of linear SPDEs

$$\begin{cases} \dfrac{\partial \mathfrak{v}}{\partial t} - \mathbf{d}(\mathbf{x},t).\Delta_\alpha \mathfrak{v} - \left(1 - \dfrac{xy}{2} + t, 1 + \dfrac{xy}{2} - t\right).\nabla \mathfrak{v} + c^{(m)}(\mathbf{x},t)\mathfrak{v} = g^{(m)}(\mathbf{x},t),\ \mathbf{x} \in \mathcal{V}, t \in \Omega_t, \\ \mathfrak{v}(\mathbf{x},0) = (x^{\alpha+1}-x^2)(y^{\alpha+1}-y^2), \quad \mathbf{x} \in \overline{\mathcal{V}}, \\ \mathfrak{v}(\mathbf{x},t) = 0, \quad (\mathbf{x},t) \in \partial\mathcal{V} \times \overline{\Omega}_t, \end{cases} \tag{7.4.3}$$

where $\mathfrak{v}(\mathbf{x},t) = u^{(m+1)}(\mathbf{x},t)$,

$$\begin{cases} c^{(m)}(\mathbf{x},t) = e^{u^{(m)}} > 0, \\ g^{(m)}(\mathbf{x},t) = u^{(m)}(\mathbf{x},t)c^{(m)}(\mathbf{x},t) - f(\mathbf{x},t,u^{(m)}(\mathbf{x},t)). \end{cases}$$

Therefore, for a fixed $m \geq 0$ we solve equation (7.4.3) using the computational method discussed earlier in Section 7.3. Upon reaching the tolerance bound specified in (7.2.2), we terminate the Newton sequence and consider the current iterate as the solution to our problem. To employ the proposed LOD technique, we express the source function as the following decomposition:

$$\begin{aligned} g_2^{(m)}(\mathbf{x},t) &= y\left(g^{(m)}(x,1,t) - g^{(m)}(x,0,t)\right) + g^m(x,0,t), \\ g_1^{(m)}(\mathbf{x},t) &= g^{(m)}(\mathbf{x},t) - g_2^{(m)}(\mathbf{x},t), \end{aligned} \tag{7.4.4}$$

so that it satisfies the compatibility condition (7.2.4). Numerical solution plot, depicted in Figure 7.1a shows the results obtained using 64 number of grid points in spatial as well as temporal directions. The errors and convergence orders for Example 7.4.1 are provided in Table 7.1, and notably, the first-order accuracy is obtained in spatial and temporal directions. Additionally, Figure 7.1b illustrates the log-log plots of the Example 7.4.1.

Next, we incorporate an example with the fractional type convection term.

Example 7.4.2. *Consider the following 2D SFDE with a fractional convection term:*

$$\begin{cases} \dfrac{\partial u}{\partial t} - \Delta_\alpha u - (1+t^2)(1+x+y, 1-x-y).\Delta_\varpi^{1/2} u + f(\boldsymbol{x},t,u) = 0,\ \boldsymbol{x} \in \mathcal{V}, t \in \Omega_t, \\ u(\boldsymbol{x},0) = (x^{\alpha+1} - 2x^3 + x^2)(y^{\alpha+1} - 2y^3 + y^2), \quad \boldsymbol{x} \in \overline{\mathcal{V}}, \\ u(\boldsymbol{x},t) = 0, \quad (\boldsymbol{x},t) \in \partial\mathcal{V} \times \overline{\Omega}_t, \end{cases} \tag{7.4.5}$$

Table 7.1: Maximum errors and convergence rates of the Example 7.4.1 for different values of N and α.

N	$\alpha = 0.3$		$\alpha = 0.5$		$\alpha = 0.8$	
	E_M^N	CO_M^N	E_M^N	CO_M^N	E_M^N	CO_M^N
16	1.1795e-02	–	3.6571e-03	–	5.0894e-04	–
32	6.6033e-03	0.8369	2.0994e-03	0.8007	2.9858e-04	0.7694
64	3.4706e-03	0.9280	1.1270e-03	0.8975	1.6385e-04	0.8657
128	1.7724e-03	0.9695	5.8284e-04	0.9513	8.6136e-05	0.9277
256	8.9478e-04	0.9861	2.9610e-04	0.9770	4.4169e-05	0.9636

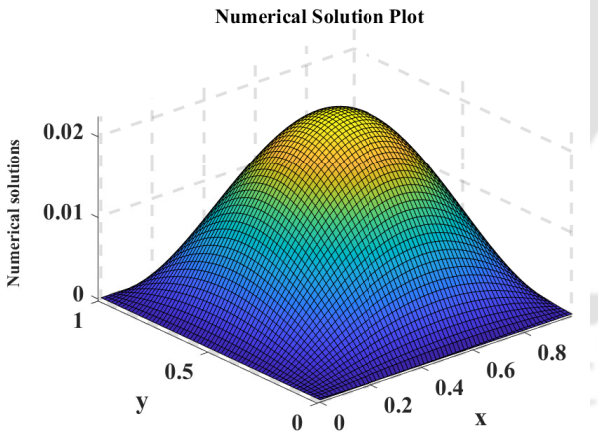

(a) Numerical solution of the Example 7.4.1 at the time $t = 1$ for $\alpha = 0.5$

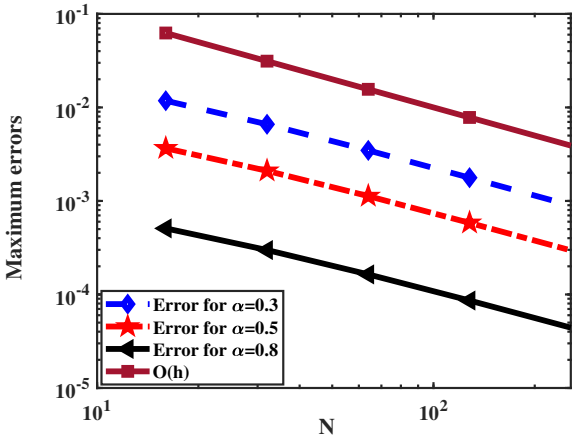

(b) Log-log plots for various α

Figure 7.1: Figures corresponding to the Table 7.1.

with the domain $\mathcal{V} = (0,1)^2, \Omega_t = (0,1)$ and the nonlinear source term is considered as $f(\mathbf{x},t,u) = u(1-u) + \widehat{\xi}(\mathbf{x},t)$, where the function $\widehat{\xi}(\mathbf{x},t)$ is selected in such a manner that the exact solution of equation (7.4.5) is $u(\mathbf{x},t) = e^{-t}(x^{\alpha+1} - 2x^3 + x^2)(y^{\alpha+1} - 2y^3 + y^2)$.

The Newton's quasilinearization technique is implemented in the same way as demonstrated in (7.4.3).

Table 7.2: Maximum errors and convergence rates of the Example 7.4.2 for various values of N, α with $\varpi = 0.8$.

N	$\alpha = 0.3$		$\alpha = 0.5$		$\alpha = 0.8$	
	E_M^N	CO_M^N	E_M^N	CO_M^N	E_M^N	CO_M^N
16	4.3440e-02	–	4.3457e-02	–	3.8965e-02	–
32	2.4320e-02	0.8369	2.5397e-02	0.7749	2.4318e-02	0.6801
64	1.2712e-02	0.9359	1.3766e-02	0.8835	1.3852e-02	0.8120
128	6.4534e-03	0.9781	7.1392e-03	0.9473	7.4400e-03	0.8967
256	3.2448e-03	0.9920	3.6271e-03	0.9769	3.8582e-03	0.9474

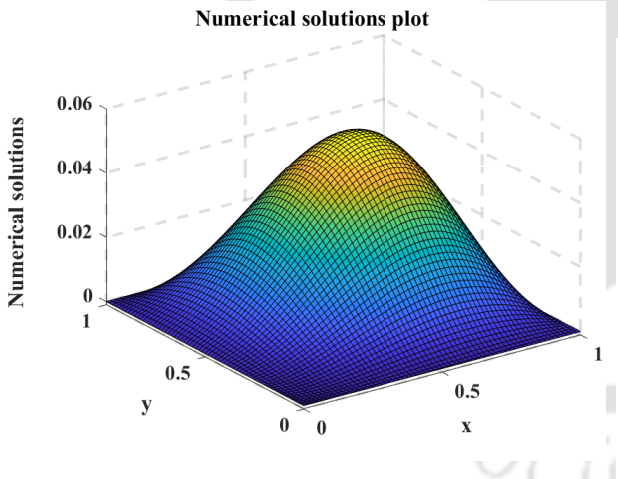

(a) Numerical solution of the Example 7.4.2 at the time $t = 1$ for $\alpha = 0.5$ and $\varpi = 0.8$

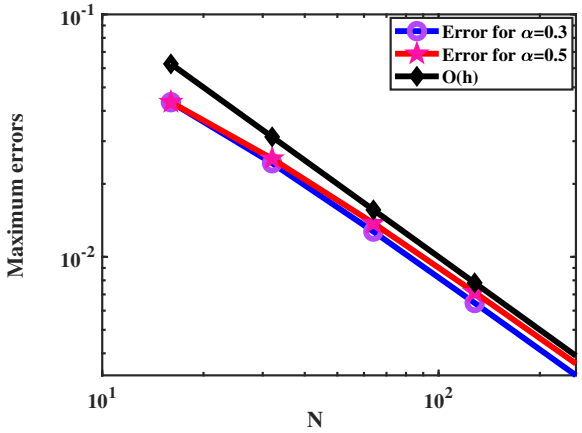

(b) Log-log plots for various α

Figure 7.2: Figures corresponding to the Table 7.2.

In Figure 7.2a, the numerical solution plot shows the results obtained using 64 grid points in both spatial and temporal directions. Table 7.2 presents the errors and convergence orders for Example 7.4.2, affirming the first-order convergence achieved in both space and time. Furthermore, Figure 7.2b displays the log-log plots of the Example 7.4.2 with $\varpi = 0.8$.

7.5 Conclusion

In this chapter, we introduced a numerical technique based on a LOD process to solve 2D nonlinear SFDE (7.1.1). Initially, the model problem has been linearized using Newton's quasilinearization process, after which it has been partitioned into two one-dimensional sub-problems along the x and y directions. The well-known $L1$-method over a uniform mesh was employed to discretize the spatial fractional term, and the discrete maximum principle was established for the discretized scheme. Further, the discrete maximum principle and convergence analysis have been discussed for the presented numerical scheme using a well-fitted discrete barrier function. Numerical results have been provided to confirm the truthfulness of the theoretical estimation.

CHAPTER 8

Concise overview and future extensions

This chapter summarizes the important results that have been carried out in the previous chapters of this thesis and discusses some future directions of the proposed concepts.

8.1 Summary of the works

Some important results of this thesis are highlighted below:

In Chapter 2, we considered a steady-state advection-diffusion-reaction type FBVP with a fractional convection term. The higher order derivative term of the model problem contains a mixed-fractional derivative. We have discussed a finite difference scheme based on the uniform $L1-$ method to discretize the fractional derivative terms. The discrete maximum principle has been addressed here. Further the related error analysis has been investigated and an error bound $CM_x^{-1}\left(\ln M_x\right)^{\alpha}$ has been proved. The convergence of the scheme was studied with the help of properly chosen discrete barrier function. An application of the proposed method was shown on the semilinear FBVPs. At last some numerical examples were established to corroborate the theory.

Chapter 3 studied the numerical solution of FBVPs with integral type boundary conditions. The numerical scheme consists of the spline approximation for the Caputo derivative, and the second-order classical finite difference for the advection-term and trapezoidal rule for the integral-type boundary conditions. Truncation error of the proposed scheme was obtained, and stability analysis has been carried out. Second-order convergent error estimate was derived. Semilinear FBVPs were also solved by the proposed method after using the Newton's quasilinearization. Some numerical experiment were carried out to validate the theoretical error estimates and efficiency of the method.

Then, Chapter 4 focused on the semi-analytical and numerical solutions of a nonlinear time-tempered **k**-Caputo FDE. The Elzaki decomposition method was considered to find the semi-analytical solution of the model problem and then it has been linearized using Newton's quasilinearization method. To discretize the quasilinearized problem, a numerical scheme namely tempered ${}_{\mathbf{k}}L2\text{-}1_{\sigma}$ method has been proposed. The stability and convergence analysis of the fully discretized problem have been carried out in the L_2-norm using the energy method, and the second-order convergence $\mathcal{O}\left(M_x^{-2}+N^{-2}\right)$ in both time and space has been established in the theoretical analysis. In support of the theoretical results, a numerical experiment has been appended.

Chapter 5 investigated an analysis of the non-uniform $L1$-method to find the numerical solution of a nonlinear time-fractional diffusion equation with generalized memory kernel. To overcome the difficulty due to the presence of singularity in the solution at $t=0$, the graded meshes $t_n = T\left(n/N\right)^r,\ n=0,1,2\ldots,N$ have been conducted as it has advantage to concentrate the mesh points near $t=0$. Complementary discrete generalized memory

kernel has been introduced to develop a generalized discrete fractional Grönwall inequality for the non-uniform $L1$-formula. Stability and the error estimate of the proposed scheme with convergence order $\mathcal{O}\left(N^{-\min(r\alpha,2-\alpha)}\right)$ were carried out in the L^2-norm. Also, a regularity parameter $\sigma \in (0,1) \cup (1,2)$ has been taken into account and the convergence rates $\mathcal{O}\left(N^{-\min(r\sigma,2-\alpha)}\right)$ have been enumerated in temporal direction under a regularity condition (5.3.15). Some numerical simulations have been comprehended in support of the performance of theoretical aspects and the computed results have shown good agreement with the presented analysis.

In Chapter 6, we have proposed the WGFEM, coupled with the ADI–type dimensional-splitting technique to find the numerical solution of a class of time-factional diffusion equation. It helped us to easily deal with the 2D time-fractional diffusion problem. This dimensional-splitting technique assists to reduce the computational cost in solving the 2D time-fractional problem. The well known $L1$-method has been used to approximate the time-fractional derivative term over a non-uniform mesh and the uniform dimensional-splitting WGFEM was used for the space discretization. We have analyzed the stability of the proposed scheme and proved the error estimate of order $\mathcal{O}\left(h^{k+1} + N^{-\min(r\alpha,2-\alpha)}\right)$. In support of the theoretical estimate, a numerical example has been proposed.

Finally, a numerical technique based on a LOD process has been introduced in Chapter 7 to solve 2D nonlinear SFDE. Initially, the model problem has been linearized using Newton's quasilinearization process, after which it has been partitioned into two one-dimensional subproblems along the x and y directions. The well-known $L1$-method over a uniform mesh was employed to discretize the spatial fractional term, and the discrete maximum principle was established for the discretized scheme. Further, the discrete maximum principle and convergence analysis have been discussed for the presented numerical scheme using a well-fitted discrete barrier function. Numerical results are provided to confirm the truthfulness of the theoretical estimation.

8.2 Future scopes

Here, we are briefly proposing some problems that can be considered as future scope in this thesis work:

8.2.1 Weak Galerkin FEM for multi-term TFDE

Multi-term fractional differential equations [78] stand out as a crucial category of FDEs, including multiple fractional differential operators. It has become increasingly important in modeling numerous significant processes, particularly those characterized by multi-rate systems. Notably, multi-term fractional order differential equations offer advantageous properties and describe complex multi-rate physical phenomena in various way [38]. We wish to extend the dimensional-splitting $L1$-WGFEM, discussed in Chapter 6 to the following multi-term TFDE. Let $\mathcal{V} \subset \mathbb{R}^d (d \geq 1)$ be a convex polyhedral domain with a boundary $\partial\mathcal{V}$. Consider the following fractional-order parabolic problem for the function $u(x,t)$:

$$\begin{cases} P_c^{(\alpha)}(\partial_t)u(\mathbf{x},t) - \nabla \cdot (\Psi(\mathbf{x},t)\nabla u(\mathbf{x},t)) = f(\mathbf{x},t), \quad (\mathbf{x},t) \in \mathcal{V} \times (0,T], \\ u(\mathbf{x},t) = 0, \quad (\mathbf{x},t) \in \partial\mathcal{V} \times (0,T], \\ u(\mathbf{x},0) = \widehat{u}_0(\mathbf{x}), \quad \mathbf{x} \in \mathcal{V}. \end{cases} \tag{8.2.1}$$

Here, $\mathcal{V} = \Omega_x \times \Omega_y \subset \mathbb{R}^2$, where $\Omega_x = (x_l, x_r)$ and $\Omega_y = (y_l, y_r)$ with the boundary $\partial\mathcal{V}$, $u(\mathbf{x},\cdot) = u(x,y,\cdot)$ and $T > 0$ is a fixed final time. The functions $f \in L^\infty(0,T;L^2(\mathcal{V}))$ and $\widehat{u}_0 \in L^2(\mathcal{V})$ are given source term and initial data, respectively, and $\Psi(\mathbf{x},t) \in \mathbb{R}^{d\times d}$ is a symmetric matrix-valued diffusion coefficient such that for some constant $\lambda \geq 1$

$$\begin{aligned} &\lambda^{-1}|\xi|^2 \leq \Psi(\mathbf{x},t)\xi \cdot \xi \leq \lambda|\xi|^2, \quad \forall \xi \in \mathbb{R}^d, \forall (\mathbf{x},t) \in \mathcal{V} \times (0,T], \\ &|\partial_t \Psi(\mathbf{x},t)| + |\nabla_x \Psi(\mathbf{x},t)| + |\nabla_x \partial_t \Psi(\mathbf{x},t)| \leq c, \quad \forall (\mathbf{x},t) \in \mathcal{V} \times (0,T]. \end{aligned} \tag{8.2.2}$$

Here, the fractional differential operator $P_c^{(\alpha)}(\partial_t)$ is defined by

$$P_c^{(\alpha)}(\partial_t)u(\mathbf{x},t) := {}^C D_{0,t}^{\alpha} u(\mathbf{x},t) + \sum_{i=1}^{m} q_i {}^C D_{0,t}^{\alpha_i} u(\mathbf{x},t),$$

where q_i are given positive constants, $1 \geq \alpha > \alpha_1 \geq \alpha_2 \geq \ldots \geq \alpha_m > 0$.

8.2.2 Weak Galerkin FEM for time-fractional Burgers' equation

Burgers' equations are a type of nonlinear partial differential equations (PDEs) that describe the movement of waves in a unique way. Those equations are often used to model traffic flow, showing how traffic behaves with nonlinear effects like spreading out and sharpening at the front. Interestingly, they share similarities with the famous Navier-Stokes equations, which describe how fluids flow without any pressure pushing them along, but they're tailored specifically for situations like traffic flow. The presented scheme of Chapter 6 can be

considered to numerically solve the following nonlinear time-fractional Burgers' problem [1] in 2D:

$$\begin{cases} {}^{C}D^{\alpha}_{0,t}u - \varepsilon\Delta u + u\left(\dfrac{\partial u}{\partial x} + \dfrac{\partial u}{\partial y}\right) = f(\mathbf{x},t), \quad (\mathbf{x},t) \in \mathcal{V}\times(0,T], \\ u(\mathbf{x},t) = \widehat{g}(\mathbf{x},t), \quad (\mathbf{x},t) \in \partial\mathcal{V}\times(0,T], \\ u(\mathbf{x},0) = \widehat{u}_0(\mathbf{x}), \quad \mathbf{x}\in\mathcal{V}. \end{cases} \tag{8.2.3}$$

Here, $\mathcal{V} = \Omega_x \times \Omega_y$, where $\Omega_x = (x_l, x_r)$ and $\Omega_y = (y_l, y_r)$ with the boundary $\partial\mathcal{V}$ in $\mathbb{R}^2$, $u(\mathbf{x},\cdot) = u(x,y,\cdot)$, $T > 0$ is a fixed final time, $\widehat{u}_0(\mathbf{x}), f(\mathbf{x},t)$ and $\widehat{g}(\mathbf{x},t)$ are given functions, the parameter $\varepsilon = \dfrac{1}{R_e}$ is diffusion constant and R_e is the Reynolds number.

8.2.3 Weak Galerkin FEM for two-dimensional time-fractional mobile/immobile equation

The time-fractional mobile/immobile model plays a central role in describing various phenomena including heat diffusion and propagation of ocean sounds, among others. Moreover, it has been verified that the long term limit of continuous time random walks can be controlled by the fractional mobile/immobile equation [89], which interprets the probabilistic nature of the latter. The dimensional-splitting WGFEM of Chapter 6 can be taken into consideration to numerically solve the following 2D time-fractional mobile/immobile equation [68]:

$$\begin{cases} \dfrac{\partial u}{\partial t} + {}^{C}D^{\alpha}_{0,t}u = \Delta u + f(\mathbf{x},t), \quad (\mathbf{x},t) \in \mathcal{V}\times(0,T], \\ u(\mathbf{x},t) = \widehat{g}(\mathbf{x},t), \quad (\mathbf{x},t) \in \partial\mathcal{V}\times(0,T], \\ u(\mathbf{x},0) = \widehat{u}_0(\mathbf{x}), \quad \mathbf{x}\in\mathcal{V}. \end{cases} \tag{8.2.4}$$

Here, $\mathcal{V} = \Omega_x \times \Omega_y$, where $\Omega_x = (x_l, x_r)$ and $\Omega_y = (y_l, y_r)$ with the boundary $\partial\mathcal{V}$ in $\mathbb{R}^2$, $u(\mathbf{x},\cdot) = u(x,y,\cdot)$, $T > 0$ is a fixed final time, $\widehat{u}_0(\mathbf{x}), f(\mathbf{x},t)$ and $\widehat{g}(\mathbf{x},t)$ are given smooth functions.

Bibliography

[1] N. Abdi, H. Aminikhah, A. R. Sheikhani, J. Alavi, and M. Taghipour, *An efficient explicit decoupled group method for solving two–dimensional fractional Burgers' equation and its convergence analysis*, Advances in Mathematical Physics, 2021 (2021), pp. 1–20.

[2] G. Adomian, *Solving frontier problems of physics: the decomposition method*, vol. 60, Springer Science & Business Media, 2013.

[3] O. P. Agrawal, *A general finite element formulation for fractional variational problems*, Journal of Mathematical Analysis and Applications, 337 (2008), pp. 1–12.

[4] J.-P. Aguilar, J. Korbel, and Y. Luchko, *Applications of the fractional diffusion equation to option pricing and risk calculations*, Mathematics, 7 (2019), p. 796.

[5] A. A. Al-Nana, I. M. Batiha, and S. Momani, *A numerical approach for dealing with fractional boundary value problems*, Mathematics, 11 (2023), p. 4082.

[6] R. B. Albadarneh, I. M. Batiha, and M. Zurigat, *Numerical solutions for linear fractional differential equations of order $1< \alpha< 2$ using finite difference method (FFDM)*, International Journal of Mathematics and Computer Science, 16 (2016), pp. 103–111.

[7] A. A. Alikhanov, *A new difference scheme for the time-fractional diffusion equation*, Journal of Computational Physics, 280 (2015), pp. 424–438.

[8] A. A. Alikhanov and C. Huang, *A high-order L2 type difference scheme for the time-fractional diffusion equation*, Applied Mathematics and Computation, 411 (2021), p. 126545.

[9] R. L. Bagley and P. J. Torvik, *A theoretical basis for the application of fractional calculus to viscoelasticity*, Journal of Rheology, 27 (1983), pp. 201–210.

[10] F. B. M. Belgacem and A. A. Karaballi, *Sumudu transform fundamental properties investigations and applications*, International Journal of Stochastic Analysis, 2006 (2006).

[11] D. A. Benson, M. M. Meerschaert, and J. Revielle, *Fractional calculus in hydrologic modeling: A numerical perspective*, Advances in Water Resources, 51 (2013), pp. 479–497.

[12] M. Caputo, *Linear models of dissipation whose Q is almost frequency independent—II*, Geophysical Journal International, 13 (1967), pp. 529–539.

[13] V. Chaurasia and J. Singh, *Application of Sumudu transform in Schrödinger equation occurring in quantum mechanics*, Applied Mathematical Sciences, 4 (2010), pp. 2843–2850.

[14] R. Diaz and E. Pariguan, *On hypergeometric functions and Pochhammer k-symbol*, Divulgaciones Matemáticas, 15 (2007), pp. 179–192.

[15] T. M. Elzaki, *Application of new transform "Elzaki transform" to partial differential equations*, Global Journal of Pure and Applied Mathematics, 7 (2011), pp. 65–70.

[16] T. M. Elzaki, *The new integral transform Elzaki transform*, Global Journal of Pure and Applied Mathematics, 7 (2011), pp. 57–64.

[17] T. M. Elzaki, *On the connections between Laplace and Elzaki transforms*, Advances in Theoretical and Applied Mathematics, 6 (2011), pp. 1–11.

[18] T. M. Elzaki, S. M. Elzaki, and E. A. Elnour, *On the new integral transform "Elzaki transform" fundamental properties investigations and applications*, Global Journal of Mathematical Sciences: Theory and Practical, 4 (2012), pp. 1–13.

[19] N. Engheta, *On fractional calculus and fractional multipoles in electromagnetism*, IEEE Transactions on Antennas and Propagation, 44 (1996), pp. 554–566.

[20] V. J. Ervin and J. P. Roop, *Variational formulation for the stationary fractional advection dispersion equation*, Numerical Methods for Partial Differential Equations, 22 (2006), pp. 558–576.

[21] L. Euler, *De progressionibus transcendentibus seu quarum termini generales algebraice dari nequeunt*, Commentarii Academiae scientiarum imperialis Petropolitanae, (1738), pp. 36–57.

[22] G. Farid, A. Javed, and A. Rehman, *On Hadamard inequalities for n-times differentiable functions which are relative convex via Caputo k-fractional derivatives*, in Nonlinear Analysis Forum, vol. 22, 2017, pp. 17–28.

[23] T. Fu, Z. Zheng, and B. Duan, *Variational formulation for fractional inhomogeneous boundary value problems*, BIT Numerical Mathematics, 60 (2020), pp. 1203–1219.

[24] L. K. Gadzova, *Nonlocal boundary-value problem for a linear ordinary differential equation with fractional discretely distributed differentiation operator*, Mathematical Notes, 106 (2019), pp. 904–908.

[25] G.-h. Gao, Z.-z. Sun, and H.-w. Zhang, *A new fractional numerical differentiation formula to approximate the Caputo fractional derivative and its applications*, Journal of Computational Physics, 259 (2014), pp. 33–50.

[26] J. L. Gracia, E. O'Riordan, and M. Stynes, *Convergence analysis of a finite difference scheme for a two-point boundary value problem with a Riemann–Liouville–Caputo fractional derivative*, BIT Numerical Mathematics, 60 (2020), pp. 411–439.

[27] J. L. Gracia and M. Stynes, *Central difference approximation of convection in Caputo fractional derivative two-point boundary value problems*, Journal of Computational and Applied Mathematics, 273 (2015), pp. 103–115.

[28] J. L. Gracia and M. Stynes, *A finite difference method for an initial–boundary value problem with a Riemann–Liouville–Caputo spatial fractional derivative*, Journal of Computational and Applied Mathematics, 381 (2021), p. 113020.

[29] G. H. Hardy, J. E. Littlewood, and G. Pólya, *Inequalities*, Cambridge University Press, 1952.

[30] M. S. Hashmi, M. Wajiha, S.-W. Yao, A. Ghaffar, and M. Inc, *Cubic spline based differential quadrature method: A numerical approach for fractional Burgers' equation*, Results in Physics, 26 (2021), p. 104415.

[31] M. M. Hosseini and H. Nasabzadeh, *On the convergence of Adomian decomposition method*, Applied Mathematics and Computation, 182 (2006), pp. 536–543.

[32] Y. Hou, C. Wen, Y. Liu, and H. Li, *A two-grid ADI finite element approximation for a nonlinear distributed-order fractional sub-diffusion equation.*, Networks & Heterogeneous Media, 18 (2023).

[33] C. Huang and M. Stynes, *Optimal spatial H1-norm analysis of a finite element method for a time-fractional diffusion equation*, Journal of Computational and Applied Mathematics, 367 (2020), p. 112435.

[34] A. J. Hussein, *A weak Galerkin finite element method for solving time-fractional coupled Burgers' equations in two dimensions*, Applied Numerical Mathematics, 156 (2020), pp. 265–275.

[35] C. Ionescu, A. Lopes, D. Copot, J. T. Machado, and J. H. Bates, *The role of fractional calculus in modeling biological phenomena: A review*, Communications in Nonlinear Science and Numerical Simulation, 51 (2017), pp. 141–159.

[36] A. Jajarmi and D. Baleanu, *A new iterative method for the numerical solution of high-order non-linear fractional boundary value problems*, Frontiers in Physics, 8 (2020), p. 220.

[37] C. Jesus and E. Sousa, *Numerical method with fractional splines for a subdiffusion problem*, BIT Numerical Mathematics, 60 (2020), pp. 1075–1111.

[38] H. Jiang, F. Liu, I. Turner, and K. Burrage, *Analytical solutions for the multi-term time-fractional diffusion-wave/diffusion equations in a finite domain*, Computers & Mathematics with Applications, 64 (2012), pp. 3377–3388.

[39] B. Jin, R. Lazarov, J. Pasciak, and Z. Zhou, *Error analysis of a finite element method for the space-fractional parabolic equation*, SIAM Journal on Numerical Analysis, 52 (2014), pp. 2272–2294.

[40] R. Kalaba and K. Spingarn, *On the rate of convergence of the quasi-linearization method*, IEEE Transactions on Automatic Control, 28 (1983), pp. 798–799.

[41] Q. D. Katatbeh and F. B. M. Belgacem, *Applications of the Sumudu transform to fractional differential equations*, Nonlinear Studies, 18 (2011), pp. 99–112.

[42] N. Kedia, A. A. Alikhanov, and V. K. Singh, *Stable numerical schemes for time-fractional diffusion equation with generalized memory kernel*, Applied Numerical Mathematics, 172 (2022), pp. 546–565.

[43] M. Khalid, M. Sultana, F. Zaidi, and U. Arshad, *Application of Elzaki transform method on some fractional differential equations*, Mathematical Theory and Modeling, 5 (2015), pp. 89–96.

[44] N. Khalid, M. Abbas, M. K. Iqbal, J. Singh, and A. I. M. Ismail, *A computational approach for solving time-fractional differential equation via spline functions*, Alexandria Engineering Journal, 59 (2020), pp. 3061–3078.

[45] N. Kopteva, *Error analysis of the L1 method on graded and uniform meshes for a fractional-derivative problem in two and three dimensions*, Mathematics of Computation, 88 (2019), pp. 2135–2155.

[46] N. Kopteva, *Error analysis of an L2-type method on graded meshes for a fractional-order parabolic problem*, Mathematics of Computation, 90 (2021), pp. 19–40.

[47] T. Langlands and B. I. Henry, *The accuracy and stability of an implicit solution method for the fractional diffusion equation*, Journal of Computational Physics, 205 (2005), pp. 719–736.

[48] G. W. Leibniz, *Mathematische Schriften: aus den Handschriften der Königlichen Bibliothek zu Hannover. Briefwechsel zwischen Leibniz, Hugens Van Zulichem und dem Marquis de L'Hospital*, vol. 1, Asher, 1850.

[49] C. Li, Q. Yi, and A. Chen, *Finite difference methods with non-uniform meshes for nonlinear fractional differential equations*, Journal of Computational Physics, 316 (2016), pp. 614–631.

[50] G. Li, Y. Chen, and Y. Huang, *A new weak Galerkin finite element scheme for general second-order elliptic problems*, Journal of Computational and Applied Mathematics, 344 (2018), pp. 701–715.

[51] M. Li, C. Huang, and P. Wang, *Galerkin finite element method for nonlinear fractional Schrödinger equations*, Numerical Algorithms, 74 (2017), pp. 499–525.

[52] X. Li, *Numerical solution of fractional differential equations using cubic B-spline wavelet collocation method*, Communications in Nonlinear Science and Numerical Simulation, 17 (2012), pp. 3934–3946.

[53] X. Li and P. J. Wong, *gL1 scheme for solving a class of generalized time-fractional diffusion equations*, Mathematics, 10 (2022), p. 1219.

[54] R. Lin, X. Ye, S. Zhang, and P. Zhu, *A weak Galerkin finite element method for singularly perturbed convection-diffusion–reaction problems*, SIAM Journal on Numerical Analysis, 56 (2018), pp. 1482–1497.

[55] Y. Lin and C. Xu, *Finite difference/spectral approximations for the time-fractional diffusion equation*, Journal of Computational Physics, 225 (2007), pp. 1533–1552.

[56] A. M. Lopes, J. T. Machado, C. M. Pinto, and A. M. Galhano, *Fractional dynamics and MDS visualization of earthquake phenomena*, Computers & Mathematics with Applications, 66 (2013), pp. 647–658.

[57] J. Ma, F. Gao, and N. Du, *Stabilizer-free weak Galerkin finite element method with second-order accuracy in time for the time-fractional diffusion equation*, Journal of Computational and Applied Mathematics, 414 (2022), p. 114407.

[58] S. J. C. Mary and A. Tamilselvan, *Numerical method for a non-local boundary value problem with Caputo fractional order*, Journal of Applied Mathematics and Computing, 67 (2021), pp. 671–687.

[59] R. Matuš, *Application of fractional order calculus to control theory*, International Journal of Mathematical Models and Methods in Applied Sciences, 5 (2011), pp. 1162–1169.

[60] G. M. Mittag-Leffler, *Sur la Nouvelle Fonction $E\alpha(x)$*, Comptes Rendus de l'Academie des Sciences Paris, 137 (1903), pp. 554–558.

[61] L. Mu, J. Wang, and X. Ye, *Weak Galerkin finite element methods on polytopal meshes*, International Journal of Numerical Analysis & Modeling, 12 (2015), pp. 31–53.

[62] S. Mubeen and G. Habibullah, *k-fractional integrals and application*, International Journal of Contemporary Mathematical Sciences, 7 (2012), pp. 89–94.

[63] K. Nedaiasl and R. Dehbozorgi, *Galerkin finite element method for nonlinear fractional differential equations*, Numerical Algorithms, 88 (2021), pp. 113–141.

[64] I. Newton, *Philosophiae naturalis principia mathematica*, vol. 1, G. Brookman, 1833.

[65] A. Pedas and E. Tamme, *Piecewise polynomial collocation for linear boundary value problems of fractional differential equations*, Journal of Computational and Applied Mathematics, 236 (2012), pp. 3349–3359.

[66] T. R. Prabhakar, *A singular integral equation with a generalized Mittag-Leffler function in the kernel*, Yokohama Mathematical Journal, 19 (1971), pp. 7–15.

[67] W. Qiu, D. Xu, H. Chen, and J. Guo, *An alternating direction implicit Galerkin finite element method for the distributed-order time-fractional mobile–immobile equation in two dimensions*, Computers & Mathematics with Applications, 80 (2020), pp. 3156–3172.

[68] F. M. Salama, U. Ali, and A. Ali, *Numerical solution of two-dimensional time-fractional mobile/immobile equation using explicit group methods*, International Journal of Applied and Computational Mathematics, 8 (2022), p. 188.

[69] S. Shen and F. Liu, *Error analysis of an explicit finite difference approximation for the space fractional diffusion equation with insulated ends*, ANZIAM Journal, 46 (2004), pp. C871–C887.

[70] E. Sousa, *Numerical approximations for fractional diffusion equations via splines*, Computers & Mathematics with Applications, 62 (2011), pp. 938–944.

[71] M. Stynes and J. L. Gracia, *A finite difference method for a two-point boundary value problem with a Caputo fractional derivative*, IMA Journal of Numerical Analysis, 35 (2015), pp. 698–721.

[72] M. Stynes, E. O'Riordan, and J. L. Gracia, *Error analysis of a finite difference method on graded meshes for a time-fractional diffusion equation*, SIAM Journal on Numerical Analysis, 55 (2017), pp. 1057–1079.

[73] F. Sultana, D. Singh, R. K. Pandey, and D. Zeidan, *Numerical schemes for a class of tempered fractional integro-differential equations*, Applied Numerical Mathematics, 157 (2020), pp. 110–134.

[74] Z.-z. Sun and X. Wu, *A fully discrete difference scheme for a diffusion-wave system*, Applied Numerical Mathematics, 56 (2006), pp. 193–209.

[75] N. Sweilam, M. Khader, and A. Mahdy, *Crank-Nicolson finite difference method for solving time-fractional diffusion equation*, Journal of Fractional Calculus and Applications, 2 (2012), pp. 1–9.

[76] V. E. Tarasov, *Generalized memory: Fractional calculus approach*, Fractal and Fractional, 2 (2018), p. 23.

[77] Ş. Toprakseven, *A weak Galerkin finite element method for time-fractional reaction-diffusion-convection problems with variable coefficients*, Applied Numerical Mathematics, 168 (2021), pp. 1–12.

[78] Ş. Toprakseven, *A weak Galerkin finite element method on temporal graded meshes for the multi-term time-fractional diffusion equations*, Computers & Mathematics with Applications, 128 (2022), pp. 108–120.

[79] R. S. Varga, *Matrix iterative analysis*, New Jersey, 322 (1962).

[80] G. W. F. von Leibniz, *Leibnizens mathematische schriften*, vol. 1, A. Asher, 1849.

[81] H. Wang, K. Wang, and T. Sircar, *A direct $O(N \log 2N)$ finite difference method for fractional diffusion equations*, Journal of Computational Physics, 229 (2010), pp. 8095–8104.

[82] J. Wang and X. Ye, *A weak Galerkin finite element method for second-order elliptic problems*, Journal of Computational and Applied Mathematics, 241 (2013), pp. 103–115.

[83] J. Wang and X. Ye, *A weak Galerkin mixed finite element method for second order elliptic problems*, Mathematics of Computation, 83 (2014), pp. 2101–2126.

[84] J. Wang and X. Ye, *A weak Galerkin finite element method for the Stokes equations*, Advances in Computational Mathematics, 42 (2016), pp. 155–174.

[85] G. K. Watugala, *Sumudu transform: a new integral transform to solve differential equations and control engineering problems*, Integrated Education, 24 (1993), pp. 35–43.

[86] J. Webb, *Existence of positive solutions for a thermostat model*, Nonlinear Analysis: Real World Applications, 13 (2012), pp. 923–938.

[87] S. Weerakoon, *Application of Sumudu transform to partial differential equations*, International Journal of Mathematical Education in Science and Technology, 25 (1994), pp. 277–283.

[88] A. Wiman, *Über die Nullstellen der Funktionen $E_a(x)$*, Acta Mathematica, 29 (1905), pp. 217–234.

[89] X. Yang, H. Zhang, and Q. Tang, *A spline collocation method for a fractional mobile–immobile equation with variable coefficients*, Computational and Applied Mathematics, 39 (2020), p. 34.

[90] Y. Yang, J. Huang, and H. Li, *An α-robust analysis of finite element method for space-time-fractional diffusion equation*, Numerical Algorithms, (2024), pp. 1–26.

[91] W. K. Zahra and S. M. Elkholy, *Quadratic spline solution for boundary value problem of fractional order*, Numerical Algorithms, 59 (2012), pp. 373–391.

[92] Y. Zhang, *A finite difference method for fractional partial differential equation*, Applied Mathematics and Computation, 215 (2009), pp. 524–529.

[93] Y.-n. Zhang, Z.-z. Sun, and H.-l. Liao, *Finite difference methods for the time-fractional diffusion equation on non-uniform meshes*, Journal of Computational Physics, 265 (2014), pp. 195–210.

[94] L. Zhao, F. Zhao, and C. Li, *Linearized finite difference schemes for a tempered fractional Burgers' equation in fluid-saturated porous rocks*, Waves in Random and Complex Media, (2021), pp. 1–25.

[95] X. Zhao, X. Hu, W. Cai, and G. E. Karniadakis, *Adaptive finite element method for fractional differential equations using hierarchical matrices*, Computer Methods in Applied Mechanics and Engineering, 325 (2017), pp. 56–76.

[96] P. Zhu and S. Xie, *A uniformly convergent weak Galerkin finite element method on Shishkin mesh for 1d convection–diffusion problem*, Journal of Scientific Computing, 85 (2020), p. 34.

List of published and communicated articles

1. Aniruddha Seal, Srinivasan Natesan, Convergence Analysis of a Second-Order Scheme for Fractional Differential Equation with Integral Boundary Conditions, Journal of Applied Mathematics and Computing, 69, 465–489, 2023.

2. Aniruddha Seal, Srinivasan Natesan, A Numerical Approach for Nonlinear Time-Fractional Diffusion Equation with Generalized Memory Kernel, Numerical Algorithms, 2023.

3. Aniruddha Seal, Srinivasan Natesan, A Dimensional-Splitting Weak Galerkin Finite Element Method for 2D Time-Fractional Diffusion Equation, Journal of Scientific Computing, 98(56), 2024.

4. Aniruddha Seal, Srinivasan Natesan, An Efficient Computational Technique for Semilinear Time–Fractional Diffusion Equation, Calcolo, 61(47), 2024.

5. Aniruddha Seal, Srinivasan Natesan, An Accurate Finite-Difference Scheme for the Numerical Solution of a Fractional Differential Equation. (Under Review)

6. Aniruddha Seal, Srinivasan Natesan, A Novel Locally One-Dimensional Method for Two-Dimensional Nonlinear Space-Fractional Diffusion Equation. (Under Review)